Effectiveness of the new ambulance air exhaust system in reducing aerosol particle concentration

Mr. Vasutorn Petrangsan

จุฬาลงกรณ์มหาวิทยาลัย
CHULALONGKORN UNIVERSITY

A Thesis Submitted in Partial Fulfillment of the Requirements
for the Degree of Master of Engineering in Mechanical Engineering
Department of Mechanical Engineering
FACULTY OF ENGINEERING
Chulalongkorn University
Academic Year 2021

Copyright of Chulalongkorn University

ประสิทธิผลของระบบดูดอากาศที่ติดตั้งใหม่ในรถพยาบาลในการลดความเข้มข้นของละอองในอากาศ

นายวสุธร เพชรรังสรรค์

จุฬาลงกรณ์มหาวิทยาลัย
CHULALONGKORN UNIVERSITY

วิทยานิพนธ์นี้เป็นส่วนหนึ่งของการศึกษาตามหลักสูตรปริญญาวิศวกรรมศาสตรมหาบัณฑิต
สาขาวิชาวิศวกรรมเครื่องกล ภาควิชาวิศวกรรมเครื่องกล
คณะวิศวกรรมศาสตร์ จุฬาลงกรณ์มหาวิทยาลัย
ปีการศึกษา 2564
ลิขสิทธิ์ของจุฬาลงกรณ์มหาวิทยาลัย

Thesis Title	Effectiveness of the new ambulance air exhaust system in reducing aerosol particle concentration
By	Mr. Vasutorn Petrangsan
Field of Study	Mechanical Engineering
Thesis Advisor	KARU CHONGSIRIPINYO, Ph.D.

Accepted by the FACULTY OF ENGINEERING, Chulalongkorn University in Partial Fulfillment of the Requirement for the Master of Engineering

..... Dean of the FACULTY OF ENGINEERING

(Professor SUPOT TEACHAVORASINSKUN, Ph.D.)

THESIS COMMITTEE

..... Chairman

(Associate Professor ALONGKORN PIMPIN, Ph.D.)

..... Thesis Advisor

(KARU CHONGSIRIPINYO, Ph.D.)

..... Examiner

(Assistant Professor SARAN SALAKIJ, Ph.D.)

..... External Examiner

(Associate Professor Vejapong Juttijudata, Ph.D.)

จุฬาลงกรณ์มหาวิทยาลัย
Chulalongkorn University

วสุธร เพชรรังสรรค์ : ประสิทธิผลของระบบดูดอากาศที่ติดตั้งใหม่ในรถพยาบาลในการลดความเข้มข้นของละอองในอากาศ. (Effectiveness of the new ambulance air exhaust system in reducing aerosol particle concentration) อ.ที่ปรึกษาหลัก : อ. ดร.การุ จงศิริภิญโญ

วัตถุประสงค์ของการศึกษานี้คือเพื่อประเมินประสิทธิผลในการลดอนุภาคในอากาศของระบบระบายอากาศ *Camfil® CC410-concealed* ที่ติดตั้งในรถพยาบาลรหัส *ER-1* (รถพยาบาลของโรงพยาบาลจุฬาลงกรณ์) การทดลองทำโดยพ่นละอองลอยเข้าไปในห้องโดยสารที่ตำแหน่งบริเวณใบหน้าของผู้ป่วยเป็นเวลา 1 นาที และวัดความเข้มข้นของละอองลอยภายในห้องโดยสารเมื่อเวลาผ่านไป การทดลองดำเนินการในสภาวะการระบายอากาศ 2 สภาวะ คือ เมื่อปิดระบบดูดอากาศและเมื่อเปิดระบบดูดอากาศที่อัตราสูงสุด ความหนาแน่นของละอองลอยถูกตีความในแง่ของความเข้มข้นเชิงปริมาตร สำหรับช่วงเวลาที่จะกล่าวด้านล่างนี้นับจากเวลาเมื่อสิ้นสุดการพ่นละอองลอยเข้าสู่ห้องโดยสาร

จากการศึกษาพบว่าละอองลอยมีกระจายไปทางส่วนหน้าของห้องโดยสารและกระจายไปทั่วห้องโดยสารหลังจากหยุดการพ่นได้ไม่นาน การกระจายเชิงพื้นที่ของละอองลอยไม่สม่ำเสมอโดยมีปริมาณสูงเมื่อเทียบกับบริเวณอื่นเกิดขึ้นพร้อมกันหลายบริเวณซึ่งแตกต่างกันระหว่างสองสภาวะ อนุภาคที่มีช่วงขนาดต่างกันจะถูกกำจัดออกจากห้องโดยสารด้วยอัตราที่ต่างกัน เมื่อปราศจากระบบดูดอากาศ อนุภาคที่มีขนาดใหญ่กว่ามีแนวโน้มในการลดลงได้เร็วกว่าอนุภาคที่มีขนาดเล็ก ในการคืนค่าความเข้มข้นของละอองลอยให้กลับมาใกล้เคียงกับระดับสถานะเริ่มต้น (หรือสถานะพื้นหลัง) สำหรับกรณีปิดระบบดูดอากาศใช้เวลาประมาณ 16 นาทีสำหรับอนุภาคในช่วงขนาด 0.5-1 ไมครอน, 12 นาทีสำหรับ 1-2.5 ไมครอน และ 9 นาทีสำหรับ 2.5-5 ไมครอน สถานะพื้นหลังกลับมาหลังจาก 18 นาทีสำหรับทุกช่วงขนาด เมื่อมีระบบดูดอากาศ ระยะเวลาการลดลงนั้นลดลงเหลือเพียงประมาณ 5 นาทีสำหรับทุกช่วงขนาดของละอองลอย ในช่วงการลดลงของกรณีปิดระบบดูดอากาศ ละอองลอยขนาดเล็กมีแนวโน้มที่จะรวมตัวกันในบริเวณด้านหลังห้องโดยสาร และ ละอองลอยขนาดใหญ่มีแนวโน้มที่จะรวมตัวกันในบริเวณด้านหน้า (ใกล้กับบริเวณหัวฉีด) สะท้อนให้เห็นถึงความสามารถ (หรือไม่สามารถ) ในการกระจายตัวของละอองลอย ซึ่งแตกต่างไปตามขนาดของละอองลอยเอง ละอองลอยขนาด 1-5 ไมครอน (ช่วงขนาดกลางถึงใหญ่) มีปริมาณค่อนข้างสูงบริเวณส่วนหน้าห้องโดยสาร (ตำแหน่งที่นั่ง 1) แต่ในช่วงขนาด 0.5-1 ไมครอนมีปริมาณมากในบริเวณส่วนท้ายของห้องโดยสาร (ตำแหน่งที่นั่ง 5) ในทางกลับกันในช่วงการลดลงเมื่อเปิดระบบดูดอากาศ อนุภาคขนาดใหญ่มีการกระจายไปยังส่วนกลางและส่วนหลังของห้องโดยสาร สำหรับละอองลอยขนาด 0.5-2.5 ไมครอน (ช่วงขนาดเล็กถึงขนาดกลาง) มีการกระจุกตัวบริเวณส่วนหน้าของห้องโดยสาร (ตำแหน่งที่นั่ง 2) ในขณะที่ในช่วงขนาด 2.5-5 ไมครอนเกิดค่าความเข้มข้นสูงสุดบริเวณกึ่งกลาง (ตำแหน่งที่นั่ง 3) และโดยเฉลี่ยบริเวณด้านหลังของห้องโดยสาร (ตำแหน่งที่นั่ง 5) ระบบดูดอากาศได้รับการพิสูจน์แล้วว่ามีประสิทธิผลในการลดความเข้มข้นของละอองลอยในห้องโดยสารของรถพยาบาล เมื่อพิจารณาจากทั้งตำแหน่งที่นั่งและขนาดอนุภาคในการทดลองนี้ ระบบดูดอากาศสามารถลดความเข้มข้นสูงสุดของละอองลอยประมาณ 25% และลดความเข้มข้นเฉลี่ยของละอองลอยประมาณ 70%

สาขาวิชา	วิศวกรรมเครื่องกล	ลายมือชื่อนิสิต .....
ปีการศึกษา	2564	ลายมือชื่อ อ.ที่ปรึกษาหลัก .....

จุฬาลงกรณ์มหาวิทยาลัย
Chulalongkorn University

6270255621 : MAJOR MECHANICAL ENGINEERING

KEYWORD: Pandemic; airborne transmission; aerosol particle; ambulance; air exhaust system

Vasutorn Petrangsan : Effectiveness of the new ambulance air exhaust system in reducing aerosol particle concentration. Advisor: KARU CHONGSIRIPINYO, Ph.D.

The objective of this work is to assess the effectiveness in reducing airborne particles of the Camfil® CC410-concealed air exhaust system, that is installed in the ER-1 ambulance (a King Chulalongkorn Memorial Hospital ambulance). This is done by diffusing aerosols into the cabin at the patient's face position for an injection period (IP) of 1 minute and measuring the aerosol concentration inside the cabin over time. The experiment is conducted for 2 ventilation conditions, when the exhaust system is off (Minimal Ventilation: MV) and at maximum speed (High Ventilation: HV). Density of the aerosol is interpreted in terms of its volume concentration. Time period is counted at the end of the IP.

Aerosol is found to disperse toward the cabin's frontal part and then throughout the entire cabin shortly after IP. Its spatial distribution is non-uniform with multiple local peaks, differs between the two cases. Particles of different size range is removed from the cabin with different rates. Without an aid from the exhaust system (MV case), larger particles tend to decay relatively faster. To recover aerosol concentration to that 'comparable' to the initial (or background) state for the MV case, it takes 16 minutes for 0.5-1 microns, 12 minutes for 1-2.5 microns, and 9 minutes for 2.5-5 microns particles. The background state is reached after 18 minutes for all size ranges. With the aid in the HV case, the decaying period is shortened to about 5 minutes for all aerosol size ranges. During the passive decay (MV), small aerosols tend to aggregate in the rear cabin and larger aerosols in the front (close to the diffusion nozzle), reflecting their "native" dispersion ability (or inability) with respect to their sizes. Aerosol of medium-to-large 1-5 microns range is relatively large at the cabin frontal part (seat 1) but 0.5-1 microns range is large at the cabin rear (seat 5). During the active decay (HV), on the other hand, larger particle is advected toward the middle and rear parts. Small-to-medium-size aerosols at 0.5-2.5 microns is concentrated at the cabin frontal part (seat 2) while that of 2.5-5 microns concentration is peaked in the middle (seat 3) and on average in the rear (seat 5). The air exhaust system is proven satisfactory effective in reducing aerosol concentration in the ambulance cabin. Considering among seats and particle size in this experiment, the system is able to reduce peak aerosol concentrations by 25% and temporal-averaged concentration by 70%.

Field of Study: Mechanical Engineering Student's Signature .....

Academic Year: 2021 Advisor's Signature .....

จุฬาลงกรณ์มหาวิทยาลัย
Chulalongkorn University

ACKNOWLEDGEMENTS

After two years and a half have passed, this thesis was successfully accomplished with great assistance and support from my thesis advisor, Karu Chongsiripinyo, who provided advice and guidance on conducting this research as well as reviewing this thesis. I am also extremely grateful to Associate Professor Alongkorn Pimpin for being the chairman of the thesis committee, Assistant Professor Saran Salakij for being the thesis examiner, and Associate Professor Vejapong Juttijudata for being the thesis external examiner.

I would like to thank Professor Thanadol Rojanasarntikul, MD, FTCEP, Director of EMS Unit of Department of Emergency Medicine of King Chulalongkorn Memorial Hospital, for providing resources in conducting the research. I really appreciate the financial support from Chulalongkorn University (CU-GR 63-34-21-02), and Micro/Nano Electro-Mechanical Integrated Device Research Unit, Faculty of Engineering, Chulalongkorn University.

Furthermore, I would like to thank Sikarin Wongsawatkul, Siraphat Wongwattanaun, and Waris Natirutthakorn, the third-year students at Department of Mechanical Engineering, Thanyakan Sukkho, PMD, and Chalermchai Taesiri, MD, for their assistance in conducting this thesis experiment. Lastly, I would like to express my appreciation to my family for always supporting me in every aspect.

จุฬาลงกรณ์มหาวิทยาลัย
Chulalongkorn University

Vasutorn Petrangsan

TABLE OF CONTENTS

Page

..... iii

ABSTRACT (THAI) iii

..... iv

ABSTRACT (ENGLISH) iv

ACKNOWLEDGEMENTS v

TABLE OF CONTENTS vi

LIST OF TABLES xii

LIST OF FIGURES xiv

CHAPTER 1 1

INTRODUCTION 1

1.1 Background and Significant of the Research Problem 1

1.1.1 Current Pandemic Situation 1

1.1.2 Transmission Pathway 2

1.1.3 Infection Statistics and Prevention Measures 2

1.1.4 Dangers and Symptoms of COVID-19 7

1.1.5 Pandemic Viruses 9

1.1.6 Virus-Size Distribution 10

1.1.7 Detection and Diagnosis of COVID-19 13

1.1.8 Particle Measurement Techniques 17

1.1.9 Ventilation Types 24

1.1.10 Cleanrooms Design (Variddhi Ungbhakorn, 2012) 26

จุฬาลงกรณ์มหาวิทยาลัย
Chulalongkorn University

1.1.11 New Ambulances for Respiratory Disease 30
1.2 Objective of the Research 32
1.3 Scopes of the Research 33
1.4 Expectation Benefits 34
CHAPTER 2 35
LITERATURE REVIEW 35
2.1 Related Research 35
2.1.1 Number and Size of Particles Emitted by People 35
2.1.2 How Far Can Particles Spread and How Long Can They Remain? 37
2.1.3 The Size of the Particle and the Severity of the Infection 39
2.1.4 Standards for Aerosol Particles and Droplets 39
2.1.5 Protection Equipment and Protection Method 40
2.1.6 Standard for the Building Ventilation System 42
2.1.7 Risks of Medical Personnel Working in an Ambulance 42
2.1.8 Ambulance Ventilation System 45
CHAPTER 3 47
RESEARCH METHODOLOGY 47
3.1 Research Instrument 51
3.1.1 Toyota Ventury 51
3.1.2 CC 410-Concealed Air Purifier 52
3.1.3 Oxylog® 3000 plus 54
3.1.4 Aeroneb® Professional Nebulizer 56
3.1.5 Handheld 3016 59
3.1.6 PMS5003 G5 (with GM1705A01 pin adapter module) 61

จุฬาลงกรณ์มหาวิทยาลัย
Chulalongkorn University

3.1.7 Arduino UNO R3 SMD (CH340G) 63
3.1.8 0.9% Sodium Chloride Solution 65
3.2 PMS5003 Usage 65
3.3 Sensor Calibration 66
3.4 Preliminary Experimental Procedure 76
3.4.1 Case 1: Turn off air exhaust system (minimal ventilation) 76
3.4.2 Case 2: Turn on air exhaust system at level 3 (medium ventilation) 77
3.4.3 Case 3: Turn on air exhaust system at level 6 (high ventilation) 78
3.5 Experimental Procedure 78
3.5.1 Case 1: Turn off air exhaust system (minimal ventilation) 79
3.5.2 Case 2: Turn on air exhaust system at level 6 (high ventilation) 80
3.6 Data Analysis 80
CHAPTER 4 84
PRELIMINARY RESULTS 84
4.1 Return to Background-State Time 84
4.2 Maximum Aerosol Volume Concentration 86
4.2.1 Size range between 0.5 and 1 micron 86
4.2.2 Size range between 1 and 2.5 micron 86
4.2.3 Size range between 2.5 and 5 micron 87
4.4 Mean Aerosol Volume Concentration 87
4.3.1 Size range between 0.5 and 1 micron 87
4.3.2 Size range between 1 and 2.5 micron 88
4.3.3 Size range between 2.5 and 5 micron 88
CHAPTER 5 90

จุฬาลงกรณ์มหาวิทยาลัย
Chulalongkorn University

RESULTS 90
5.1 Three-Dimensional Visualization 92
5.1.1 Size range between 0.5 and 1 micron 92
5.1.2 Size range between 1 and 2.5 micron 95
5.1.3 Size range between 2.5 and 5 micron 97
5.2 Horizontal Contour Plane at Face Level of EMS workers 100
5.2.1 Size range between 0.5 and 1 micron 100
5.2.2 Size range between 1 and 2.5 micron 113
5.2.3 Size range between 2.5 and 5 micron 128
5.3 Vertical Contour Plane at Injection Position along Patient Cot 142
5.3.1 Size range between 0.5 and 1 micron 142
5.3.2 Size range between 1 and 2.5 micron 155
5.3.3 Size range between 2.5 and 5 micron 169
5.4 Spatial-Averaged Aerosol Volume Concentration over Time 182
5.5 Aerosol Volume Concentration over Time at EMS Workers' Face 186
5.6 Maximum Aerosol Volume Concentration at EMS Workers' Face 197
5.6.1 Size range between 0.5 and 1 micron 197
5.6.2 Size range between 1 and 2.5 micron 198
5.6.3 Size range between 2.5 and 5 micron 200
5.7 Temporal-Averaged Aerosol Volume Concentration at EMS Workers' Face 204
5.7.1 Size range between 0.5 and 1 micron 204
5.7.2 Size range between 1 and 2.5 micron 205
5.7.3 Size range between 2.5 and 5 micron 206
CHAPTER 6 209

จุฬาลงกรณ์มหาวิทยาลัย
Chulalongkorn University

DISCUSSION 209
CHAPTER 7 212
SUMMARY AND CONCLUSION 212
REFERENCES 216
APPENDIX A 2
PMS5003 WIRING DIAGRAM FOR PRELIMINARY EXPERIMENT (ACTIVE MODE) 2
APPENDIX B 3
CODE FOR PMS5003 (ACTIVE MODE) 3
APPENDIX C 7
PMS5003 WIRING DIAGRAM (PASSIVE MODE) 7
APPENDIX D 8
CODE FOR PMS5003 (PASSIVE MODE) 8
APPENDIX E 12
PYTHON CODE FOR CALIBRATION AND CONVERSION 12
APPENDIX F 15
PYTHON CODE FOR CUBIC SPLINE INTERPOLATION 15
APPENDIX G 16
PYTHON CODE FOR WINDOW MOVING AVERAGE 16
APPENDIX H 17
PYTHON CODE FOR WRITING VTK FILE 17
APPENDIX I 19
SUPPLEMENTAL MATERIALS FOR PRELIMINARY RESULTS 19
APPENDIX J 28
CONFERENCE PROCEEDING 28

จุฬาลงกรณ์มหาวิทยาลัย
Chulalongkorn University

1 Introduction 29

2 Experiment 30

2.1 Experimental procedure 30

2.2 Data analysis 31

3 PMS5003 calibration 32

4 Results 32

4.1 Aerosol volume concentration over time 32

4.2 Maximum aerosol volume concentration 33

4.3 Mean Aerosol Volume Concentration 34

5 Summary and Conclusions 34

6 Acknowledgement 35

7 References 35

APPENDIX K 38

PRESENTATION MATERIAL 38

VITA 92

จุฬาลงกรณ์มหาวิทยาลัย
CHULALONGKORN UNIVERSITY

LIST OF TABLES

Page

Table 1 Operating Specification of Camfil® CC 410-Concealed Air Purifier (Camfil, 2021c).....53

Table 2 Time to Return to the Background-State Concentration in a Second Unit at Seat 1.....84

Table 3 Time to Return to the Background-State Concentration in a Second Unit at Seat 2.....85

Table 4 Time to Return to the Background-State Concentration in a Second Unit at Seat 3.....85

Table 5 Time to Return to the Background-State Concentration in Second at Seat 1 189

Table 6 Time to Return to the Background-State Concentration in Second at Seat 2 190

Table 7 Time to Return to the Background-State Concentration in Second at Seat 3 190

Table 8 Time to Return to the Background-State Concentration in Second at Seat 4 190

Table 9 Time to Return to the Background-State Concentration in Second at Seat 5 191

Table 10 Maximum Volume concentration in 0.5-1-micron size range at all positions 197

Table 11 Maximum Volume concentration in 1-2.5-micron size range in all positions 198

Table 12 Maximum Volume concentration in 2.5-5-micron size range in all positions 200

จุฬาลงกรณ์มหาวิทยาลัย
CHULALONGKORN UNIVERSITY

Table 13 Temporal-Averaged Volume concentration in 0.5-1-micron size range in all positions 204

Table 14 Temporal-Averaged Volume concentration in 1-2.5-micron size range in all positions 205

Table 15 Temporal-Averaged Volume concentration in 2.5-5-micron size range in all positions 206

จุฬาลงกรณ์มหาวิทยาลัย
Chulalongkorn University

LIST OF FIGURES

Page

Figure 1 Number of COVID-19 Daily Reported Cases around the World with 7-Day Moving Average (as of March 15, 2021) (Worldometer, 2021a) 3

Figure 2 Number of COVID-19 Daily Death Cases around the World (as of March 15, 2021) (Worldometer, 2021a) 3

Figure 3 Number of COVID-19 Daily Reported Cases of United States with 7-Day Moving Average (as of March 15, 2021) (Worldometer, 2021b) 4

Figure 4 Number of COVID-19 Daily Death Cases of United States (as of March 15, 2021) (Worldometer, 2021b) 4

Figure 5 Number of COVID-19 Daily Reported Cases of China with 7-Day Moving Average (as of March 15, 2021) (Worldometer, 2021c) 5

Figure 6 Number of COVID-19 Daily Death Cases of China (as of March 15, 2021) (Worldometer, 2021c) 6

Figure 7 Number of COVID-19 Daily Reported Cases of Thailand with 7-Day Moving Average (as of March 15, 2021) (Worldometer, 2021d) 7

Figure 8 Number of COVID-19 Daily Death Cases of Thailand (as of February 21, 2021) (Worldometer, 2021d) 7

Figure 9 Size Comparison of Viruses (Verras, 2021) 10

Figure 10 The Relative Size of Particles (Visual Capitalist, 2020) 12

Figure 11 Throat Swab (Centers for Disease Control and Prevention, 2017) 13

Figure 12 Nasopharyngeal Swab (Centers for Disease Control and Prevention, 2017) 13

Figure 13 Nasal Swab (Centers for Disease Control and Prevention, 2017) 14

Figure 14 Molecular Test (American Society for Microbiology, 2020) 15

จุฬาลงกรณ์มหาวิทยาลัย
Chulalongkorn University

Figure 15 Rapid Antigen Test (American Society for Microbiology, 2020) 15

Figure 16 Finger Prick (Left) (King, 2020) and Blood Draw (Right) (Neoteryx, 2020)..... 16

Figure 17 Antibody Test (American Society for Microbiology, 2020) 16

Figure 18 Air Jet Sieving (Le et al., 2012)..... 18

Figure 19 5-Stage Cascade Impactor (Kwon et al., 2003)..... 19

Figure 20 Gravity Sedimentation Instrument (Merkus, 2009) 20

Figure 21 Coulter Counter (Doroszkowski, 1999) 21

Figure 22 Dynamic Light Scattering (Aleandri et al., 2018)..... 22

Figure 23 Laser Diffraction (Sympatec GmbH, 2017) 24

Figure 24 Turbulent Mixed Flow Cleanroom (Baixardoc, n.d.)..... 27

Figure 25 Horizontal Laminar Flow (crossflow) Cleanroom (Variddhi Ungbhakorn, 2012)..... 28

Figure 26 Vertical Laminar Flow Cleanroom (National Direct Network, 2020) 29

Figure 27 Examples of an Isolation Tent for the Patient (Jeju Tourism Organization, 2020)..... 30

Figure 28 AUTECH Solati (H-350) (Autech, 2020) 31

Figure 29 SAIC Motor Co., Ltd. Ambulances Construction (Xinhuanet, 2020) 32

Figure 30 Negative Pressure Ambulance of Qingdao Ruvii Vehicle Co.,Ltd (Ruvii Vehicle, 2020)..... 32

Figure 31 The proportions of Coronaviruses in different sizes of aerosol particle (Herrmann et al., 2020)..... 36

Figure 32 Comparison of Size of Aerosol or Droplet Nuclei and Droplet from Different Studies 38

Figure 33 Ambulance Patient Compartment with Installation of Preliminary Experimental Equipment and Air Exhaust System 48

Figure 34 The Installation Location of the Experimental Equipment..... 49

Figure 35 The Location of the Experiment's Measurement Points in the Patient Compartment. 50

Figure 36 Toyota Ventury ER-1 (Plane Boi, 2019) 51

Figure 37 Patient Compartment of Toyota Ventury 51

Figure 38 CC 410 (Concealed) Air Purifier 52

Figure 39 Oxylog® 3000 plus (Dräger, 2020a) 54

Figure 40 Aeroneb® Professional Nebulizer (Medplan, 2021) 56

Figure 41 Particle Size Distribution for Albuterol as per EN 13544-1 (Aerogen®, 2015) 58

Figure 42 Handheld 3016 (Lighthouse Worldwide Solutions, 2019) 59

Figure 43 PMS5003 61

Figure 44 GM1705A01 Pin Adapter Module 61

Figure 45 Functional Block Diagram of PMS5003 (Plantower, 2017) 62

Figure 46 Arduino UNO R3 63

Figure 47 0.9% Sodium Chloride Solution 65

Figure 48 Number of Particles between 0.5 and 1 Micron per Cubic Feet over Time from Test 1 68

Figure 49 Number of Particles between 0.5 and 1 Micron per Cubic Feet over Time from Test 2 68

Figure 50 Number of Particles between 0.5 and 1 Micron per Cubic Feet over Time from Test 3 68

Figure 51 Number of Particles between 1 and 2.5 Microns per Cubic Feet over Time from Test 1 69

Figure 52 Number of Particles between 1 and 2.5 Microns per Cubic Feet over Time from Test 2 69

Figure 53 Number of Particles between 1 and 2.5 Microns per Cubic Feet over Time from Test 3 69

Figure 54 Number of Particles between 2.5 and 5 Microns per Cubic Feet over Time from Test 1 70

Figure 55 Number of Particles between 2.5 and 5 Microns per Cubic Feet over Time from Test 2 70

Figure 56 Number of Particles between 2.5 and 5 Microns per Cubic Feet over Time from Test 3 70

Figure 57 Mean Number of Particles between 0.5 and 1 Micron per Cubic Feet over Time and Standard Deviation of Three Tests 71

Figure 58 Mean Number of Particles between 1 and 2.5 Microns per Cubic Feet over Time and Standard Deviation of Three Tests 71

Figure 59 Mean Number of Particles between 2.5 and 5 Microns per Cubic Feet over Time and Standard Deviation of Three Experiments 71

Figure 60 Calibration Curve between PMS5003 and Handheld3016 for the Particle size between 0.5 and 1 micron 72

Figure 61 Calibration Curve between PMS5003 and Handheld3016 for the Particle Size between 1 and 2.5 Microns 73

Figure 62 Calibration Curve between PMS5003 and Handheld3016 for the Particle Size between 2.5 and 5 Microns 73

Figure 63 Mean Number of Particles between 0.5 to 1 Micron per Cubic Feet over Time between Handheld3016 and PMS5003 after Using Calibration Curve 74

Figure 64 Mean Number of Particles between 1 to 2.5 Microns per Cubic Feet over Time between Handheld3016 and PMS5003 after Using Calibration Curve 75

Figure 65 Mean Number of Particles between 2.5 to 5 Microns per Cubic Feet over Time between Handheld3016 and PMS5003 after Using Calibration Curve 75

Figure 66 Refine Grid (12558 Points) 83

จุฬาลงกรณ์มหาวิทยาลัย
Chulalongkorn University

Figure 67 Ambulance Patient Compartment 89

Figure 68 An Example of Mean Number of Particles over Time at a Position. The Line Shows the Ensemble Mean of Three Experiments. A Vertical Line on top of the Mean Values Represents Standard Deviation of the Collected Data at that Point in Time. . 91

Figure 69 Volume Rendering of Aerosol Volume Concentration in the Size Range between 0.5 and 1 Micron of the Minimal Ventilation Case (MV). The Subfigures are Sorted, (a) - (f), by Time Since the Beginning of Experiment and to Recall, the Aerosol Injection Starts at t = 60 sec. 93

Figure 70 Volume Rendering of Aerosol Volume Concentration in the Size Range between 0.5 and 1 Micron of the High Ventilation Case (HV). The Subfigures are Sorted, (a) - (f), by Time Since the Beginning of Experiment and to Recall, the Aerosol Injection Starts at t = 60 sec. 94

Figure 71 Volume Rendering of Aerosol Volume Concentration in the Size Range between 1 and 2.5 Micron of the Minimal Ventilation Case (MV). The Subfigures are Sorted, (a) - (f), by Time Since the Beginning of Experiment and to Recall, the Aerosol Injection Starts at t = 60 sec. 95

Figure 72 Volume Rendering of Aerosol Volume Concentration in the Size Range between 1 and 2.5 Micron of the High Ventilation Case (HV). The Subfigures are Sorted, (a) - (f), by Time Since the Beginning of Experiment and to Recall, the Aerosol Injection Starts at t = 60 sec. 96

Figure 73 Volume Rendering of Aerosol Volume Concentration in the Size Range between 2.5 and 5 Micron of the Minimal Ventilation Case (MV). The Subfigures are Sorted, (a) - (f), by Time Since the Beginning of Experiment and to Recall, the Aerosol Injection Starts at t = 60 sec. 98

Figure 74 Volume Rendering of Aerosol Volume Concentration in the Size Range between 2.5 and 5 Micron of the High Ventilation Case (HV). The Subfigures are Sorted, (a) - (f), by Time Since the Beginning of Experiment and to Recall, the Aerosol Injection Starts at t = 60 sec. 99

จุฬาลงกรณ์มหาวิทยาลัย
Chulalongkorn University

Figure 75 Contour Plane at EMS workers' Face Level at time = 0 second of Minimal Ventilation and High Ventilation with Different Colormap Ranges 102

Figure 76 Contour Plane at EMS workers' Face Level at time = 60 second of Minimal Ventilation and High Ventilation with Different Colormap Ranges 102

Figure 77 Contour Plane at EMS workers' Face Level at time = 64 second of Minimal Ventilation and High Ventilation with Different Colormap Ranges 103

Figure 78 Contour Plane at EMS workers' Face Level at time = 66 second of Minimal Ventilation and High Ventilation with Different Colormap Ranges 103

Figure 79 Contour Plane at EMS workers' Face Level at time = 68 second of Minimal Ventilation and High Ventilation with Different Colormap Ranges 104

Figure 80 Contour Plane at EMS workers' Face Level at time = 74 second of Minimal Ventilation and High Ventilation with Different Colormap Ranges 104

Figure 81 Contour Plane at EMS workers' Face Level at time = 84 second of Minimal Ventilation and High Ventilation with Different Colormap Ranges 105

Figure 82 Contour Plane at EMS workers' Face Level at time = 107 second of Minimal Ventilation and High Ventilation..... 105

Figure 83 Contour Plane at EMS workers' Face Level at time = 121 second of Minimal Ventilation and High Ventilation..... 107

Figure 84 Contour Plane at EMS workers' Face Level at time = 137 second of Minimal Ventilation and High Ventilation..... 107

Figure 85 Contour Plane at EMS workers' Face Level at time = 180 second of Minimal Ventilation and High Ventilation..... 107

Figure 86 Contour Plane at EMS workers' Face Level at time = 247 second of Minimal Ventilation and High Ventilation with Different Colormap Ranges 108

Figure 87 Contour Plane at EMS workers' Face Level at time = 300 second of Minimal Ventilation and High Ventilation with Different Colormap Ranges 108

จุฬาลงกรณ์มหาวิทยาลัย
Chulalongkorn University

Figure 88 Contour Plane at EMS workers' Face Level at time = 350 second of Minimal Ventilation and High Ventilation with Different Colormap Ranges 109

Figure 89 Contour Plane at EMS workers' Face Level at time = 400 second of Minimal Ventilation and High Ventilation with Different Colormap Ranges 109

Figure 90 Contour Plane at EMS workers' Face Level at time = 459 second of Minimal Ventilation and High Ventilation with Different Colormap Ranges 110

Figure 91 Contour Plane at EMS workers' Face Level at time = 600 second of Minimal Ventilation and High Ventilation with Different Colormap Ranges 110

Figure 92 Contour Plane at EMS workers' Face Level at time = 800 second of Minimal Ventilation with Different Colormap Ranges 111

Figure 93 Contour Plane at EMS workers' Face Level at time = 950 second of Minimal Ventilation with Different Colormap Ranges 111

Figure 94 Contour Plane at EMS workers' Face Level at time = 1050 second of Minimal Ventilation with Different Colormap Ranges 112

Figure 95 Contour Plane at EMS workers' Face Level at time = 1150 second of Minimal Ventilation with Different Colormap Ranges 112

Figure 96 Contour Plane at EMS workers' Face Level at time = 1200 second of Minimal Ventilation with Different Colormap Ranges 112

Figure 97 Contour Plane at EMS workers' Face Level at time = 0 second of Minimal Ventilation and High Ventilation with Different Colormap Ranges 115

Figure 98 Contour Plane at EMS workers' Face Level at time = 60 second of Minimal Ventilation and High Ventilation with Different Colormap Ranges 116

Figure 99 Contour Plane at EMS workers' Face Level at time = 63 second of Minimal Ventilation and High Ventilation with Different Colormap Ranges 116

Figure 100 Contour Plane at EMS workers' Face Level at time = 64 second of Minimal Ventilation and High Ventilation with Different Colormap Ranges 117

จุฬาลงกรณ์มหาวิทยาลัย
Chulalongkorn University

Figure 101 Contour Plane at EMS workers' Face Level at time = 66 second of Minimal Ventilation and High Ventilation with Different Colormap Ranges 117

Figure 102 Contour Plane at EMS workers' Face Level at time = 68 second of Minimal Ventilation and High Ventilation with Different Colormap Ranges 118

Figure 103 Contour Plane at EMS workers' Face Level at time = 74 second of Minimal Ventilation and High Ventilation with Different Colormap Ranges 118

Figure 104 Contour Plane at EMS workers' Face Level at time = 85 second of Minimal Ventilation and High Ventilation with Different Colormap Ranges 119

Figure 105 Contour Plane at EMS workers' Face Level at time = 89 second of Minimal Ventilation and High Ventilation with Different Colormap Ranges 119

Figure 106 Contour Plane at EMS workers' Face Level at time = 107 second of Minimal Ventilation and High Ventilation 120

Figure 107 Contour Plane at EMS workers' Face Level at time = 121 second of Minimal Ventilation and High Ventilation 121

Figure 108 Contour Plane at EMS workers' Face Level at time = 137 second of Minimal Ventilation and High Ventilation 121

Figure 109 Contour Plane at EMS workers' Face Level at time = 180 second of Minimal Ventilation and High Ventilation 122

Figure 110 Contour Plane at EMS workers' Face Level at time = 271 second of Minimal Ventilation and High Ventilation with Different Colormap Ranges 122

Figure 111 Contour Plane at EMS workers' Face Level at time = 300 second of Minimal Ventilation and High Ventilation with Different Colormap Ranges 123

Figure 112 Contour Plane at EMS workers' Face Level at time = 350 second of Minimal Ventilation and High Ventilation with Different Colormap Ranges 123

Figure 113 Contour Plane at EMS workers' Face Level at time = 400 second of Minimal Ventilation and High Ventilation with Different Colormap Ranges 124

จุฬาลงกรณ์มหาวิทยาลัย
Chulalongkorn University

Figure 114 Contour Plane at EMS workers' Face Level at time = 487 second of Minimal Ventilation and High Ventilation with Different Colormap Ranges 124

Figure 115 Contour Plane at EMS workers' Face Level at time = 600 second of Minimal Ventilation and High Ventilation with Different Colormap Ranges 125

Figure 116 Contour Plane at EMS workers' Face Level at time = 880 second of Minimal Ventilation with Different Colormap Ranges 126

Figure 117 Contour Plane at EMS workers' Face Level at time = 950 second of Minimal Ventilation with Different Colormap Ranges 126

Figure 118 Contour Plane at EMS workers' Face Level at time = 1050 second of Minimal Ventilation with Different Colormap Ranges 126

Figure 119 Contour Plane at EMS workers' Face Level at time = 1150 second of Minimal Ventilation with Different Colormap Ranges 127

Figure 120 Contour Plane at EMS workers' Face Level at time = 1200 second of Minimal Ventilation with Different Colormap Ranges 127

Figure 121 Contour Plane at EMS workers' Face Level at time = 0 second of Minimal Ventilation and High Ventilation with Different Colormap Ranges 130

Figure 122 Contour Plane at EMS workers' Face Level at time = 60 second of Minimal Ventilation and High Ventilation with Different Colormap Ranges 130

Figure 123 Contour Plane at EMS workers' Face Level at time = 63 second of Minimal Ventilation and High Ventilation with Different Colormap Ranges 131

Figure 124 Contour Plane at EMS workers' Face Level at time = 64 second of Minimal Ventilation and High Ventilation with Different Colormap Ranges 131

Figure 125 Contour Plane at EMS workers' Face Level at time = 66 second of Minimal Ventilation and High Ventilation with Different Colormap Ranges 132

Figure 126 Contour Plane at EMS workers' Face Level at time = 68 second of Minimal Ventilation and High Ventilation with Different Colormap Ranges 132

จุฬาลงกรณ์มหาวิทยาลัย
Chulalongkorn University

Figure 127 Contour Plane at EMS workers' Face Level at time = 74 second of Minimal Ventilation and High Ventilation with Different Colormap Ranges 133

Figure 128 Contour Plane at EMS workers' Face Level at time = 89 second of Minimal Ventilation and High Ventilation with Different Colormap Ranges 133

Figure 129 Contour Plane at EMS workers' Face Level at time = 96 second of Minimal Ventilation and High Ventilation with Different Colormap Ranges 134

Figure 130 Contour Plane at EMS workers' Face Level at time = 107 second of Minimal Ventilation and High Ventilation 134

Figure 131 Contour Plane at EMS workers' Face Level at time = 121 second of Minimal Ventilation and High Ventilation 135

Figure 132 Contour Plane at EMS workers' Face Level at time = 137 second of Minimal Ventilation and High Ventilation 136

Figure 133 Contour Plane at EMS workers' Face Level at time = 180 second of Minimal Ventilation and High Ventilation 136

Figure 134 Contour Plane at EMS workers' Face Level at time = 263 second of Minimal Ventilation and High Ventilation with Different Colormap Ranges 136

Figure 135 Contour Plane at EMS workers' Face Level at time = 300 second of Minimal Ventilation and High Ventilation with Different Colormap Ranges 137

Figure 136 Contour Plane at EMS workers' Face Level at time = 350 second of Minimal Ventilation and High Ventilation with Different Colormap Ranges 137

Figure 137 Contour Plane at EMS workers' Face Level at time = 400 second of Minimal Ventilation and High Ventilation with Different Colormap Ranges 138

Figure 138 Contour Plane at EMS workers' Face Level at time = 503 second of Minimal Ventilation and High Ventilation with Different Colormap Ranges 138

Figure 139 Contour Plane at EMS workers' Face Level at time = 600 second of Minimal Ventilation and High Ventilation with Different Colormap Ranges 139

จุฬาลงกรณ์มหาวิทยาลัย
Chulalongkorn University

Figure 140 Contour Plane at EMS workers' Face Level at time = 861 second of Minimal Ventilation with Different Colormap Ranges 140

Figure 141 Contour Plane at EMS workers' Face Level at time = 950 second of Minimal Ventilation with Different Colormap Ranges 140

Figure 142 Contour Plane at EMS workers' Face Level at time = 1050 second of Minimal Ventilation with Different Colormap Ranges 140

Figure 143 Contour Plane at EMS workers' Face Level at time = 1150 second of Minimal Ventilation with Different Colormap Ranges 141

Figure 144 Contour Plane at EMS workers' Face Level at time = 1200 second of Minimal Ventilation with Different Colormap Ranges 141

Figure 145 Contour Plane at Injection Position along Patient Cot at time = 0 second of Minimal Ventilation and High Ventilation with Different Colormap Ranges 144

Figure 146 Contour Plane at Injection Position along Patient Cot at time = 60 second of Minimal Ventilation and High Ventilation with Different Colormap Ranges 144

Figure 147 Contour Plane at Injection Position along Patient Cot at time = 62 second of Minimal Ventilation and High Ventilation with Different Colormap Ranges 145

Figure 148 Contour Plane at Injection Position along Patient Cot at time = 63 second of Minimal Ventilation and High Ventilation with Different Colormap Ranges 145

Figure 149 Contour Plane at Injection Position along Patient Cot at time = 67 second of Minimal Ventilation and High Ventilation with Different Colormap Ranges 146

Figure 150 Contour Plane at Injection Position along Patient Cot at time = 72 second of Minimal Ventilation and High Ventilation with Different Colormap Ranges 146

Figure 151 Contour Plane at Injection Position along Patient Cot at time = 76 second of Minimal Ventilation and High Ventilation with Different Colormap Ranges 147

Figure 152 Contour Plane at Injection Position along Patient Cot at time = 81 second of Minimal Ventilation and High Ventilation with Different Colormap Ranges 147

จุฬาลงกรณ์มหาวิทยาลัย
Chulalongkorn University

Figure 153 Contour Plane at Injection Position along Patient Cot at time = 108 second of Minimal Ventilation and High Ventilation 148

Figure 154 Contour Plane at Injection Position along Patient Cot at time = 116 second of Minimal Ventilation and High Ventilation 148

Figure 155 Contour Plane at Injection Position along Patient Cot at time = 126 second of Minimal Ventilation and High Ventilation 149

Figure 156 Contour Plane at Injection Position along Patient Cot at time = 160 second of Minimal Ventilation and High Ventilation 149

Figure 157 Contour Plane at Injection Position along Patient Cot at time = 200 second of Minimal Ventilation and High Ventilation 150

Figure 158 Contour Plane at Injection Position along Patient Cot at time = 235 second of Minimal Ventilation and High Ventilation with Different Colormap Ranges 150

Figure 159 Contour Plane at Injection Position along Patient Cot at time = 300 second of Minimal Ventilation and High Ventilation with Different Colormap Ranges 151

Figure 160 Contour Plane at Injection Position along Patient Cot at time = 350 second of Minimal Ventilation and High Ventilation with Different Colormap Ranges 151

Figure 161 Contour Plane at Injection Position along Patient Cot at time = 395 second of Minimal Ventilation and High Ventilation with Different Colormap Ranges 152

Figure 162 Contour Plane at Injection Position along Patient Cot at time = 600 second of Minimal Ventilation and High Ventilation with Different Colormap Ranges 152

Figure 163 Contour Plane at Injection Position along Patient Cot at time = 807 second of Minimal Ventilation with Different Colormap Ranges 153

Figure 164 Contour Plane at Injection Position along Patient Cot at time = 950 second of Minimal Ventilation with Different Colormap Ranges 153

Figure 165 Contour Plane at Injection Position along Patient Cot at time = 1050 second of Minimal Ventilation with Different Colormap Ranges 154

จุฬาลงกรณ์มหาวิทยาลัย
Chulalongkorn University

Figure 166 Contour Plane at Injection Position along Patient Cot at time = 1150 second of Minimal Ventilation with Different Colormap Ranges 154

Figure 167 Contour Plane at Injection Position along Patient Cot at time = 1200 second of Minimal Ventilation with Different Colormap Ranges 154

Figure 168 Contour Plane at Injection Position along Patient Cot at time = 0 second of Minimal Ventilation and High Ventilation with Different Colormap Ranges 157

Figure 169 Contour Plane at Injection Position along Patient Cot at time = 60 second of Minimal Ventilation and High Ventilation with Different Colormap Ranges 158

Figure 170 Contour Plane at Injection Position along Patient Cot at time = 62 second of Minimal Ventilation and High Ventilation with Different Colormap Ranges 158

Figure 171 Contour Plane at Injection Position along Patient Cot at time = 63 second of Minimal Ventilation and High Ventilation with Different Colormap Ranges 159

Figure 172 Contour Plane at Injection Position along Patient Cot at time = 67 second of Minimal Ventilation and High Ventilation with Different Colormap Ranges 159

Figure 173 Contour Plane at Injection Position along Patient Cot at time = 72 second of Minimal Ventilation and High Ventilation with Different Colormap Ranges 160

Figure 174 Contour Plane at Injection Position along Patient Cot at time = 77 second of Minimal Ventilation and High Ventilation with Different Colormap Ranges 160

Figure 175 Contour Plane at Injection Position along Patient Cot at time = 80 second of Minimal Ventilation and High Ventilation with Different Colormap Ranges 161

Figure 176 Contour Plane at Injection Position along Patient Cot at time = 108 second of Minimal Ventilation and High Ventilation 161

Figure 177 Contour Plane at Injection Position along Patient Cot at time = 112 second of Minimal Ventilation and High Ventilation 161

Figure 178 Contour Plane at Injection Position along Patient Cot at time = 124 second of Minimal Ventilation and High Ventilation 163

จุฬาลงกรณ์มหาวิทยาลัย
Chulalongkorn University

Figure 179 Contour Plane at Injection Position along Patient Cot at time = 160 second of Minimal Ventilation and High Ventilation 163

Figure 180 Contour Plane at Injection Position along Patient Cot at time = 200 second of Minimal Ventilation and High Ventilation 163

Figure 181 Contour Plane at Injection Position along Patient Cot at time = 277 second of Minimal Ventilation and High Ventilation with Different Colormap Ranges 164

Figure 182 Contour Plane at Injection Position along Patient Cot at time = 300 second of Minimal Ventilation and High Ventilation with Different Colormap Ranges 164

Figure 183 Contour Plane at Injection Position along Patient Cot at time = 350 second of Minimal Ventilation and High Ventilation with Different Colormap Ranges 165

Figure 184 Contour Plane at Injection Position along Patient Cot at time = 470 second of Minimal Ventilation and High Ventilation with Different Colormap Ranges 165

Figure 185 Contour Plane at Injection Position along Patient Cot at time = 600 second of Minimal Ventilation and High Ventilation with Different Colormap Ranges 166

Figure 186 Contour Plane at Injection Position along Patient Cot at time = 930 second of Minimal Ventilation with Different Colormap Ranges 167

Figure 187 Contour Plane at Injection Position along Patient Cot at time = 950 second of Minimal Ventilation with Different Colormap Ranges 167

Figure 188 Contour Plane at Injection Position along Patient Cot at time = 1050 second of Minimal Ventilation with Different Colormap Ranges 167

Figure 189 Contour Plane at Injection Position along Patient Cot at time = 1150 second of Minimal Ventilation with Different Colormap Ranges 168

Figure 190 Contour Plane at Injection Position along Patient Cot at time = 1200 second of Minimal Ventilation with Different Colormap Ranges 168

Figure 191 Contour Plane at Injection Position along Patient Cot at time = 0 second of Minimal Ventilation and High Ventilation with Different Colormap Ranges 171

จุฬาลงกรณ์มหาวิทยาลัย
Chulalongkorn University

Figure 192 Contour Plane at Injection Position along Patient Cot at time = 60 second of Minimal Ventilation and High Ventilation with Different Colormap Ranges 171

Figure 193 Contour Plane at Injection Position along Patient Cot at time = 62 second of Minimal Ventilation and High Ventilation with Different Colormap Ranges 172

Figure 194 Contour Plane at Injection Position along Patient Cot at time = 63 second of Minimal Ventilation and High Ventilation with Different Colormap Ranges 172

Figure 195 Contour Plane at Injection Position along Patient Cot at time = 67 second of Minimal Ventilation and High Ventilation with Different Colormap Ranges 173

Figure 196 Contour Plane at Injection Position along Patient Cot at time = 72 second of Minimal Ventilation and High Ventilation with Different Colormap Ranges 173

Figure 197 Contour Plane at Injection Position along Patient Cot at time = 78 second of Minimal Ventilation and High Ventilation with Different Colormap Ranges 174

Figure 198 Contour Plane at Injection Position along Patient Cot at time = 81 second of Minimal Ventilation and High Ventilation with Different Colormap Ranges 174

Figure 199 Contour Plane at Injection Position along Patient Cot at time = 108 second of Minimal Ventilation and High Ventilation 175

Figure 200 Contour Plane at Injection Position along Patient Cot at time = 112 second of Minimal Ventilation and High Ventilation 175

Figure 201 Contour Plane at Injection Position along Patient Cot at time = 117 second of Minimal Ventilation and High Ventilation 175

Figure 202 Contour Plane at Injection Position along Patient Cot at time = 160 second of Minimal Ventilation and High Ventilation 176

Figure 203 Contour Plane at Injection Position along Patient Cot at time = 200 second of Minimal Ventilation and High Ventilation 177

Figure 204 Contour Plane at Injection Position along Patient Cot at time = 254 second of Minimal Ventilation and High Ventilation with Different Colormap Ranges 177

จุฬาลงกรณ์มหาวิทยาลัย
Chulalongkorn University

Figure 205 Contour Plane at Injection Position along Patient Cot at time = 300 second of Minimal Ventilation and High Ventilation with Different Colormap Ranges 178

Figure 206 Contour Plane at Injection Position along Patient Cot at time = 350 second of Minimal Ventilation and High Ventilation with Different Colormap Ranges 178

Figure 207 Contour Plane at Injection Position along Patient Cot at time = 500 second of Minimal Ventilation and High Ventilation with Different Colormap Ranges 179

Figure 208 Contour Plane at Injection Position along Patient Cot at time = 600 second of Minimal Ventilation and High Ventilation with Different Colormap Ranges 179

Figure 209 Contour Plane at Injection Position along Patient Cot at time = 745 second of Minimal Ventilation with Different Colormap Ranges 180

Figure 210 Contour Plane at Injection Position along Patient Cot at time = 950 second of Minimal Ventilation with Different Colormap Ranges 180

Figure 211 Contour Plane at Injection Position along Patient Cot at time = 1050 second of Minimal Ventilation with Different Colormap Ranges 181

Figure 212 Contour Plane at Injection Position along Patient Cot at time = 1150 second of Minimal Ventilation with Different Colormap Ranges 181

Figure 213 Contour Plane at Injection Position along Patient Cot at time = 1200 second of Minimal Ventilation with Different Colormap Ranges 181

Figure 214 Spatial-Averaged Aerosol Volume Concentration over Time in the Case of Minimal Ventilation (MV) 183

Figure 215 Spatial-Averaged Aerosol Volume Concentration over Time in the Case of High Ventilation (HV) 184

Figure 216 Spatial-Averaged Aerosol Volume Concentration over Time in each Size Bin 185

Figure 217 Aerosol Volume Concentration over Time at Five Different Seat Positions with Aerosol Particles in the Range between 0.5 and 1 Micron for Minimal Ventilation Case (MV) 186

จุฬาลงกรณ์มหาวิทยาลัย
Chulalongkorn University

Figure 218 Aerosol Volume Concentration over Time at Five Different Seat Positions with Aerosol Particles in the Range between 0.5 and 1 Micron for High Ventilation Case (HV) 187

Figure 219 Aerosol Volume Concentration over Time at Five Different Seat Positions with Aerosol Particles in the Range between 1 and 2.5 Microns for Minimal Ventilation Case (MV) 187

Figure 220 Aerosol Volume Concentration over Time at Five Different Seat Positions with Aerosol Particles in the Range between 1 and 2.5 Microns for High Ventilation Case (HV) 188

Figure 221 Aerosol Volume Concentration over Time at Five Different Seat Positions with Aerosol Particles in the Range between 2.5 and 5 Microns for Minimal Ventilation Case (MV) 188

Figure 222 Aerosol Volume Concentration over Time at Five Different Seat Positions with Aerosol Particles in the Range between 2.5 and 5 Microns for High Ventilation Case (HV) 189

Figure 223 Aerosol Volume Concentration over Time in each Size Bin of Seat1 192

Figure 224 Aerosol Volume Concentration over Time in each Size Bin of Seat2 193

Figure 225 Aerosol Volume Concentration over Time in each Size Bin of Seat3 194

Figure 226 Aerosol Volume Concentration over Time in each Size Bin of Seat4 195

Figure 227 Aerosol Volume Concentration over Time in each Size Bin of Seat5 196

Figure 228 Contour Plot of Highest Maximum Concentration at EMS Workers' Face Position 198

Figure 229 Contour Plot of Highest Maximum Concentration at EMS Workers' Face Position 199

Figure 230 Contour Plot of Highest Maximum Concentration at EMS Workers' Face Position 201

จุฬาลงกรณ์มหาวิทยาลัย
Chulalongkorn University

Figure 231 Maximum Volume Concentration at Five Different Locations in each Size Bin 203

Figure 232 Temporal-Averaged Aerosol Volume Concentration at Five Different Locations in each Size Bin 208

Figure 233 Aerosol Volume Concentration over Time with Three Different Ventilation Rate at Seat 1 with Aerosol Particles in the Range between 0.5 and 1 micron. Each Line Shows the Mean and Standard Deviation of Six Experiments. 19

Figure 234 Aerosol Volume Concentration over Time with Three Different Ventilation Rate at Seat 2 with Aerosol Particles in the Range between 0.5 and 1 micron. Each Line Shows the Mean and Standard Deviation of Six Experiments 20

Figure 235 Aerosol Volume Concentration over Time with Three Different Ventilation Rate at Seat 3 with Aerosol Particles in the Range between 0.5 and 1 micron. Each Line Shows the Mean and Standard Deviation of Six Experiments 21

Figure 236 Aerosol Volume Concentration over Time with Three Different Ventilation Rate at Seat 1 with Aerosol Particles in the Range between 1 and 2.5 microns. Each Line Shows the Mean and Standard Deviation of Six Experiments 22

Figure 237 Aerosol Volume Concentration over Time with Three Different Ventilation Rate at Seat 2 with Aerosol Particles in the Range between 1 and 2.5 microns. Each Line Shows the Mean and Standard Deviation of Six Experiments 23

Figure 238 Aerosol Volume Concentration over Time with Three Different Ventilation Rate at Seat 3 with Aerosol Particles in the Range between 1 and 2.5 microns. Each Line Shows the Mean and Standard Deviation of Six Experiments 24

Figure 239 Aerosol Volume Concentration over Time with Three Different Ventilation Rate at Seat 1 with Aerosol Particles in the Range between 2.5 and 5 microns. Each Line Shows the Mean and Standard Deviation of Six Experiments 25

Figure 240 Aerosol Volume Concentration over Time with Three Different Ventilation Rate at Seat 2 with Aerosol Particles in the Range between 2.5 and 5 microns. Each Line Shows the Mean and Standard Deviation of Six Experiments 26

จุฬาลงกรณ์มหาวิทยาลัย
Chulalongkorn University

Figure 241 Aerosol Volume Concentration over Time with Three Different Ventilation Rate at Seat 3 with Aerosol Particles in the Range between 2.5 and 5 microns. Each Line Shows the Mean and Standard Deviation of Six Experiments..... 27

จุฬาลงกรณ์มหาวิทยาลัย
CHULALONGKORN UNIVERSITY

CHAPTER 1
INTRODUCTION

1.1 Background and Significant of the Research Problem

1.1.1 Current Pandemic Situation

Nowadays there are respiratory infection outbreaks throughout the world and the most obvious example in these days is Coronavirus disease, also known as COVID-19. For the disease, severe acute respiratory syndrome coronavirus 2 (SARS-CoV-2) infection was first discovered in Wuhan, China in December 2019 but it was not possible (at least to the outside world) to determine how the infection began. The World Health Organization (WHO) considered this an uncommon occurrence that could pose public health hazards to neighbouring countries due to disease transmission across borders, necessitating a coordinated international response, and declared it as Public Health Emergency of International Concern (PHEIC) on 30 January 2020. Soon after COVID-19 had spread worldwide, WHO made an announcement on 11 March 2020 regarding the pandemic COVID-19. At the start of this pandemic, many countries began screening measures for people entering or leaving the country to control the spread. Some countries are able to control the epidemic and limit its area very well, but many countries have delayed and ignored the danger, causing many people to become infected and lose their lives. In the current situation, pharmaceutical companies have developed and produced vaccines, including COVID-19 Vaccine Janssen by Johnson & Johnson, COVID-19 Vaccine AstraZeneca by BARDA and OWS, Comirnaty by Pfizer and BioNTech, Sputnik V by Gamaleya Research Institute and Acellena Contract Drug Research and Development, CoronaVac by Sinovac and Moderna COVID-19 Vaccine by Moderna, BARDA, and NIAID.

จุฬาลงกรณ์มหาวิทยาลัย
Chulalongkorn University

1.1.2 Transmission Pathway

The transmission from infected person to other people of SARS-CoV-2 can be transmitted by both direct contact and indirect contact. This virus can be spread by coughing, talking, sneezing, or breathing of an infected person. The liquid particles, generated from these actions, can be large respiratory droplets or small aerosol particles. Direct contact transmission occurs by touching or interchanging body fluids such as respiratory droplets with an infected person. Indirect contact transmission occurs by touching a contaminated object such as doorknob, table, chair, etc. and touching mouth, nose, or eyes before washing or cleaning hands well. This type of indirect contact transmission is also known as fomite transmission. Another type of indirect contact transmission is airborne transmission. The airborne transmission is caused by the dispersion of aerosol particles, which contain viruses, that spread through the air over a wide area from an infected source. This type of transmission usually occurs in places where a number of people reside for a period of time in a place such as office, restaurant, nightclub, or even home or place with insufficient ventilation.

จุฬาลงกรณ์มหาวิทยาลัย
Chulalongkorn University

1.1.3 Infection Statistics and Prevention Measures

Globally, there are more than 120 million COVID-19 cases worldwide, of which 97 million have been healed, but more than 2.66 million have died (as of March 15, 2021). Histogram of daily infected cases and daily death cases around the world are shown in Figure 1 and Figure 2, respectively. While the spreading of COVID-19 for each country has different rates depending on the control policies of the country's administrators, the important thing is how people in the country protect themselves.

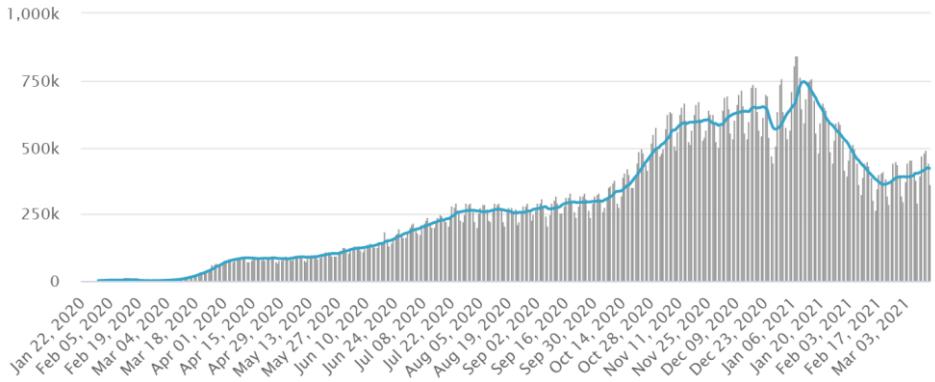

Figure 1 Number of COVID-19 Daily Reported Cases around the World with 7-Day Moving Average (as of March 15, 2021) (Worldometer, 2021a)

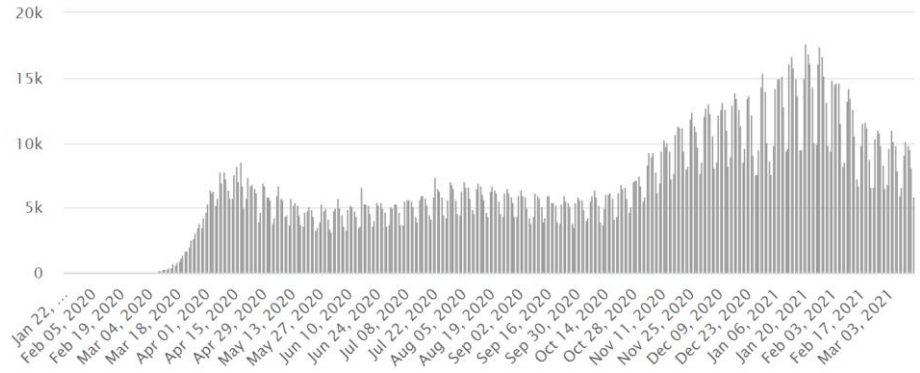

Figure 2 Number of COVID-19 Daily Death Cases around the World (as of March 15, 2021) (Worldometer, 2021a)

จุฬาลงกรณ์มหาวิทยาลัย
Chulalongkorn University

As an example, the United States has a very high number of daily infections. There are currently 30,081,831 cumulative cases with 22,169,240 cases of cured patients and a cumulative total of 547,235 deaths (as of March 15, 2021). This high infection rate could be caused by little mistakes like the contact greetings such as shaking hands. The early spread of COVID-19 in the United States was partly arised from the absence of using SARS-CoV-2 testing equipment and the initial test like fever and symptom observation is clearly insufficient. In addition, America is a very liberal country and Americans love to host festivals, such as Mardi Gras, or Fat Tuesday in New Orleans, Louisiana on February 25, 2020, and Spring Break in Miami, Florida on March 19, 2020. Both of these festivals took place despite that the White

House had already announced the ban on protests due to the COVID-19 outbreak. These two incidents greatly spread the virus, resulting in an increasing in the number of cases in Florida in early April as the first place and Louisiana as the second place in the United States. It can be said that these events marked the beginning of a major outbreak in the United States, as evidenced by Figure 3 and Figure 4, where the number of infections and deaths began to rise during that time. Another reason that cannot be overlooked is the misleading public broadcast from the political leader in indicating that SARS-CoV-2 was not a dangerous virus, much less severe than influenza and body could recover from this disease by itself.

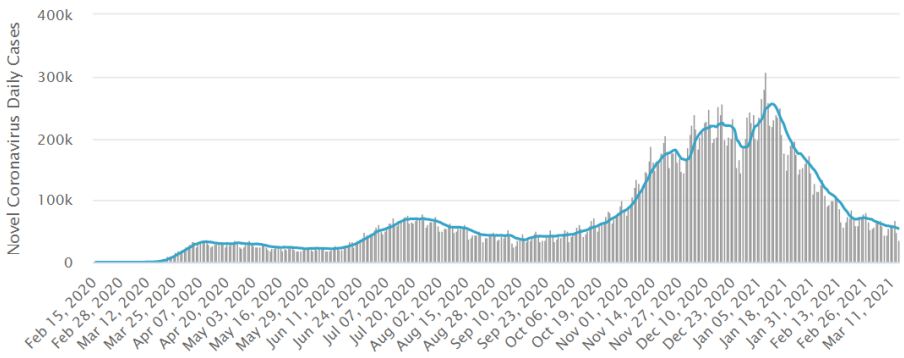

Figure 3 Number of COVID-19 Daily Reported Cases of United States with 7-Day Moving Average (as of March 15, 2021) (Worldometer, 2021b)

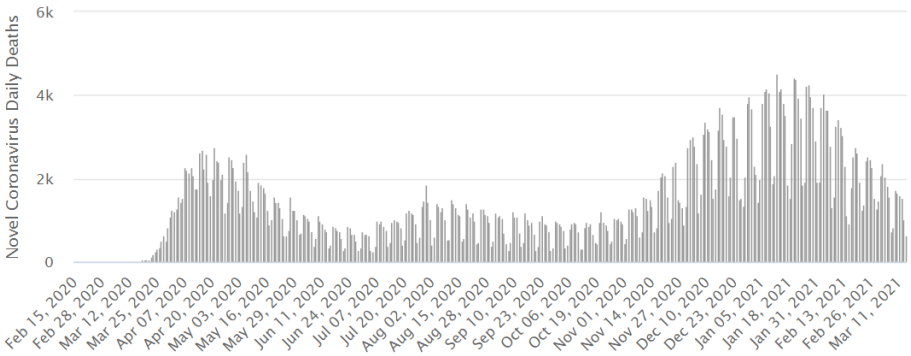

Figure 4 Number of COVID-19 Daily Death Cases of United States (as of March 15, 2021) (Worldometer, 2021b)

Another example, on the contrary, is the case of China; China was the first country to encounter with COVID-19 cases in Hubei Province, Wuhan. China handled with the situation by announcing the closure of Hubei, the epicentre of the pandemic, on January 23, 2020. After that, China implemented the measure to deal with COVID-19 patients by building an "emergency hospital" in a week and by sending health workers from all over the country to the pandemic centre. The next proactive measures were to cancel all major events such as sporting events, ordered ~~the~~ closure of theatres, cinemas, factories and stores, extended school holidays and asked people to wear face masks when going outside. China also took advantage of the payment application technology such as Alipay or WeChat, which can be used as a means to monitor people's movement. Consequently, China's cashless society has also helped reduce the epidemic. The good response of China is reflected in Figure 5 and Figure 6; after the outbreak occurred in the early stages of infection and the rapid increase in deaths, the outbreak was under control in a short period of time. China currently has 85,238 cases of total cured patients from 90,049 COVID-19 cases and 4,636 deaths (as of March 15, 2021).

จุฬาลงกรณ์มหาวิทยาลัย

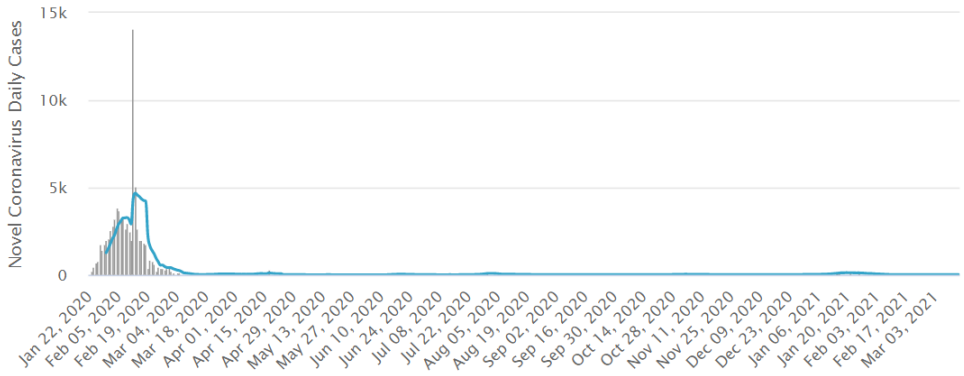

Figure 5 Number of COVID-19 Daily Reported Cases of China with 7-Day Moving Average (as of March 15, 2021) (Worldometer, 2021c)

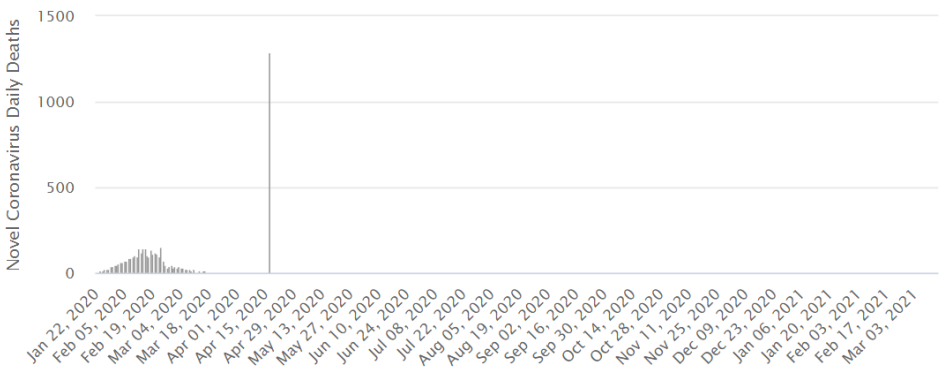

Figure 6 Number of COVID-19 Daily Death Cases of China (as of March 15, 2021) (Worldometer, 2021c)

Thailand is the second country to report COVID-19 cases after China because Thailand received more than a million Chinese tourists in January 2020. The first reported case was confirmed by the Ministry of Public Health on January 12, 2020, that the first COVID-19 patient in Thailand was a 61-year-old Chinese female tourist coming from Wuhan. On February 29, 2020, the Ministry of Health declared COVID-19 as a contagious disease according to Communicable Disease Act B.E. 2015 (A.D. 2015), resulting in the provincial governor having the power to issue orders so as to quarantine suspected infections or to close risky locations. Later on March 26, 2020, the Prime Minister announced the use of the emergency decree nationwide to bring power to the centre and set up a management centre for the situation of the pandemic of COVID-19, followed by an order to close the night clubs and shopping malls, prohibited activities in crowded places and closed the border. Through these measures, Thailand had been in control of the COVID-19 situation for a long period until the end of 2020, foreign workers, who have SARS-CoV-2, were smuggled into Thailand illegally, causing a new outbreak as shown in Figure 7 and Figure 8. The current number of patients diagnosed with SARS-CoV-2 is 27,005 cases with 26,154 recovered patients and 87 deaths (as of March 15, 2021).

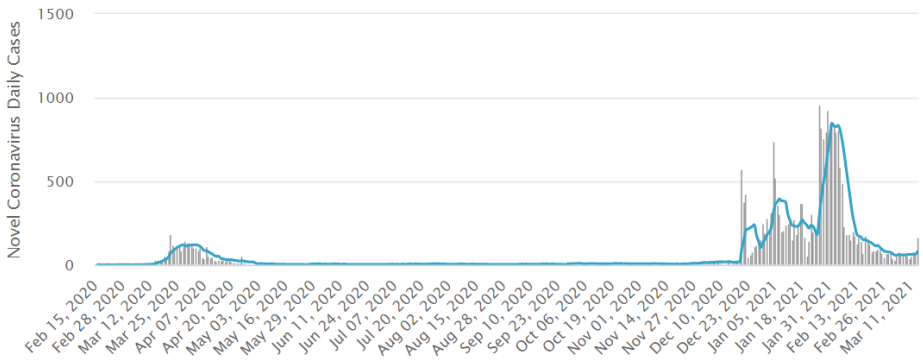

Figure 7 Number of COVID-19 Daily Reported Cases of Thailand with 7-Day Moving Average (as of March 15, 2021) (Worldometer, 2021d)

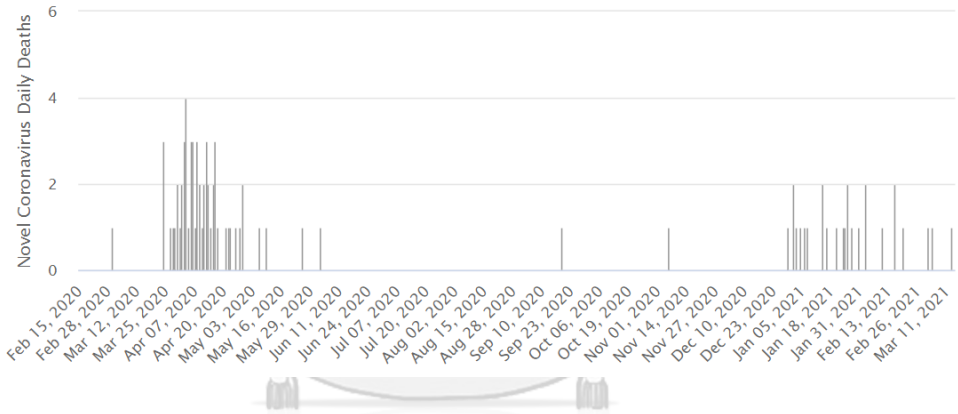

Figure 8 Number of COVID-19 Daily Death Cases of Thailand (as of February 21, 2021) (Worldometer, 2021d)

จุฬาลงกรณ์มหาวิทยาลัย
CHULALONGKORN UNIVERSITY

1.1.4 Dangers and Symptoms of COVID-19

SARS-CoV-2 usually enters the body through the respiratory system, including the lungs. In the early stages of being infected with SARS-CoV-2, the body cannot recognize that it has been exposed to the virus. Normally, our body's cells begin to release chemicals called interferons when the virus hijack a host cell, and this is a warning to the rest of the body and the immune system. However in this case, SARS-CoV-2 can inhibit this chemical and cause the body to not respond to the virus promptly. The symptoms of COVID-19 start as lung disease and may later affect the entire body. SARS-CoV-2 not only kills lung cells like conventional viruses, but it also

destroys them and induces syncytia formation, which is the agglutination of cells, causing them to become large and malfunctions. In addition, COVID-19 patients also suffer from blood clotting disorders. These effects are due to the viral S protein receptor-binding domain or spike binds to ACE2-receptor to enter the host cell by implantation into the host cell, which can be found throughout the body. Viruses can cause inflammation in some patients, causing the immune system to go into overreaction, which negatively affects the rest of the body. Patients with diabetes disease, chronic kidney disease, lung and respiratory disease, obesity, liver disease, immunodeficiency disease, heart disease, and patients using immunosuppressants are likely to have severe symptoms and die from COVID-19. In addition to patients with complication diseases mentioned above. Children under 12 months of age are also more likely to catch a serious illness from COVID-19. One thing to be aware of with COVID-19 is that a host of SARS-CoV-2 may not show signs of illness, but the virus can still be transmitted.

Symptoms of a SARS-CoV-2 infection vary greatly. Fever, weariness, and a dry cough were the most prevalent symptoms, followed by sore throat, diarrhea, aches and pains, conjunctivitis, headache, ageusia, hyposmia or anosmia, skin rash, and fingers or toes discoloration. In addition to the symptoms listed above, there are serious symptoms and patients with these symptoms require immediate medical attention: discomfort or pressure in the chest, breathing difficulty or shortness of breath, and speaking or motion impairments. For all of the symptoms of COVID-19 listed above, symptoms may not be present even after receiving the SARS-CoV-2, as the incubation period varies from person to person. On average, symptoms of COVID-19 develop five to six days after exposure to the virus, but in some cases it can last up to 14 days.

จุฬาลงกรณ์มหาวิทยาลัย
Chulalongkorn University

1.1.5 Pandemic Viruses

Apart from COVID-19, in the past our world has faced the same highly contagious disease as COVID-19 and killed many people including smallpox, Middle East Respiratory Syndrome (MERS), Severe Acute Respiratory Syndrome (SARS), Spanish flu, and other diseases.

Smallpox was first believed to occur around 12,000 years ago as a result of variola virus. This virus can be spread through droplets emitted by patients such as coughing, sneezing, and exposure to contaminated objects. It starts with high fever, body aches, and fatigue. After a few days, a red, smooth rash begins on the body and bulges later, and some deaths occur.

The Spanish flu first occurred in 1918 and it can be transmitted via airborne transmission, droplet transmission, and fomite transmission like COVID-19. Infected person has symptoms such as fever, cough, sneezing, nausea, aches and diarrhoea, similar to common flu symptoms. Importantly, the virus can evolve and mutate into a new and more deadly virus, causing patients to develop bleeding in parts, suffocation and rapid death; whether it's a kid, an old man or even a young man. More than 500 million people were infected worldwide and deaths estimated to range from 20 to 50 million.

จุฬาลงกรณ์มหาวิทยาลัย
Chulalongkorn University

Severe Acute Respiratory Syndrome (SARS) spread during the year 2002-2003. This disease was capable of spreading through small droplets emitted by patients. Infected people develop muscle cramps, fever and muscle soreness, as well as rapid respiratory ailments, which include coughing and shortness of breath, and possibly diarrhoea. The SARS is spread in 29 countries around the world and there were 8,439 recorded cases with 812 deaths.

In 2012, the Middle East Respiratory Syndrome (MERS) was discovered. The disease is easily transmitted to people who are close to the patient like other

respiratory ailments. Patients may have symptoms or may not have symptoms. The most common ailments are sickness, cough, and breathing difficulty. About 3 out of 10 to 4 out of 10 of the patients have reported deaths.

As you know, there are viruses that are easily spread and can spread all over the world. Some viruses are so dangerous and kills many people. In addition, it is not possible to know which virus would return to the epidemics or the pandemics and emerging diseases can occur at any time.

1.1.6 Virus-Size Distribution

Generally, viruses generally ranging in size from 0.005 to 0.3 micron, e.g., porcine circovirus is from 0.017 to 0.022 micron, poliovirus is approximately 0.030 micron, Epstein-Barr virus is from 0.12 to 0.15 micron, etc. but there are also viruses bigger than general such as Mimi virus and Pithovirus which are called giant viruses as shown in Figure 9.

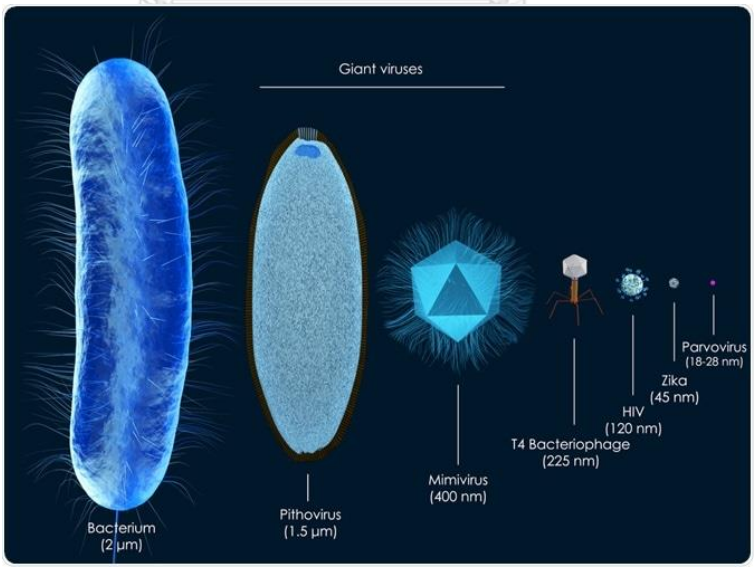

Figure 9 Size Comparison of Viruses (Verras, 2021)

These viruses are very small and can bind with particles of all sizes, whether they are small droplets or large particles like dust, which are released from infected sources. If particles are large, they can contain large amounts of viruses. In addition, particle of different size will have a different aerodynamic behaviour. In general, the criteria specified whether a particle is large or small is 5 microns, but some researchers have suggested that the particle size divider according to aerodynamic behaviour should be 100 microns. The large particles often fall to the ground by the gravitational force after coming out of the source within 2 meters, while smaller particles can remain airborne for a long period under most indoor condition after coming out of the source. Researchers also measured the size of infectious particles and have shown that pathogens are most commonly found in particles which are smaller than 5 microns. Difference in the size of viruses, respiratory droplets, and other particles is shown in Figure 10.

จุฬาลงกรณ์มหาวิทยาลัย
Chulalongkorn University

Figure 10 The Relative Size of Particles (Visual Capitalist, 2020)

1.1.7 Detection and Diagnosis of COVID-19

Today, around the world, including in Thailand, there are various screening methods for COVID screening, such as body temperature testing or symptom observation. These tests may be able to tell if the person is suffering from the illness, but it cannot be specific that the person has COVID-19. To obtain better result, it is necessary to directly detect the SARS-CoV-2. The methods used for the detection of COVID-19 can be divided into three main types: molecular test, rapid antigen test, and antibody test.

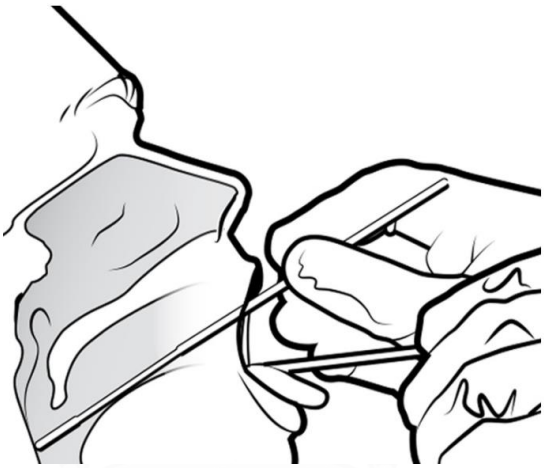

Figure 11 Throat Swab (Centers for Disease Control and Prevention, 2017)

Figure 12 Nasopharyngeal Swab (Centers for Disease Control and Prevention, 2017)

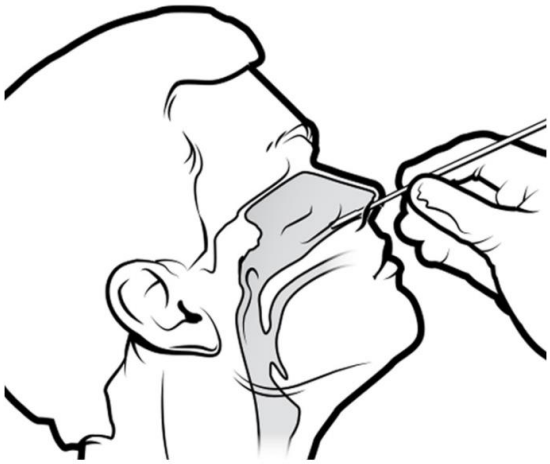

Figure 13 Nasal Swab (Centers for Disease Control and Prevention, 2017)

Molecular test, which is also referred to a viral test, nucleic acid amplification test (NAAT), diagnostic examination, LAMP test, and RT-PCR test, is the method employed to determine whether or not a patient has the virus in the body at that time; however, it is impossible to tell if the person had COVID-19 in the past. Molecular method is an effective and diagnostic technique that only requires a good knowledge of the genomic and proteomic composition of the SARS-CoV-2. This method relies on the identification of RNA viruses or virus fragment by using signal amplification techniques to assist in the detection because the nucleic acids which are discovered in clinical specimens frequently have low copy counts. The signal amplification techniques are divided into three groups according to their applications: amplifying target nucleic acids, amplifying probes that attach to the target nucleic acids, and amplifying signals produced by target nucleic acids. This method can be summarized in 4 steps as shown in Figure 14. Most of the specimens from the throat swab (Figure 11) can also be taken from nasopharyngeal swab (Figure 12), nasal swab (Figure 13) or saliva in some cases. Although this method is accurate and does not take a long time to process, the main disadvantage of this method is the need for a certified laboratory, specialists, expensive equipment and dedicated space.

จุฬาลงกรณ์มหาวิทยาลัย
CHULALONGKORN UNIVERSITY

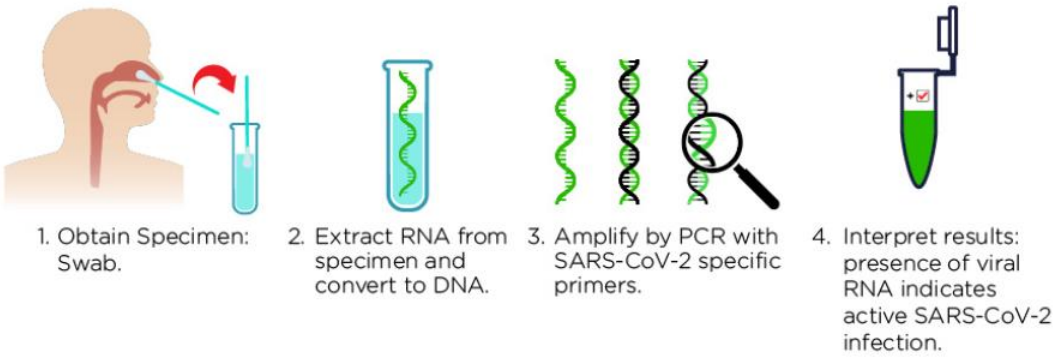

Figure 14 Molecular Test (American Society for Microbiology, 2020)

Rapid antigen test is to detect virus-specific proteins, which is also known as antigens as shown in Figure 15. This method is used to determine whether the tester is infected with SARS-CoV-2 at that time but cannot be used to determine if the tester had been infected with the virus as in the molecular test. This method is not generally as sensitive as the molecular test. Specimens from the tester can be obtained from a nasal or nasopharyngeal swab. The method takes only 15-30 minutes and it is very accurate if the result is positive. The test for negative coronavirus infection result is, however, often inaccurate compared to the molecular test. Therefore, even if the person was tested negative but with symptoms of COVID-19, another molecular test is needed.

จุฬาลงกรณ์มหาวิทยาลัย
Chulalongkorn University

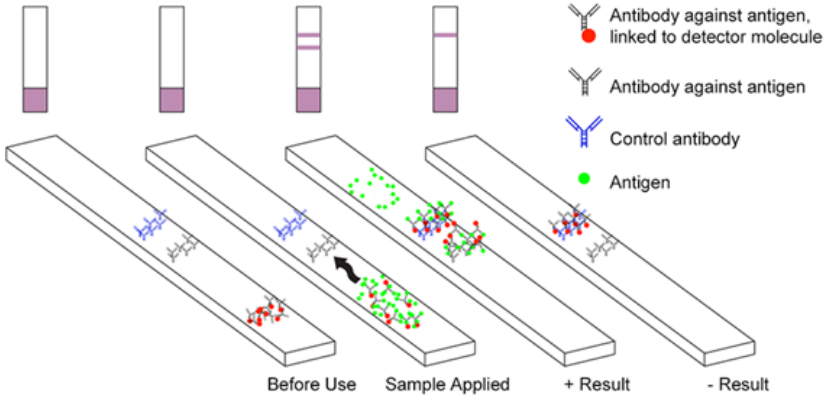

Figure 15 Rapid Antigen Test (American Society for Microbiology, 2020)

Antibody test, which is shown in Figure 17, is also known as serological test or serology test. This test examines antibodies caused by the body's response to SARS-CoV-2. Specimen samples can be taken from a finger prick or blood draw (Figure 16) and the result can be obtained within 1 day. This test can tell whether the person taking the test has been infected with SARS-CoV-2, but it cannot tell if the person is infected with the virus at that time or has already recovered from COVID-19.

Figure 16 Finger Prick (Left) (King, 2020) and Blood Draw (Right) (Neoteryx, 2020)

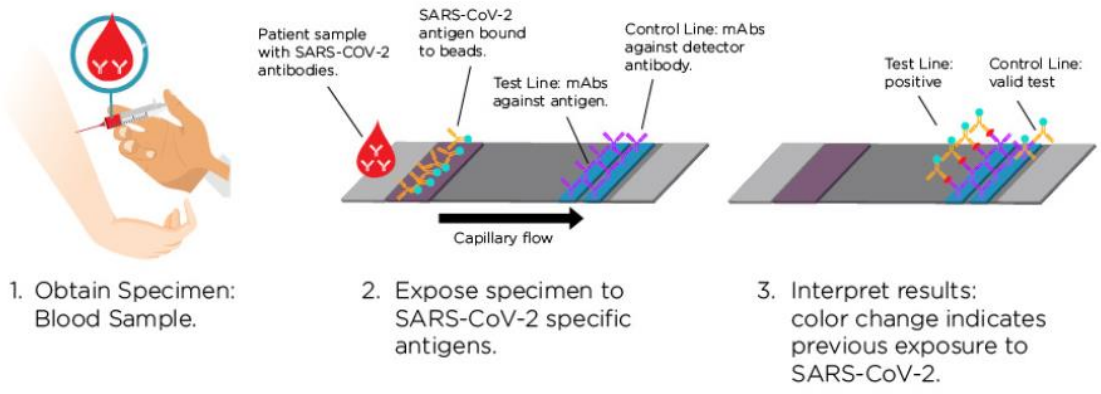

Figure 17 Antibody Test (American Society for Microbiology, 2020)

1.1.8 Particle Measurement Techniques

The measurement of particles of different sizes has different methods of measurement to suit the sample to be measured, such as wet, dry or it may be in solution form. In addition, particles have a different shape, possibly in width, length, thickness, or asymmetric shape. Therefore, the particle size used is its size relative to the spherical particles, which is called the equivalent spherical diameter. Equivalent spherical diameter can be categorized into 4 types: equivalent Stokes diameter, equivalent volume diameter, equivalent surface diameter, and equivalent projected area diameter. Equivalent surface diameter indicates the size of the particle, having a surface area equal to the surface area of a spherical particle. Equivalent volume diameter indicates the size of the particle, having a volume equal to the volume of the spherical particle. Equivalent projected area diameter indicates the size of the particle, whose cross-sectional area is equal to the area under the contour of the spherical particle when the particle is placed horizontally in the most stable state. Equivalent Stokes diameter indicates the size of the particle whose sedimentation rate in a liquid is equal to the sedimentation rate of the spherical particle.

Sieve Method

จุฬาลงกรณ์มหาวิทยาลัย

The first method, which is discussed here, is a long-standing and still useful method, known as the sieve method which is used to measure large particles. This can be done by sifting samples through a stack of wire mesh sieves with oscillations at the desired time and frequency, allowing irregularly shaped particles to orient themselves upon falling through the stack of wire mesh sieves, the particles size can be separated along the sieve on each layer. Nowadays, it is commonly used as a standard for production control in the food, pharmaceutical or chemical industries. The sieve method can be classified into three main types, separated by size range: air jet sieving (Figure 18), which has a range of sizes from 10 microns to 200 microns,

wet sieving with a measuring range of 20 microns to 20 millimetres, and dry sieving with a measuring range of 40 microns to 125 millimetres.

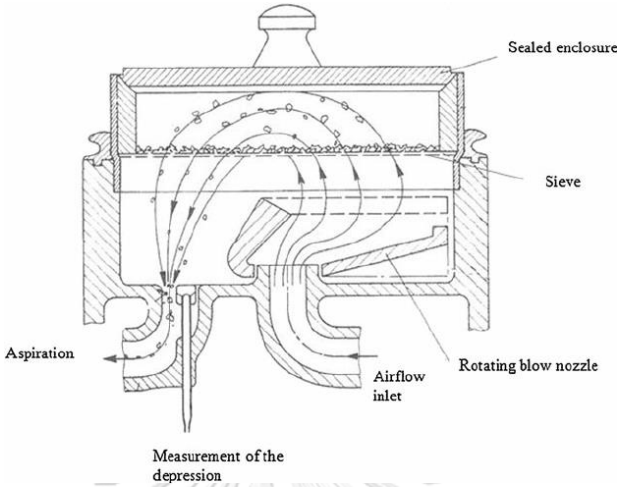

Figure 18 Air Jet Sieving (Le et al., 2012)

Particle Motion Inertia Method

The next method is based on the principle of particle motion inertia. The device is called the cascade impactor, where air enters the upper nozzle by the vacuum suction pump and has a diaphragm at the outlet called the impaction plate. Larger particles with high inertia impact to impaction plates because they cannot move around to the other side of the impaction plate. Smaller particles with low inertia follow the flow of fluid around the impaction plate. The function of the cascade impactor is to stack these kits into layers, as shown in Figure 19, to separate the particle size as many layers as required. The cascade impactor, which controls air flow, is a simple, easy-to-use device, but the disadvantage is that if it is used for a long time it will reduce the performance of the device due to the greater sedimentation at the impaction plates and need to be cleaned periodically.

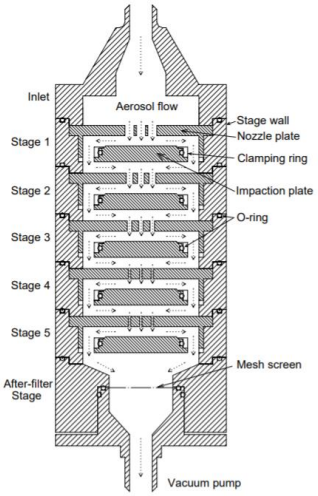

Figure 19 5-Stage Cascade Impactor (Kwon et al., 2003)

Gravitational Sedimentation Method

There is also a method called gravitational sedimentation method which is often used to measure particles with a diameter ranging from 0.1 to 300 microns. The principle of this method is to measure the velocity of particles from sedimentation within a liquid medium. The device that implements this principle is the Andreasen pipette, shown in Figure 20. This speed can be used to determine the particle diameter using Stokes's law:

จุฬาลงกรณ์มหาวิทยาลัย
CHULALONGKORN UNIVERSITY

$$V = \frac{d_{st}^2(\rho_s - \rho_0)g}{18\eta_0}$$

where V is a sedimentation speed

d_{st} is *an* equivalent Stokes diameter

ρ_s is *a* particle density

ρ_0 is *a* medium liquid density

η_0 is a viscosity of the medium liquid

g is a gravitational acceleration

The disadvantage of this method is that it is not possible to determine the size of the coagulating particles and the flow of the liquid medium has to be laminar which means that the sedimentation rate must not be too fast to disturb the flow or streamline of the liquid medium.

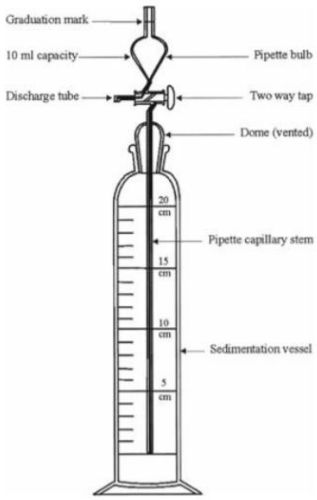

Figure 20 Gravity Sedimentation Instrument (Merkus, 2009)

Electrical Stream Sensing Zone Method

The next method is the electrical stream sensing zone method, whereby the device that uses this method is coulter counter, shown in Figure 21. This instrument is suitable for measuring particles with a diameter ranging from 1 to 500 microns. The detector identifies the particle size by volume and counts the number of particles. The principle of this counter is to use an insulating particle to form a suspension in a conductive solution such as sodium chloride, trisodium phosphate, and sodium acetate. After that, the particle is stimulated to travel through the orifice, called sensing zone, one by one along the path created by an electric current. In the normal state (without particle through sensing zone), the electrode at that point will have a constant electrical potential difference, and when particle passes, it is considered to increase the electrical resistance according to the particle's volume,

causing the changing in electrical potential difference. After that, the electrical potential difference signal is amplified by an amplifier, analysed and converted to equivalent volume diameter. This measurement can be done regardless of the refractive index of particles, shape, colour or density, by allowing particles to pass through sensing zone only one particle at a time. This creates a limitation on the concentration of the suspension to avoid repeating particle counts. This counter also needs to select the appropriate sensing zone size for the particle size.

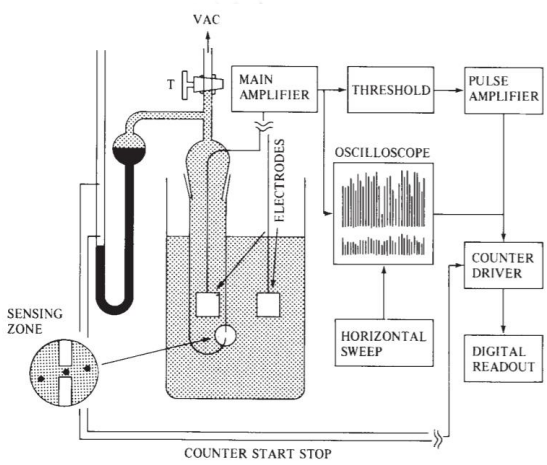

Figure 21 Coulter Counter (Doroszkowski, 1999)

จุฬาลงกรณ์มหาวิทยาลัย
CHULALONGKORN UNIVERSITY

Dynamic Light Scattering

Dynamic light scattering (DLS), shown in Figure 22, is the most common measurement technique. Dynamic light scattering is suitable for detecting the size of particles in the range of 5 nanometre to 5 microns, because particles smaller than 5 microns transverse randomly in all directions (Brownian motion) and collide with the medium molecule evenly over time. Collisions between molecules cause energy to transfer that have a big effect on smaller particles. Smaller particles thus obtain a greater movement speed than that of larger particles. Larger particles are slow-moving, causing scattering light with low frequency, while smaller, fast-moving

particles are associated with higher frequency scattering light. We can find the size of the particles with the Stokes-Einstein equation:

$$D_t = \frac{k_B T}{6\pi\eta R_H}$$

where D_t is a translational diffusion coefficient

k_B is *a* Boltzmann constant

R_H is a hydrodynamic radius

η is *a* solvent dynamic viscosity

T is *a* solvent temperature

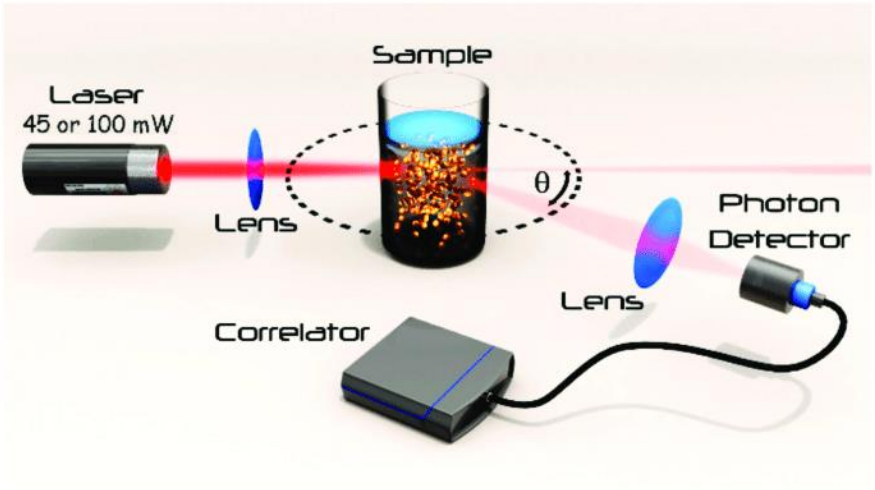

Figure 22 Dynamic Light Scattering (Aleandri et al., 2018)

Static Light Scattering

Static light scattering, shown in Figure 23, which is also known as laser diffraction is a technique that is often used in measuring instruments today due to its short analysis time, high accuracy, precise repeatability, and can be used with a variety of samples: liquid, aerosol or dry powder. The principle of the diffraction technique is that when light travels through particles suspended in a fluid medium, it

causes the angular fluctuation in light intensity caused by a laser beam passes through a dispersed particle sample. Light diffracted by particles has a specific pattern of intensity. Bigger particles scatter light at smaller angles, whereas smaller particles scatter light at larger angles compared to laser beams. Fraunhofer diffraction and MIE Scattering are the two basic theories used to calculate the type of light intensity distribution patterns created by particles of varying sizes. The measurement range of Laser diffraction ranges from 0.02 micron to 2 mm.

Fraunhofer diffraction is a theory which assumes that the particles interacting with the laser beam are considered to be spherical and the particles are not transparent (the laser light cannot enter into the particles). The refractive index, adsorption and light reflection of the particles and the dispersant are not considered. In this theory, calculations were simplified and were initially used to create laser particle size analysers. Fraunhofer diffraction is suitable for analysing particle sizes larger than 25 microns or at least 10 times of the wavelength of the beam. The error occurs when the particles are less than 25 microns; the smaller the particles, the greater the error.

MIE Scattering was born from Maxwell's electromagnetic theory which explain the analysis of the mechanism of light scattering from a smooth sphere. MIE Scattering takes into account all types of optical properties: absorptivity and reflectivity of particles, refractive index, and the refractive index of a dispersant. Therefore, it can provide accurate analysis for samples with different optical properties and more accurate results for smaller particle sizes compared to Fraunhofer diffraction. MIE Scattering is applicable to particle sizes ranging from microns to millimetres. The past limitation of this theory is that computation is very complex, but nowadays it is possible to use advanced techniques in computation, so today's laser diffraction particle size analyser uses this theory as a basis for building tools.

จุฬาลงกรณ์มหาวิทยาลัย
CHULALONGKORN UNIVERSITY

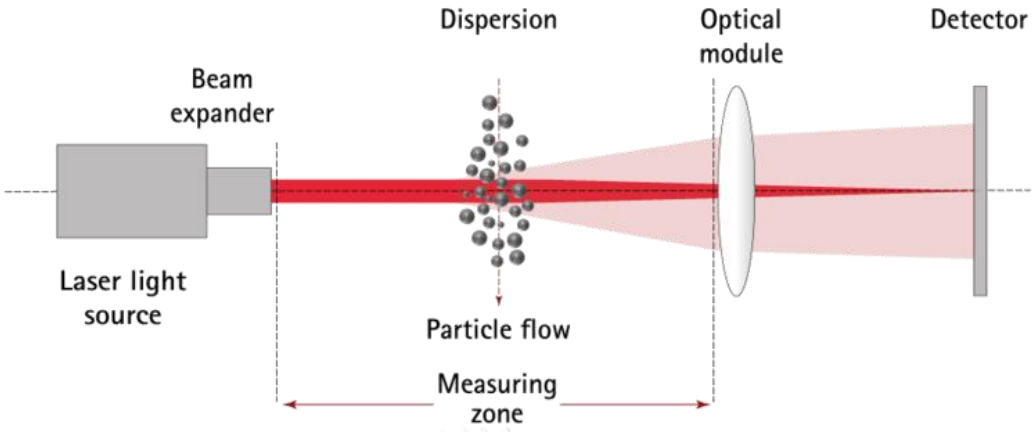

Figure 23 Laser Diffraction (Sympatec GmbH, 2017)

1.1.9 Ventilation Types

Mixing ventilation can be found everywhere in buildings. This ventilation type is to fill fresh air into system or building at the ceiling or ceiling position. After that, the air coming out of the inlet at high velocity would have a strong buoyancy force to cling to the ceiling for more air distribution. As a result, the air added into the building or system mixes with the pre-existing air and drops to an occupied zone with the velocity of approximately 0.25 to 0.40 m/s. In a mixing ventilated room , humidity, air velocity, and temperature will be dispersed uniformly, and the air quality should be the same across the room. The main disadvantage of this type of ventilation is that the cleanest air is located around the inlet, which means that the air in the occupied zone may be the least clean. If the system contains high levels of contaminants such as dust, smell or aerosol particles, this type of ventilation will allow these contaminants to spread easily throughout the system.

Displacement ventilation differs from mixing ventilation in that fresh air that fills into the system fills from the bottom or in the occupied zone. The fresh air that fills this system has a lower velocity than in the mixing ventilation to prevent people inside the building from being exposed to high-speed wind. After filling the occupied

zone with fresh air, hot air accumulates in the occupied zone so that the airborne contaminants lighter than air will rise to the top. For displacement ventilation, upper-level opening near the ceiling or on the top of the system is required to allow the contaminated rising air to escape to the outside of the system.

Natural ventilation, unlike mechanical ventilation, occurs as a result of the pressure difference caused by wind or buoyancy effect, resulting in air movement throughout the building or system. The wind or buoyant effect is caused by temperature and humidity differences. The amount of ventilation rate in the building or system depends on the size and the position of various openings within the system. The purpose of such ventilation is to fill the system with fresh air and remove contaminated air that is contaminated with odours, dust or aerosol particles out of the building or system.

Natural ventilation can be divided into three main types; cross ventilation, single-sided ventilation, and stack ventilation. Cross ventilation, a wind-driven ventilation, occurs when both sides of the building or system with openings (windows, doors, etc.) have different pressure. Single-sided ventilation occurs when there is a temperature difference across openings, which serves as both an air inlet and outlet, and the wind forces. Stack ventilation, which is buoyancy-driven ventilation, occurs when the air in the lower zone or occupied zone gets warmer and becomes less dense so it becomes more buoyant and rises up to the top of the system or building. This results in positive pressure zone at the top of the system and negative pressure zone at the bottom so the fresh air can flow into the system through openings at lower zone and exhaust out of the system at upper zone.

จุฬาลงกรณ์มหาวิทยาลัย
CHULALONGKORN UNIVERSITY

1.1.10 Cleanrooms Design (Variddhi Ungbhakorn, 2012)

Before designing and choosing the level of cleanroom, two important things need to be thought of are what level of cleanliness to use in our cleanroom design and how can we design it to achieve that level of cleanliness?

The particles emitted by the people in the room as well as the particles produced by activities within the room which are carried in the airflow stream in the controlled space combined must not be more than the "level of cleanliness" that is set for the cleanroom design. Therefore, adequate air circulation within this control volume or cleanroom is needed. As an example from the Clean Room Design Manual (Variddhi Ungbhakorn, 2012) for an ISO 6 (Class 1000) controlled volume, the generation rate of 0.5-micron particle is 70,600 particles per cubic meter per minute in order to have number of particles not more than 35,300 particles per cubic meter in the room. The ventilation rate of the room can be found from the relationship as follows.

$$ACH = \frac{60x}{y}$$

where ACH is room air change per hour

x is a maximum particle generation rate (number of particle/m^3/minute)

y is number of particle/m^3 (According to the desired level of cleanroom standards)

From the example above we will get

$$ACH = \frac{60(70600)}{35300} = 120$$

จุฬาลงกรณ์มหาวิทยาลัย
Chulalongkorn University

Clean rooms can be categorized based on their air flow characteristics through the inlet and outlet locations into three categories:

1. Conventional Cleanroom or Turbulent Mixed Flow Cleanroom

The turbulent-flow cleanroom type, shown in Figure 24, is the least clean cleanroom type of the three. Air is supplied with a chaotic flow through the diffuser at the ceiling position and outlets are installed at low area around the walls (the outlets should not be installed in the ceiling position because this will cause air short circuit). The design of this type of clean room is similar to the typical air-conditioned room but equipped with a HEPA filter at the inlet, a much higher air flow rate than a typical air-conditioned room (10-100 ACH). This turbulence in the cleanroom helps removing contaminants. In addition to the ventilation rate, the pressure difference must also be taken into account to ensure that contaminated air cannot be pushed back into the cleanroom. In general, the pressure difference between a clean room and an adjacent non-clean room should be 15 Pa, and the pressure difference between the two cleanrooms is 10 Pa. In the event that this pressure difference is not achieved, the pressure difference should be at least *5* Pa.

The disadvantage of this type of clean room is that due to the uneven air flow, it cannot remove very small particles from the room very well. Most contaminants can linger on floors and have a chance to go back into the air flow. In addition, each location of the room has an uneven level of cleanliness.

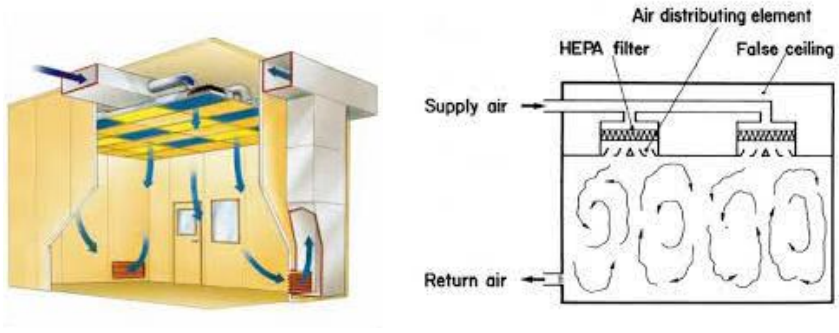

Figure 24 Turbulent Mixed Flow Cleanroom (Baixardoc, n.d.)

2. Horizontal Laminar Flow (Crossflow) Cleanroom

The construction principle of this type of cleanroom is that one wall is created as a wall for air filtering (wall composed of HEPA filter lined up), also known as filter wall to allow air to move into the room, and the opposite wall is made of perforated panels with pre-filter installed (efficiency *90-95%)* as a channel for reintroducing fresh air into the room again, shown in Figure 25. The principle of choosing whether to use a filter wall for short side or long side of the wall depends on the application. If the narrow side is the filter wall, the air entering the room will take longer distance and time to move to the perforated panels. On the other hand, if the longer side is selected for the filter wall, the air entering the room will not take as long of a distance or time to reach perforated panels on the opposite wall. The air entering the system is cleaned after passing through the filter wall and the cleanliness is gradually reduced as the air entering the room starts to become contaminated by various particles that occur as a result of various activities in the room and will be most contaminated at the pre-filter position at perforated panels.

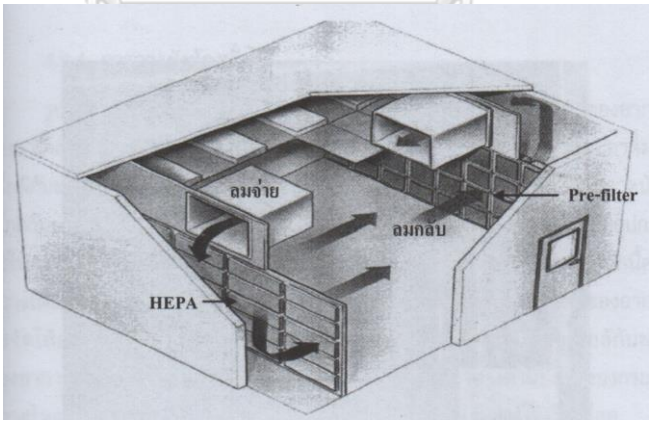

Figure 25 Horizontal Laminar Flow (crossflow) Cleanroom (Variddhi Ungbhakorn, 2012)

For the layout of Horizontal Laminar Flow Cleanroom, in addition to positioning the filter wall and perforated panels opposite each other, special room

layouts can be arranged according to different application requirements, including U-shape, W-shape, C- shape, L-shape, twin laminar flow, and double cross flow.

3. Vertical Laminar Flow Cleanroom

This type of clean room is similar to a horizontal laminar flow type clean room, but instead of air flowing into the wall location where the HEPA filter panel is installed; for in this type of cleanroom, air flows into the room through the ceiling where the HEPA or ULPA filters panel is installed. The floor is formed into a raised floor and covered with perforated rectangular sheets, called perforated floor panels (returning air grating), allowing the air to flow vertically, shown in Figure 26. The advantages of this kind of clean room are that the dirt that is generated at each area in the room will not spread to other areas and due to the short distance between the ceiling and perforated floor panels, the air for this cleanroom is low in contamination. The main disadvantage of this type of cleanroom is the high construction costs.

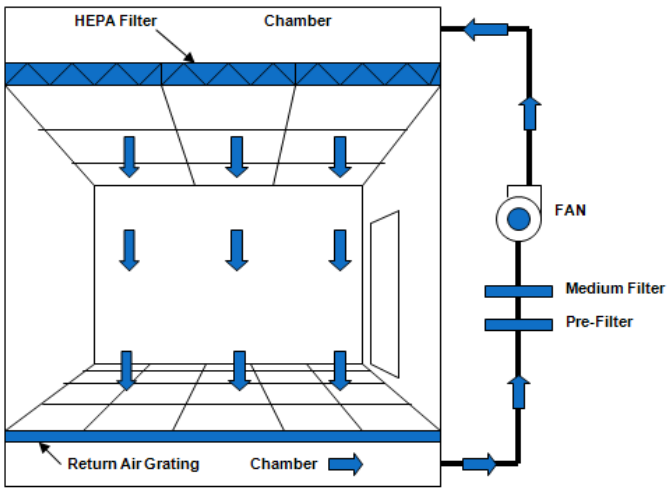

Figure 26 Vertical Laminar Flow Cleanroom (National Direct Network, 2020)

1.1.11 New Ambulances for Respiratory Disease

Today's ambulances do not have ventilation systems installed in the ambulances in the first place, at least a sufficiently well-performed system capable of handling a pandemic situation, which makes it possible for medical personnel to become infected from transporting patients, who can later transmit disease through the air. Many countries have begun to develop the ambulance to transport COVID-19 patients by developing a negative pressure ambulance to help preventing pathogens from the patient to leave the ambulance to the outside environment without filtering. It is equipped with an oxygen concentration monitoring system and an automatic ventilation system (can be manually controlled) inside the patient compartment to prevent the oxygen concentration being too low while transporting patients. If the concentration is lower than that set, the ventilation system will automatically work to maintain the oxygen concentration within the patient compartment. It also includes an isolation tent, shown in Figure 27, for infected patient that is at risk of infecting medical personnel or doctors inside the ambulance. The increased equipment inside the patient compartment made the new ambulances larger than the existing ones and to increase first aid space. Example of countries where the new ambulance has begun to be built and sold are South Korea, China, etc.

จุฬาลงกรณ์มหาวิทยาลัย
Chulalongkorn University

Figure 27 Examples of an Isolation Tent for the Patient (Jeju Tourism Organization, 2020)

An example of an ambulance equipped with a negative pressure system in South Korea is the AUTECH special ambulance Solati (H-350), shown in Figure 28, which is specially designed to transport patients safely and quickly.

There are a wide variety of medical equipment inside the vehicle, including a separate tent for the patient to prevent disease transmission to ambulance personnel and for speedy transportation. The ventilation system can be adjusted up to 7 levels and can be adjusted until inside of the patient compartment reach -200 Pa if needed, and its tight seal makes the patient compartment separate from the driver and the external environment. In addition, HEPA H14 grade filter are installed at the outlet of the ventilation system and there is also a negative pressure air conditioner air conditioning system.

CHULALONGKORN UNIVERSITY

Figure 28 AUTECH Solati (H-350) (Autech, 2020)

For China, a number of ambulances were promptly created to control the distribution of SARS-CoV-2 as quickly as possible with the cooperation of SAIC Motor Co., Ltd. to build a negative pressure ambulance as shown in Figure 29. In addition to the SAIC Motor Co., Ltd., there is also negative pressure ambulances that can be adjusted to -30Pa of the Qingdao Ruvii Vehicle Co., Ltd, shown in Figure 30, which has received the CE, ISO 9001 standards. It is capable of transferring up to 35 ACH of ambulance patient compartment, and the company claims to have a filtration

efficiency of up to 99.95% to filter infectious diseases, biological viruses and also chemical agents.

Figure 29 SAIC Motor Co., Ltd. Ambulances Construction (Xinhuanet, 2020)

Figure 30 Negative Pressure Ambulance of Qingdao Ruvii Vehicle Co.,Ltd (Ruvii Vehicle, 2020)

1.2 Objective of the Research

1.2.1 To assess the effectiveness of an ambulance air exhaust system in reducing the volume density of airborne particles

1.3 Scopes of the Research

1.3.1 The assessment is to be done experimentally inside a particular ambulance, currently deployed in the King Chulalongkorn Memorial Hospital. The result cannot directly be generalized to an ambulance deployed elsewhere.

1.3.2 The experiments take place while the vehicle is parked. Due to the limitation in terms of vehicle availability and traffic condition, it is difficult to achieve control environments, during the experiment duration, of moving ambulance.

1.3.3 Particles to be measured are not virus themselves but their corresponding carriers which in this case are wet airborne particle or the so-called wet aerosol. This aerosol is detectable by our particle counter. In place of real respiratory droplet carrier, 0.9% sodium chloride solution diffused in aerosol form is utilized instead as a carrier to avoid potential health problems to the experimenter. The aerosol particles, whose sizes range from 0.5 to about 5 micron, while representing a limiting number of respiratory pathogens; in the exclusion of Fungi, Spores, and large Bacteria; cover large viruses of interest.

1.3.4 The size ranges of aerosol particles measurement are considered in three ranges: 0.5 to 1 micron, 1 to 2.5 micron and 2.5 to 5 micron.

จุฬาลงกรณ์มหาวิทยาลัย
Chulalongkorn University

1.3.5 Aerosol concentration is measured for 200 positions (grid base volume discretization). The air exhaust system is adjusted for maximum of 3 settings; turned off (very low ACH or minimal ventilation (MV)); medium (roughly 40 ACH); high (roughly 80 ACH or high ventilation (HV)).

1.3.6 Due to the additional thesis challenges lie in acquiring the three-dimensional field experimentally, making measurement without interfering with the flows inside the cabin is not feasible for the current setup with the affordable measurement units.

1.4 Expectation Benefits

This research will at the very least provide a database for a future development of high safety ambulances.

จุฬาลงกรณ์มหาวิทยาลัย
Chulalongkorn University

CHAPTER 2
LITERATURE REVIEW

2.1 Related Research

2.1.1 Number and Size of Particles Emitted by People

In the past, many diseases have been studied. Methods of transmission of pathogens can be broadly divided into indirect contact, direct contact, airborne transmission, droplet transmission and common vehicle transmission. The most common causes of contagious transmission are airborne transmission and droplet transmission which can remain in air for a while (Centers for Disease Control and Prevention, 2020). One of most obvious examples today is COVID-19, with the primary cause of transmission of these infections due to droplets and droplet nuclei, which carry microorganisms, released by humans.

Gralton et al. (2011) has reviewed 26 studies and found that healthy people can generate particles with sizes ranging from 0.01 to 500 microns from breathing, coughing, sneezing, and talking. In the event that patients are infected, they can generate particles from 0.05 to 500 microns. As mentioned before, it can be seen that the particle size generated by human behaviour is in a very wide range, so further studies have to be done on how the behaviour of particles in different size ranges and how they affect humans. The respiratory viral RNA carrier was studied in various particle sizes released by both young and old patients by Gralton et al. While breathing, 58% of those who took the test generated particles, which are larger than 5 microns, containing respiratory viruses and 80% of participants generated particles, which are less than or equal to 5 microns, containing respiratory viruses. While coughing, 57% of participants in the experiment generated particles of a large size carrying respiratory viruses and 82% of test participants released small particles with

จุฬาลงกรณ์มหาวิทยาลัย
Chulalongkorn University

respiratory viral RNA. Research of Gralton et al. (2013) improves the understanding between particle size and respiratory viral carriers. Research of Fernstrom and Goldblatt (2013) stated the number of airborne microorganisms or droplets released from human activities, for example, one sneezing can generate approximately 40,000 particles, bowel evacuation can emit approximately 20,000 particle counts per event, one vomiting can release about 1,000 particles, a single cough can generate as many as 710 particles and talking can release approximately 36 particles per 100 words. Although the amount of particles emitted is large in some human behaviour, Gupta et al. (2010) found that cumulative number of particles particle generate by coughing and sneezing, which is an event that does not happen very often, is significantly less than breathing and talking for the same period of time.

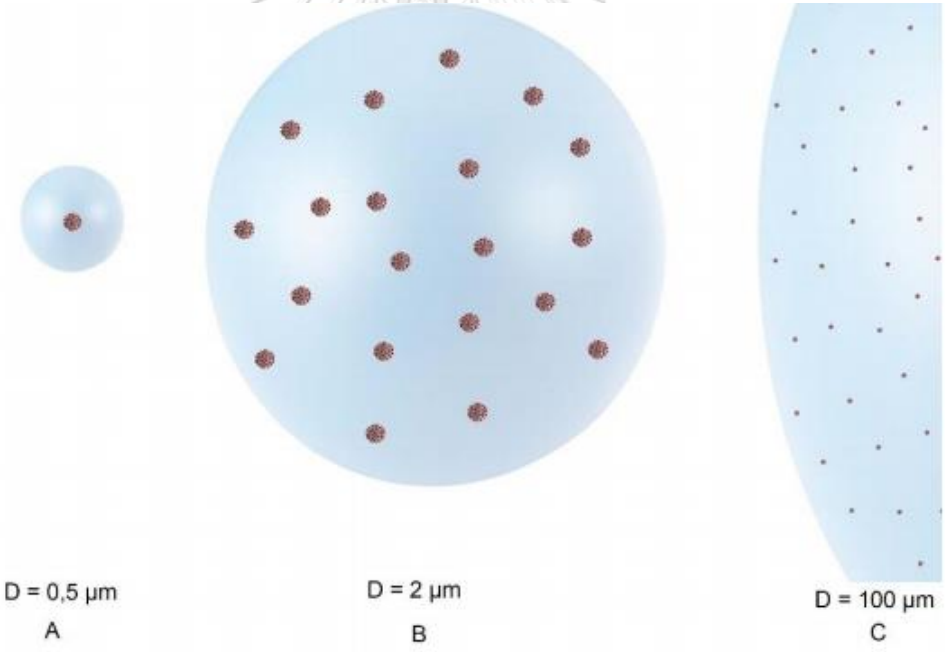

Figure 31 The proportions of Coronaviruses in different sizes of aerosol particle (Herrmann et al., 2020)

2.1.2 How Far Can Particles Spread and How Long Can They Remain?

In addition to studying the number of pathogens which are in different particle sizes. There are also studies about how far and how long particles of various sizes can spread from an infectious source and how long they can remain airborne. Liu, Li, et al. (2017) studied an expiratory droplet transmission range between two persons by using two thermal manikins as the representative of two people. The studies found that the aerosols and droplets exhaled by the source manikin which is about 1.5 m far from another manikin can be direct deposited on body surface and transmitted by both small and large particle which are called short-range airborne transmission and droplet transmission, respectively.

Liu, Wei, et al. (2017) also studied on how particle size affects the distance that particles can travel and found that the larger the particles size, the shorter the distance dispersed from the source. From this study, Liu, Wei, et al. suggested that the threshold of droplet size should be 10 microns. The droplet nuclei smaller than 10 microns may stay in the air for an extended period of time and all size of droplet can be droplet transmission.

Furthermore, Kutter et al. (2018) studied about human-to-human respiratory virus transmission routes which are adenovirus, parainfluenza (PIV), measles virus (MV) , respiratory syncytial virus (RSV), human metapneumovirus (HMPV), influenza A virus, rhinovirus, and coronavirus. Kutter et al. found that most of the respiratory viruses can be transmitted by droplet transmission and airborne transmission. This study also stated that droplet is a particle with diameter larger than 5 microns and can only be dispersed for only a short range of less than one metre, and aerosol and droplet nuclei are particle with diameter smaller than 5 micron and can be dispersed over long distance more than 1 m.

Knight (1980) studied the role of particle size in transmission and found that particle in the range of 1 to 3 microns can remain airborne for an infinite of time, particle with diameter about 10 microns could remain in air less than 17 minutes, 20-micron diameter particle would fall to ground in 4 minutes, and particle with 100-micron diameter can remain only shortly in air less than 10 seconds.

According to studies by Liu, Wei, et al., Kutter et al., and Knight, the size range of aerosol particles and droplet particles are different as shown in Figure 32, but all these three studies indicate that aerosol particles can linger in the atmosphere for a very long period and can spread for a long distance, while larger particles, or droplets, can only spread near the source and linger in the air for only a small span of time.

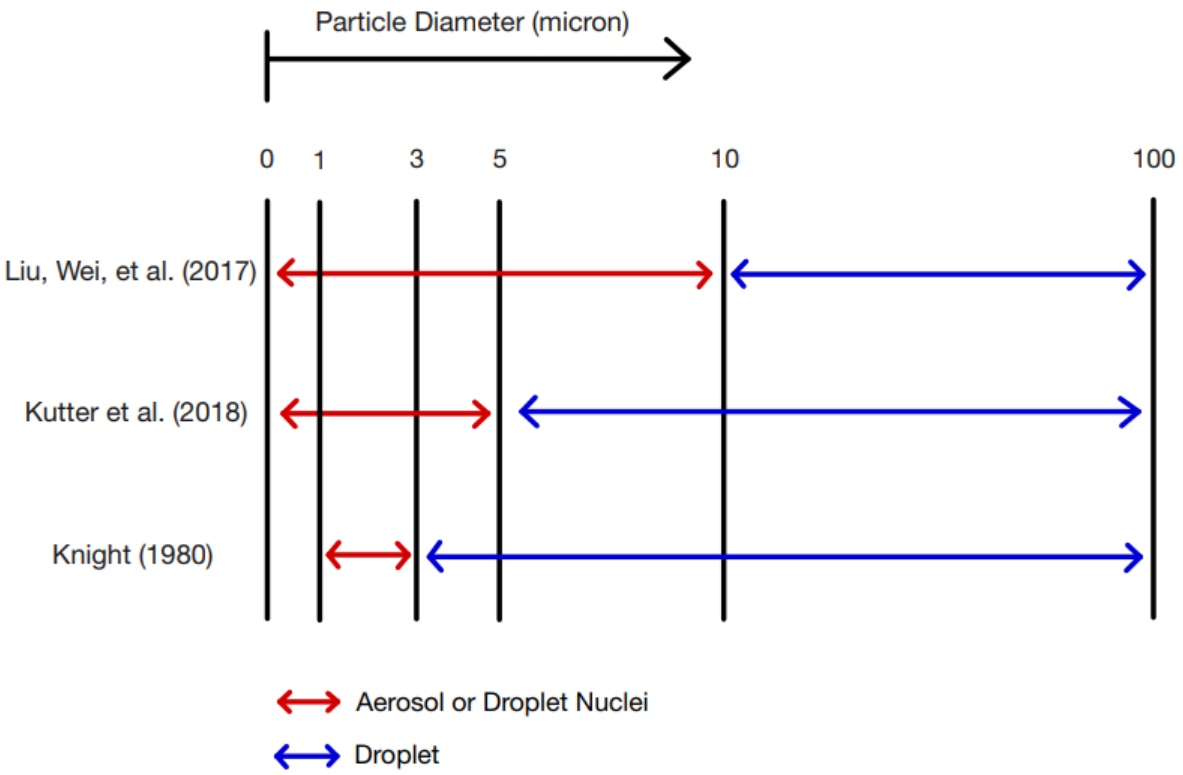

Figure 32 Comparison of Size of Aerosol or Droplet Nuclei and Droplet from Different Studies

2.1.3 The Size of the Particle and the Severity of the Infection

In addition to particle size differences affecting aerodynamic behaviour, differences in particle size also affect the respiratory system in different parts of the body. Thomas (2013) studied about how particle size affects pathogenicity and respiratory tract. Small aerosol particles are easily inbreathed and affect the lower respiratory system whether it be larynx below the vocal folds, trachea, bronchus, or lungs, whereas large droplets can be deposited in the upper respiratory system such as the larynx above the vocal folds, pharynx, nasal cavity, and nose. Research of Kutter et al. (2018) also showed the similar data to Thomas's research which are particles with a diameter less than 5 microns affect the lower airway respiratory system and particles larger than 5 microns deposit on upper respiratory tract and mucous membrane. Besides that, research studies by Alford et al. (1966) and Wonderlich et al. (2017) can concluded that aerosol particles are more likely to exacerbate infection or disease symptoms than droplet particles.

2.1.4 Standards for Aerosol Particles and Droplets

The previous studies above have found that particles of different sizes behave differently; there are few studies that specify the break point between aerosol particles and droplet particles; there are also various standards for the world to use as a threshold of particle size regulations. Centers for Disease Control and Prevention (CDC) (Siegel et al., 2007) and World Health Organization (WHO) (World Health Organization, 2014) consider the threshold of droplet size at 5 microns. Particles with aerodynamic diameter more than 5 microns are considered as droplets which cause droplet transmission and particles with aerodynamic diameter of 5 microns or less are considered as droplet nuclei or aerosol particles which cause airborne transmission. Most of droplets fall out of the air very quickly within 6 feet from the infectious source in a period of seconds to minutes, whereas aerosol particles can

linger in the atmosphere for many minutes to hours and are able to travel farther from the infectious source than droplets.

2.1.5 Protection Equipment and Protection Method

As aforementioned, infectious particles, whether they are droplets or droplet nuclei emitted by patients, are extremely dangerous to those around them. At present, many protective equipment has been studied, such as research of Belkin (1997) which is about filtering efficiency and effectiveness of surgical mask in preventing particles from exhalation, research of Willeke et al. (1996) which is about penetrating ability of airborne microorganisms through surgical mask, and research of Lindsley et al. (2014) which is about efficacy of the face shield in protecting face from aerosol droplets emitted by cough simulator.

Not only protective equipment which has been studied but many protection methods also have been studied too. Escombe et al. (2007) studied natural ventilation in building for the avoidance of airborne transmission in 368 tests by monitoring ventilation rate with a carbon dioxide tracer gas approach. This study found that open up doors and windows have median air change rate of 28 air changes per hour (ACH) which is higher than nowadays rooms that are mechanically ventilated which are normally operated at 12 ACH. However, the disadvantage which cannot be overlook of natural ventilation is that the air ventilated into or out of the patient's room is not filtered to prevent harmful effects from outside to inside and from inside to outside. Jurelionis et al. (2015) studied about the effects of air distribution systems on aerosol particle behavior and found that at low air change rates, particles were routed more efficiently to the diffusers by one-way mixing ventilation, whereas ventilation with four-way mixing allowed leftover particles to suspend in the air. At high air change rates, aerosol particles could not be moved to the other side of the room due to the combination of mixing ventilation and a one-

จุฬาลงกรณ์มหาวิทยาลัย
CHULALONGKORN UNIVERSITY

way air supply. Because of the comparatively high age of the air, displacement air distribution was poor at removing particles from the room when compared to mixing ventilation.

Yang et al. (2015) studied the importance of unidirectional ventilation system by using computational fluid dynamics (CFD) program for the airflow field and particle concentration distribution from the human breathe and body simulation for three situations which were standing, sitting, and lying. The results showed that at least 0.25 m/s of supply air velocity is necessary for standing and sitting positions, and 0.2 m/s for lying positions.

Bhagat et al. (2020) studied about the impacts of ventilation on the indoor dissemination of COVID-19 in three types of ventilation: wind-driven ventilation, displacement ventilation (mechanical and natural), and mixing ventilation. This study was divided into four scenarios. First scenario was a person in the mixing ventilation system. This scenario showed that hot air from human body and body plume rose to the top of the system and all air in the system remained uniform except at inlet and outlet. Second scenario was a person without surgical mask in the displacement ventilation system. This scenario showed that hot air and body's thermal plume rose to the top layer of the system and expiratory plume stratified below the hot upper layer. After that, the expiratory plume got entrained into the hot air and body plume and exhausted out of the system. Third scenario was a person with surgical mask in the displacement ventilation system. This scenario showed that hot air and body plume rose to the top layer of the system and expiratory plume got entrained into the body's thermal plume near its origin and exhausted out of the system at the ceiling. The last scenario was a person without surgical mask in the natural ventilation system (open doors and windows with upper-level opening), disregarding the wind's effect. The result was the same as displacement ventilation when the surgical mask is not on. Bhagat R. et al. also studied on people movement and

จุฬาลงกรณ์มหาวิทยาลัย
Chulalongkorn University

plumes generated by exhalation. Bhagat R. et al. also studied about body's thermal plume and the interaction with expiratory plumes in six scenarios which were sitting quietly breathing through their nose (with and without surgical mask), sitting and saying the word "also" with conversational volume (with and without surgical mask), and laughing (with and without surgical mask) and studied about thermal wake and forced convection generated by a person travelling through an inactive room.

2.1.6 Standard for the Building Ventilation System

In addition to various related research about ventilation system in building for reducing chance of airborne transmission, there is also a standard for ventilation system rates for rooms. American Society of Heating, Refrigerating and Air-Conditioning Engineers (ASHRAE, 2017) had come out to set standards for required minimum ventilation rates for rooms depended on their function and space such as airborne infection isolation anteroom which requires minimum total air change rates per hour of ten, and airborne infection isolation room whose pressure needs to be negative compared to adjacent areas. Airborne infection isolation room requires minimum total air change rates per hour of 12 and requires minimum outdoor air change rates per hour of two.

จุฬาลงกรณ์มหาวิทยาลัย
Chulalongkorn University

2.1.7 Risks of Medical Personnel Working in an Ambulance

As you can see, there have been many studies done on indoor or hospital ventilation systems, and standards were also set. In addition to the medical personnel who are close to the patients in the hospital, the high-risk group, which is sometimes overlooked, is the medical staff working in the ambulance traveling with the patient or EMS workers. Gibson (2019) studied about fomite transmission of methicillin-resistant Staphylococcus aureus (MRSA) on the surface of oxygen tank and oxygen regulator, as well as other surfaces in the ambulance cabin. Review by

Hudson et al. (2018) summarized the literatures on the ubiquity of microorganisms in ambulance patient compartment for understanding safety and biological hazards in ambulance. Although there is a lot of research about pathogen prevalence and disease transmission in ambulance, only few research have been done on airborne transmission in the ambulances.

Pipitsangjan et al. (2011) did experimental research about droplet and airborne infections among EMS workers by collecting air samples from ambulance before and during ambulance service, a total of 318 air samples. A history of medical personnel exposed to droplet and airborne for a month while working on the EMS service found that 92.5% of medical workers were exposed to suspected TB patients, 83.9% of workers were exposed to patients with coughing or sneezing, 80.1% of EMS workers were exposed to chickenpox patients, and 79.5% of medical personnel were exposed to suspected influenza or avian flu. It was also found that 87% of medical workers wore sterile gloves during contacting with mucous membrane or sterile zone of the patient, 64% used an N95 masks while exposing to tuberculosis, chickenpox, SARS, avian flu, influenza 2009, and measles, and approximately 85.7% wore a normal surgical mask while giving service to rubella and influenza patient. The number of airborne pathogens in an ambulance during service was notably higher than in non-service cases.

จุฬาลงกรณ์มหาวิทยาลัย
Chulalongkorn University

Bielawska-Drózd et al. (2017) studied about surface contamination and microbiological air quality in office spaces and ambulances. The experiments were done by using cyclone wet technology method (swab methods, imprint, and coriolis recon apparatus) for collecting air samples and Kruskal–Wallis and Mann-Whitney statistical tests were used to analyse data with $\alpha = 0.05$. Significant was defined as a P value of less than or equal to 0.05. The results for ambulances' microbial air quality (N = 28) showed the concentrations of tainted air were in the range from 0 to 2.3×10^1 colony-forming unit (CFU)/m^3 (Median = 6.2×10^0) for bacteria and from 0 to

1.8 $\times 10^1$ CFU/m^3 (Median = 4.6 $\times 10^0$) for filamentous fungi and yeast. The results for offices' microbial air quality (N = 10) showed the concentrations of air contamination were in the range from 2 to 4.2 $\times 10^1$ CFU/m^3 (Median = 1.35 $\times 10^1$) for bacteria and from 0 to 1.9 $\times 10^1$ CFU/m^3 (Median = 6.8 $\times 10^0$) for yeast and filamentous fungi. The results of research from Bielawska-Drózd et al. can indicate that ambulance paramedics have a high chance of developing respiratory infections by airborne during patient transport.

Bielawska-Drózd et al. (2018) also collected number of bioaerosol from 10 hospital emergency departments, 9 ambulances, 9 offices, and 13 outdoors by using Button Sampler device inserted with gelatine filters and Kruskal–Wallis and Mann-Whitney statistical tests were used to analyse data with α = 0.05. Significant was defined as a P value of less than or equal to 0.05. In hospital emergency departments, the concentration of bacteria was between 1.3 $\times 10^2$ and 4.2 $\times 10^3$ CFU/m^3 (Median = 4.7 $\times 10^2$), and the concentration of fungi was between 3.4 $\times 10^0$ and 8.1 $\times 10^1$ CFU/m^3 (Median = 6.7 $\times 10^0$). In ambulances, the concentration of bacteria was from 1.3 $\times 10^2$ to 1.4 $\times 10^3$ CFU/m^3 (Median = 3.0 $\times 10^2$), and the concentration of fungi was from 6.7 $\times 10^0$ to 6.5 $\times 10^2$ CFU/m^3 (Median = 6.7 $\times 10^1$). In offices, the concentration of bacteria was between 4.2 $\times 10^1$ and 5.0 $\times 10^3$ CFU/m^3 (Median = 2.3 $\times 10^2$), and the concentration of fungi was between 0 and 7.9 $\times 10^2$ CFU/m^3 (Median = 2.4 $\times 10^1$). Outdoor air, the concentration of bacteria was from 1.0 $\times 10^2$ to 5.9 $\times 10^2$ CFU/m^3 (Median = 2.2 $\times 10^2$), and the concentration of fungi was from 1.5 $\times 10^2$ to 8.2 $\times 10^2$ CFU/m^3 (Median = 3.2 $\times 10^2$). From these results, it can be inferred that the concentrations of bacteria and fungi in the ambulance were significantly increased during ambulance use.

From both studies of Bielawska-Drózd et al. are able to indicate that when the ambulance is taken to transport the patient, the concentration of pathogens and

viruses that were distributed in the air was higher which could be dangerous for the medical services workers who are on duty in the ambulance.

In addition to the above studies, Sayed et al. (2011) studied about detailed analysis of occupational health hazards at Boston EMS emergency medical care system from 2007 to 2009. The results showed that the most reported exposure to pathogens was meningitis (32.9%) which can be transmitted through coughing, sneezing, or contaminated objects. The second highest reported exposure was tuberculosis (TB) (17.1%) which can be transmitted through the air by inhaling droplet nuclei containing M. tuberculosis, followed by H1N1 or influenza (15.4%) which can be transmitted through droplets produced while coughing or sneezing. This study by Sayed et al. can indicate that ambulance workers are at a high chance of encountering patient with an airborne transmission disease.

2.1.8 Ambulance Ventilation System

Although there are few studies on the airborne transmission inside ambulances during the transportation of patients, with the past studies we can infer that the personnel working in the ambulance are at high risk of being infected disease by airborne transmission from the droplet or droplet nuclei emitted by patient. Ambulance airborne transmission problems can be solved in the same way as indoors which is the ventilation system. Lindsley et al. (2019) studied about how ambulance ventilation system affects airborne particles released by the patient's cough and EMS workers are exposed to aerosols and droplets while transporting patients. Lindsley et al. used NIOSH cough aerosol simulator (Lindsley et al., 2013) as a source of aerosol particles and measured number of particles by optical particle counters at different locations and patient cot angles in the ambulance (2005 Wheeled Coach Type III). In this study, Lindsley W. G. et al. divided the experiment into 2 types which were using cough aerosol nebulizer loaded with 28% KCl and

จุฬาลงกรณ์มหาวิทยาลัย
Chulalongkorn University

using airborne influenza virus. In the experiments, Lindsley et al. adjusted ventilation rates to 0, 5, and 12 ACH and recorded the change of the number of particles over time at each ventilation rate.

The results showed that raising the ventilation rate greatly lowered the volume concentration of airborne particles in all positions. At 0 ACH, changing the cot angle affected the volume concentration, but at 5 and 12 ACH, the cot angle had little effect on the particle volume concentration. Lindsley W. G. et al. also found out that ventilation system could reduce but could not get rid of exposure of EMS workers to airborne particles. According to a study by Lindsley et al., the ventilation system installed inside the ambulance can be effective in reducing volume concentration of particles at any location within the ambulance. However, in different models of the ambulance, ventilation system, including the difference in installing location of the ventilation system may have different effects in each case.

จุฬาลงกรณ์มหาวิทยาลัย
Chulalongkorn University

CHAPTER 3
RESEARCH METHODOLOGY

This chapter describes the process of conducting research studies. The set of experimental studies is performed to assess the effectiveness of an ambulance air exhaust system in reducing the aerosol particle concentration by measuring volume concentration of particles in different size ranges at different locations when the ambulance is not moving.

The ambulance used, is a Toyota Ventury ambulance. The patient compartment is 1500 mm wide, 2730 mm long, and 1400 mm high. Particles are introduced into the patient compartment in the form of pulses by portable ventilator, Oxylog® 3000 plus, connected to the nebulizer, Aeroneb® Professional Nebulizer uses for aerosolizing solutions. This process simulates the patient's breathing pattern. Throughout the process of particle injection into the cabin, we measure the number of particles with the PMS5003 measuring instrument at 200 positions over time. The PMS5003 is previously calibrated against a more-accurate, Handheld 3016 particle counter. The released aerosol particles are 0.9% sodium chloride solution to ensure the safety of the experimenter.

จุฬาลงกรณ์มหาวิทยาลัย
Chulalongkorn University

For the preliminary experiment, the data are collected not only at 3 different seat positions but at three different ventilation rates. Ventilation rate is controlled by adjusting the air exhaust system's fan speeds for the intake fan at the top of the patient compartment and an air exhaust blower on the right side of the ambulance next to the patient cot. The adjustment is made for three levels: minimal ventilation (very small ACH), medium ventilation (roughly 40 ACH), and high ventilation (roughly 80 ACH). The preliminary experiment setup is depicted as in Figure 33. Note that the sensors of the preliminary result are placed on the centre of the seat positions.

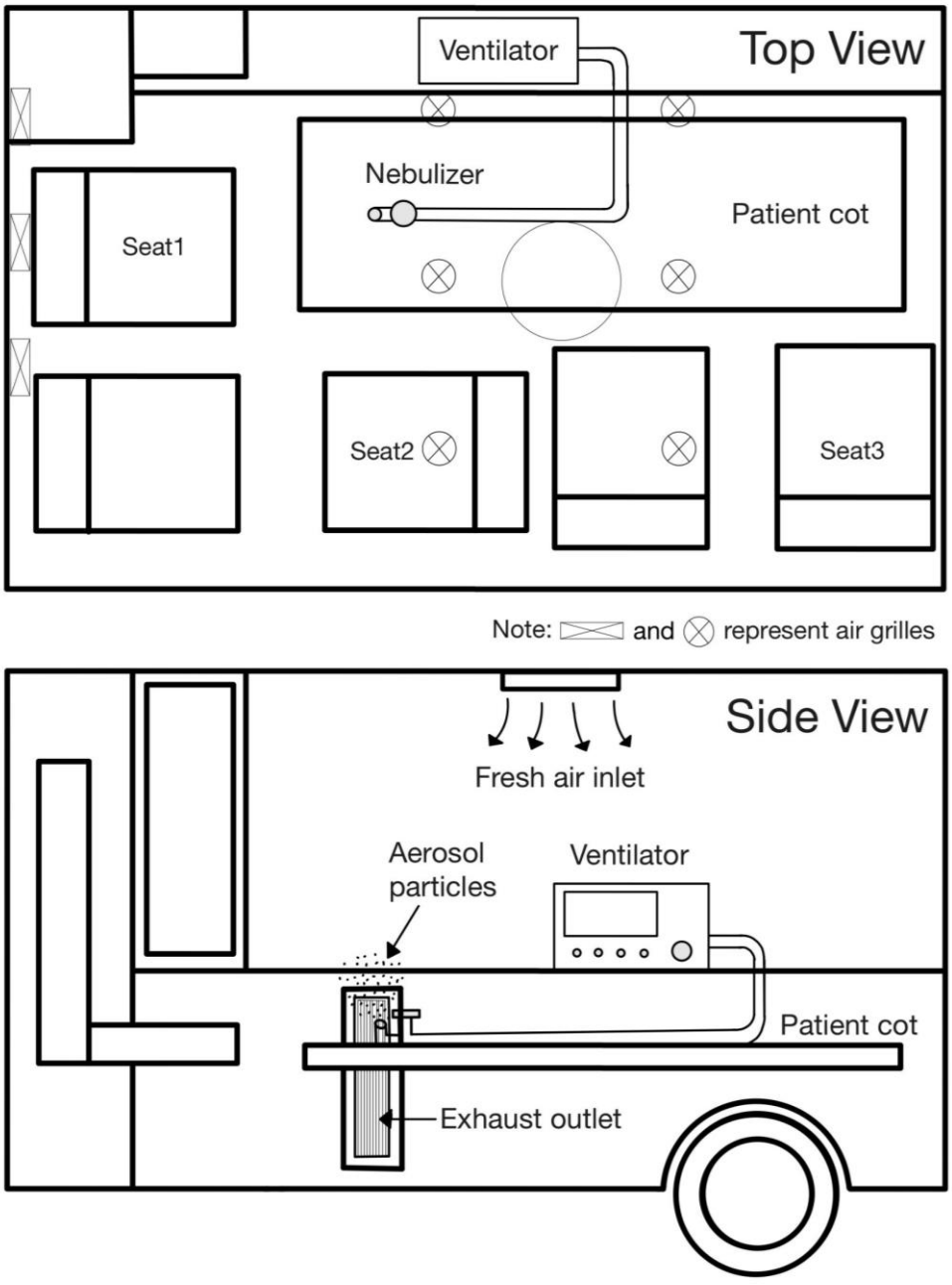

Figure 33 Ambulance Patient Compartment with Installation of Preliminary Experimental Equipment and Air Exhaust System

For the experiment of this research, the locations of the devices and sensors are shown in Figure 34. The sensors used in the measurement are mounted hanging from the ceiling of the patient compartment and all 200 data positions are measured by sliding the bar in the Figure 34 to various points on the ceiling. All 200 points are divided into 10 points along the x-axis (20 centimeters apart), 5 points on the y-axis (20 centimeters apart), and 4 points on the z-axis (16 centimeters apart) as shown in Figure 35 below. The experiments are divided into two cases: minimal ventilation (very small ACH) and high ventilation (roughly 80 ACH). The procedures of each case will be discussed later.

Figure 34 The Installation Location of the Experimental Equipment

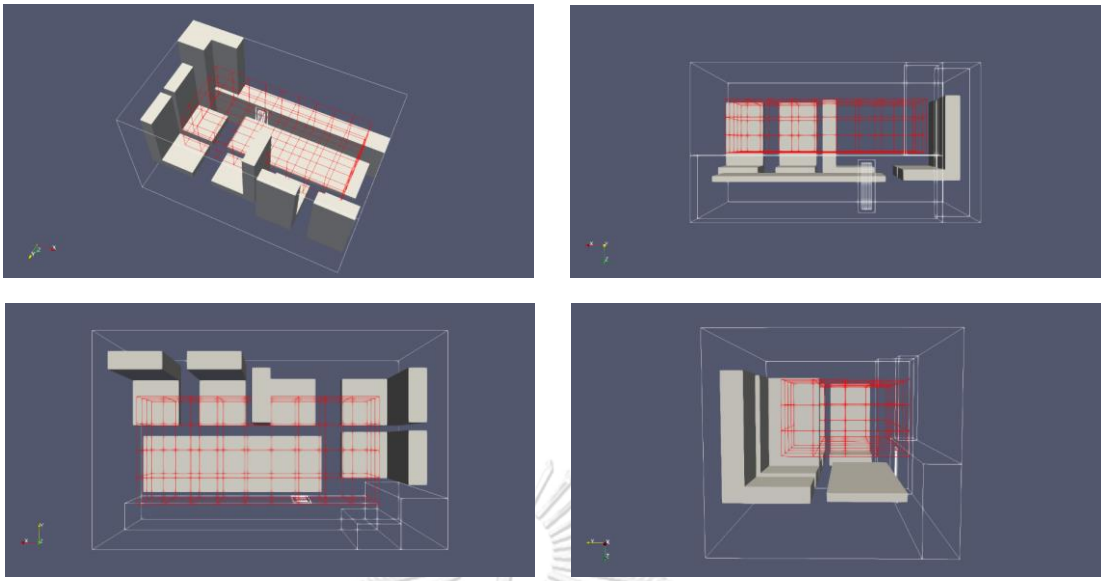

Figure 35 The Location of the Experiment's Measurement Points in the Patient Compartment.

จุฬาลงกรณ์มหาวิทยาลัย
Chulalongkorn University

3.1 Research Instrument

3.1.1 Toyota Ventury

Figure 36 Toyota Ventury ER-1 (Plane Boi, 2019)

Figure 37 Patient Compartment of Toyota Ventury

The ambulance used in this research is Emergency-1 (ER-1), Toyota Ventury model of King Chulalongkorn Memorial Hospital, shown in Figure 36 and Figure 37,

equipped with an air exhaust system model CC 410-Concealed Air Purifier from Camfil®.

3.1.2 CC 410-Concealed Air Purifier

Figure 38 CC 410 (Concealed) Air Purifier

The Camfil® air purifier, shown in Figure 38, installed in the ambulance has three classes of air filters: the pre filter (30/30 Pre filter-G4), which has an initial pressure drop of 80 Pa (Camfil, 2021a), UVC, and HEPA filter H14 (Absolute CET14-H14) which has an initial pressure drop of 250 Pa (Camfil, 2021b).The pre filter is made of cotton and synthetic fibres. The filter media is densed and reinforced with wire mesh to increase its strength. This filter has passed EN 779 efficiency test standard with no less than G4 level of filtration or dust collection efficiency with a dust capture efficiency greater than 90% or equivalent to ASHRAE Test Standard 52.2-2007 or MERV 8. The second layer of pathogens capture is to use two 16 Watts UVC lamps installed inside the machine, while in use the machine must be completely closed so that the light cannot come outside the machine. The final filter is the HEPA Filter, the Absolute model CET14-H14, which is compliant with the EN 1822:2009 standard for trapping pathogens and microscopic particles. The material is made from glass fibres with hot-melt beads with dust filtration efficiency up to 99.995% at particle size 0.1 to 0.2 micron.

จุฬาลงกรณ์มหาวิทยาลัย
Chulalongkorn University

As for the fan section, it is used for 1-way inlet and 1-way outlet air circulation, with a maximum speed of 2810 rounds per minute and maximum flow rate of 490 CMH or 288 CFM and a total of 6 adjustable levels. Motor is an ECblue motor which needs a voltage of 1 ~ 230 V and a frequency of 50 Hz.

Table 1 Operating Specification of Camfil® CC 410-Concealed Air Purifier (Camfil, 2021c)

Fan Level	Flow Rate (m^3/hr)	Noise Level (dB)	Power Consumption (W)
1	45	23	2.5
2	124	28.1	8.3
3	271	44.7	37.9
4	412	55.3	101
5	442	58.9	155
6	490	63.3	165

The flow rate values in Table 1 are the default values of CC 410-concealed air purifier. However, with continuous usage, a higher pressure drop results in a lower flow rate, resulting in non-constant air change rate throughout the experiments. The patient compartment volume is also difficult to measure since the equipment within the ambulance, such as the patient cot and seats, makes calculating the exact air change rate complicated. In this study, the air change rate is estimated from the size of the patient compartment and from the flow rate in the Table 1; When the air exhaust system is opened at level 3, it is roughly 40 ACH and roughly 80 ACH when opening at the maximum rate.

จุฬาลงกรณ์มหาวิทยาลัย
Chulalongkorn University

3.1.3 Oxylog® 3000 plus

Figure 39 Oxylog® 3000 plus (Dräger, 2020a)

The Oxylog® 3000 plus, shown in Figure 39, is a transport ventilator which helps transporting air in or out patient's lungs. It is necessary for people with respiratory failure which means a condition which is difficult to breathe or get enough oxygen into blood.

จุฬาลงกรณ์มหาวิทยาลัย
CHULALONGKORN UNIVERSITY

Operating Specification (Dräger, 2020b)

Ventilation Modes:	VC-CMV, VC-AC, VC-SIMV, SpnCPAP, PC-BIPAP
Ventilation Setting:	Pressure support: VC-SIMV, PC-BIPAP and SpnCPAP
	Apnoea ventilation: SpnCPAP
	AutoFlow (optional): VC-CMV, VC-AC and VC-SIMV
	NIV: SpnCPAP (/PS), PC-BIPAP (/PS), VC-CMV/AF, VC-AC/AF and VC-SIMV/AF
Ventilation Respiratory Rate:	2 to 60 / min (VC-SIMV, PC-BIPAP)
	5 to 60 / min (VC-CMV, VC-AC)

	12 to 60 / min for apnoea ventilation
Tidal Volume:	0.05 to 2.0 L; BTPS
Ti / I:E:	I:E or Ti configurable for all ventilation modes
Ventilation Time Ratio I:E:	1:100 to 50:1
Inspiratory Time Ti:	0.2 to 10 seconds
Inspiratory Pressure Pinsp:	PEEP +3 to +55 mbar
O2 Concentration:	40 to 100 Vol.%
PEEP/CPAP:	0 to 20 mbar
Trigger Sensitivity (Flow Trigger):	1 to 15 L/min
Pressure Support ΔPsupp:	0 to 35 mbar (relative to PEEP)
Slope (Pressure Rise Time):	Slow, Standard, Fast
Max. Inspiration Flow:	100 L/min @ supply pressures > 350 kPa / 51 PSI; 80 L/min @ supply pressures < 350 kPa / 51 PSI; 39 L/min @ supply pressures <270 kPa / 39 PSI
Displayed Measured Values:	MVe, FiO2, RR, VTe, PEEP, Pmean, PIP, Pplat, MVesp, RRspon, etCO2
Display Type:	Technology Electro-luminescence (EL) Pixels 240 x 128 Visible area 108 x 56 mm
Curve Display:	Airway pressure Paw curve, flow curve, CO2 curve (optional)
Patient Hose Types:	Reusable adult hose (1.5 m / 3 m), Disposable adult hose (1.5 m / 3 m), Disposable pediatric hose (1.9 m)

จุฬาลงกรณ์มหาวิทยาลัย
CHULALONGKORN UNIVERSITY

3.1.4 Aeroneb® Professional Nebulizer

Figure 40 Aeroneb® Professional Nebulizer (Medplan, 2021)

The Aeroneb® Professional nebulizer, shown in Figure 40, is a multi-patient portable medical device. It's designed to aerosolize medicines or doctor-prescribed solutions for patients to inhale.

Aeroneb® Professional consists of 5 main components, including 1) nebulizer unit, used to aerosolize solutions or medications. 2) Control module is used to control the aerosolization duration between 15 and 30 minutes or to turn nebulizer on or off. 3) Control module cable is used to connect between nebulizer unit and control module. 4) AC/DC adapter is used to connect the power supply to the control module. 5) T-piece is used to connect nebulizer unit into breathing circuit.

Specification (Aerogen®, 2015)

Operating:	Maintains specified performance at circuit pressures up to 90cm H2 O and temperatures from 5 ºC (41ºF) up to 45 ºC (113ºF) Atmospheric Pressure: 450 to 1100 hPa Humidity: 15% to 95% relative humidity Noise Level: < 35 dB measured at 0.3 m distance
Storage & Transport:	Transient Temperature Range: -20 to +60°C (-4 to +140°F) Atmospheric Pressure: 450 to 1100 hPa Humidity: 15% to 95% relative humidity
Power Source:	Can operate from AC/DC Adapter (input 100 to 240 VAC 50 – 60 Hz, output 9 V) or internal rechargeable battery (4.8 V nominal output)
Power Consumption:	< 6.5 Watts (charging), 2.0 Watts (nebulising)
Patient Isolation:	Controller circuitry provides 4 kilovolt (kV) patient isolation and complies with IEC/EN 60601-1
Nebulizer Capacity:	Maximum 10 mL
Flow Rate:	> 0.2 mL/min (Average ~ 0.4 mL/min)
Particle Size:	As measured with the Andersen Cascade Impactor: Specification Range: 1-5 microns Average Tested: 3.1 microns As per EN 13544-1, with a starting dose of 2 mL: Aerosol Output rate: 0.24 mL/min Aerosol Output: 1.08 mL emitted of 2.0 mL dose Residual Volume: <0.1 mL for 3 mL dose6

จุฬาลงกรณ์มหาวิทยาลัย
Chulalongkorn University

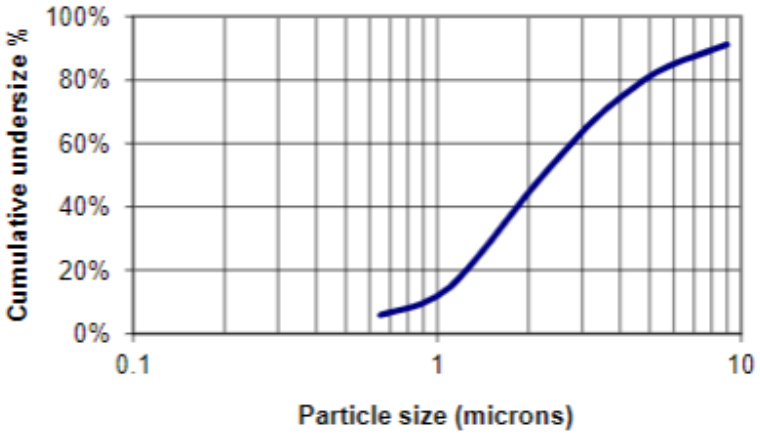

Figure 41 Particle Size Distribution for Albuterol as per EN 13544-1 (Aerogen®, 2015)

Figure 41 shows *Albuterol* particle size distribution nebulized by Aeroneb® Professional Nebulizer. The nebulizer's performance may vary based on the type of medicine or solution and environment in the use of nebulizer.

จุฬาลงกรณ์มหาวิทยาลัย
Chulalongkorn University

3.1.5 Handheld 3016

Figure 42 Handheld 3016 (Lighthouse Worldwide Solutions, 2019)

Handheld 3016, shown in Figure 42, is a particle counter which has a sensitivity range of 0.3 micron to 25 microns with 0.1 CFM flow rate. The Handheld 3016 can display data on both cumulative and differential particle counts as well as relative humidity and temperature data on the colour touch screen and there are six particle size channels that can be counted at the same time.

จุฬาลงกรณ์มหาวิทยาลัย
CHULALONGKORN UNIVERSITY

Specification (Lighthouse Worldwide Solutions, 2018)

Flowrate:	0.1 CFM (2.83 LPM)
Laser Source:	Extreme Light Laser Diode with > 20 years MTTF
Zero Count Level:	< 1 count / 5 minutes (per ISO 21501-4)
Concentration Limits:	8,000,000 particles/cu.ft. at 10% coincidence loss

Calibration:	Meets ISO 21501-4 calibration using NIST traceable PSL spheres
Count Modes:	Automatic, manual, beep, concentration, cumulative/differential
Data Storage:	3,000 sample records, rotating buffer, includes particle and environmental data, location, and time
Communication Mode:	RS-232 via RJ-45 to PC or optional printer
Supporting Software:	LMS Express, LMS Express RT, LMS Pharma, LMS Pro
Environmental Sensors:	Direct Mount Temperature/Relative Humidity probe: 0-150°F (-17.8 to 65.6°C) ± 1.8°F at 77°F, 0-100% ± 5% at 33%
Touch Screen Display:	3.5 inch (8.89 cm), colour TFT display
Reports:	FS-209E, ISO-14644-1 (1999, 2015) & EU GMP (Model 3016-IAQ no report standards)
Alarms:	Internal, adjustable alarm on counts, low battery, sensor failure
Sample Inlet:	Isokinetic sampling probe
Sample Output:	Internally filtered to HEPA standards (>99.97% @ 0.3 µm)
Vacuum Source:	Internal pump, automatic flow control
Enclosure:	High impact injection molded plastic
Power:	External power supply: 12 VDC, 1.25 A
Battery:	Li-Ion, removable and rechargeable
Dimensions:	8.75 in. (l) x 5.0 in. (w) x 2.5 in. (h), (22.23 x 12.70 x 6.35 cm)
Weight:	2.2 lbs (1 kg)
Languages:	English (U.S.), Deutsch, Espanol, Italiano, Français, Russian, Japanese, Korean and Chinese

จุฬาลงกรณ์มหาวิทยาลัย
Chulalongkorn University

3.1.6 PMS5003 G5 (with GM1705A01 pin adapter module)

Figure 43 PMS5003

Figure 44 GM1705A01 Pin Adapter Module

PMS5003, shown in Figure 43, need to be used with pin adapter module, shown in Figure 44, in order to connect with microcontroller. PMS5003 is a digital universal particle concentration sensor. The sensor uses static light scattering method to get the number of particles in the atmosphere. In the process the instrument uses laser to radiate suspended particulate matters in the atmosphere and collects a certain degree of scattering light. Finally, a microprocessor based on MIE theory

determines the equivalent particle diameter and the number of particles. This process is shown in functional block diagram in Figure 45.

There are passive and active for digital output. In default mode, sensor automatically returns serial data to the host after power up. There are two modes in active mode which are fast mode and stable mode. If the concentration changes over a wide range, the laser beam is emitted every 200 to 800 milliseconds which is called fast mode. If the concentration changes over a small range, the laser beam is emitted every 2.3 seconds which is called stable mode. The time interval is shorter if the concentration is higher.

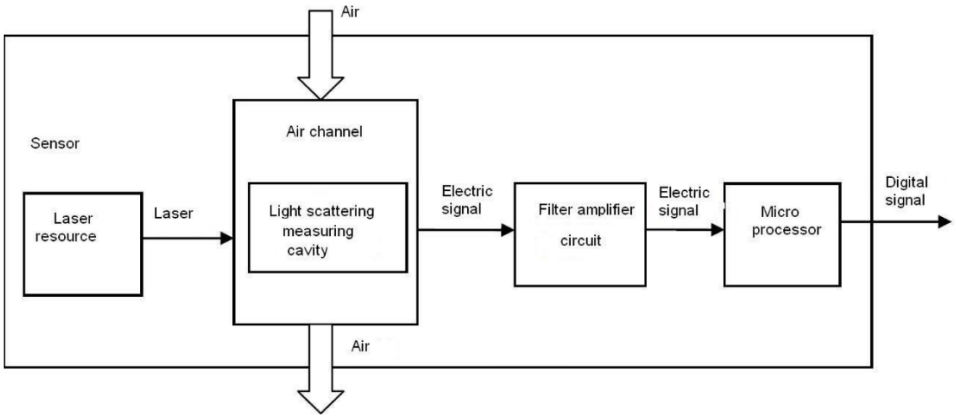

จุฬาลงกรณ์มหาวิทยาลัย
Chulalongkorn University

Figure 45 Functional Block Diagram of PMS5003 (Plantower, 2017)

Specification (Plantower, 2017)

Range of Measurement:	0.3~1.0; 1.0~2.5; 2.5~10 micron
Counting Efficiency:	50% at 0.3 micron, 98% at ≥ 0.5 micron
Effective Range (PM2.5 Standard):	0~500 μg/cu.m.
Maximum Range (PM2.5 Standard):	≥ 1000 μg/cu.m.
Resolution:	1 μg/cu.m.
Maximum Consistency Error:	±10% at 100~500 μg/cu.m., ±10 μg/cu.m. at

	0~100 µg/cu.m.
Standard Volume:	0.1 Litre
Single Response Time:	< 1 second
Total Response Time:	≤ 10 seconds
DC Power Supply:	Typ: 5.0 Volt, Min: 4.5 Volt, Max: 5.5 Volt
Active Current:	≤ 100 mA
Standby Current:	≤ 200 µA
Interface Level:	L < 0.8 at 3.3 H > 2.7 at 3.3 Volt
Working Temperature Range:	-10~60 °C
Working Humidity Range:	0~99%
Storage Temperature Range:	-40~+80 °C
Mean Time to Failure:	≥ 3 years
Size:	50 x 38 x 21 mm

3.1.7 Arduino UNO R3 SMD (CH340G)

Figure 46 Arduino UNO R3

The Arduino Uno SMD R3, shown in Figure 46, is a microcontroller board based on the ATmega328. There are 14 digital pins that can be utilized for any input or output, with 6 of them serving as PWM outputs, a 16 MHz crystal oscillator, an

ICSP header, a power jack, 6 analogue inputs, a USB connection, and a reset button. It can be started by attaching it to a computer via a USB cable or by powering it using an AC/DC adaptor.

Specification (Magyc Now, 2019)

Microcontroller:	ATmega328
Operating Voltage:	5V
Supply Voltage (recommended):	7-12V
Maximum Supply Voltage (not recommended):	20V
Digital I/O Pins:	14 (of which 6 provide PMW output)
Analog Input Pins:	6
DC Current per I/O Pin:	40 mA
DC Current for 3.3V Pin:	50 mA
Flash Memory:	32 KB (ATmega328) of which 0.5 KB used by bootloader
SRAM:	2KB (ATmega328)
EEPROM:	1KB (ATmega328)
Clock Speed:	16 MHz

จุฬาลงกรณ์มหาวิทยาลัย
Chulalongkorn University

3.1.8 0.9% Sodium Chloride Solution

Figure 47 0.9% Sodium Chloride Solution

0.9% Sodium Chloride solution, volume 100 ml, shown in Figure 47, consisting of 900 mg sodium chloride in water which is equal to the salt concentration of normal human blood.

3.2 PMS5003 Usage

In order to connect the PMS5003 to the Arduino board you need an adapter module, which in this research we chose to use GM1705A01 pin adapter module. After that, connect between pin adapter module and Arduino board. The first wire is connected between positive power pin (VCC) of adapter module and 5V pin of the board, second wire is connected between ground pin (GND) of the board and adapter module. For the first and second wires, do the aforementioned for every PMS5003 sensor. The last wires are connected between transferring serial port pin (TXD) of adapter modules and digital input pin of Arduino boards by which here choose to use digital pin 2, 4, and 7 along with leaving digital pin 3, 5, and 6 disconnected for the active mode. The wiring diagram for preliminary experiment (active mode) is shown in appendix A. For the latter experiment, the wiring diagram (passive mode) is shown in appendix C.

จุฬาลงกรณ์มหาวิทยาลัย
CHULALONGKORN UNIVERSITY

After finish wiring, the next step is coding with Arduino 1.8.5 to extract the data obtained from PMS5003 to be displayed on the serial monitor with 115200 baud rates with the code in active mode as shown in appendix B and the code in passive mode is shown in appendix D. The number of particle data can be obtained from PMS5003 transport protocol-Active Mode in 2016 product data manual of PLANTOWER (Plantower, 2017); Data7, Data8, Data9, Data10, and Data11 indicate the number of particles per 0.1 lite of air with diameter beyond 0.3, 0.5, 1.0, 2.5, and 5 microns, respectively. The data which are chosen to display here are the number of particles beyond 0.3, 0.5, 1.0, 2.5, and 5.0 microns per cubic feet unit for ease of calibration compared to Handheld3016 instrument.

3.3 Sensor Calibration

There are many sensors in the market that can measure number of airborne particles, for example, Handheld3016, Extech VPC300 Particle Counter, Handilaz® Mini II Handheld Airborne Particle Counter, Handheld Particle Counter KC-51, Handheld Particle Counter KC-52, etc. The airborne particle counter sensors mentioned above are all very expensive which made it impossible to buy and use in this research.

จุฬาลงกรณ์มหาวิทยาลัย
Chulalongkorn University

Since these sensors, which are the sensor with high precision, are expensive and difficult to borrow for a long period of time so we choose to use PMS5003, which is inexpensive and easy to buy, instead; however, the replaced sensor is not as accurate and precise as the airborne particle counter sensors mentioned above, resulting in the need for calibration between the sensors.

We borrow Handheld3016 from Lighthouse Worldwide Solutions and use it to calibrate the PMS5003 against. Starting with installing two sensor devices in the same patient compartment environment at the same location to compare the measured

values of both sensors. In the test, we introduce particle into the system to see the response values in the various sensor ranges. The test is done 3 times with the steps as follow.

1. Install all instruments together as well as install the PMS5003 and Handheld3016 in the location which is set to be measured

2. Turn on air conditioner at 25 °C with all air grilles at the centre position

3. Pour 0.9% Sodium Chloride Solution into Aeroneb® Professional Nebulizer unit

4. Turn on oxylog 3000 plus, choose VC-CMV mode, set tidal volume (VT) to 500 mL, ventilation time ratio (I:E) to 1:2 and adjust respiratory rate (RR) to 12, in order to get inspiratory time (Ti) to be 1.7 seconds

5. Turn on air exhaust system at maximum rate for 15 minutes for reducing the number of particles in the patient compartment

6. After that, turn on PMS5003 and Handheld3016 to log data at the same time

7. After 3 minute, turn on Aeroneb® Professional Nebulizer to introduce particles into the ambulance for 1 minute

8. Log data for 15 more minutes

The data obtained from these three experiments, which were divided into three size ranges: 0.5-1 microns, 1-2.5 microns and 2.5-5 microns, are shown in Figure 48 to Figure 59.

จุฬาลงกรณ์มหาวิทยาลัย
Chulalongkorn University

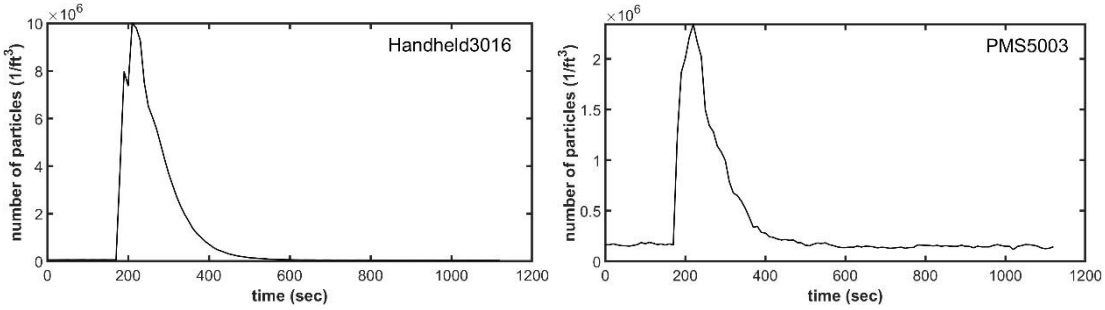

Figure 48 Number of Particles between 0.5 and 1 Micron per Cubic Feet over Time from Test 1

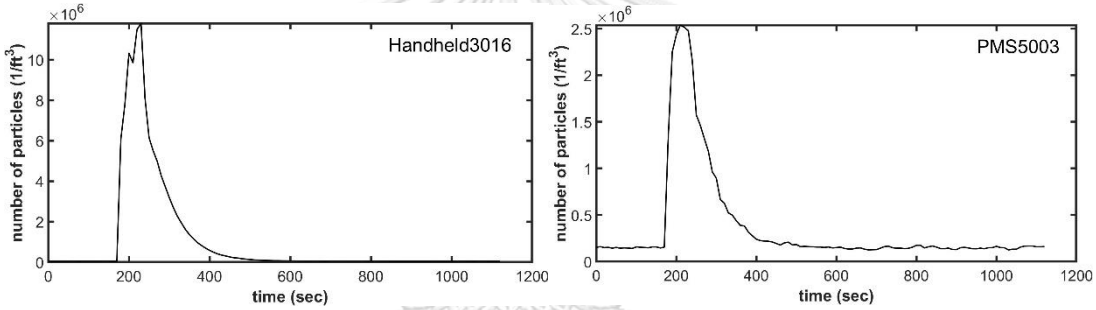

Figure 49 Number of Particles between 0.5 and 1 Micron per Cubic Feet over Time from Test 2

จุฬาลงกรณ์มหาวิทยาลัย
Chulalongkorn University

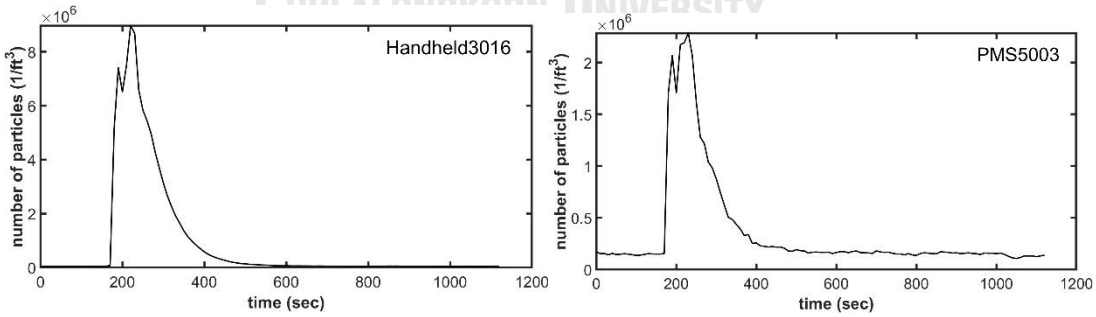

Figure 50 Number of Particles between 0.5 and 1 Micron per Cubic Feet over Time from Test 3

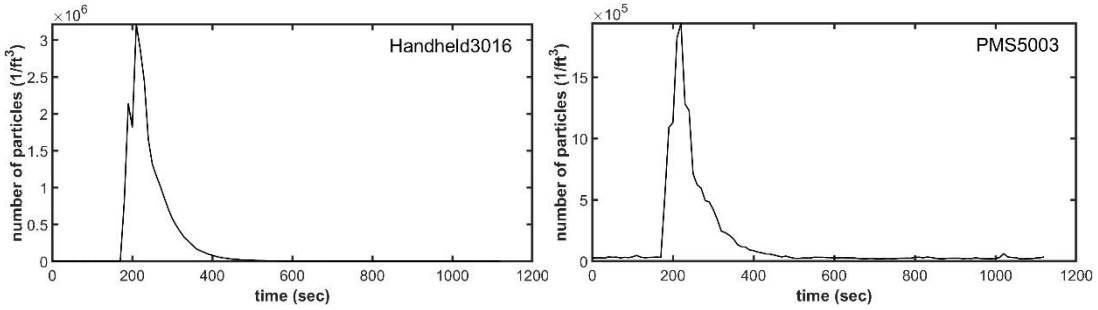

Figure 51 Number of Particles between 1 and 2.5 Microns per Cubic Feet over Time from Test 1

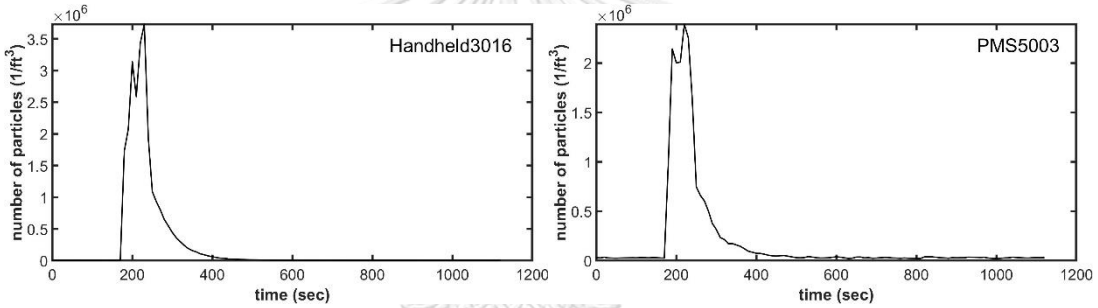

Figure 52 Number of Particles between 1 and 2.5 Microns per Cubic Feet over Time from Test 2

จุฬาลงกรณ์มหาวิทยาลัย
Chulalongkorn University

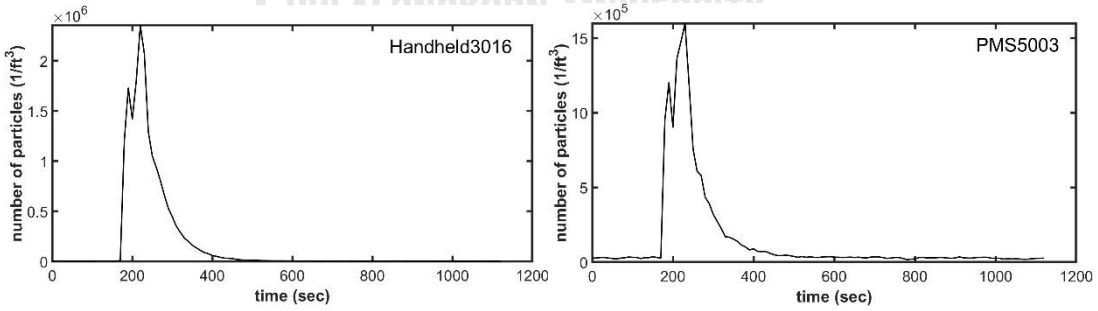

Figure 53 Number of Particles between 1 and 2.5 Microns per Cubic Feet over Time from Test 3

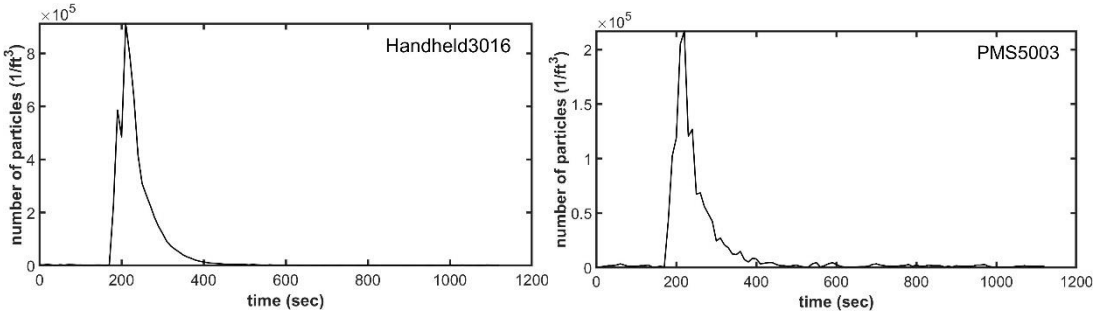

Figure 54 Number of Particles between 2.5 and 5 Microns per Cubic Feet over Time from Test 1

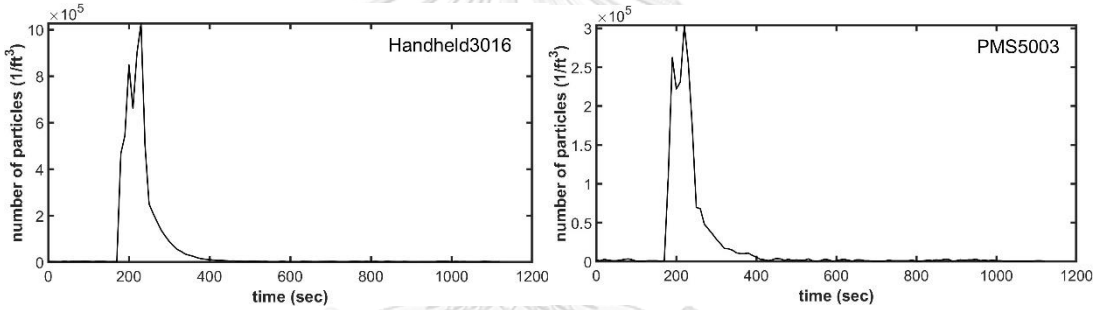

Figure 55 Number of Particles between 2.5 and 5 Microns per Cubic Feet over Time from Test 2

จุฬาลงกรณ์มหาวิทยาลัย
Chulalongkorn University

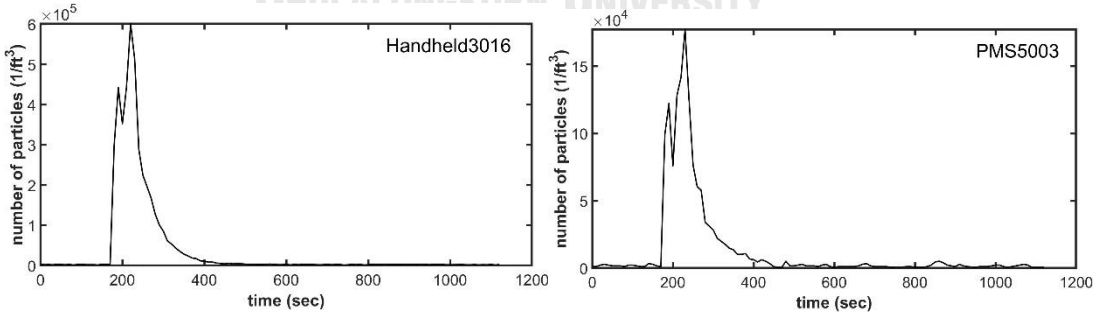

Figure 56 Number of Particles between 2.5 and 5 Microns per Cubic Feet over Time from Test 3

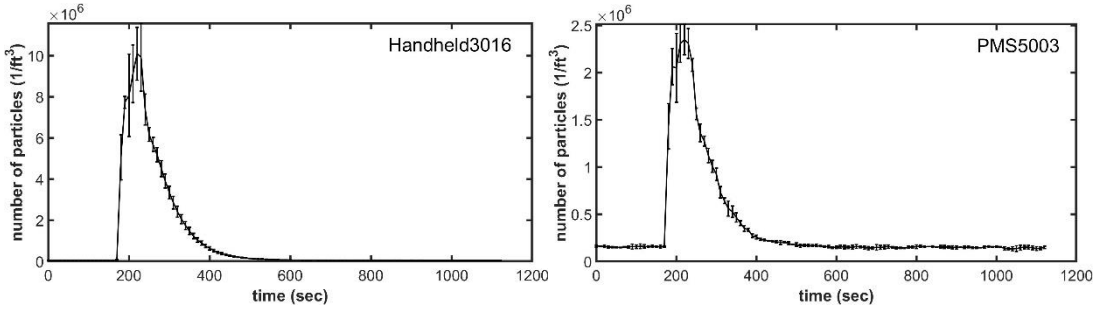

Figure 57 Mean Number of Particles between 0.5 and 1 Micron per Cubic Feet over Time and Standard Deviation of Three Tests

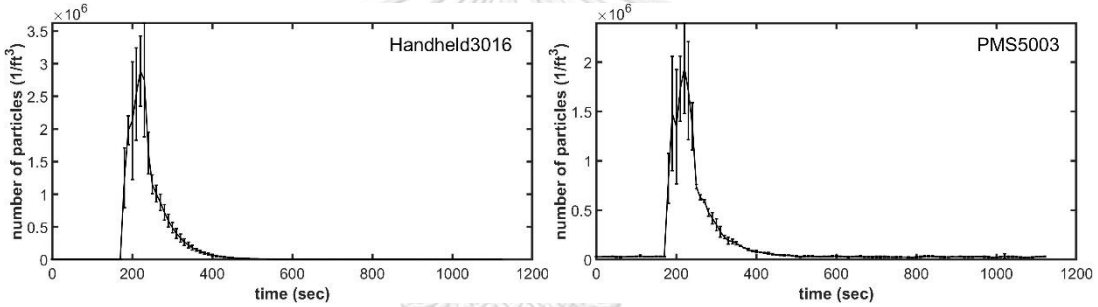

Figure 58 Mean Number of Particles between 1 and 2.5 Microns per Cubic Feet over Time and Standard Deviation of Three Tests

จุฬาลงกรณ์มหาวิทยาลัย
Chulalongkorn University

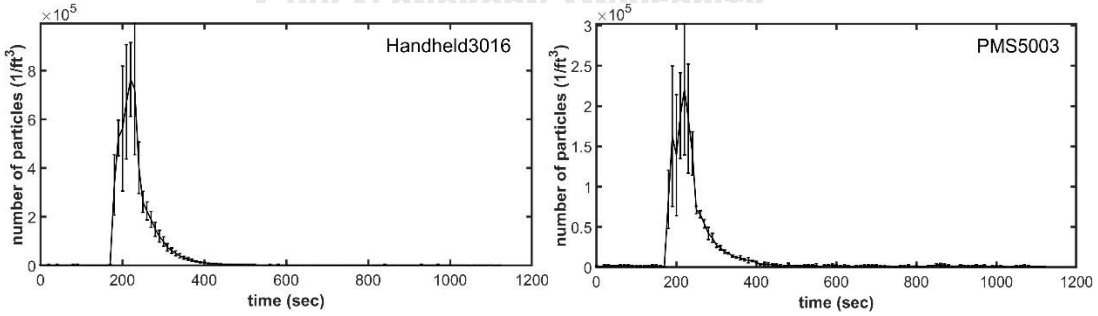

Figure 59 Mean Number of Particles between 2.5 and 5 Microns per Cubic Feet over Time and Standard Deviation of Three Experiments

After receiving the data of all 3 tests, combined all data together and categorized them into three different size bins; 0.5 to 1 micron, 1 to 2.5 microns and 2.5 to 5 microns. Since the data read from PMS5003 at low number of particles per cubic feet highly fluctuates, it is necessary not to consider those data of such low concentration from the PMS5003 in constructing calibration curves. Sort all data in each size bin in ascending order based on handheld3016 value and cut off the values which were considered to be that at the background state. Then plot the data for each size bin. The calibration curves are plotted in logarithmic scale for both axes. We found that the data on the log scales is linear in 2 ranges for every size bin as shown in Figure 60, Figure 61, and Figure 62.

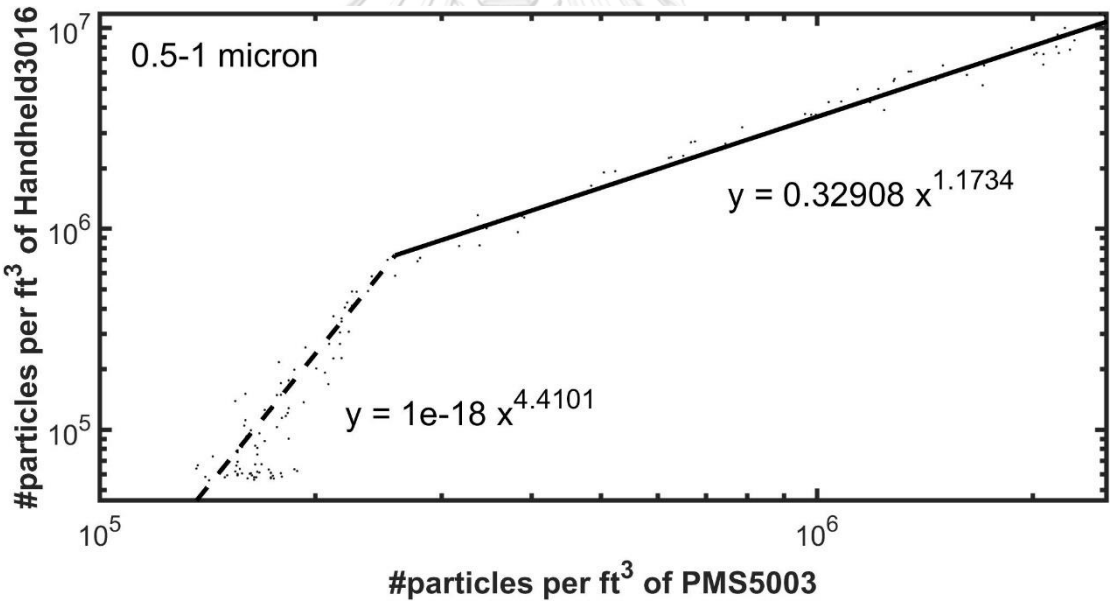

Figure 60 Calibration Curve between PMS5003 and Handheld3016 for the Particle size between 0.5 and 1 micron

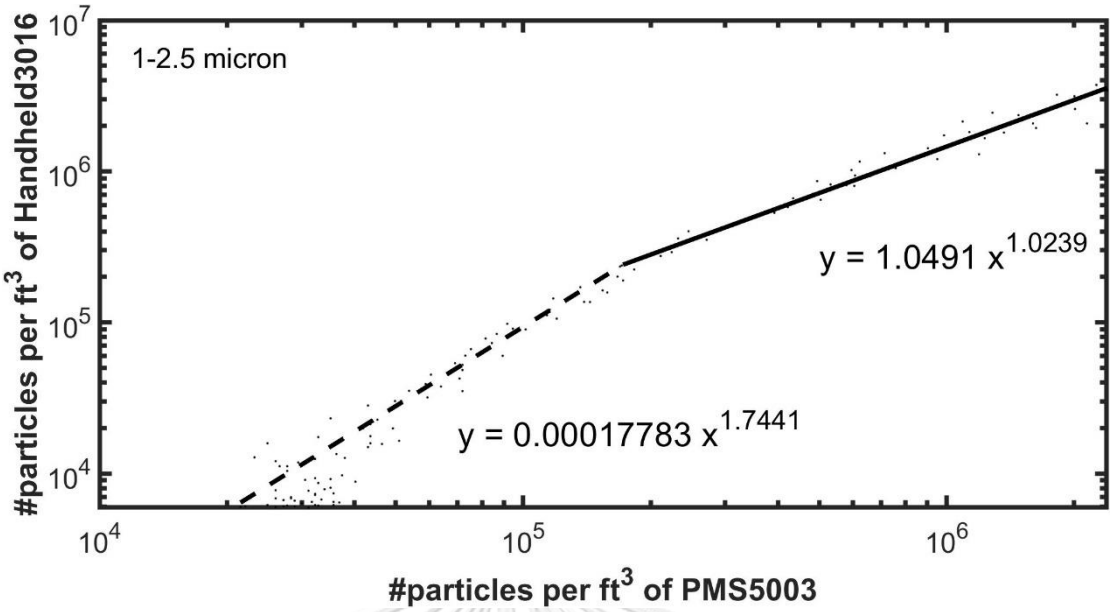

Figure 61 Calibration Curve between PMS5003 and Handheld3016 for the Particle Size between 1 and 2.5 Microns

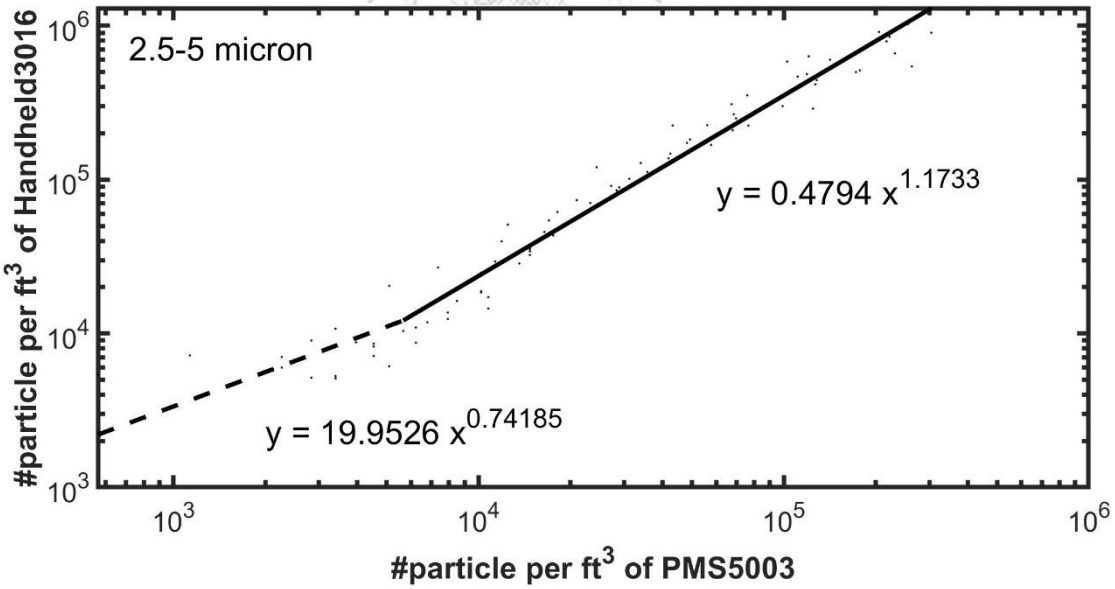

Figure 62 Calibration Curve between PMS5003 and Handheld3016 for the Particle Size between 2.5 and 5 Microns

For the size range between 0.5 and 1 micron, the number of particles per cubic feet of air from 258249 to 2538036 was considered to use $y = 0.32908 \times x^{1.1734}$ and the data below 258249 was considered to use $y = 10^{-18} \times x^{4.4101}$. For the size range between 1 and 2.5 micron, the number of particles per cubic feet of air from 172166 to 2393903 was considered to use $y = 1.0491 \times x^{1.0239}$ and the data below 172166 was considered to use $y = 0.00017783 \times x^{1.7441}$. For the size range between 2.5 and 5 micron, the number of particles per cubic feet of air from 5664 to 304123 was considered to use $y = 0.4794 \times x^{1.1733}$ and the data below 5664 was considered to use $y = 19.9526 \times x^{0.74185}$.

After receiving calibration curves, the resulting equation will be used for converting the PMS5003's data to be comparable to Handheld3016's data. The results for sizes 0.5-1 micron, 1-2.5 microns and 2.5-5 micron are shown in Figure 63, Figure 64, and Figure 65, respectively.

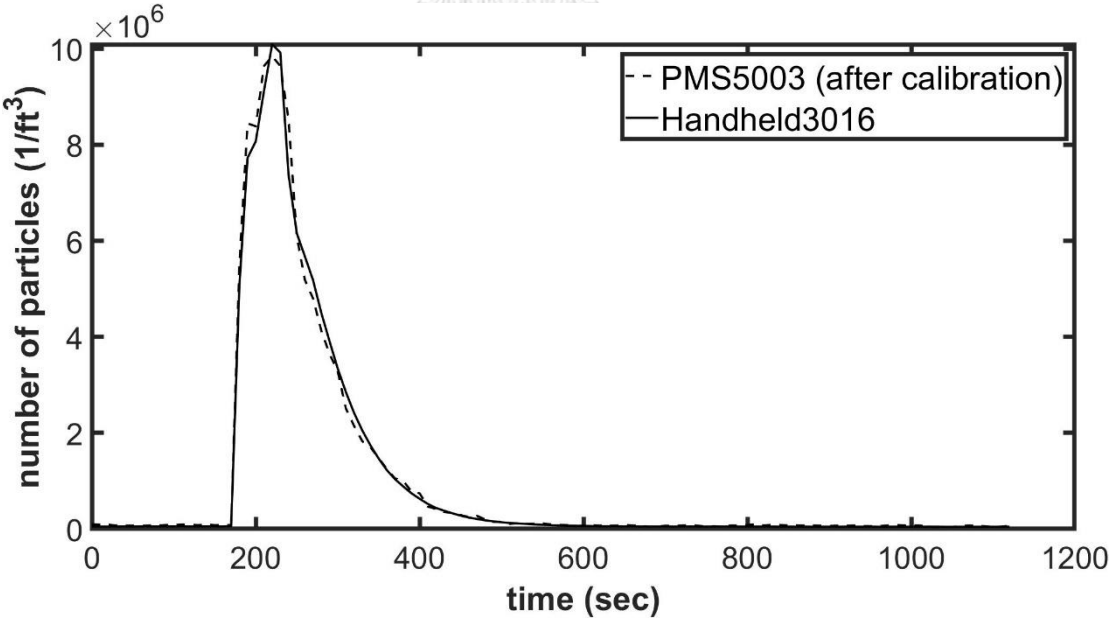

Figure 63 Mean Number of Particles between 0.5 to 1 Micron per Cubic Feet over Time between Handheld3016 and PMS5003 after Using Calibration Curve

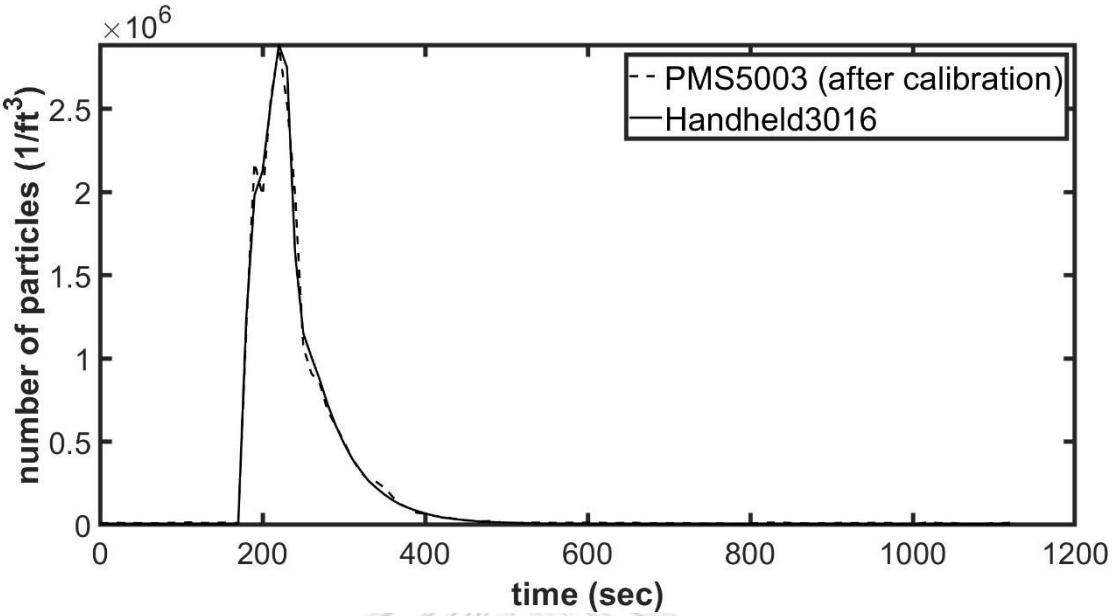

Figure 64 Mean Number of Particles between 1 to 2.5 Microns per Cubic Feet over Time between Handheld3016 and PMS5003 after Using Calibration Curve

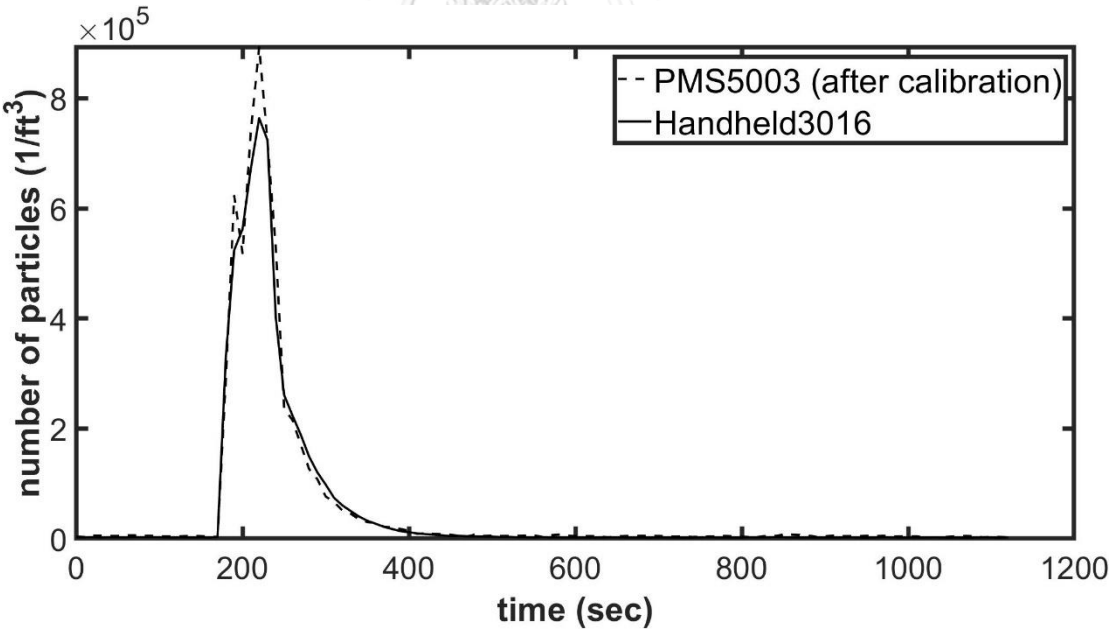

Figure 65 Mean Number of Particles between 2.5 to 5 Microns per Cubic Feet over Time between Handheld3016 and PMS5003 after Using Calibration Curve

3.4 Preliminary Experimental Procedure

The preliminary experiment procedures are divided into three cases: in case of turning off the air exhaust system (minimal ventilation case or very low ACH), in the case of turning on the air exhaust system at level 3 (medium ventilation case or roughly 40 ACH), and in the case of turning on the air exhaust system at level 6 (high ventilation case or roughly 80 ACH). The experiments are done six times for each case.

3.4.1 Case 1: Turn off air exhaust system (minimal ventilation)

1. Get into the ambulance and close the door

2. Turn on air conditioner at 25 °C with all air grilles at the centre position

3. Install all instruments together as well as install the PMS5003 in the location which is set to be measured

4. Pour 0.9% Sodium Chloride Solution into Aeroneb® Professional Nebulizer unit

จุฬาลงกรณ์มหาวิทยาลัย
Chulalongkorn University

5. Turn on oxylog 3000 plus, choose VC-CMV mode, set tidal volume (VT) to 500 mL, ventilation time ratio (I:E) to 1:2 and adjust respiratory rate (RR) to 12, in order to get inspiratory time (Ti) to be 1.7 seconds

6. Turn on air exhaust system at maximum rate (level 6) for 15 minutes to let the number of particles concentration in the patient compartment return to the background state

7. After finish preconditioning, turn off the air exhaust system and let the air in the patient compartment stabilize for 5 minutes

8. After that, turn on PMS5003 to log data

9. After 3 minutes, turn on Aeroneb® Professional Nebulizer to introduce particles into the patient compartment for 1 minute

10. After that log data for 26 minutes

3.4.2 Case 2: Turn on air exhaust system at level 3 (medium ventilation)

1. Get into the ambulance and close the door

2. Turn on air conditioner at 25 °C with all air grilles at the centre position

3. Install all instruments together as well as install the PMS5003 in the location which is set to be measured

4. Pour 0.9% Sodium Chloride Solution into Aeroneb® Professional Nebulizer unit

5. Turn on oxylog 3000 plus, choose VC-CMV mode, set tidal volume (VT) to 500 mL, ventilation time ratio (I:E) to 1:2 and adjust respiratory rate (RR) to 12, in order to get inspiratory time (Ti) to be 1.7 seconds

จุฬาลงกรณ์มหาวิทยาลัย
Chulalongkorn University

6. Turn on air exhaust system at maximum rate (level 6) for 15 minutes to let the number of particles concentration in the patient compartment return to the background state

7. After finish preconditioning, turn the air exhaust system to medium rate (level 3) and let the air in the patient compartment stabilize for 5 minutes

8. After that, turn on PMS5003 to log data

9. After 3 minutes, turn on Aeroneb® Professional Nebulizer to introduce particles into the patient compartment for 1 minute

10. After that log data for 16 minutes

3.4.3 Case 3: Turn on air exhaust system at level 6 (high ventilation)

1. Get into the ambulance and close the door

2. Turn on air conditioner at 25 ℃ with all air grilles at the centre position

3. Install all instruments together as well as install the PMS5003 in the location which is set to be measured

4. Pour 0.9% Sodium Chloride Solution into Aeroneb® Professional Nebulizer unit

5. Turn on oxylog 3000 plus, choose VC-CMV mode, set tidal volume (VT) to 500 mL, ventilation time ratio (I:E) to 1:2 and adjust respiratory rate (RR) to 12, in order to get inspiratory time (Ti) to be 1.7 seconds

6. Turn on air exhaust system at maximum rate (level 6) for 15 minutes to let the number of particles concentration in the patient compartment return to the background state

จุฬาลงกรณ์มหาวิทยาลัย
Chulalongkorn University

7. After that, turn on PMS5003 to log data

8. After 3 minutes, turn on Aeroneb® Professional Nebulizer to introduce particles into the patient compartment for 1 minute

9. After that log data for 16 minutes

3.5 Experimental Procedure

The experiment procedures are divided into two cases: in case of turning off the air exhaust system (minimal ventilation case or very low ACH) and in the case of

turning on the air exhaust system at level 6 (high ventilation case or roughly 80 ACH). The experiments are done three times for each case.

3.5.1 Case 1: Turn off air exhaust system (minimal ventilation)

1. Get into the ambulance and close the door

2. Turn on air conditioner at 25 ℃ with all air grilles at the centre position

3. Install all instruments together as well as install the PMS5003 in the location which is set to be measured

4. Pour 0.9% Sodium Chloride Solution into Aeroneb® Professional Nebulizer unit

5. Turn on oxylog 3000 plus, choose VC-CMV mode, set tidal volume (VT) to 500 mL, ventilation time ratio (I:E) to 1:2 and adjust respiratory rate (RR) to 12, in order to get inspiratory time (Ti) to be 1.7 seconds

6. Turn on air exhaust system at maximum rate (level 6) for 15 minutes to let the number of particles concentration in the patient compartment return to the background state

7. After finish preconditioning, turn off the air exhaust system and let the air in the patient compartment stabilize for 5 minutes

8. After that, turn on PMS5003 to log data

9. After 1 minutes, turn on Aeroneb® Professional Nebulizer to introduce particles into the patient compartment for 1 minute

10. After that log data for 18 minutes

3.5.2 Case 2: Turn on air exhaust system at level 6 (high ventilation)

1. Get into the ambulance and close the door

2. Turn on air conditioner at 25 °C with all air grilles at the centre position

3. Install all instruments together as well as install the PMS5003 in the location which is set to be measured

4. Pour 0.9% Sodium Chloride Solution into Aeroneb® Professional Nebulizer unit

5. Turn on oxylog 3000 plus, choose VC-CMV mode, set tidal volume (VT) to 500 mL, ventilation time ratio (I:E) to 1:2 and adjust respiratory rate (RR) to 12, in order to get inspiratory time (Ti) to be 1.7 seconds

6. Turn on air exhaust system at maximum rate (level 6) for 15 minutes to let the number of particles concentration in the patient compartment return to the background state

7. After that, turn on PMS5003 to log data

8. After 1 minutes, turn on Aeroneb® Professional Nebulizer to introduce particles into the patient compartment for 1 minute

9. After that log data for 8 minutes

3.6 Data Analysis

The value obtained from PMS5003 particle counter is the number of particles per unit volume in each particle size bin. According to the research, association of airborne virus infectivity and survivability with its carrier particle size (Zuo et al.,

2013), it was found that the carrier capacity of various particles depends not only on the number of particles, but equally important on the particle size, which affects the number of pathogens, viruses, and microorganisms directly. Larger particles can contain large amounts of pathogens, viruses, and microorganisms, and vice versa, smaller particles can contain small amounts of pathogens, viruses, and microorganisms. Therefore, volume concentration (in μL per cubic meter of air) is used in this research. The volume concentration in this unit can be determined by assuming that every particle is a spherical shape, then multiplying number of particles with volume of a particle using mean diameter (μm) in each size bin, multiplying with one thousand to change the unit to microlitre (μL), and dividing by 0.028317 for changing cubic feet of air to cubic meter of air. These relations can be summed up as the following equation.

$$\sigma = 4.71\times10^{-8}N\pi r^{3}$$

where σ is volume concentration ($\mu L/m^3$)

N is number of particles ($1/ft^3$)

r is mean radius in each size bin (μm)

จุฬาลงกรณ์มหาวิทยาลัย
CHULALONGKORN UNIVERSITY

Although the particle size distribution of aerosol particle is likely a log-normal distribution (Yali et al., 2020), the mean radius in the equation above is chosen based on a simple uniform-in-size aerosol particle size distribution due to our instrument limitation in determining the standard deviation that is important in specifying the exact log-normal size distribution for our particle cloud. For example in a log-normal distribution changing the standard deviation from 0.5 to 0.75 and 1, the resulting means are practically the same as that of the normal distribution in the size range of 0.5-1 micron, 1-2.5 micron, and 2.5-5 micron.

For the preliminary results, the particle number concentration data obtained experimentally from the three seat positions are calibrated against Handheld3016 and converted to volume concentrations by the above equation; the code for these processes are shown in appendix E. It is then interpreted as three types of results: mean aerosol volume concentration over time, maximum volume concentration, and mean volume concentration. The volume concentration over time are plots to see how long concentration took to return to the background concentration value, as well as the rate of increase and decrease of volume concentration. The maximum volume concentration is the maximum value during 30 minutes for the minimal ventilation case, and 19 minutes for the medium and maximum ventilation case. The mean volume concentration is determined by summing the aerosol volume concentration in each size bin and then averaging the total volume concentration over 19 minutes (starting measurement 3 minutes before start introducing aerosol particle into the patient compartment).

For the research results, the measured data with pms5003 obtained as particle number concentration, concentration in all 200 measured positions are calibrated and converted to volume concentration as in the case of preliminary result. As the measurement is done in set of multiple of experiments where not all positions are measured at the same time, interpolation is done using cubic spline whenever data is needed at an exact location either in time or space, the code is included in appendix F.

จุฬาลงกรณ์มหาวิทยาลัย
Chulalongkorn University

Volume concentration values which obtained for each period are then taken to a window moving average for removing the noise; the code is shown in appendix G, after that cubic spline interpolation is performed again in all three dimensions to increase the resolution of the data for further analysis, this will increase the number of nodes from 200 to 12558 nodes. The spacing of each node is 4 cm on all axes as shown in Figure 66. After that, the concentration in all nodes is subtracted by the

background concentration value, which is the average concentration of each point from first second to 59th second. Finally, the values in the form of the comma-separated values (CSV) file are converted to visualization toolkit (VTK) file via code in appendix H for further analysis in ParaView which is an open-source visualization and data analysis tool. The results are divided into 7 major topics: three-dimensional visualization, horizontal contour plane at EMS workers' face level, vertical contour plane at injection position along patient cot, spatial-averaged aerosol volume concentration over time, aerosol volume concentration over time at EMS workers' face, maximum aerosol volume concentration at EMS workers' face, and temporal-averaged aerosol volume concentration at EMS workers' face. Details of the results for each topic are discussed in Chapter 5.

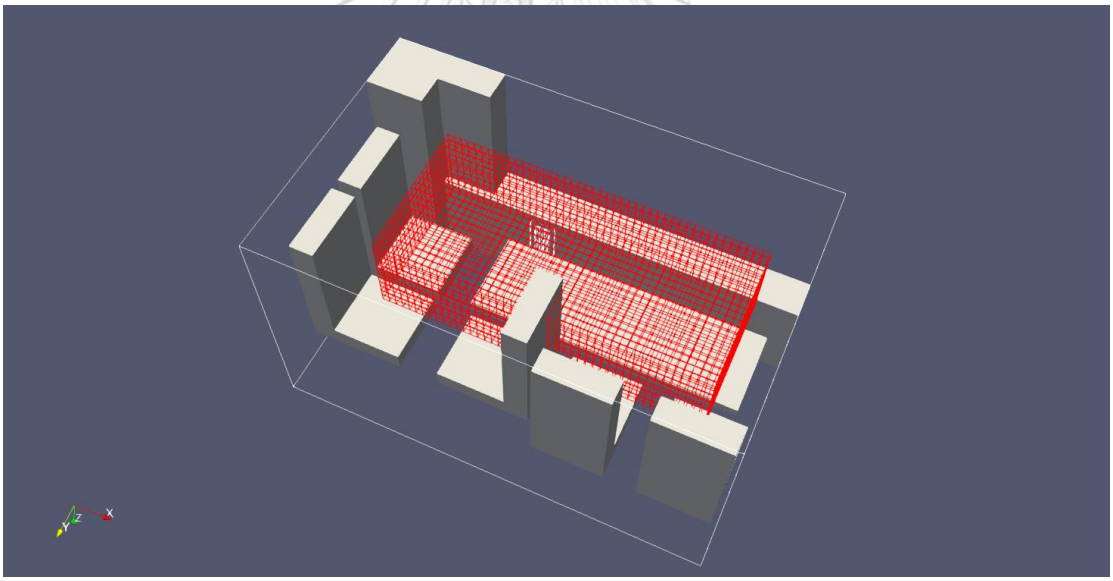

Figure 66 Refine Grid (12558 Points)

CHAPTER 4

PRELIMINARY RESULTS

This chapter is part of the experimental results from the preliminary experimental steps of chapter 3. The results of this chapter are divided into three main sections: return to background-state time, maximum aerosol volume concentration (the highest value in 30 minutes for minimal ventilation case (very low ACH) and 20 minutes for medium (roughly 40 ACH) and high ventilation case (roughly 80 ACH)), and mean aerosol volume concentration over 20 minutes. The results in each section can be divided according to three measurement locations: seat 1, seat 2, and seat 3 with three levels of ventilation: off, medium, and high. All seat positions in this chapter refer to Figure 33. A further plot of the results in this chapter can be found in appendix I.

4.1 Return to Background-State Time

The background state value is the average concentration values in the period before the injection is started. The time to return to the background-state concentration after starting the particles injection can be summarized as follows:

Table 2 Time to Return to the Background-State Concentration in a Second Unit at Seat 1

Seat 1			
Ventilation Rate / Size Range (micron)	Off	Medium	High
0.5-1	840	360	260
1-2.5	860	360	260
2.5-5	810	360	280

Table 3 Time to Return to the Background-State Concentration in a Second Unit at Seat 2

Seat 2			
Ventilation Rate / Size Range (micron)	Off	Medium	High
0.5-1	880	340	260
1-2.5	860	360	260
2.5-5	760	340	270

Table 4 Time to Return to the Background-State Concentration in a Second Unit at Seat 3

Seat 3			
Ventilation Rate / Size Range (micron)	Off	Medium	High
0.5-1	760	360	280
1-2.5	760	380	260
2.5-5	660	370	260

จุฬาลงกรณ์มหาวิทยาลัย
CHULALONGKORN UNIVERSITY

From Table 2, Table 3, and Table 4, we can see that the aerosol volume concentration after starting the particles injection takes more or less time to return to the background state, depending mostly on the ventilation rate. The results for all positions and all size ranges combined show that it takes approximately 800 seconds at minimal ventilation rate, 360 seconds at medium ventilation rate, and about 260 seconds at maximum ventilation rate.

4.2 Maximum Aerosol Volume Concentration

4.2.1 Size range between 0.5 and 1 micron

At seat 1, maximum aerosol volume concentration at minimal ventilation rate is 0.049441211 $\mu L/m^3$ (standard deviation, SD = 3.41%), at medium ventilation rate is 0.038015593 $\mu L/m^3$ (SD = 10.29%), and at maximum ventilation rate is 0.03579140 $\mu L/m^3$ (SD = 3.85%).

At seat 2, maximum aerosol volume concentration at minimal ventilation rate is 0.054777542 $\mu L/m^3$ (SD = 4.09%), at medium ventilation rate is 0.047530166 $\mu L/m^3$ (SD = 4.41%), and at maximum ventilation rate is 0.04363647 $\mu L/m^3$ (SD = 4.91%).

At seat 3, maximum aerosol volume concentration at minimal ventilation rate is 0.043374268 $\mu L/m^3$ (SD = 5.13%), at medium ventilation rate is 0.031284951 $\mu L/m^3$ (SD = 4.73%), and at maximum ventilation rate is 0.041191841 $\mu L/m^3$ (SD = 3.52%).

4.2.2 Size range between 1 and 2.5 micron

At seat 1, maximum aerosol volume concentration at minimal ventilation rate is 0.103323377 $\mu L/m^3$ (SD = 3.07%), at medium ventilation rate is 0.075161071 $\mu L/m^3$ (SD = 12.76%), and at maximum ventilation rate is 0.071581085 $\mu L/m^3$ (SD = 5.52%).

จุฬาลงกรณ์มหาวิทยาลัย
Chulalongkorn University

At seat 2, maximum aerosol volume concentration at minimal ventilation rate is 0.119153215 $\mu L/m^3$ (SD = 3.74%), at medium ventilation rate is 0.096802686 $\mu L/m^3$ (SD = 4.36%), and at maximum ventilation rate is 0.08790387 $\mu L/m^3$ (SD = 6.88%).

At seat 3, maximum aerosol volume concentration at minimal ventilation rate is 0.088897049 $\mu L/m^3$ (SD = 5.12%), at medium ventilation rate is 0.0644736 $\mu L/m^3$ (SD = 5.52%), and at maximum ventilation rate is 0.093860957 $\mu L/m^3$ (SD = 4.22%).

4.2.3 Size range between 2.5 and 5 micron

At seat 1, maximum aerosol volume concentration at minimal ventilation rate is 0.232673959 $\mu L/m^3$ (SD = 20.55%), at medium ventilation rate is 0.164921218 $\mu L/m^3$ (SD = 30.22%), and at maximum ventilation rate is 0.158213079 $\mu L/m^3$ (SD = 10.61%).

At seat 2, maximum aerosol volume concentration at minimal ventilation rate is 0.271465357 $\mu L/m^3$ (SD = 17.20%), at medium ventilation rate is 0.212237675 $\mu L/m^3$ (SD = 15.63%), and at maximum ventilation rate is 0.185901927 $\mu L/m^3$ (SD = 17.14%).

4.4 Mean Aerosol Volume Concentration

4.3.1 Size range between 0.5 and 1 micron

At seat 1, mean aerosol volume concentration at minimal ventilation rate is 0.010635349 $\mu L/m^3$ (SD = 1.93%), at medium ventilation rate is 0.00392927 $\mu L/m^3$ (SD = 6.39%), and at maximum ventilation rate is 0.003064489 $\mu L/m^3$ (SD = 1.63%).

จุฬาลงกรณ์มหาวิทยาลัย
Chulalongkorn University

At seat 2, mean aerosol volume concentration at minimal ventilation rate is 0.014620139 $\mu L/m^3$ (SD = 3.37%), at medium ventilation rate is 0.005454018 $\mu L/m^3$ (SD = 3.58%), and at maximum ventilation rate is 0.00416486 $\mu L/m^3$ (SD = 2.75%).

At seat 3, mean aerosol volume concentration at minimal ventilation rate is 0.010047908 $\mu L/m^3$ (SD = 1.98%), at medium ventilation rate is 0.003987922 $\mu L/m^3$ (SD = 2.84%), and at maximum ventilation rate is 0.004295735 $\mu L/m^3$ (SD = 2.23%).

4.3.2 Size range between 1 and 2.5 micron

At seat 1, mean aerosol volume concentration at minimal ventilation rate is 0.01886851 μL/m^3 (SD = 2.91%), at medium ventilation rate is 0.007504381 μL/m^3 (SD = 7.40%), and at maximum ventilation rate is 0.006034162 μL/m^3 (SD = 2.90%).

At seat 2, mean aerosol volume concentration at minimal ventilation rate is 0.026491041 μL/m^3 (SD = 4.28%), at medium ventilation rate is 0.010526544 μL/m^3 (SD = 5.57%), and at maximum ventilation rate is 0.008071205 μL/m^3 (SD = 5.98%).

At seat 3, mean aerosol volume concentration at minimal ventilation rate is 0.017844697 μL/m^3 (SD = 2.57%), at medium ventilation rate is 0.007461255 μL/m^3 (SD = 4.38%), and at maximum ventilation rate is 0.009000734 μL/m^3 (SD = 4.55%).

4.3.3 Size range between 2.5 and 5 micron

At seat 1, mean aerosol volume concentration at minimal ventilation rate is 0.038820502 μL/m^3 (SD = 15.44%), at medium ventilation rate is 0.017845471 μL/m^3 (SD = 18.23%), and at maximum ventilation rate is 0.015183931 μL/m^3 (SD = 15.12%).

จุฬาลงกรณ์มหาวิทยาลัย
Chulalongkorn University

At seat 2, mean aerosol volume concentration at minimal ventilation rate is 0.047651422 μL/m^3 (SD = 11.51%), at medium ventilation rate is 0.024641207 μL/m^3 (SD = 15.71%), and at maximum ventilation rate is 0.018391762 μL/m^3 (SD =7.02%).

At seat 3, mean aerosol volume concentration at minimal ventilation rate is 0.033506952 μL/m^3 (SD = 16.06%), at medium ventilation rate is 0.016129081 μL/m^3 (SD = 9.13%), and at maximum ventilation rate is 0.022500604 μL/m^3 (SD = 10.67%).

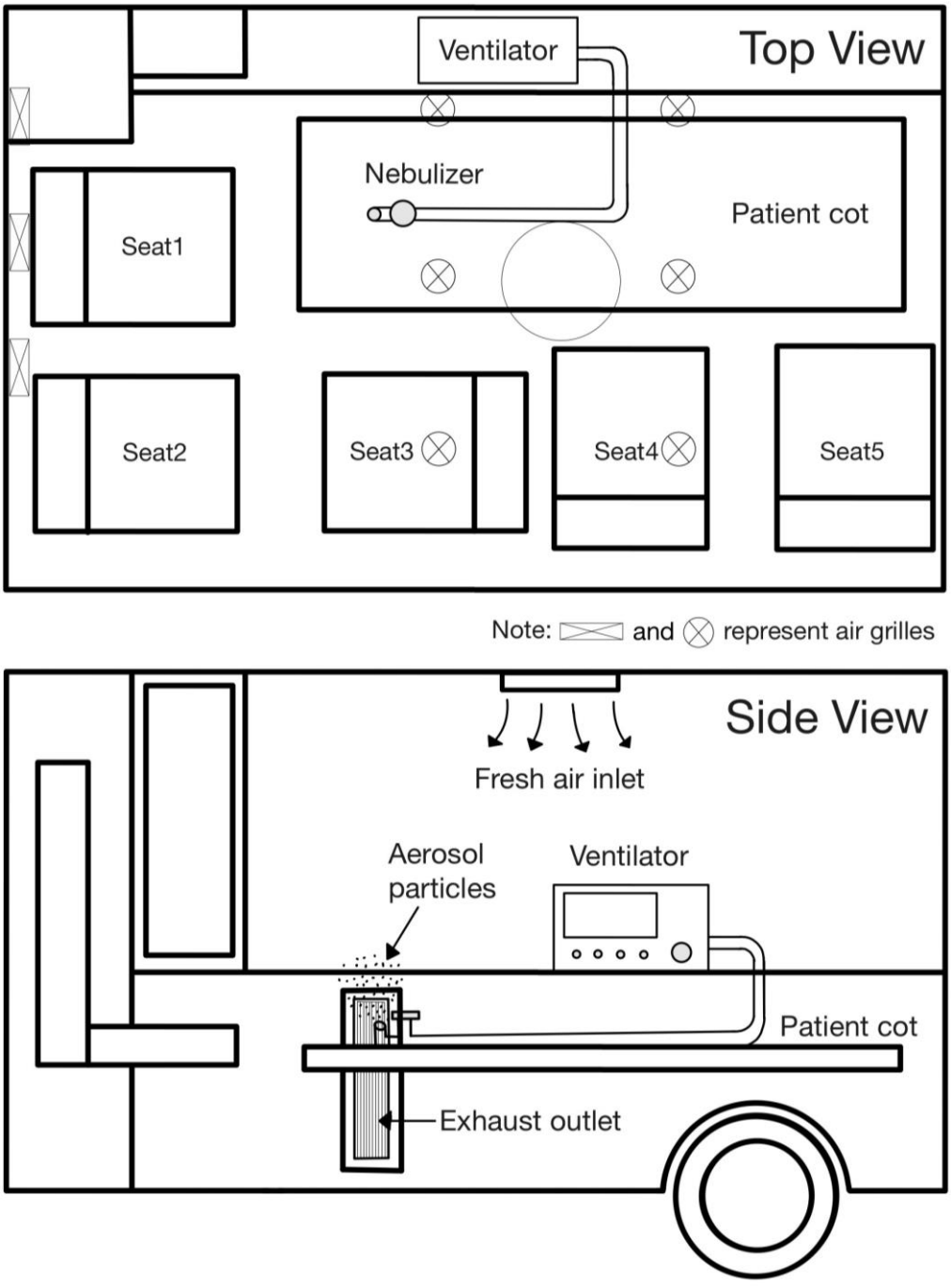

Figure 67 Ambulance Patient Compartment

CHAPTER 5
RESULTS

This chapter describes results of this research. The results are divided into 6 topics: 5.1) Three-dimensional visualization of aerosol volume concentration by means of volume rendering, 5.2) The concentration on the horizontal plane positioned at EMS workers' face level (32.2 cm. from top of the patient compartment), 5.3) The concentration on the vertical plane at injection position along patient cot (55 cm. from the right of the patient compartment), 5.4) Aerosol volume concentration that is averaged over the entire measurement space over time, 5.5) Aerosol volume concentration over time at EMS workers' face, 5.6) Maximum aerosol volume concentration at EMS workers' face, and 5.7) Temporal-averaged aerosol volume concentration at EMS workers' face. The ventilation rates mentioned in this chapter are divided into two cases: minimal ventilation (very low ACH), which denoted by "MV", and high ventilation (approximately 80 ACH), denoted by "HV". All seat positions in this chapter refer to Figure 67.

The coefficient of variation (standard deviation divided by mean) of the PMS5003 from all experiments and locations combined is close to 10 percent, 12 percent, and 25 percent for the 0.5-1-, 1-2.5-, and 2.5-5-micron size ranges, respectively.

จุฬาลงกรณ์มหาวิทยาลัย
Chulalongkorn University

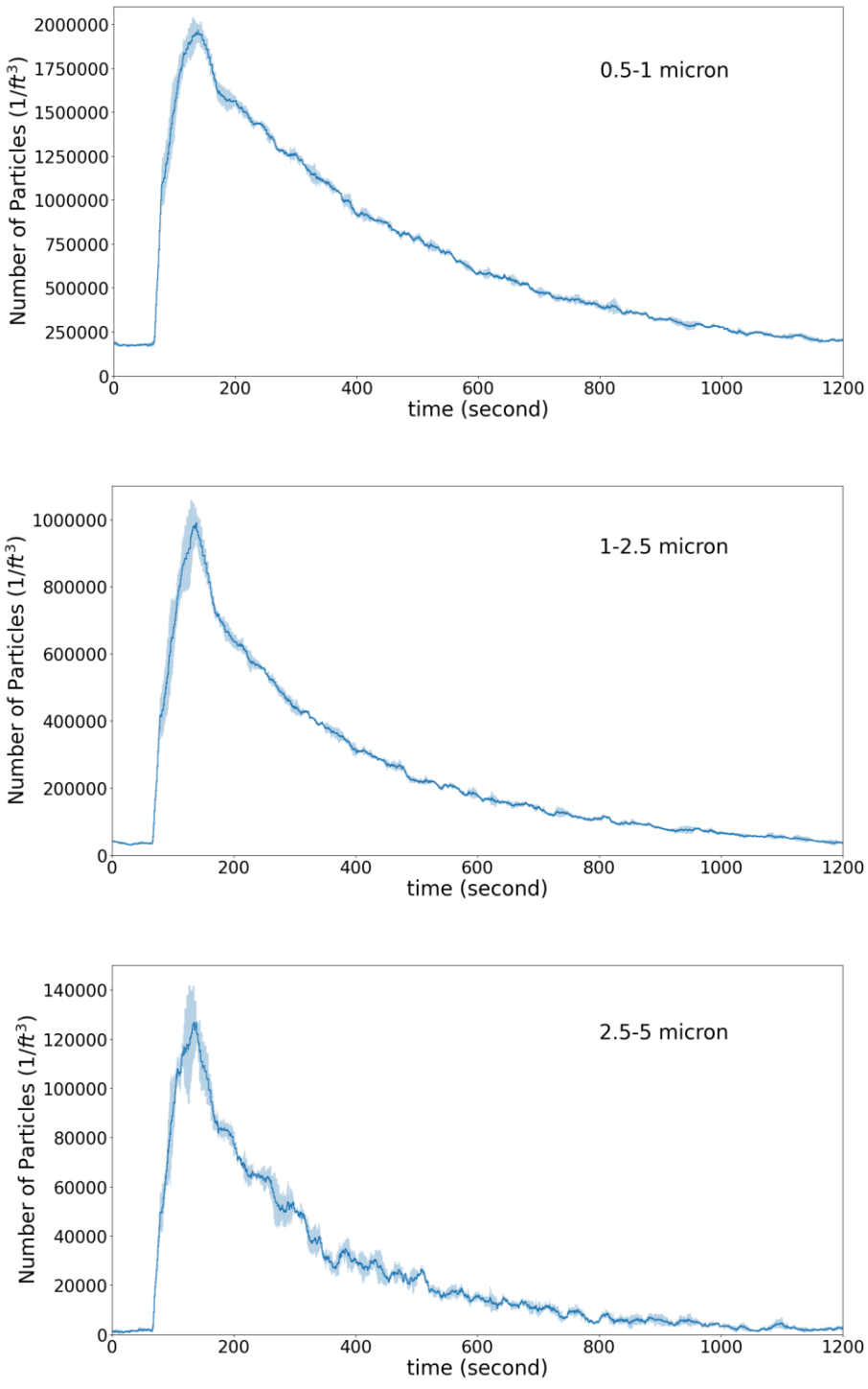

Figure 68 An Example of Mean Number of Particles over Time at a Position. The Line Shows the Ensemble Mean of Three Experiments. A Vertical Line on top of the Mean Values Represents Standard Deviation of the Collected Data at that Point in Time.

5.1 Three-Dimensional Visualization

For interpretation of the results in this section, concentration values higher than 10^{-6} μL/m^3 are considered to be the presence of particles in the considered control volume. The maximum concentration values in the colormap are the maximum values which occur in each size range and ventilation rate. Modifying the colormap's range yields different contour in terms of its visibility but the interpretation of the results that follow remains unchanged.

5.1.1 Size range between 0.5 and 1 micron

Figure 69 shows a set of volume renderings of aerosol volume concentration of 0.5-1-micron size range of the MV case. Looking at subfigure (a), it can be seen that the first region where the concentration is becoming noticeable after starting particle injection (t = 60 sec) is right above the injection or the area above the patient's face. Thereafter, the concentration at this particular region is higher and distributes over a wider area, particularly at seat 1, and especially the side adjacent to the air exhaust system outlet which can be observed in subfigure (b). The concentration continues to rise and the distribution area (observable from the chosen contour level) is wider as shown in subfigure (c). However, the high concentration remains in the same region as the previous period. Until shortly after the stop of particle injection, peak concentration occurs (to be elaborated quantitatively afterward) and the high concentration maintains a wider area distribution across the control volume, which can be seen in subfigure (d). After that, the concentration begins to decrease, especially in the high concentration area compared to the other regions until the high concentration distributes across the control volume to almost uniform, as observed in subfigure (e). Finally, the concentration throughout the control volume is comparable to that of the background state as shown in subfigure (f).

จุฬาลงกรณ์มหาวิทยาลัย
CHULALONGKORN UNIVERSITY

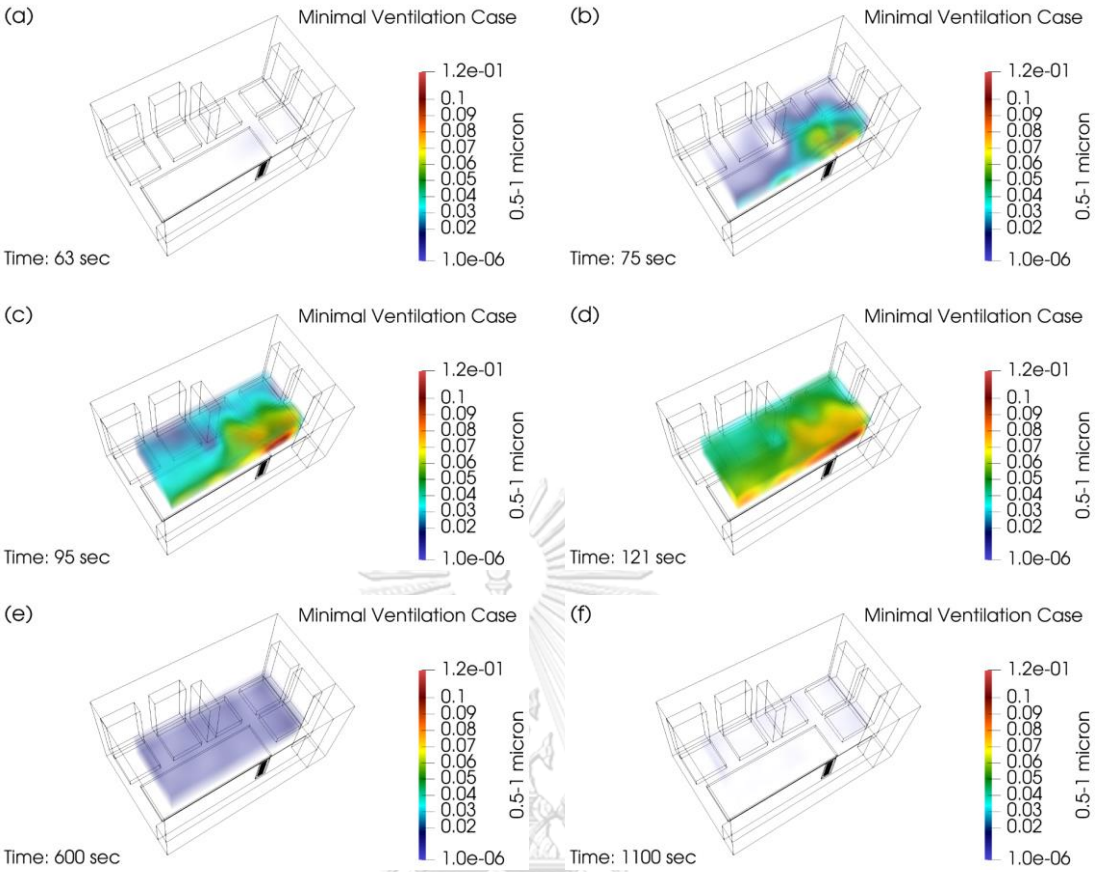

Figure 69 Volume Rendering of Aerosol Volume Concentration in the Size Range between 0.5 and 1 Micron of the Minimal Ventilation Case (MV). The Subfigures are Sorted, (a) - (f), by Time Since the Beginning of Experiment and to Recall, the Aerosol Injection Starts at t = 60 sec.

จุฬาลงกรณ์มหาวิทยาลัย
Chulalongkorn University

Figure 70 shows a set of volume renderings of aerosol volume concentration of 0.5-1-micron size range for the HV case. High concentration relative to other sites begins to be observed a few seconds after the initiation of particle injection (t = 60 sec) in the area above the patient's face, which can be seen in subfigure (a). After that, the concentration increases and the distribution area of the high concentration compared to that of subfigure (a) is wider, especially in the area that corresponds to the outlet of the air exhaust system, including seat 1, seat 2, seat 3, and at the end of the patient cot which can be seen from subfigure (b). From subfigure (c), the overall concentration in control volume is higher and high concentration spread over

a larger area comparing to subfigure (b). The area of the higher concentration compared to the other regions in subfigure (c) remains in the same area as in subfigure (b). The highest concentration is reached at about 121st second, with the highest concentration relative to the surrounding area remaining at the outlet as shown in subfigure (d). Thereafter, concentration throughout the control volume declines, especially in the higher concentration regions, and decreases until concentration is almost uniform across the control volume, as shown in subfigure (e) and the concentration decreases until it is finally comparable to the background state, which can be seen from subfigure (f).

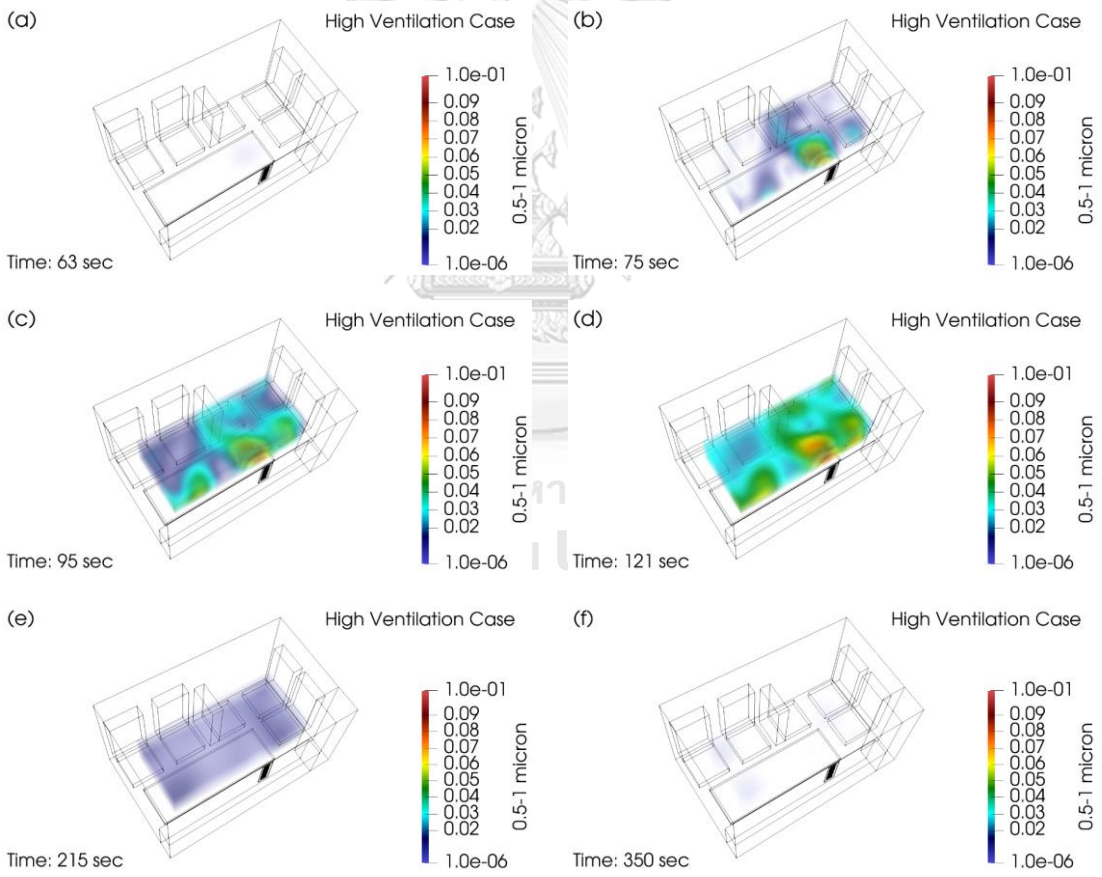

Figure 70 Volume Rendering of Aerosol Volume Concentration in the Size Range between 0.5 and 1 Micron of the High Ventilation Case (HV). The Subfigures are Sorted, (a) - (f), by Time Since the Beginning of Experiment and to Recall, the Aerosol Injection Starts at t = 60 sec.

5.1.2 Size range between 1 and 2.5 micron

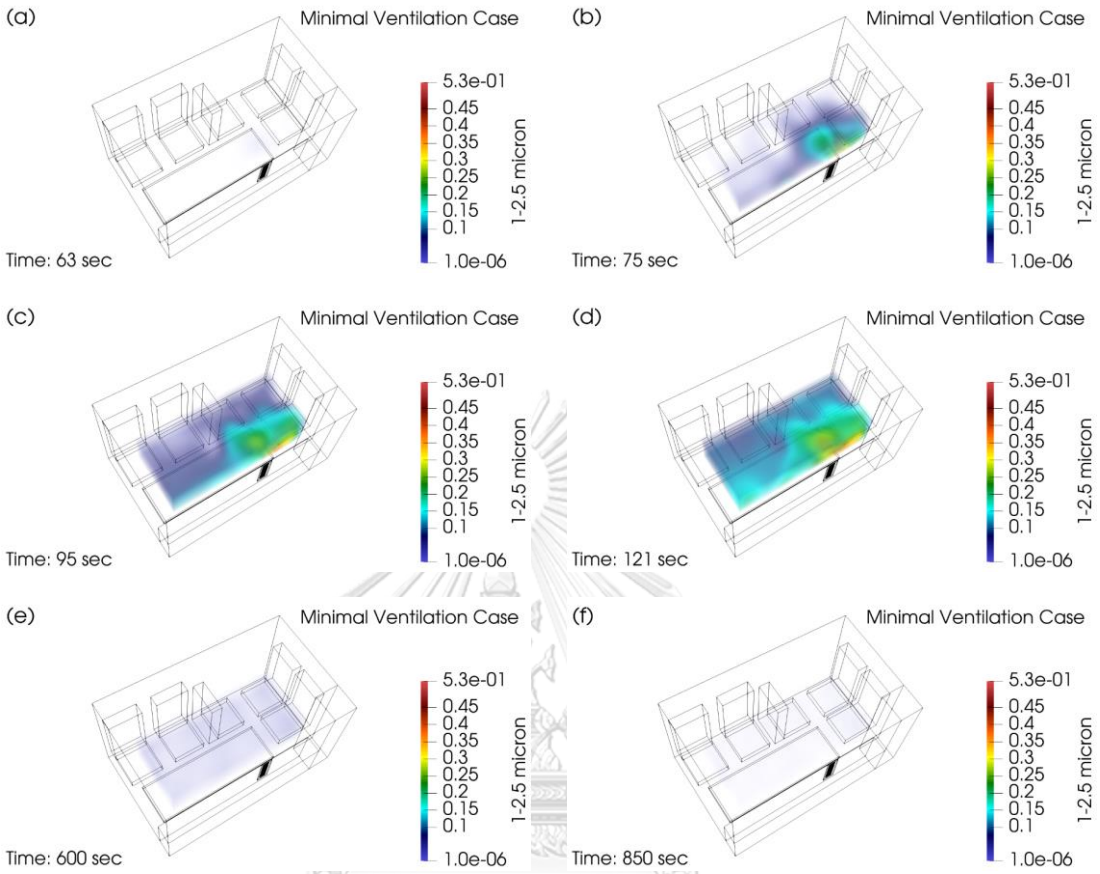

Figure 71 Volume Rendering of Aerosol Volume Concentration in the Size Range between 1 and 2.5 Micron of the Minimal Ventilation Case (MV). The Subfigures are Sorted, (a) - (f), by Time Since the Beginning of Experiment and to Recall, the Aerosol Injection Starts at t = 60 sec.

Figure 71 shows set of volume renderings of aerosol volume concentration of 1-2.5-micron size range of the MV case. Concentrations begins to noticeably increase after initiation of particle injection (t = 60 sec) in the region above the injection position or above patient's face as shown in subfigure (a). Thereafter, the concentration at this area is higher and the distributions of these concentration areas are larger (at least, with respect to the chosen colormap), especially above the patient's face and at seat 1 position, which can be seen in subfigure (b). As shown in

subfigure (c), the area of higher concentration relative to the other regions at the same time remains in the same region as in subfigure (b). Concentration continues to increase until peak concentration is reached at 121 second, as shown in subfigure (d). Thereafter, the concentration begins to decrease simultaneously in many areas, especially in areas with high concentration value relative to other areas, until the concentration distribution is almost uniform within the control volume as shown in subfigure (e), and the concentration is finally comparable to the background which can be seen from subfigure (f).

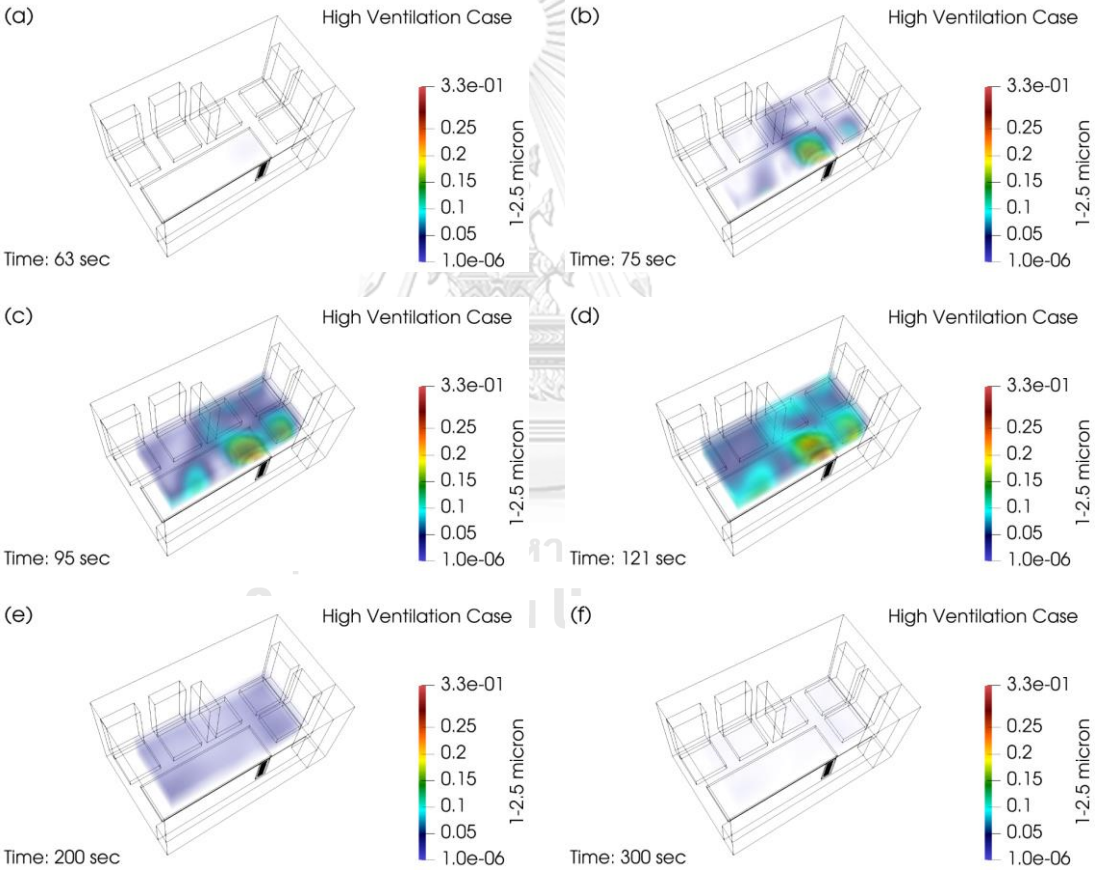

Figure 72 Volume Rendering of Aerosol Volume Concentration in the Size Range between 1 and 2.5 Micron of the High Ventilation Case (HV). The Subfigures are Sorted, (a) - (f), by Time Since the Beginning of Experiment and to Recall, the Aerosol Injection Starts at t = 60 sec.

Figure 72 shows a set of volume renderings of aerosol volume concentration of 1-2.5-micron size range of the HV case. The observable concentration still occurs after particle injection (t = 60 sec) in the same region as in the previous size range which can be observed in subfigure (a). Concentration at this location is higher and the areas of high concentration relative to other regions more extensively distribute to seat 1, seat 2, and seat 3 regions, and the highest concentration area is found in the location corresponding to the air exhaust system outlet, as shown in subfigure (b). Onward from subfigure (c), the concentration still increases from the previous period and distributes almost across the control volume, with a high concentration region compared to the other regions close to the area in the previous period, with higher concentration. The concentration increases until after particle injection is stopped for 1 second, the highest concentration occurs at this time. Concentration at the seat 1, seat 2, seat 3, and at the foot of the patient cot is higher compared to the subfigure (c) but the area of the highest concentration remains in the same area as before (adjacent to the outlet), which can be seen in subfigure (d). Thereafter, the concentration begins to decrease until it is almost uniform (at least, with respect to the chosen contour level) across the control volume and finally comparable to the background state as shown in subfigure (e) and subfigure (f), respectively.

จุฬาลงกรณ์มหาวิทยาลัย
Chulalongkorn University

5.1.3 Size range between 2.5 and 5 micron

Figure 73 shows set of volume renderings of aerosol volume concentration of 2.5-5-micron size range of the MV case. Detectable concentration occurs in the area above the patient's face after the particle injection (t = 60 sec) as observed in subfigure (a). Concentration in this specific region begins to increase and spread over a larger area in the area above patient’s face area and seat 1 region, as can be seen from subfigure (b) and subfigure (c). Until 121st second shown in subfigure (d), the highest concentration occurs and the concentration value is higher and distributes across the control volume. However, the high concentration remains in the same

region as the previous period (adjacent to the outlet). Thereafter, the concentration decreases gradually, with the most decreasing region being the region of high concentration relative to the other regions until the concentration is almost uniform across the control volume, as shown in subfigure (e), and finally comparable to the background state, as can be seen from subfigure (f).

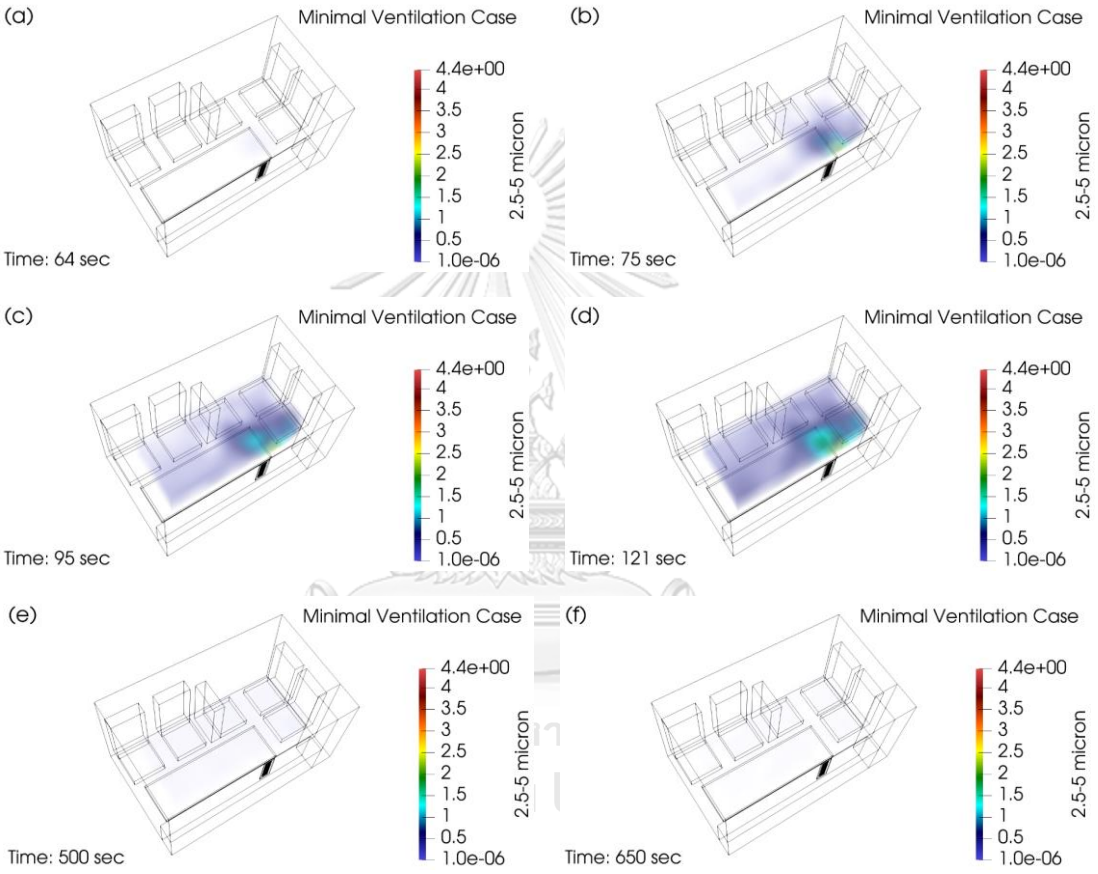

Figure 73 Volume Rendering of Aerosol Volume Concentration in the Size Range between 2.5 and 5 Micron of the Minimal Ventilation Case (MV). The Subfigures are Sorted, (a) - (f), by Time Since the Beginning of Experiment and to Recall, the Aerosol Injection Starts at t = 60 sec.

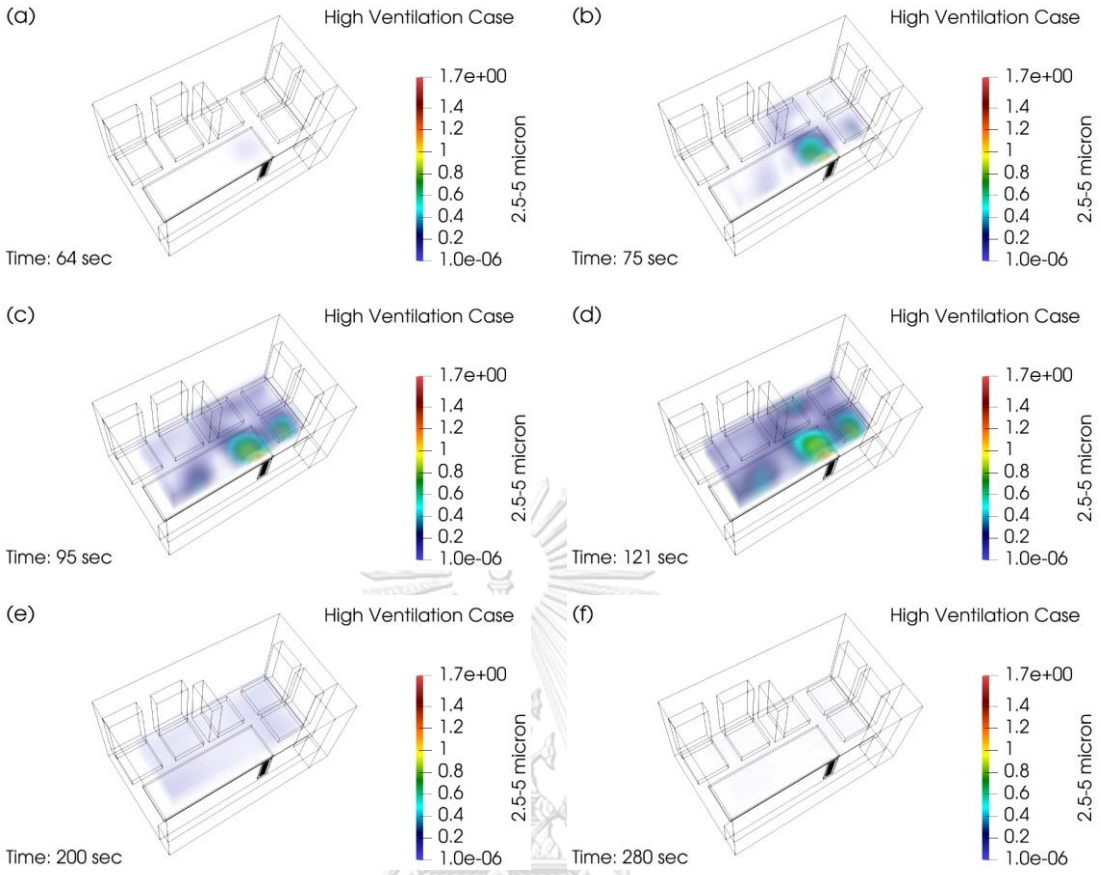

Figure 74 Volume Rendering of Aerosol Volume Concentration in the Size Range between 2.5 and 5 Micron of the High Ventilation Case (HV). The Subfigures are Sorted, (a) - (f), by Time Since the Beginning of Experiment and to Recall, the Aerosol Injection Starts at t = 60 sec.

จุฬาลงกรณ์มหาวิทยาลัย
Chulalongkorn University

Figure 74 shows a set of volume renderings of aerosol volume concentration of 2.5-5-micron size range of the HV case. From subfigure (a), higher concentration compared to other areas after initiation of particle injection (t = 60 sec) occurs in the area above the patient's face. Concentration value begins to rise and the distribution area becomes wider as shown in subfigure (b), with the highest concentration relative to the other areas still above the patient's face toward outlet of air exhaust system. The increase concentration distributes over a wide area almost throughout the control volume, with the markedly high concentration area compared to others being located above the patient's face toward the outlet, and in the seat 1 as shown

in subfigure (c). Until peak concentration occurs 1 second after the stop of particle injection, high concentration relative to the surrounding area occurs in the same area as in subfigure (c), which can be seen in subfigure (d). Thereafter, the concentration decreases until the concentration values are nearly equal across the control volume (at least, with respect to the chosen contour level), as shown in subfigure (e), and the concentration is finally comparable to the background state which can be seen in subfigure (f).

5.2 Horizontal Contour Plane at Face Level of EMS workers

This section presents concentration contour on the horizontal plane at face position of the ambulance personnel working in the ambulance at different times. The results are divided into three sections according to particles in the size range: 0.5-1 micron, 1-2.5 micron, and 2.5-5 micron.

5.2.1 Size range between 0.5 and 1 micron

Figure 75 to Figure 81 and Figure 86 to Figure 91 show the contours of the aerosol volume concentration for MV and HV cases at the face level of the EMS workers in the ambulance at each time interval. Subfigure (a) and subfigure (b) show colormaps that compare with the background value at the start of the measurement or at the zeroth second, in order to investigate the change in the concentration in comparison to when it started. Subfigure (c) and (d) help indicate the location of high concentration at that time. The period of time when the change in concentration is not visible relative to the background state colormap is shown in Figure 82 to Figure 85. For contours at time intervals greater than 600^{th} second, the time interval after the termination of the HV case, are shown in Figure 92 to Figure 96, where subfigure (a) shows a colormap relative to the background state and subfigure (b) is a visible range colormap for each time period of the MV case.

จุฬาลงกรณ์มหาวิทยาลัย
Chulalongkorn University

For the start, zeroth second is at which the measurement is started. The contours of this time are displayed in Figure 75. It can be seen that the overall picture of concentration in the case of MV is higher than in the case of HV due to the presence of particles outside the ambulance entering the leak area in the process of letting the air stabilize while the air exhaust system is turned off. Although the HV case results in more particles entering the patient compartment than the MV case, since the MV case does not have the same particle reduction capability as in the HV case; as a result, the background concentration of the MV case is thus higher. Figure 76 shows the contours when particles injection is initiated. It is found that the concentration and the distribution are not much different from Figure 75 in both MV and HV cases. Concentration on this plane begins to rise abruptly at 64^{th} second shown in Figure 77, with the peak concentration in the case of MV being approximately twice higher than the HV case. However, the peak concentrations in both cases occur in the same area which is the area above the patient's face. Figure 78 shows the distribution on plane at 66^{th} second. For the MV case, the concentration mainly distributes to seat1 and slightly distributes to seat2, seat3, and seat4. In the case of HV case, the concentration mainly distributes to seat4. After that, at 68^{th} second shown in Figure 79, the concentration distribution area is wider in the front of the patient compartment for the MV case, while for the HV case the distribution area is large but in the centre of the patient compartment. In the 74^{th} second, the MV concentration distributes to all seat locations and nearly distributes across the entire plane relative to the background state colormap. In the case of the HV, the distribution area is narrower than the MV case, with minimal distribution to seat 5. These can be seen from Figure 80.

If we look at the Figure 78 to Figure 80, while the peak concentration still occurs in the position above the patient's face explained previously, relative high concentration compared to the background state colormap diffuses to seat1 and seat2 for MV case and to seat4 for HV case. Until the 84^{th} second shown in Figure 81,

จุฬาลงกรณ์มหาวิทยาลัย
Chulalongkorn University

the concentration is relatively large (compared to the background state colormap) across the entire plane. However, the concentration continues to rise, noticeable in the snapshot at 107th second as shown in Figure 82.

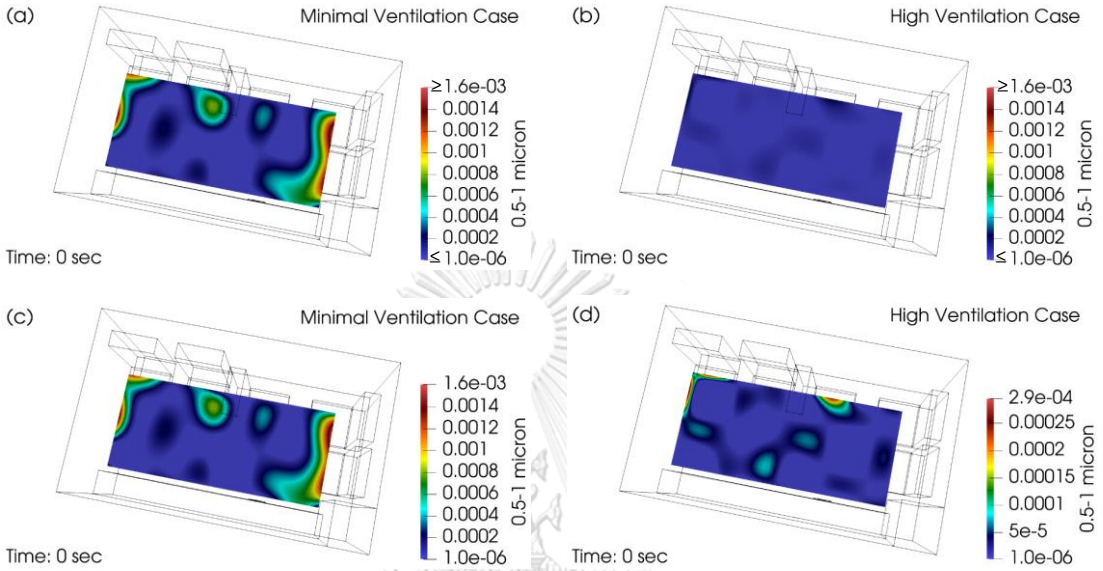

Figure 75 Contour Plane at EMS workers' Face Level at time = 0 second of Minimal Ventilation and High Ventilation with Different Colormap Ranges

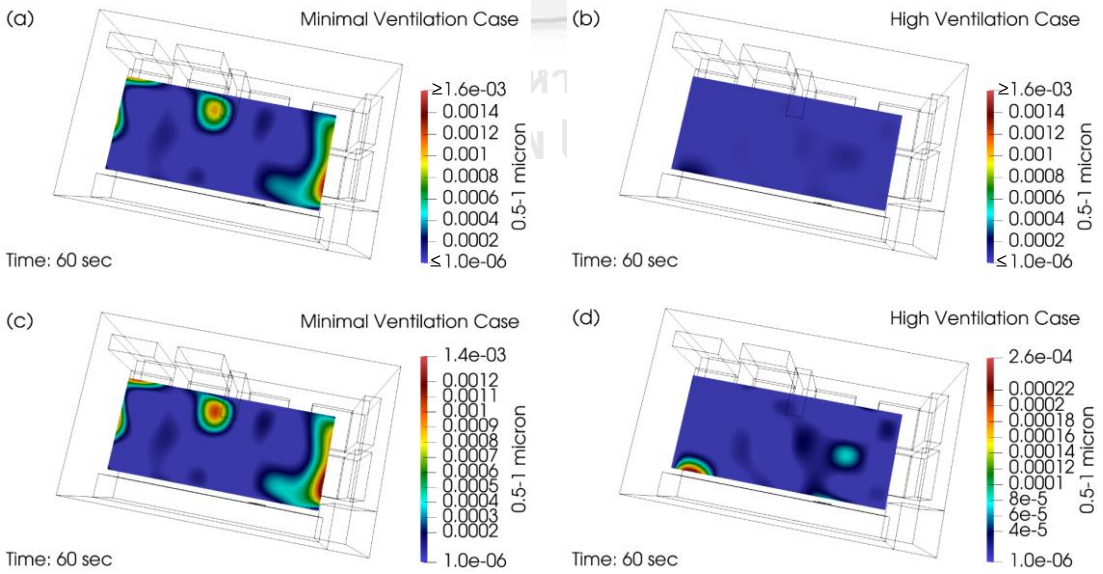

Figure 76 Contour Plane at EMS workers' Face Level at time = 60 second of Minimal Ventilation and High Ventilation with Different Colormap Ranges

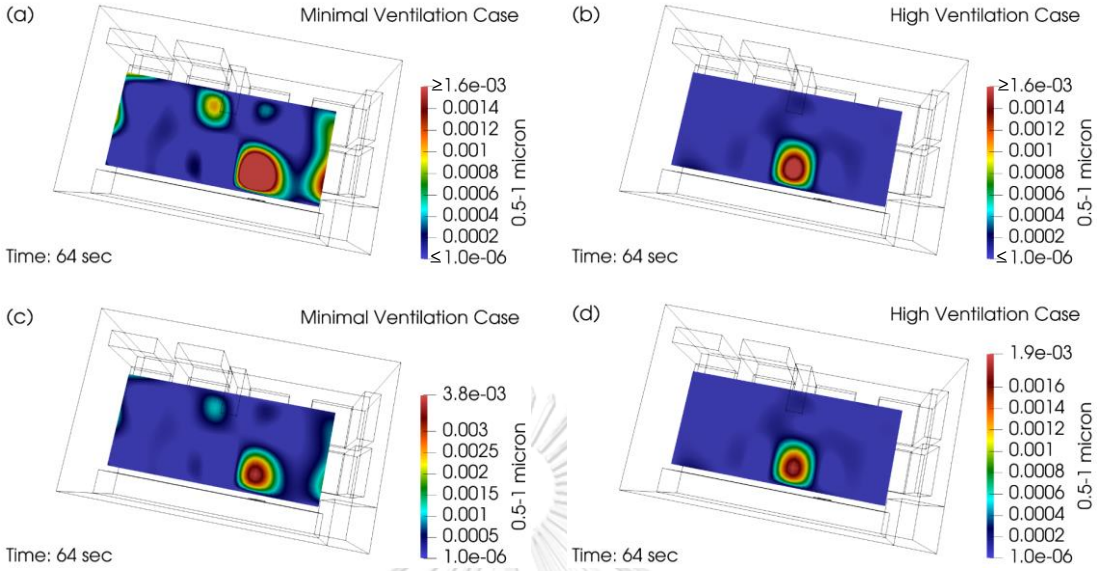

Figure 77 Contour Plane at EMS workers' Face Level at time = 64 second of Minimal Ventilation and High Ventilation with Different Colormap Ranges

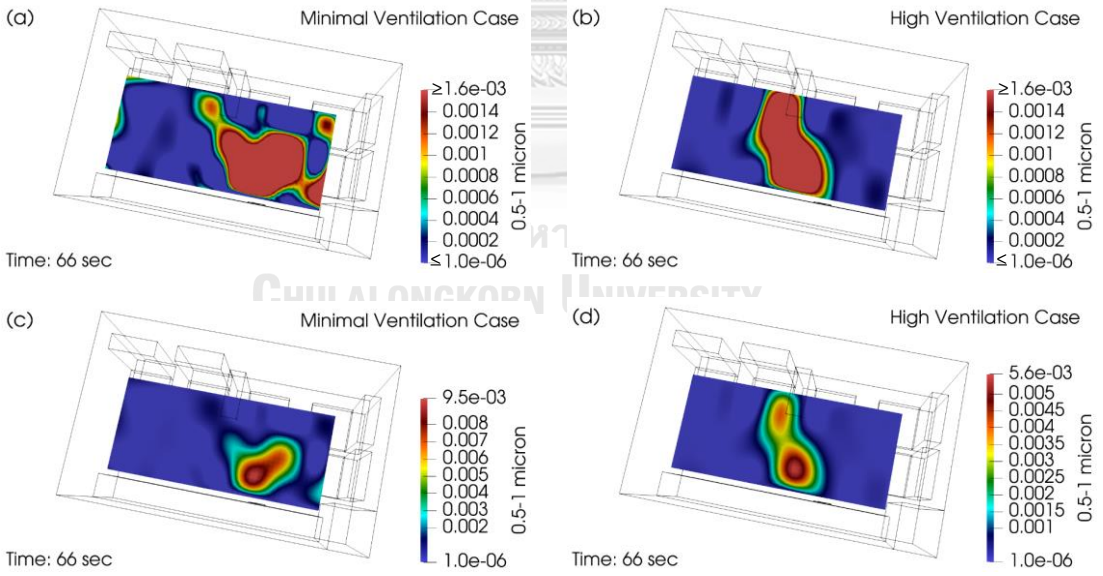

Figure 78 Contour Plane at EMS workers' Face Level at time = 66 second of Minimal Ventilation and High Ventilation with Different Colormap Ranges

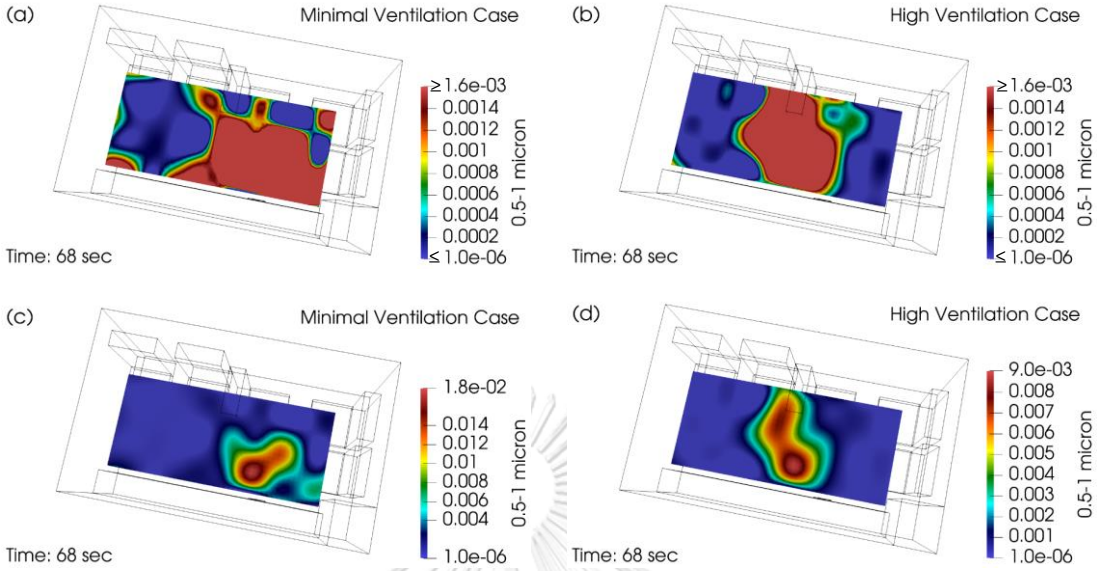

Figure 79 Contour Plane at EMS workers' Face Level at time = 68 second of Minimal Ventilation and High Ventilation with Different Colormap Ranges

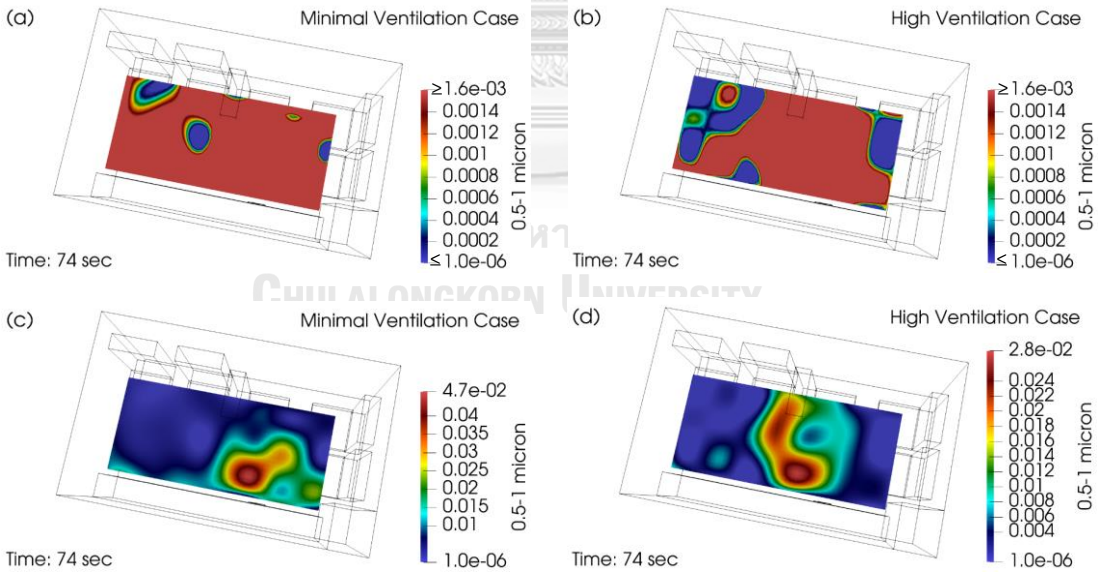

Figure 80 Contour Plane at EMS workers' Face Level at time = 74 second of Minimal Ventilation and High Ventilation with Different Colormap Ranges

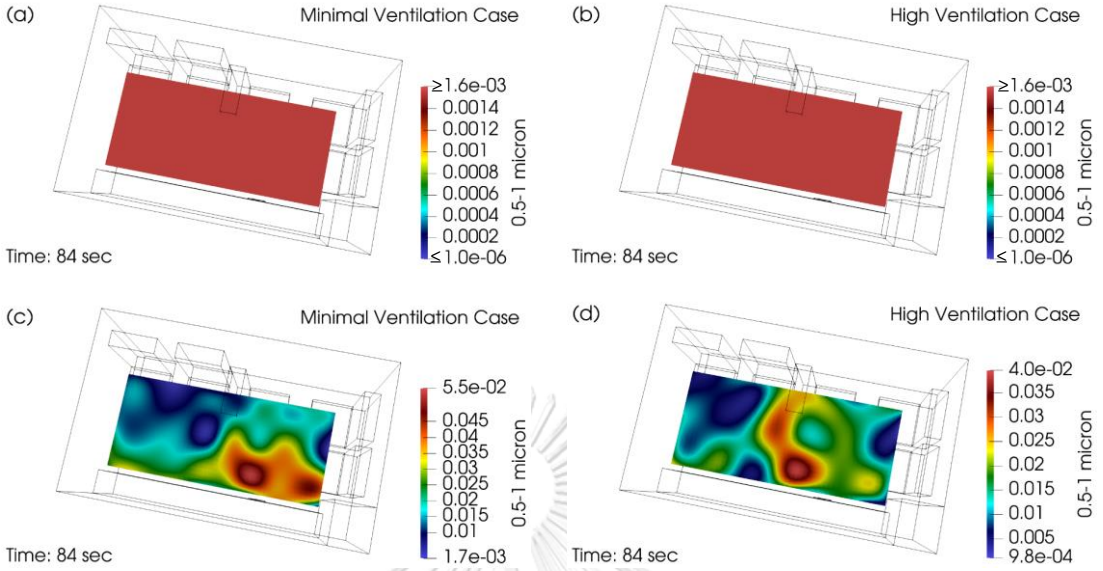

Figure 81 Contour Plane at EMS workers' Face Level at time = 84 second of Minimal Ventilation and High Ventilation with Different Colormap Ranges

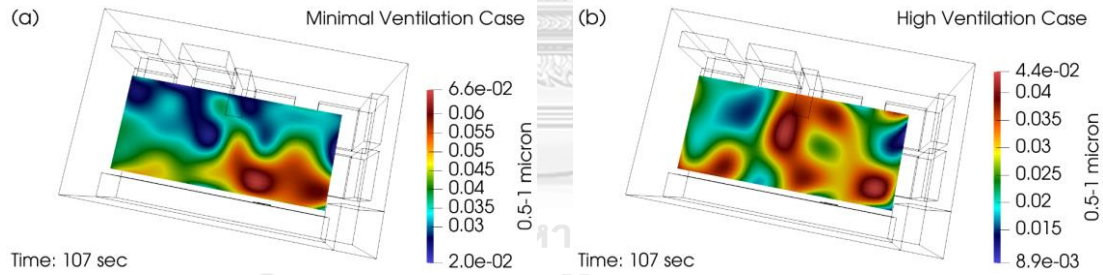

CHULALONGKORN UNIVERSITY

Figure 82 Contour Plane at EMS workers' Face Level at time = 107 second of Minimal Ventilation and High Ventilation

After stopping the particle injection at the 120th second, the peak concentration occurs right after at about 121st second for both cases as shown in Figure 83. It is obvious that in the case of MV, the distribution area of high concentration compared to the background state is significantly wider than the HV case, and the peak concentration of the MV case is also higher than HV case. The peak concentration is 0.0671 μL/m^3 and 0.0580 μL/m^3 for the MV case and HV case;

Thereafter, the concentrations compared to background state for both cases begin to decline starting from the region above patient's face as observed in Figure 84 showing the contour plane of the 137th second. Subsequently, the reduction occurs over a wide area across the plane for both cases, as shown in Figure 85, which shows the contour plane of the 180th second. Until about 247th second shown in Figure 86, the concentration on the plane of the HV case begins to be visible with the background state colormap, with the first region that decreases to the background state is the seat1, while the concentration in the case of MV also decreases but has not entered the background state colormap in any location. Figure 87, a snapshot of the 300th second, shows that the HV case concentration declines sharply at the seat1, seat2, seat3, and seat4, but at the seat5, the concentration is still high compared to the background state colormap, while the MV case does not begin to decline to background state. In the 350th second of the HV case, as shown in subfigure (b) of Figure 88, the concentration at seat1, seat2, seat3, and seat4 is lowered to the background state and found that high concentration regions occur at three areas: one region above the upper edge of the patient cot and two regions at the end of the patient compartment, including seat5. Figure 89 shows that at 400th second, the HV case concentration almost completely drops to the background state, leaving only at the end of the patient compartment. When considering peak concentration that occurs in the reduction process of the HV case, it is found that the local peak concentration occurs at multiple locations, especially at the end of the patient compartment, which can be viewed in Figure 86 to Figure 89. The entire plane concentration returns to the background value at about 459th second as shown in Figure 90. Although the HV case has returned to the background state across the entire plane, in the case of the MV, none of the positions begins to decrease to the background value. Figure 91 shows the end time of the experiment of the HV case.

จุฬาลงกรณ์มหาวิทยาลัย
Chulalongkorn University

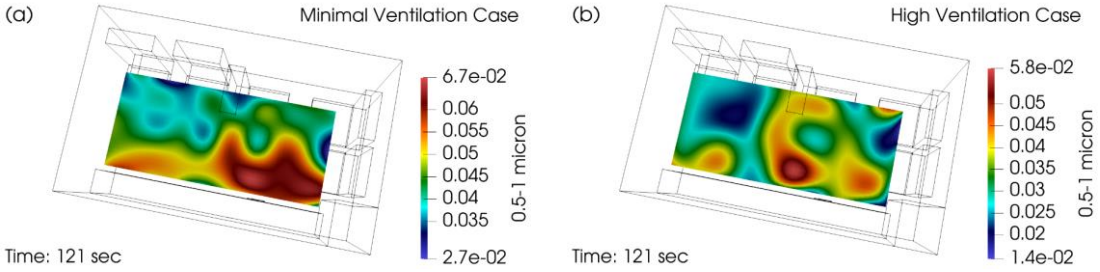

Figure 83 Contour Plane at EMS workers' Face Level at time = 121 second of Minimal Ventilation and High Ventilation

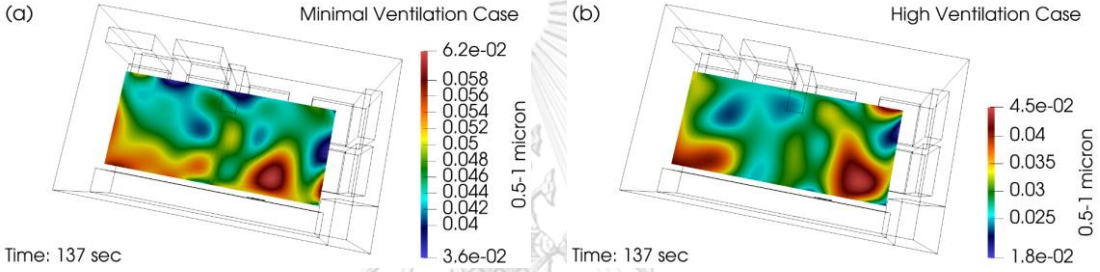

Figure 84 Contour Plane at EMS workers' Face Level at time = 137 second of Minimal Ventilation and High Ventilation

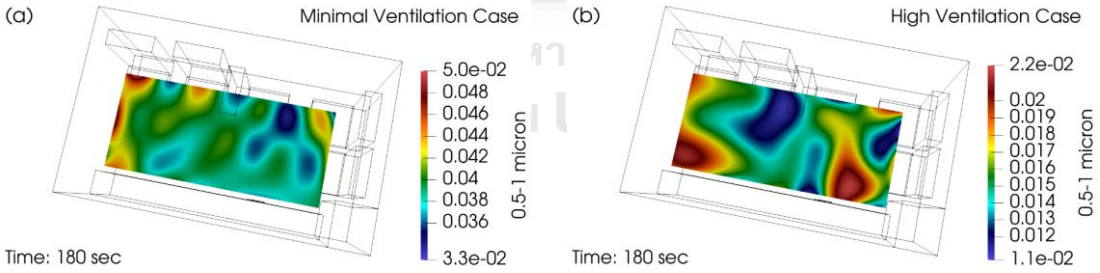

Figure 85 Contour Plane at EMS workers' Face Level at time = 180 second of Minimal Ventilation and High Ventilation

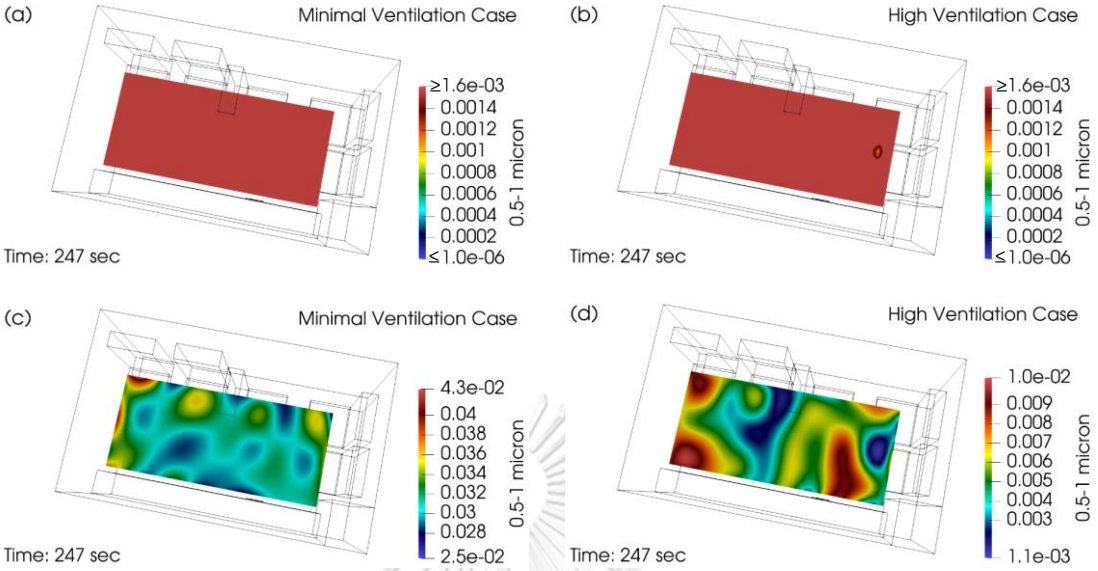

Figure 86 Contour Plane at EMS workers' Face Level at time = 247 second of Minimal Ventilation and High Ventilation with Different Colormap Ranges

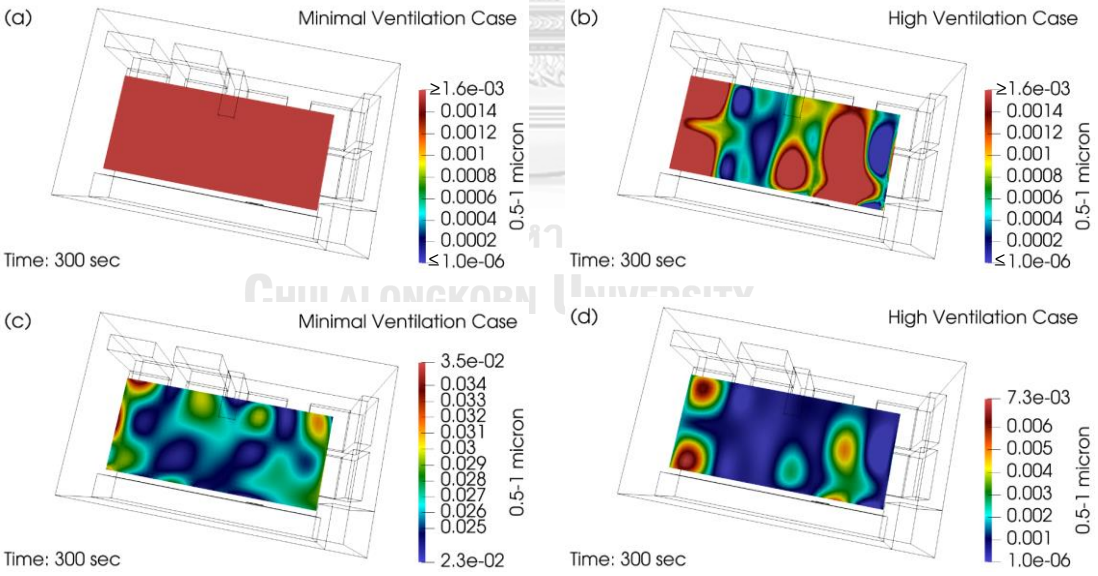

Figure 87 Contour Plane at EMS workers' Face Level at time = 300 second of Minimal Ventilation and High Ventilation with Different Colormap Ranges

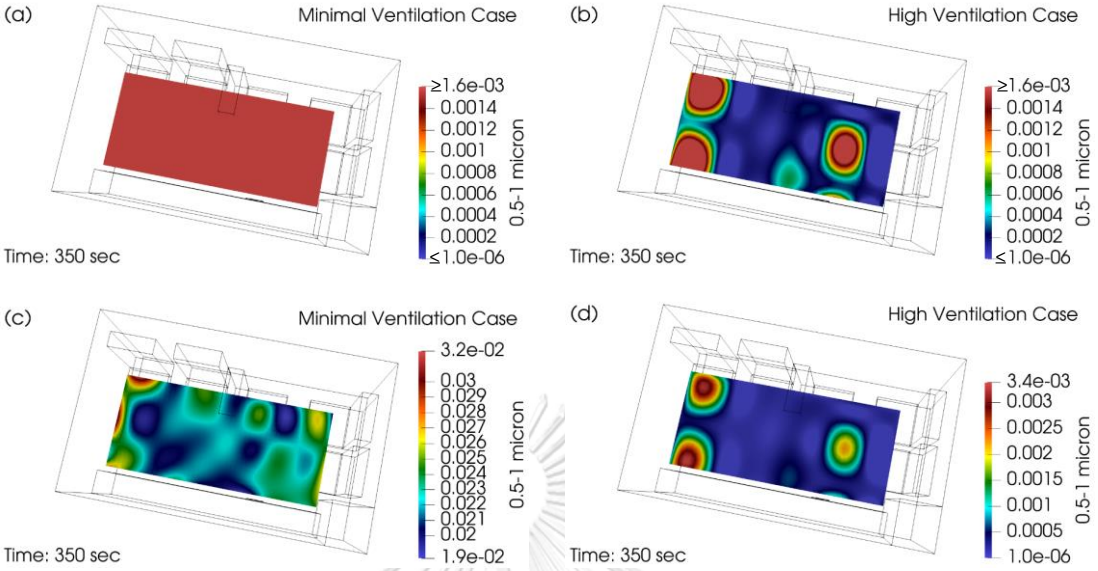

Figure 88 Contour Plane at EMS workers' Face Level at time = 350 second of Minimal Ventilation and High Ventilation with Different Colormap Ranges

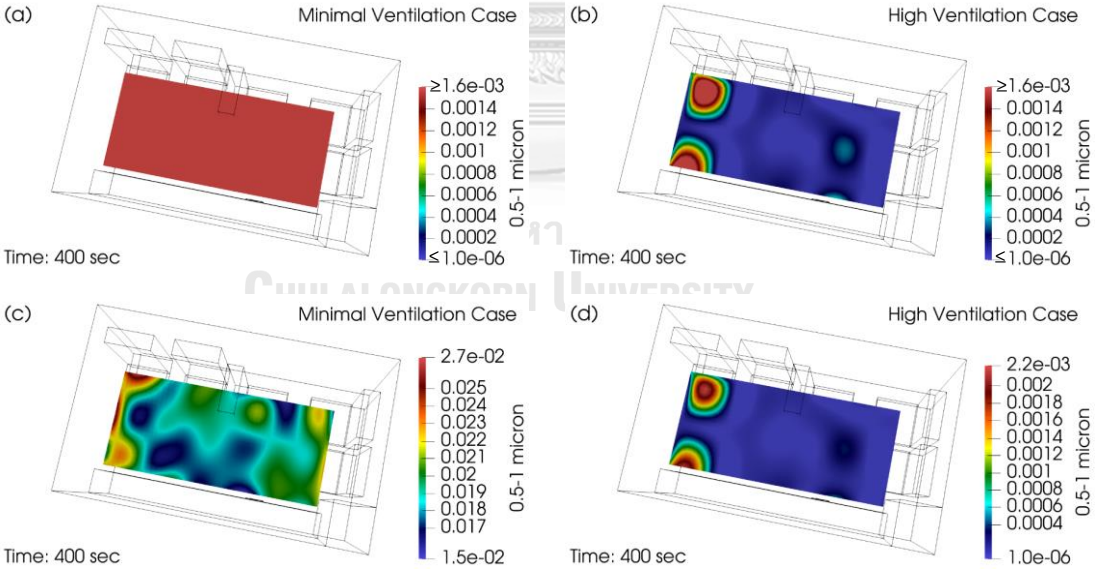

Figure 89 Contour Plane at EMS workers' Face Level at time = 400 second of Minimal Ventilation and High Ventilation with Different Colormap Ranges

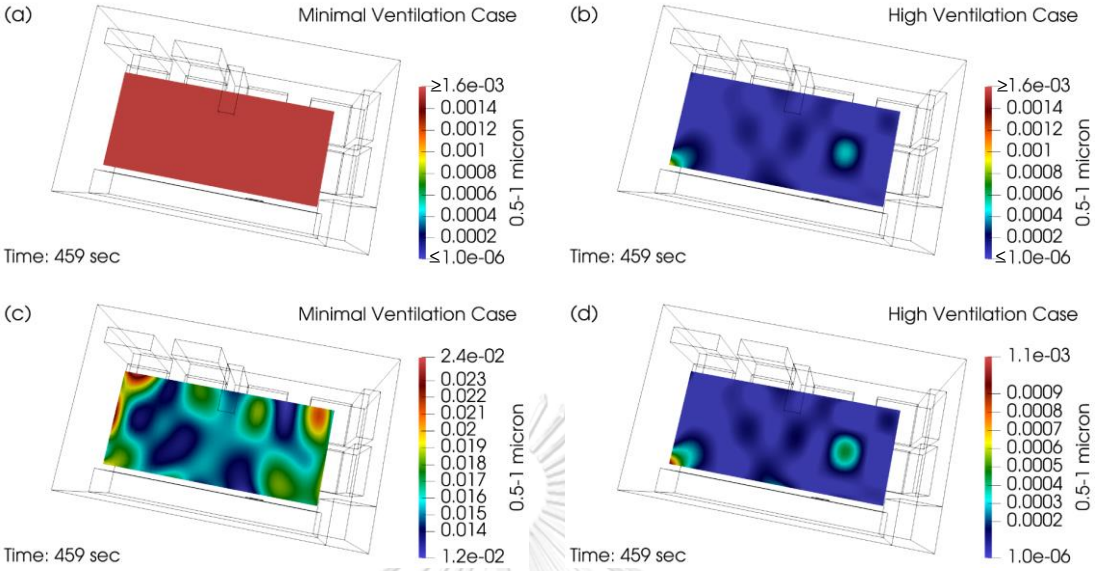

Figure 90 Contour Plane at EMS workers' Face Level at time = 459 second of Minimal Ventilation and High Ventilation with Different Colormap Ranges

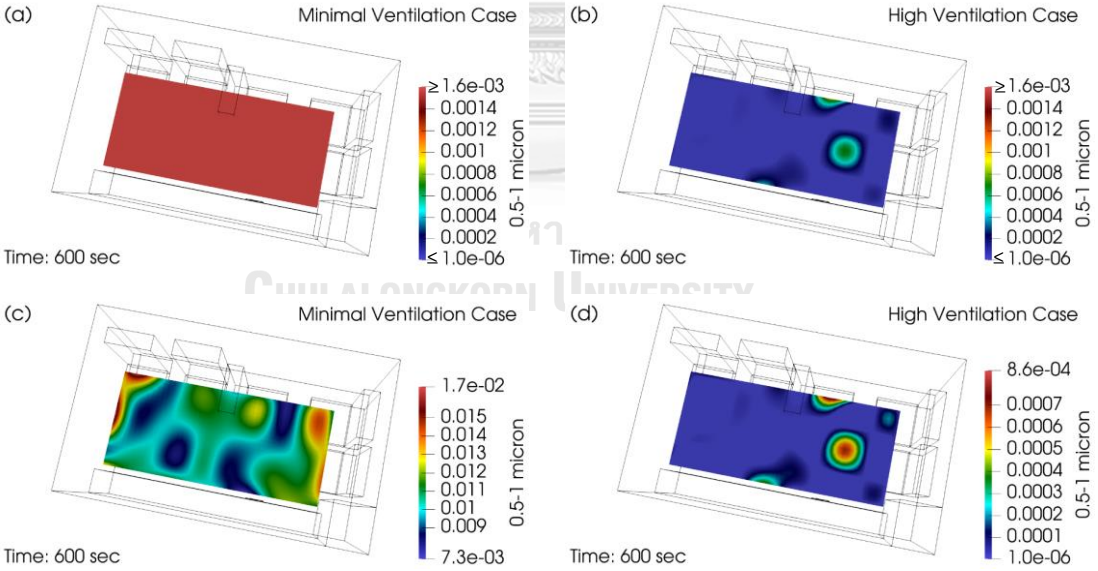

Figure 91 Contour Plane at EMS workers' Face Level at time = 600 second of Minimal Ventilation and High Ventilation with Different Colormap Ranges

Additional figures are added for the case of MV at further time. Figure 92 shows that the concentration on the plane begins to return to background state in the region between seat2 and seat3 at about 800th second with the high concentration area compared to its visible range at seat2 and seat5. After that concentration slowly drops back to the background state in several areas simultaneously as shown in Figure 93, showing a snapshot at 950th second. At 1050th second, shown in Figure 94, the concentration above the patient cot drops to the background state before all seating positions. After that, the decrease of the concentration at seat1 to seat5 occurs at 1150th second as shown in Figure 95. The end of the MV case experiment is shown in Figure 96.

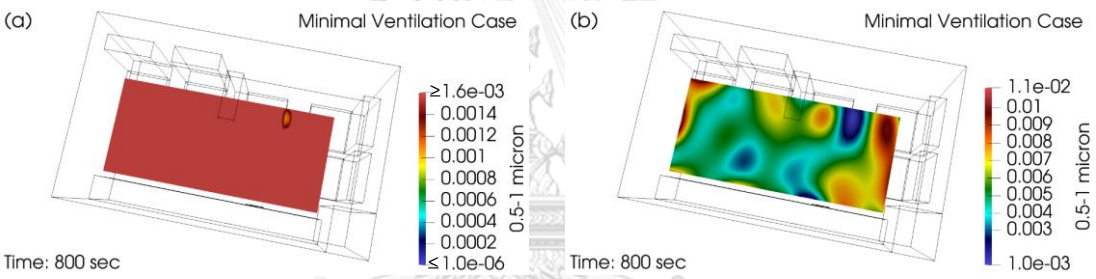

Figure 92 Contour Plane at EMS workers' Face Level at time = 800 second of Minimal Ventilation with Different Colormap Ranges

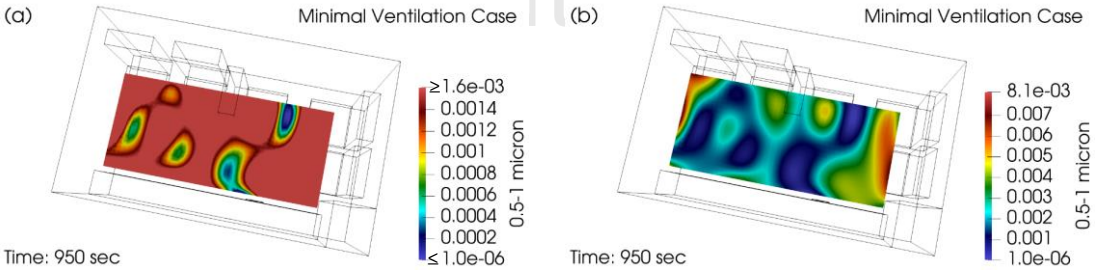

Figure 93 Contour Plane at EMS workers' Face Level at time = 950 second of Minimal Ventilation with Different Colormap Ranges

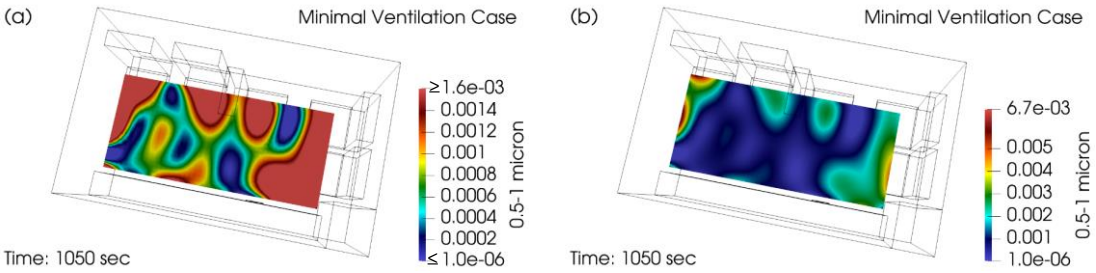

Figure 94 Contour Plane at EMS workers' Face Level at time = 1050 second of Minimal Ventilation with Different Colormap Ranges

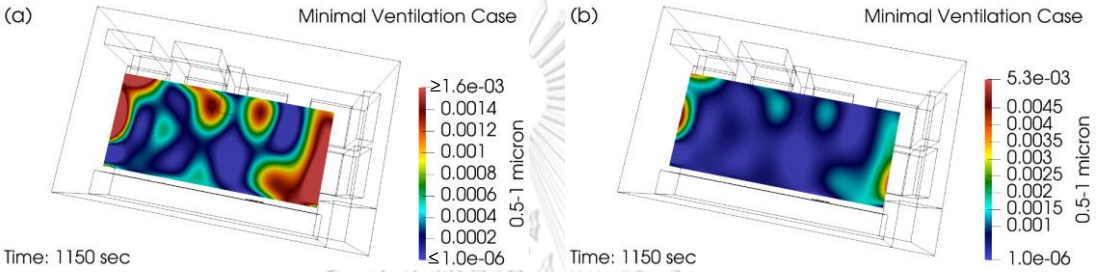

Figure 95 Contour Plane at EMS workers' Face Level at time = 1150 second of Minimal Ventilation with Different Colormap Ranges

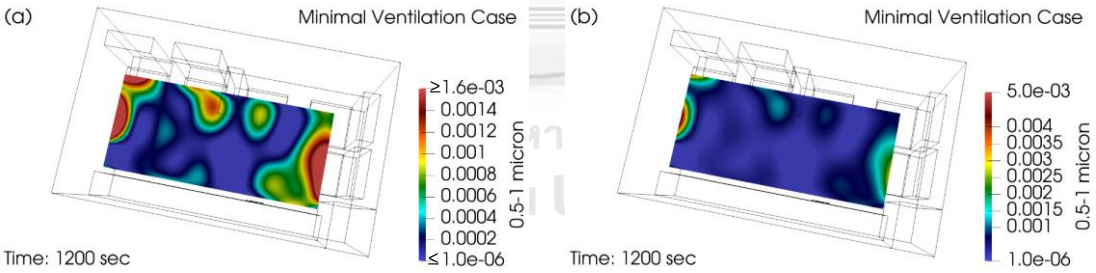

Figure 96 Contour Plane at EMS workers' Face Level at time = 1200 second of Minimal Ventilation with Different Colormap Ranges

To summarize, this section investigates the distribution of concentration of particles in the 0.5-1-micron size range. High concentration of particles is found just after the particle injection is initiated (t = 60 sec) in the region above the upper part of patient cot for both cases. Initially, the distribution area of the MV case is mainly to the front of the patient compartment, whereas the distribution area of the HV

case is mainly in the centre of the patient compartment. The concentration across the horizontal planes (at face level) of both cases reach high value compared to the background state colormap at about 20 seconds after the injection is started. The peak concentration value across all experiments occurs on this plane at about 120th second in both cases. HV concentration begins to decline back to background at about three minutes after the injection is started where the first region at seat 1 and returns to the background state across the entire plane at about 459th second. The MV case begins to decline to the background state colormap at about 12 minutes after particle injection has begun with the first region is the area between the seat 2 and seat 3. However, even after the end of the experiment of the MV case at 1200th second, the concentration has not decreased to background value for the whole plane.

5.2.2 Size range between 1 and 2.5 micron

Figure 97 to Figure 105 and Figure 110 to Figure 115 show the contours of the aerosol volume concentration for MV and HV cases at the face level of the EMS workers in the ambulance at each time interval. Subfigure (a) and subfigure (b) show colormaps that compare with the background value at the start of the measurement or at the zeroth second, in order to investigate the change in the concentration in comparison to when it started. Subfigure (c) and (d) help indicate the location of high concentration at that time. The period of time when the change in concentration is not visible relative to the background state colormap is shown in Figure 106 to Figure 109. For contours at time intervals greater than 600th second, the time interval after the termination of the HV case, are shown in Figure 116 to Figure 120, where subfigure (a) shows a colormap relative to the background state and subfigure (b) is a visible range colormap for each time period of the MV case.

Figure 97 shows the start of the experiments for both MV and HV cases, where the overall picture of concentration of the MV case is higher than the HV as the

reason discussed in section 5.2.1. The 60th second shown in Figure 98 is the contour at which the particle injection is started. From the Figure 97 and Figure 98, it can be seen that the background concentration at zeroth second and the concentration at 60th second of both MV and HV cases are not much different implying steady background state. For the MV case, the concentration on contour plane increases sharply compared to the background state colormap in the region above the patient's face at the 63rd second, as shown in Figure 99. The distribution of concentration of the case of HV is shown in Figure 100; higher concentration relative to the background state colormap occurs on the plane at 64th second in the same vicinity as the MV case at the 63rd second. The peak concentration of MV case occurring during this period is approximately 6 times higher than that of the HV case. The difference in distribution compared to the background state colormap of MV and HV cases can be seen from Figure 101 to Figure 103.

Figure 101 shows the contour plane at the 66th second. It is evident that high concentration (compared to background state colormap) distribution are of the MV case mainly distributes to seat1 and seat2 and slightly to seat3 and seat4. Whereas almost all the high concentration of HV case distributes to seat4. Figure 102 shows the concentration distribution of 68th second. It is found that the high concentration distribution area on the plane compared to the background state is wider. It also can be observed that the MV case concentration at seat3 and seat4 is higher relative to background but still remains low at seat 5 (shown in subfigure (a)). For the HV case, high concentration compared to background begins to distribute to the seat3 (shown in subfigure (b)). Concentration distribution area distributes almost across the plane at the 74th second, as shown in Figure 103.

However, although the distribution areas shown in Figure 101 to Figure 103 are different in terms of time as well as different in ventilation rate during each time period, the local peak concentration positions still occur at the same region (above of patient's face). By the 85th second, the HV case concentration is relatively large

(compared to the background state colormap) and at the 89th second for the MV case; the contour can be seen in Figure 104 and Figure 105. Although the HV concentration at 85th second is relatively large compared to the background state colormap, the concentration of HV case still increases and can be noticed from Figure 104 to Figure 106. The same is true for the MV case when considering Figure 105 and Figure 106, representing a time of 89th second and 107th second, where the concentration still increases even though it is already high across the plane compared to the background state since the 89th second (subfigure (a) of Figure 105).

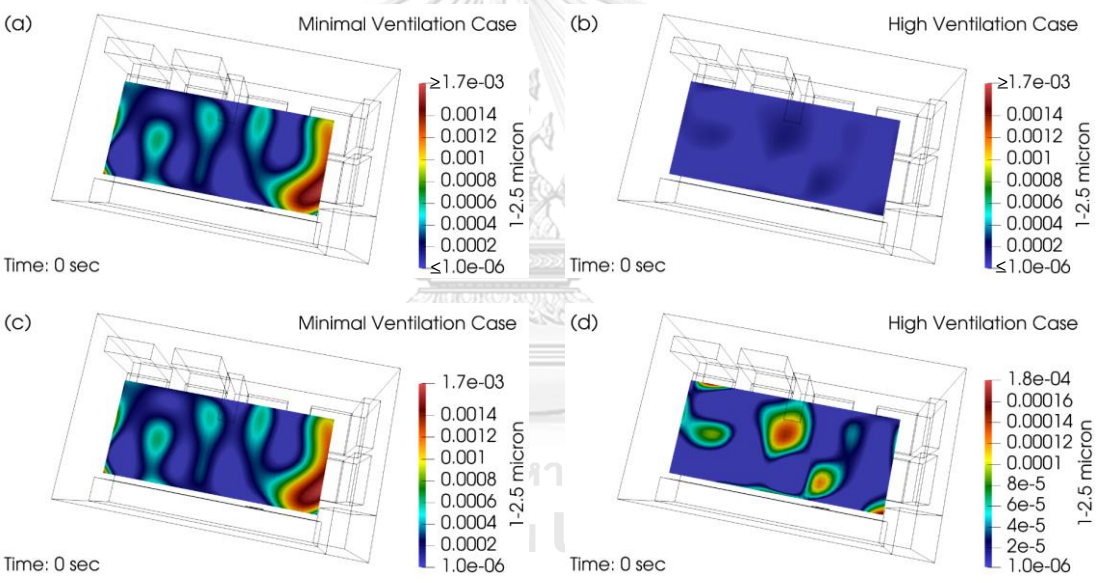

Figure 97 Contour Plane at EMS workers' Face Level at time = 0 second of Minimal Ventilation and High Ventilation with Different Colormap Ranges

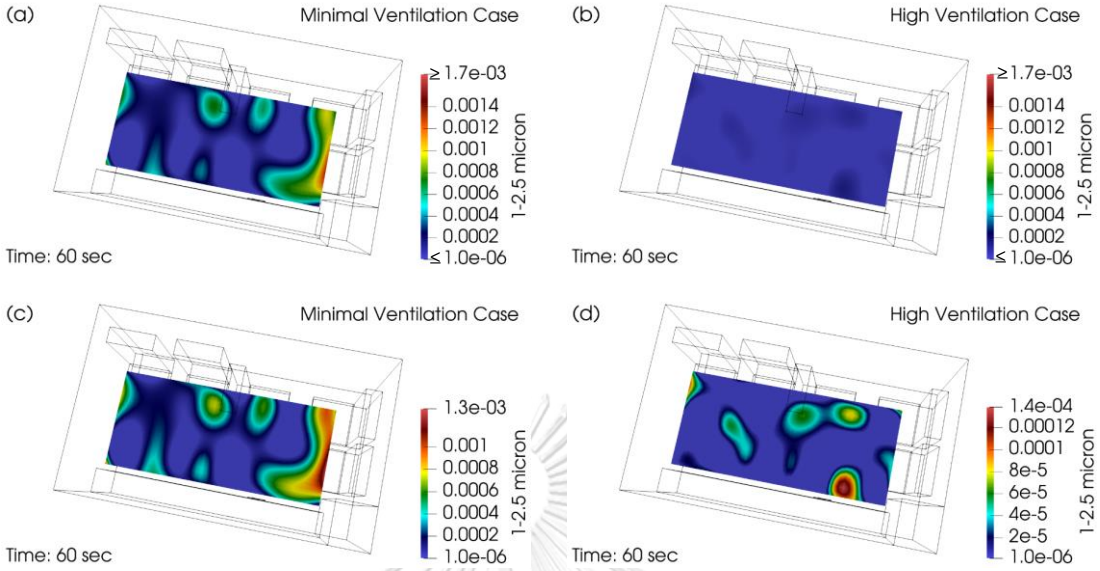

Figure 98 Contour Plane at EMS workers' Face Level at time = 60 second of Minimal Ventilation and High Ventilation with Different Colormap Ranges

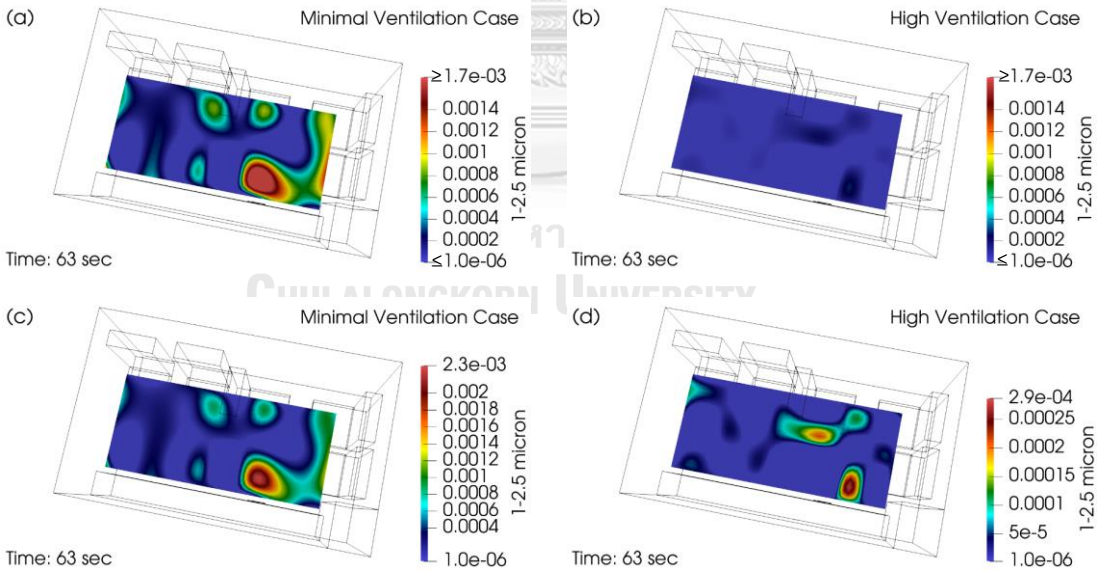

Figure 99 Contour Plane at EMS workers' Face Level at time = 63 second of Minimal Ventilation and High Ventilation with Different Colormap Ranges

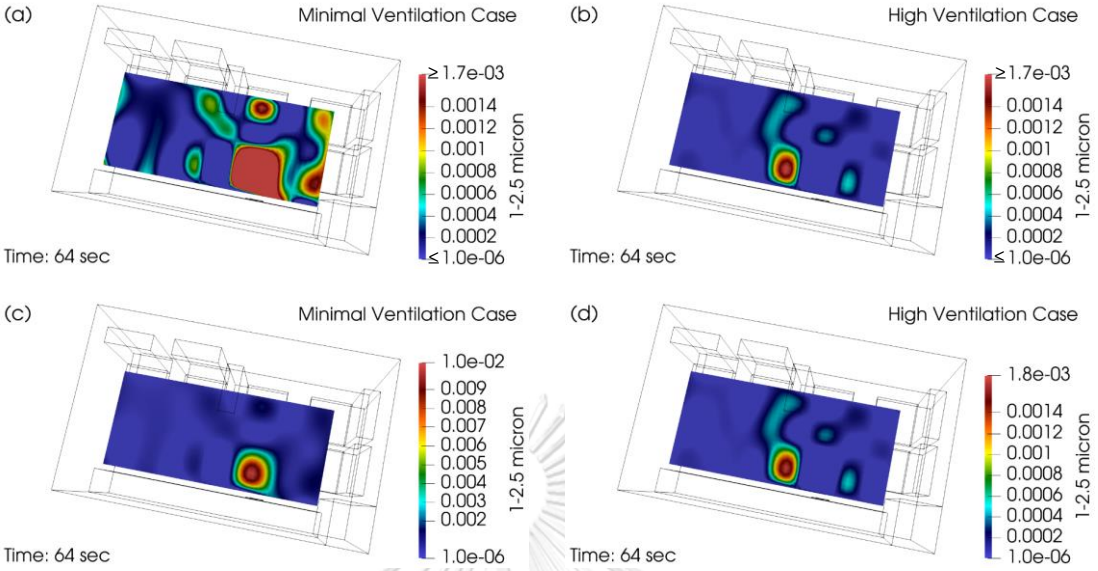

Figure 100 Contour Plane at EMS workers' Face Level at time = 64 second of Minimal Ventilation and High Ventilation with Different Colormap Ranges

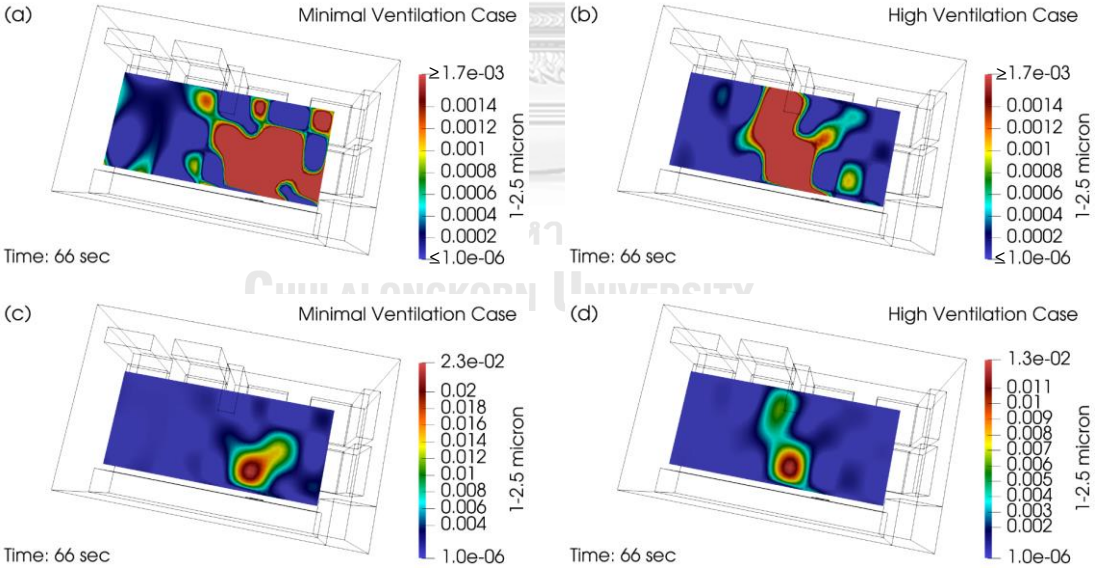

Figure 101 Contour Plane at EMS workers' Face Level at time = 66 second of Minimal Ventilation and High Ventilation with Different Colormap Ranges

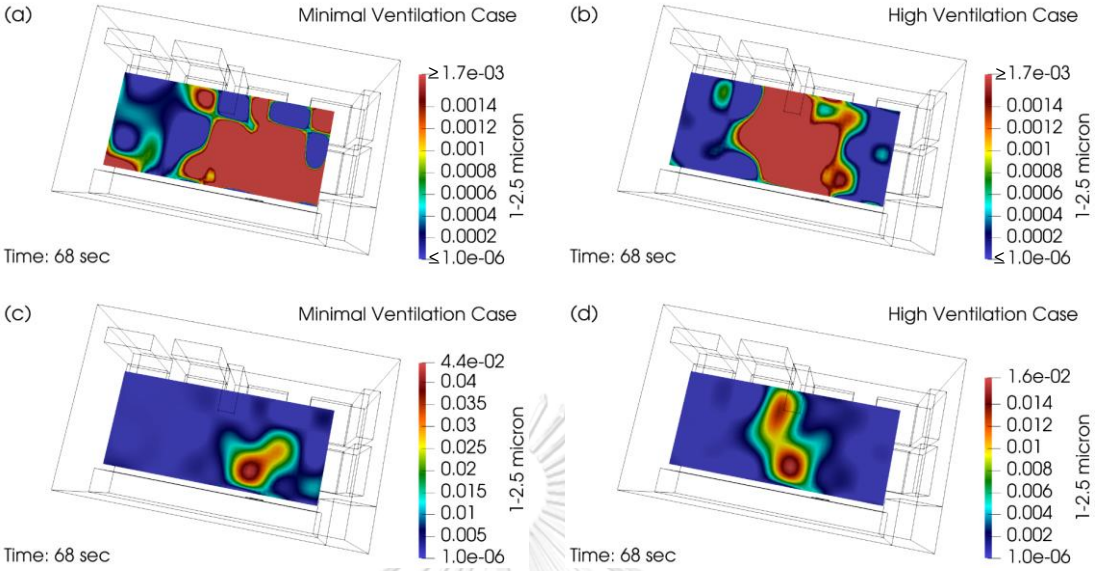

Figure 102 Contour Plane at EMS workers' Face Level at time = 68 second of Minimal Ventilation and High Ventilation with Different Colormap Ranges

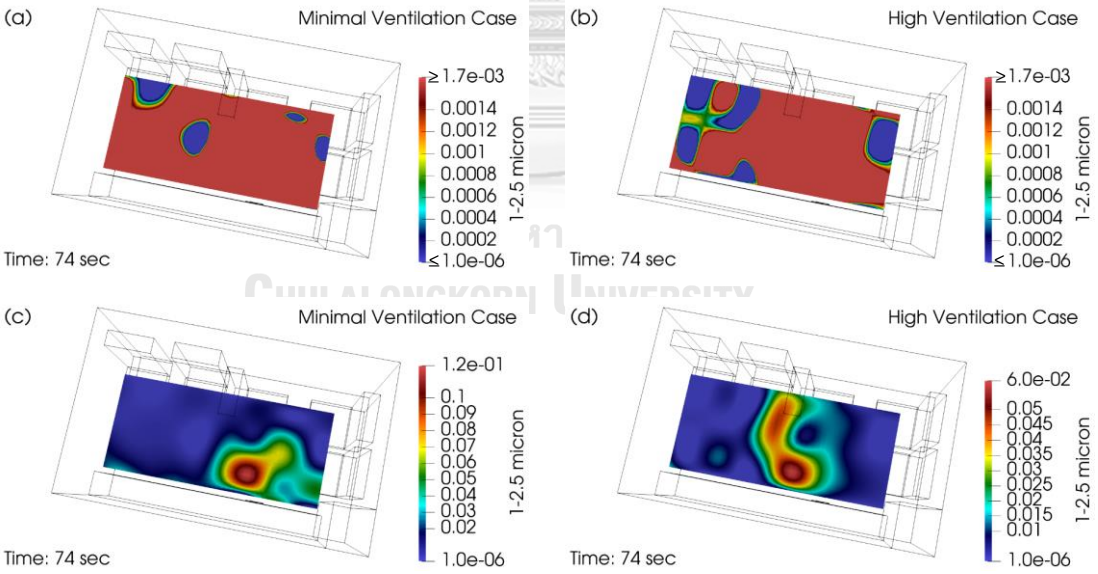

Figure 103 Contour Plane at EMS workers' Face Level at time = 74 second of Minimal Ventilation and High Ventilation with Different Colormap Ranges

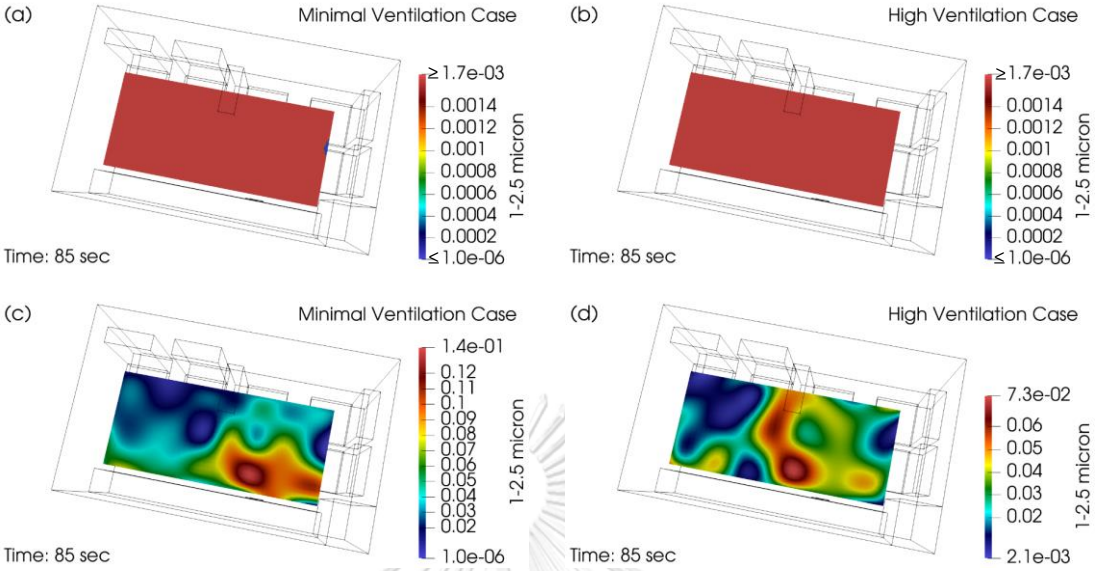

Figure 104 Contour Plane at EMS workers' Face Level at time = 85 second of Minimal Ventilation and High Ventilation with Different Colormap Ranges

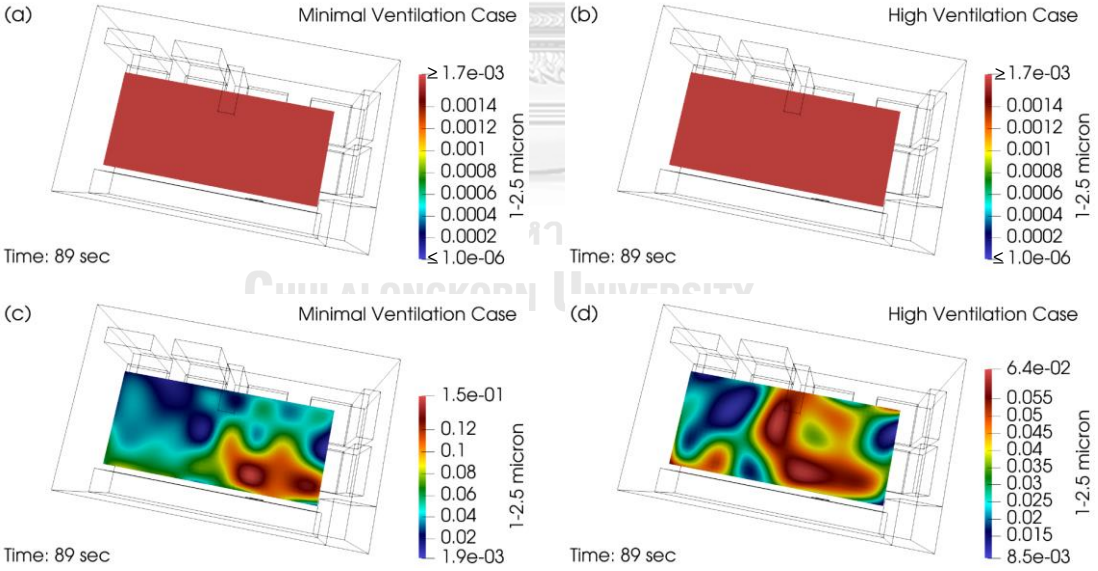

Figure 105 Contour Plane at EMS workers' Face Level at time = 89 second of Minimal Ventilation and High Ventilation with Different Colormap Ranges

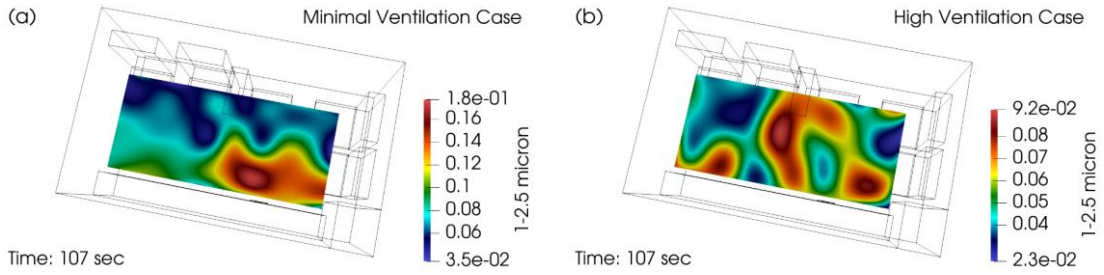

Figure 106 Contour Plane at EMS workers' Face Level at time = 107 second of Minimal Ventilation and High Ventilation

Particle injection is stopped at the 120th second, but concentration continues to rise, and the highest value occurs at about the 121st second in the area above the patient's face for both cases, as shown in Figure 107. The peak concentration of the MV case is 0.185 μL/m^3 and the peak concentration of the HV case is 0.146 μL/m^3. After that, the concentration of MV and HV cases begins to decline across the plane, but the areas that the concentration drops sharply for both cases are where the local peak concentration occurs at the 121st second. Then, the concentration in both cases continues to decline in multiple regions which can be observed from Figure 107 to Figure 109.

High concentration compared to background state colormap of HV cases begins to be visible with the background state colormap at about 271st second, shown in Figure 110, with the first region at seat4, while the MV case has no region where the concentration is reduced to be visible with the background state colormap. At 300th second, shown in Figure 111, the HV case concentration declines back to background state colormap in a wider area at the centre of the patient compartment and begins to decline to its background value in a small region at seat1. Concentration of the HV case continues to decrease simultaneously in several areas. However, at the 350th second, there are still high concentration relative to the background values at three areas, one above the patient's face and two at the end of the patient compartment, as shown in Figure 112.

จุฬาลงกรณ์มหาวิทยาลัย
CHULALONGKORN UNIVERSITY

Later at 400th second, the HV case concentration decreases to background state colormap almost across the plane, leaving high concentration area relative to the background only at the end of the patient compartment as shown in Figure 113. Until about 487th second, as shown in Figure 114, the concentration across the plane of the HV case returns to the background value and concentration contour at the end of the experimental period of the HV case is shown in Figure 115. Although the HV case concentration has returned to the background state across the entire plane at about 487th second, no region of the MV case is visible with the background state colormap. However, the value concentration of the MV case starts to decline since the 121st second.

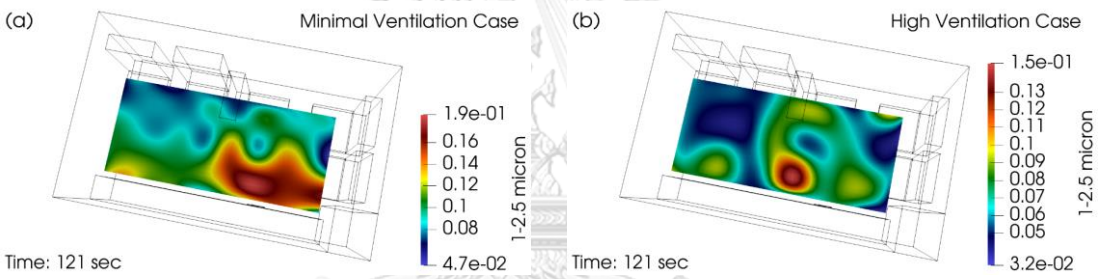

Figure 107 Contour Plane at EMS workers' Face Level at time = 121 second of Minimal Ventilation and High Ventilation

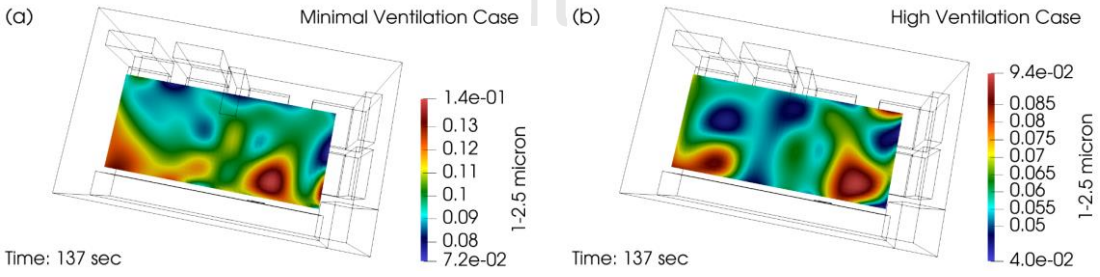

Figure 108 Contour Plane at EMS workers' Face Level at time = 137 second of Minimal Ventilation and High Ventilation

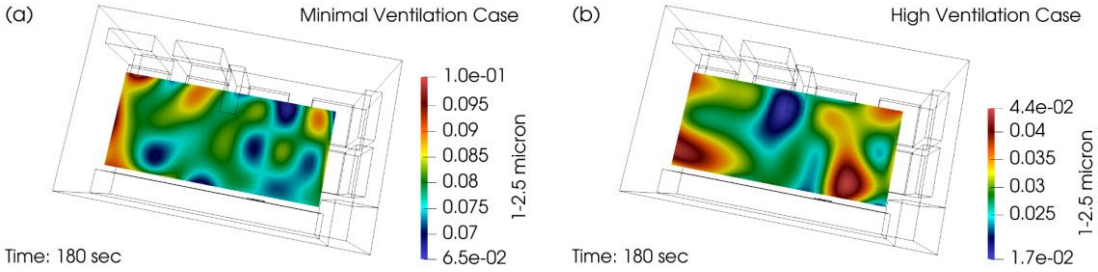

Figure 109 Contour Plane at EMS workers' Face Level at time = 180 second of Minimal Ventilation and High Ventilation

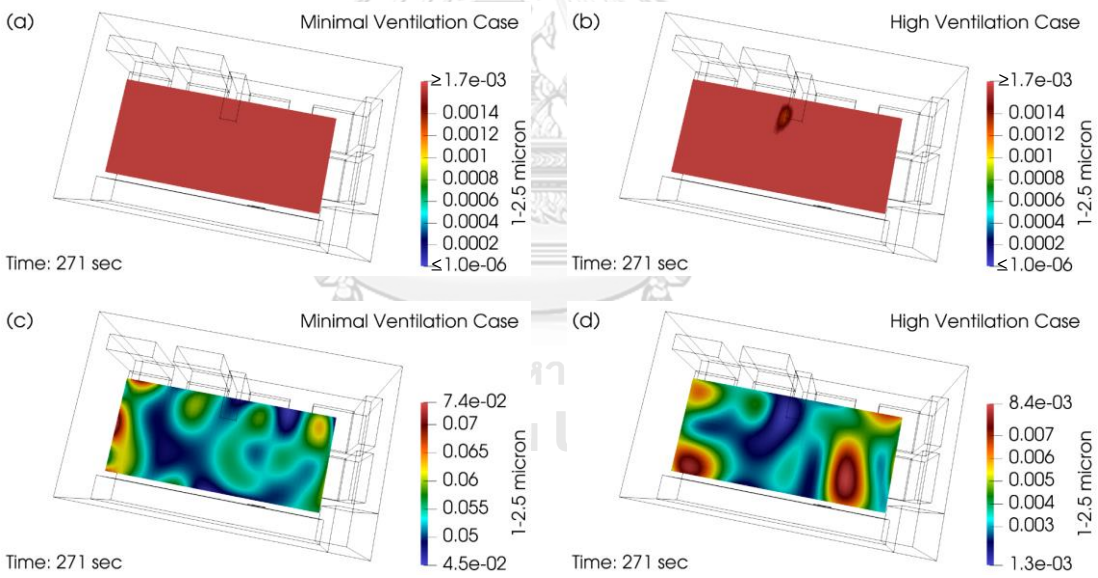

Figure 110 Contour Plane at EMS workers' Face Level at time = 271 second of Minimal Ventilation and High Ventilation with Different Colormap Ranges

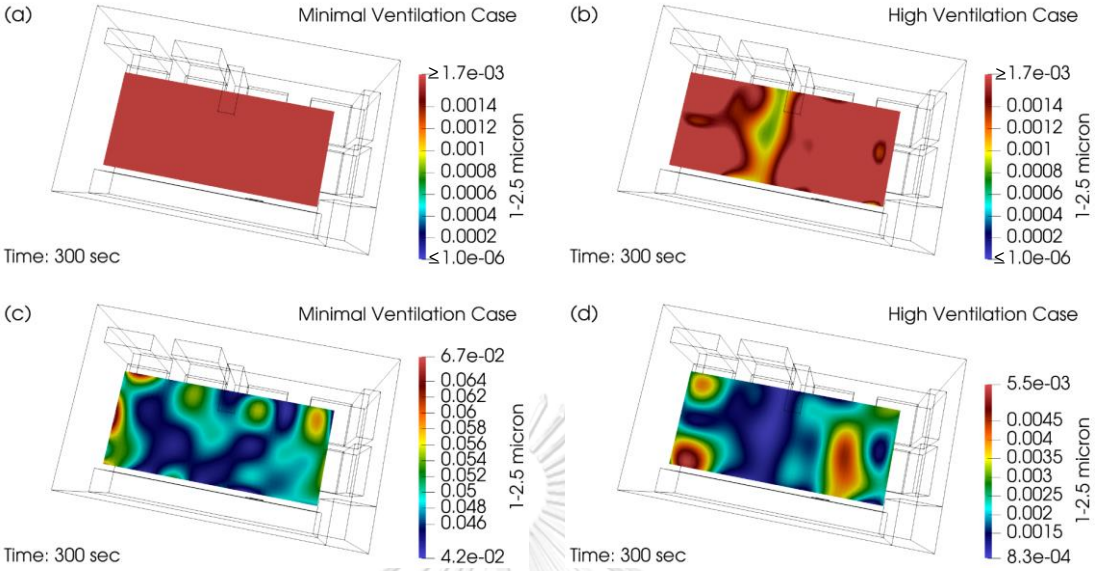

Figure 111 Contour Plane at EMS workers' Face Level at time = 300 second of Minimal Ventilation and High Ventilation with Different Colormap Ranges

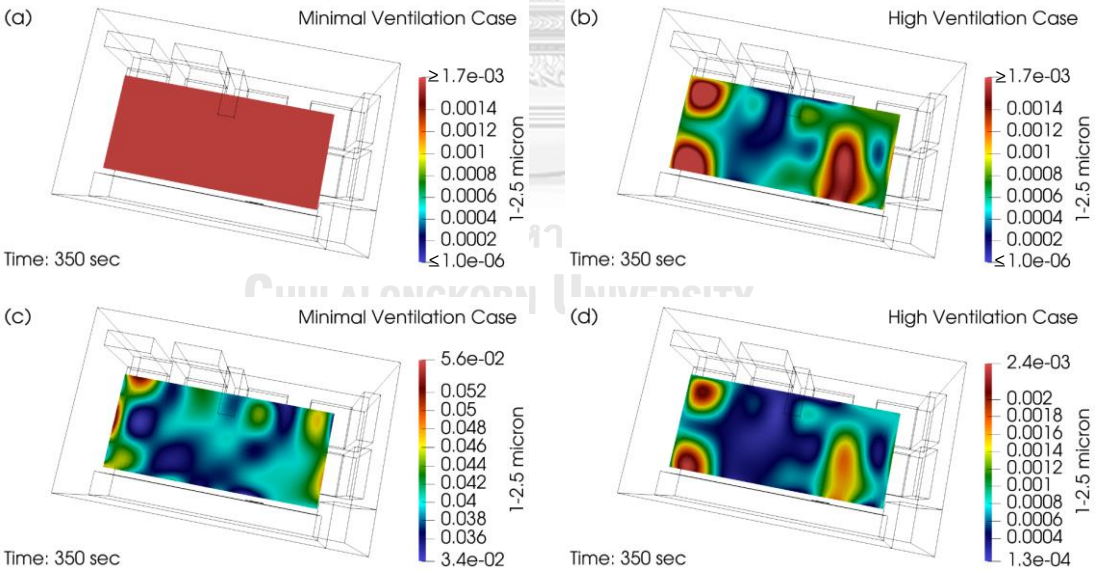

Figure 112 Contour Plane at EMS workers' Face Level at time = 350 second of Minimal Ventilation and High Ventilation with Different Colormap Ranges

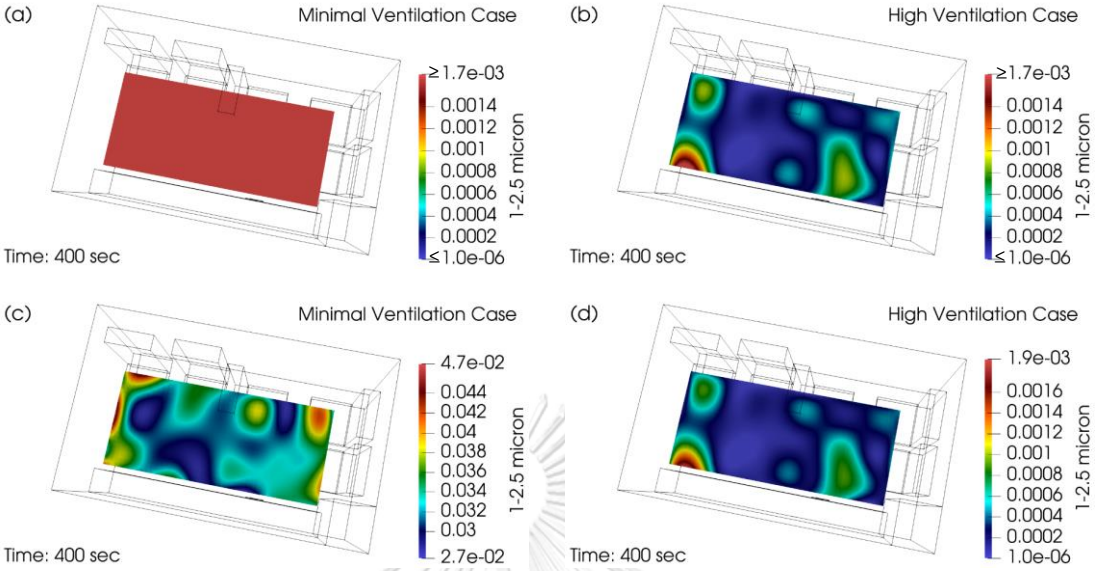

Figure 113 Contour Plane at EMS workers' Face Level at time = 400 second of Minimal Ventilation and High Ventilation with Different Colormap Ranges

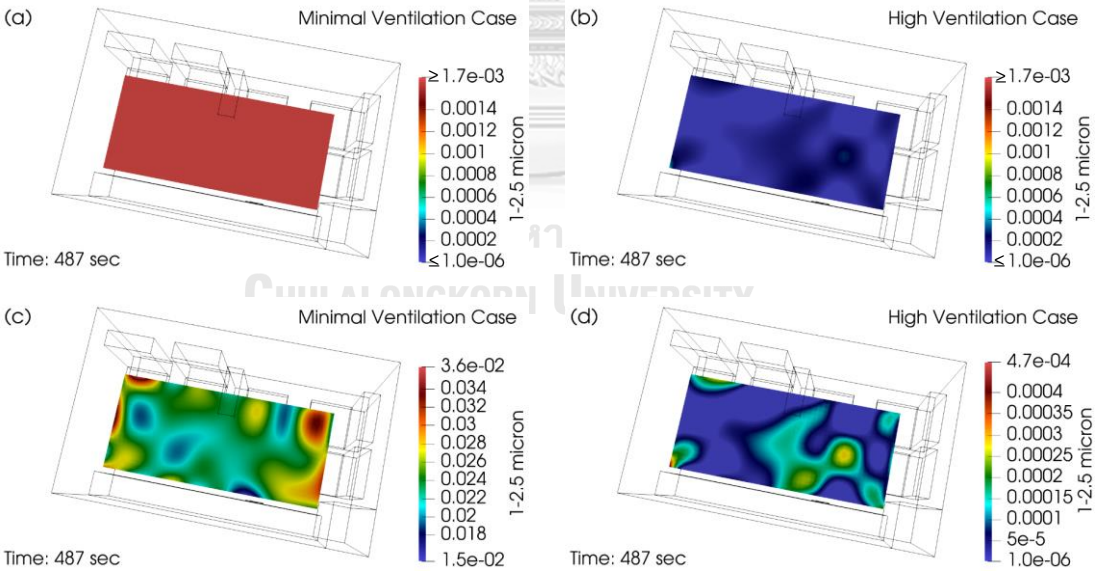

Figure 114 Contour Plane at EMS workers' Face Level at time = 487 second of Minimal Ventilation and High Ventilation with Different Colormap Ranges

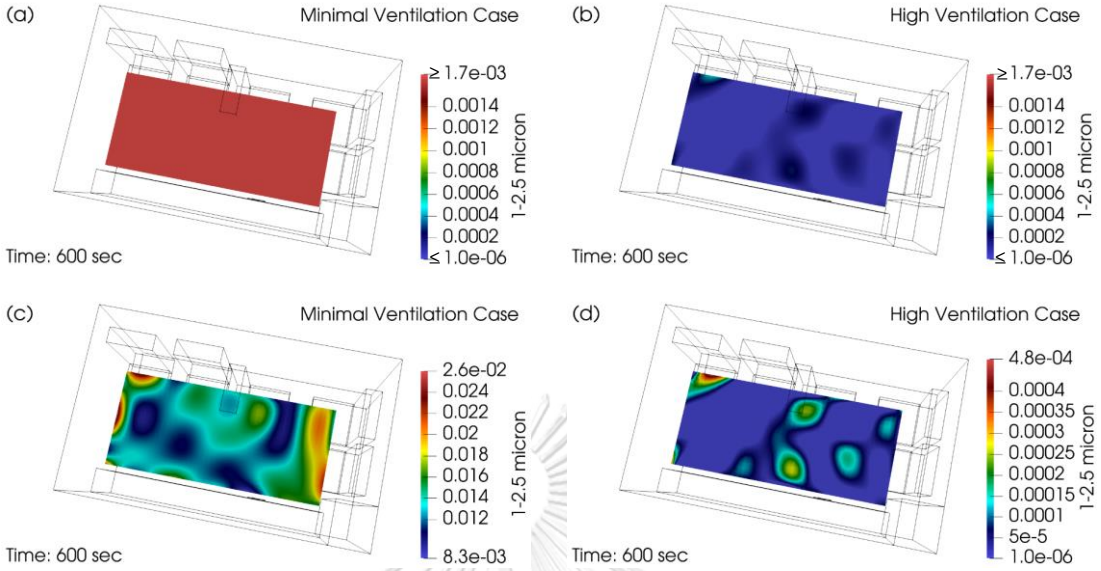

Figure 115 Contour Plane at EMS workers' Face Level at time = 600 second of Minimal Ventilation and High Ventilation with Different Colormap Ranges

Additional figures are added for the case of MV at further time. For the MV case, high concentration compared to background state colormap starts to be visible with the background state colormap for the first time at about 880th second in the region shown in Figure 116. After that, high concentration area compared to background state in the decreased region at 880th second begins to be wider which can be observed in Figure 117, which shows the concentration distribution area of 950th second. High concentration area relative to background continues to decline to a larger area at 1050th second, as observed in Figure 118. Until the 1150th second shown in Figure 119, concentration in the centre of patient compartment decreases more rapidly than in the front and rear of patient compartment. Figure 120 shows the contour plane of the experimental end time of the MV case.

จุฬาลงกรณ์มหาวิทยาลัย
CHULALONGKORN UNIVERSITY

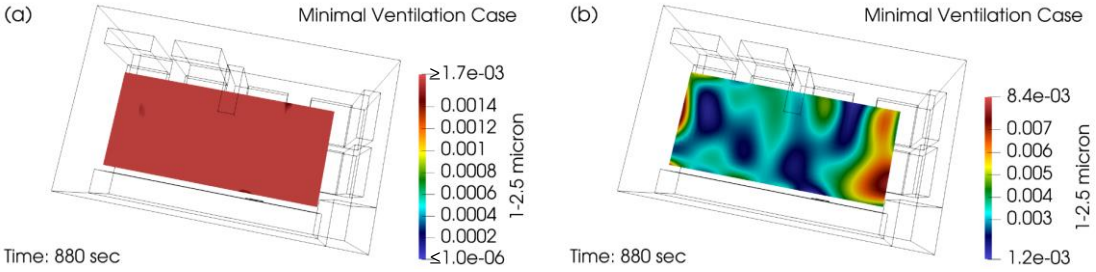

Figure 116 Contour Plane at EMS workers' Face Level at time = 880 second of Minimal Ventilation with Different Colormap Ranges

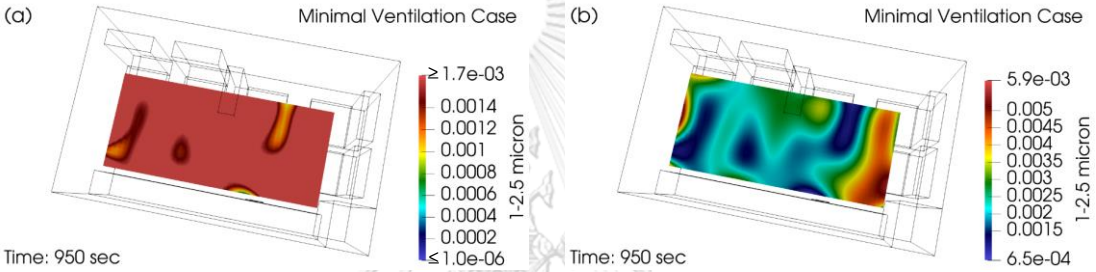

Figure 117 Contour Plane at EMS workers' Face Level at time = 950 second of Minimal Ventilation with Different Colormap Ranges

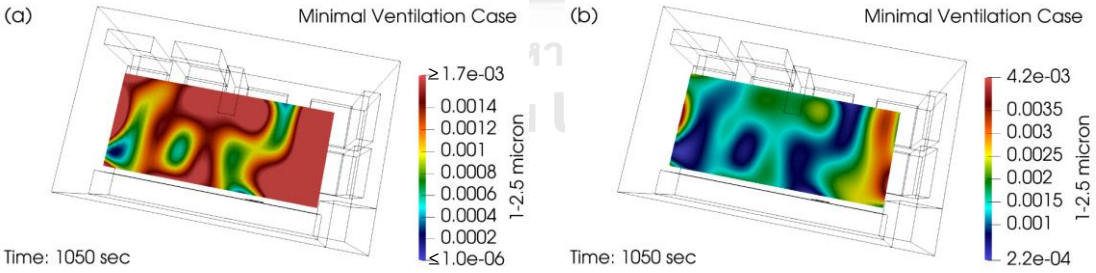

Figure 118 Contour Plane at EMS workers' Face Level at time = 1050 second of Minimal Ventilation with Different Colormap Ranges

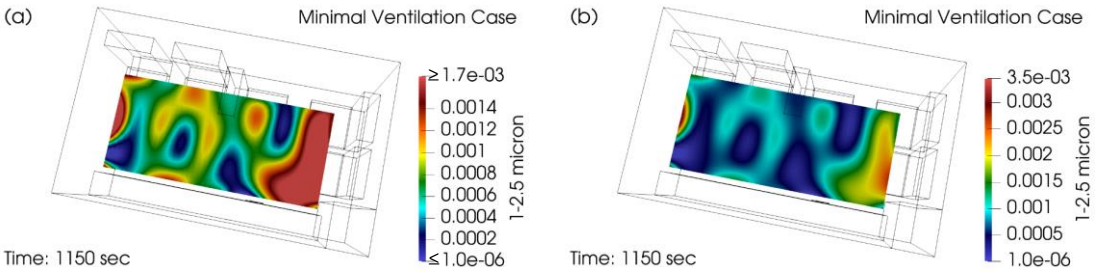

Figure 119 Contour Plane at EMS workers' Face Level at time = 1150 second of Minimal Ventilation with Different Colormap Ranges

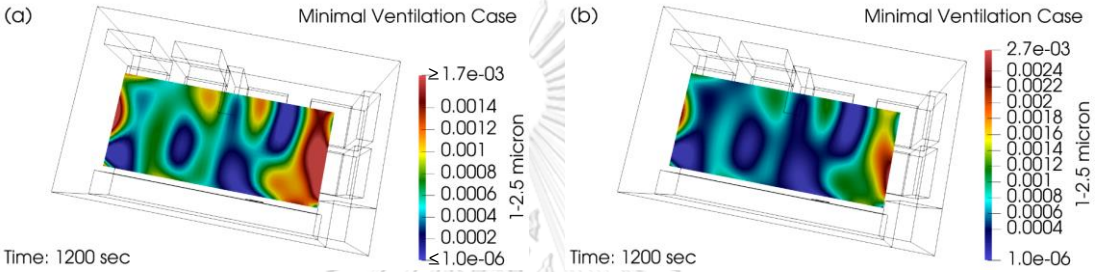

Figure 120 Contour Plane at EMS workers' Face Level at time = 1200 second of Minimal Ventilation with Different Colormap Ranges

To summarize, this section investigates the distribution of concentration of particles in the 1-2.5-micron size range. The high concentration is noticed on the plane only few seconds after the start of particle injection which occurs above in the region above patient cot of both cases. At first, the concentration distribution areas on the plane remain similar as in the 0.5-1-micron size range which are mostly in the front of the patient compartment for the MV case and in the centre of the patient compartment for the HV case. The concentration across the horizontal planes (at face level) of both cases reach high value compared to the background state colormap at about 20 to 30 seconds after the injection is launched. The peak concentration of both cases from all experiments occurs at about 120th second. About three minutes after the particles are introduced into patient compartment, the high concentration of the HV case begins to decline to the background state with the first region at seat 4 and returns to background across the plane at 487th second. For

the MV case, high concentration begins to decline to the background state in several regions at about 13 minutes after the injection is started. However, even at the end of the experiment of the MV case, the concentration has not decreased to background value for the whole plane.

5.2.3 Size range between 2.5 and 5 micron

Figure 121 to Figure 129 and Figure 134 to Figure 139 show the contours of the aerosol volume concentration for MV and HV cases at the face level of the EMS workers in the ambulance at each time interval. Subfigure (a) and subfigure (b) show colormaps that compare with the background value at the start of the measurement or at the zeroth second, in order to investigate the change in the concentration in comparison to when it started. Subfigure (c) and (d) help indicate the location of high concentration at that time. The period of time when the change in concentration is not visible relative to the background state colormap is shown in Figure 130 to Figure 133. For contours at time intervals greater than 600th second, the time interval after the termination of the HV case, are shown in Figure 140 to Figure 144, where subfigure (a) shows a colormap relative to the background state and subfigure (b) is a visible range colormap for each time period of the MV case.

จุฬาลงกรณ์มหาวิทยาลัย
Chulalongkorn University

The contour of the concentration at the start of the experiment is shown in Figure 121. It can be observed that the concentration of the MV case has a higher concentration and the concentration distribution area is wider than that of the HV case. Figure 122 shows the start of particle injection into the patient compartment, with concentration value and distribution characteristic remain close to zeroth second. In the MV case, a noticeable concentration relative to the background state colormap occurs at 63rd second, as shown in Figure 123. After one second at 64th second, as seen in Figure 124, the concentration of the HV case begins to rise compared to the background state colormap in the same region as the MV case in one second before, above the patient's face. At the 66th second the distribution area

of concentration compared to the background state of both MV and HV cases is wider, with the MV case spreading across the front half of the patient compartment, including seat1 to seat4.

For the HV case, the concentration mostly distributes to seat4 which can be seen in Figure 125. Figure 126 shows the concentration distribution at 68th second, it can be seen that the MV case has the distribution area of high concentration relative to the background state at the rear region of patient compartment, but there is only small dispersion of high concentration relative to background to seat5. For the HV case the high concentration disperses to seat3. Looking at the 74th second, as shown in Figure 127, high concentration compared to background state colormap of both the MV and HV cases distributes almost across the entire plane compared to the background state. It is observed during this period that the HV distribution is more rapid compared to the MV case, with more distribution area to seat1 and seat2 than the previous period as well as at the end of the patient compartment. When we observe the increasing of the distribution area in Figure 123 to Figure 127, we can see that although the distribution area of the MV and HV cases varies from time to time, the local peak concentration still occurs in the adjacent area which is above the patient's face (injection position). High concentration compared to background state colormap spreads over a larger area until about 89th second shown in Figure 128, the HV case concentration is relatively large (compared to background state colormap) across the entire plane, and the same is true for the MV case after 7 seconds which can be seen in Figure 129. The local peak concentration area in Figure 128 also occurs in the same area as the previous period, but with a wider distribution area to the seat1 region for the MV case and to the seat3 and seat4 areas for the HV case. The local peak concentration area at 96th second is the same area as at 89th second for the MV case. For the HV case, local peak concentration is seen in several regions, as shown in Figure 129. Although the concentration of the MV and HV cases is relatively large compared to the background state colormap across the entire plane,

the concentration continues to increase, like the other size ranges of particles, which can be seen in Figure 130, which shows the concentration contour at 107th second.

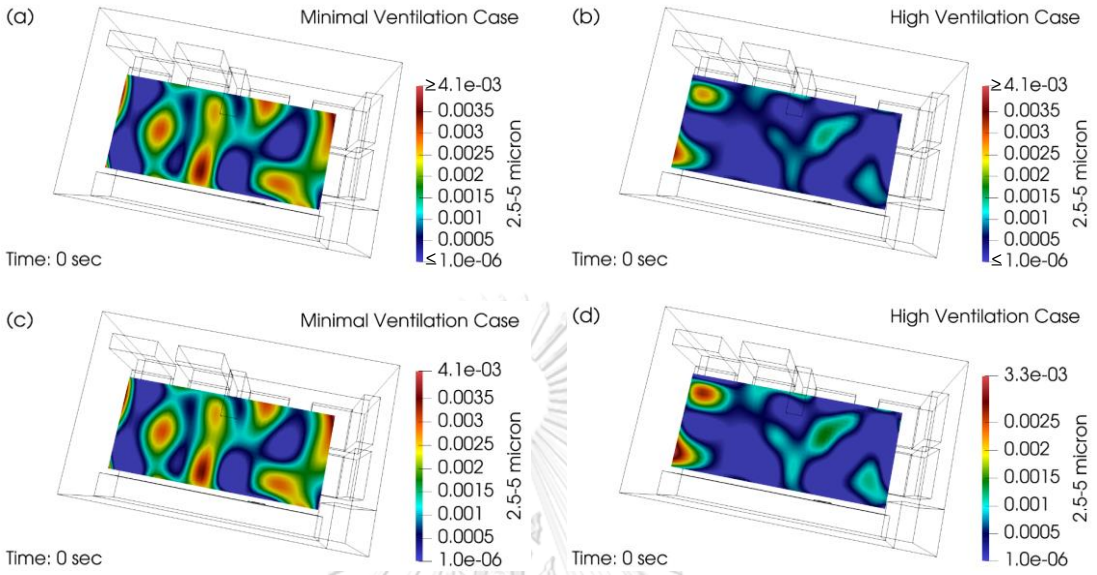

Figure 121 Contour Plane at EMS workers' Face Level at time = 0 second of Minimal Ventilation and High Ventilation with Different Colormap Ranges

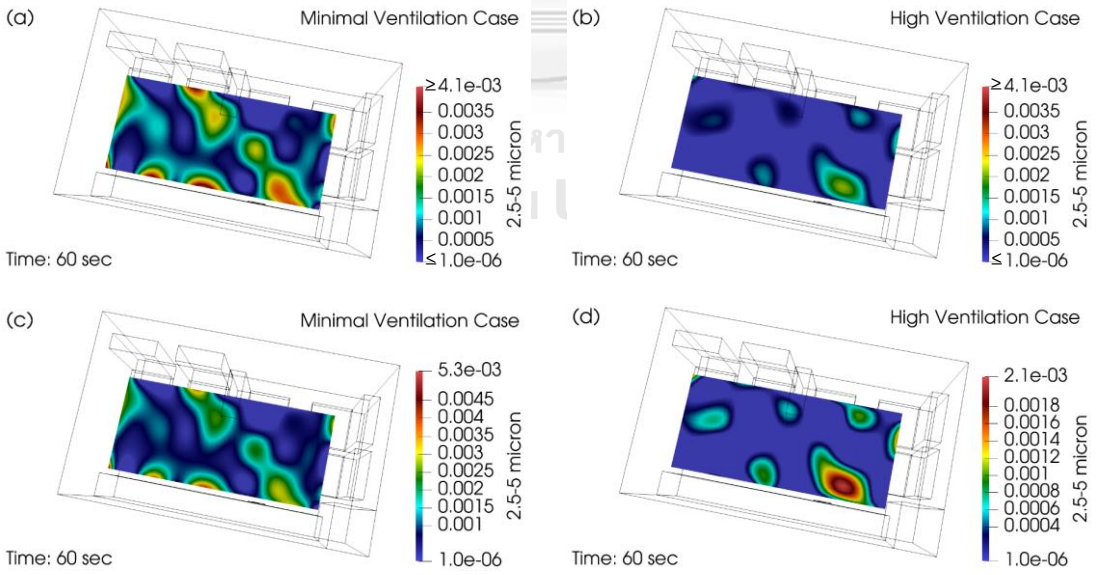

Figure 122 Contour Plane at EMS workers' Face Level at time = 60 second of Minimal Ventilation and High Ventilation with Different Colormap Ranges

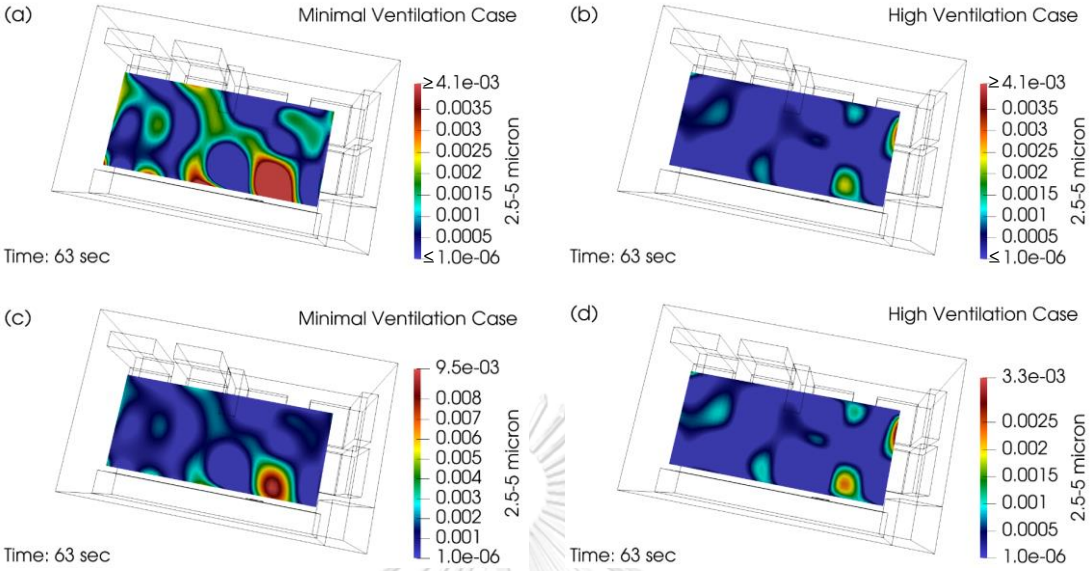

Figure 123 Contour Plane at EMS workers' Face Level at time = 63 second of Minimal Ventilation and High Ventilation with Different Colormap Ranges

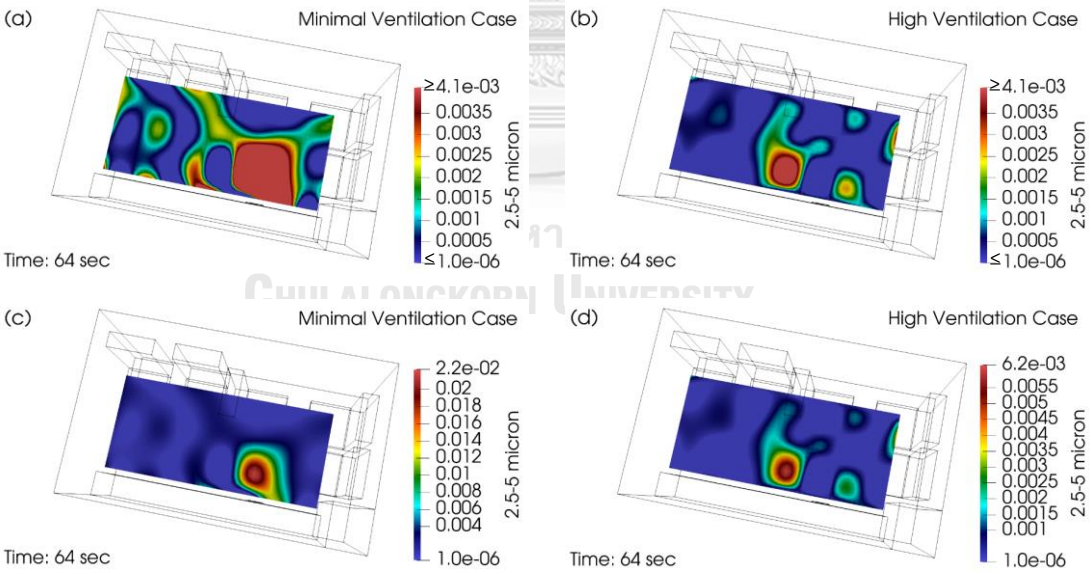

Figure 124 Contour Plane at EMS workers' Face Level at time = 64 second of Minimal Ventilation and High Ventilation with Different Colormap Ranges

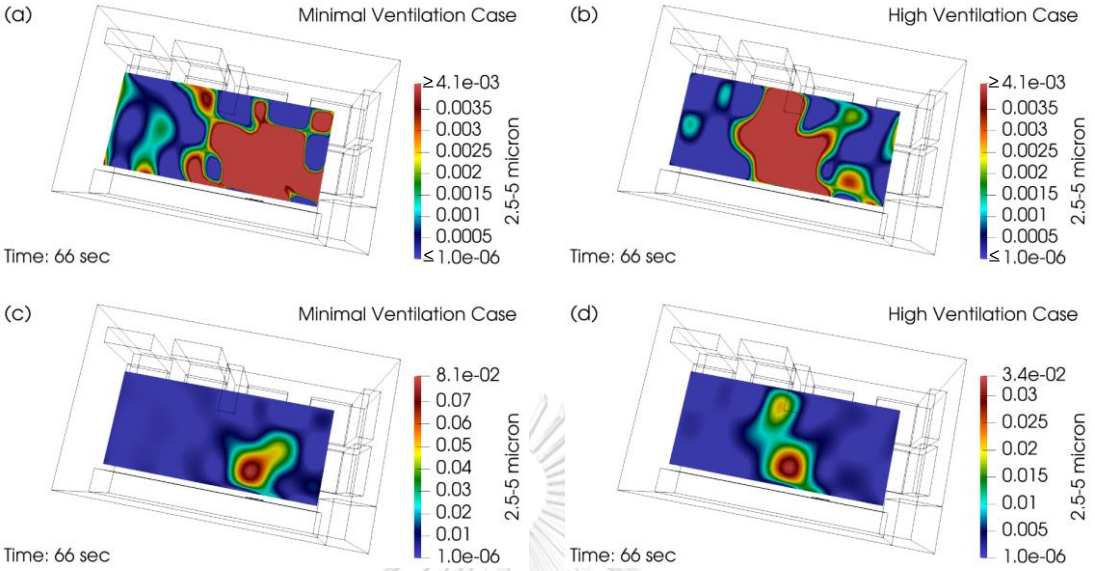

Figure 125 Contour Plane at EMS workers' Face Level at time = 66 second of Minimal Ventilation and High Ventilation with Different Colormap Ranges

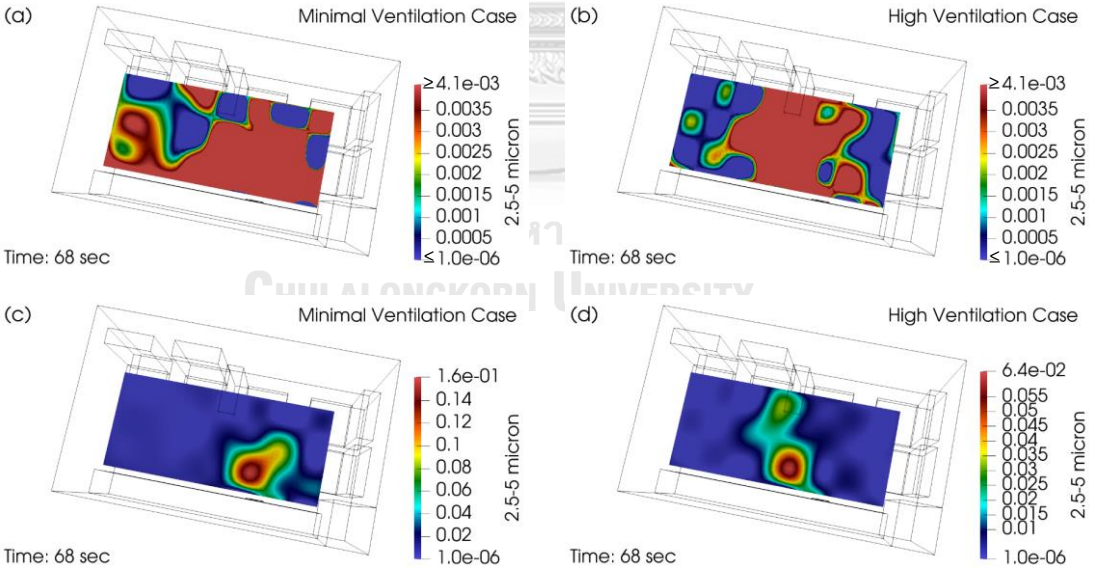

Figure 126 Contour Plane at EMS workers' Face Level at time = 68 second of Minimal Ventilation and High Ventilation with Different Colormap Ranges

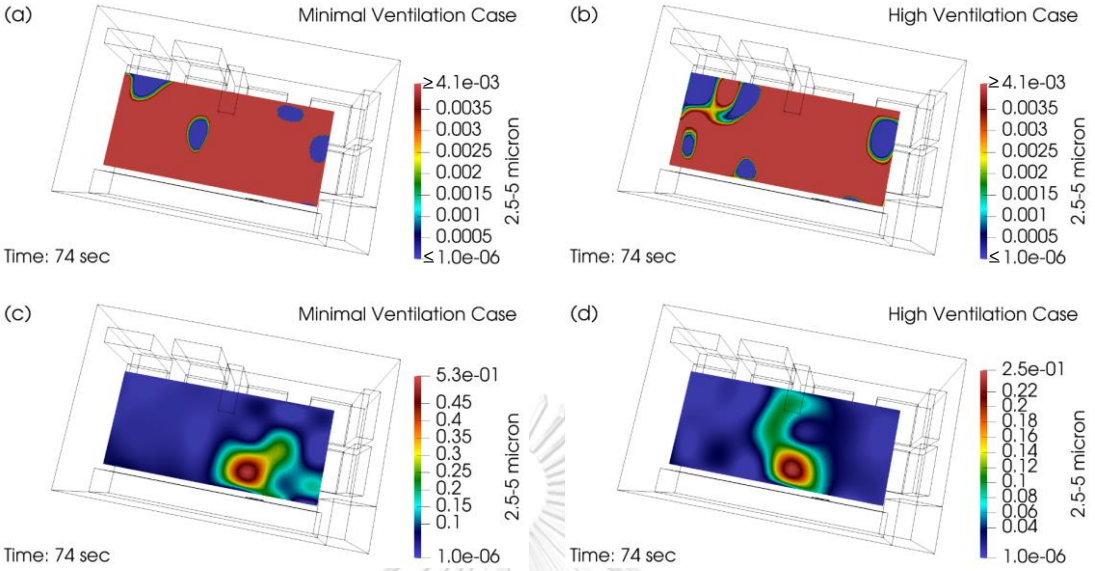

Figure 127 Contour Plane at EMS workers' Face Level at time = 74 second of Minimal Ventilation and High Ventilation with Different Colormap Ranges

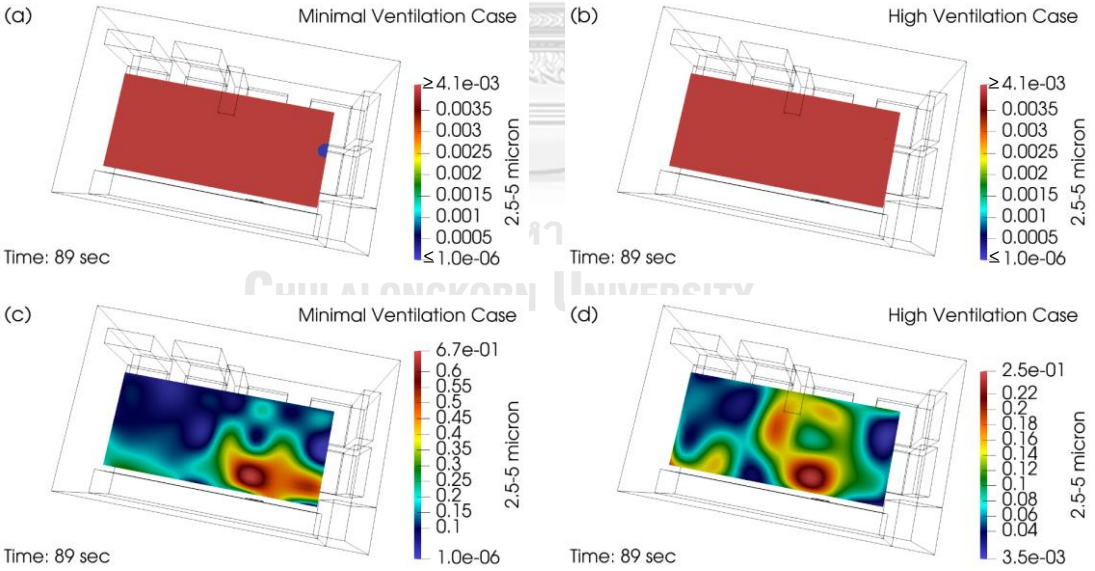

Figure 128 Contour Plane at EMS workers' Face Level at time = 89 second of Minimal Ventilation and High Ventilation with Different Colormap Ranges

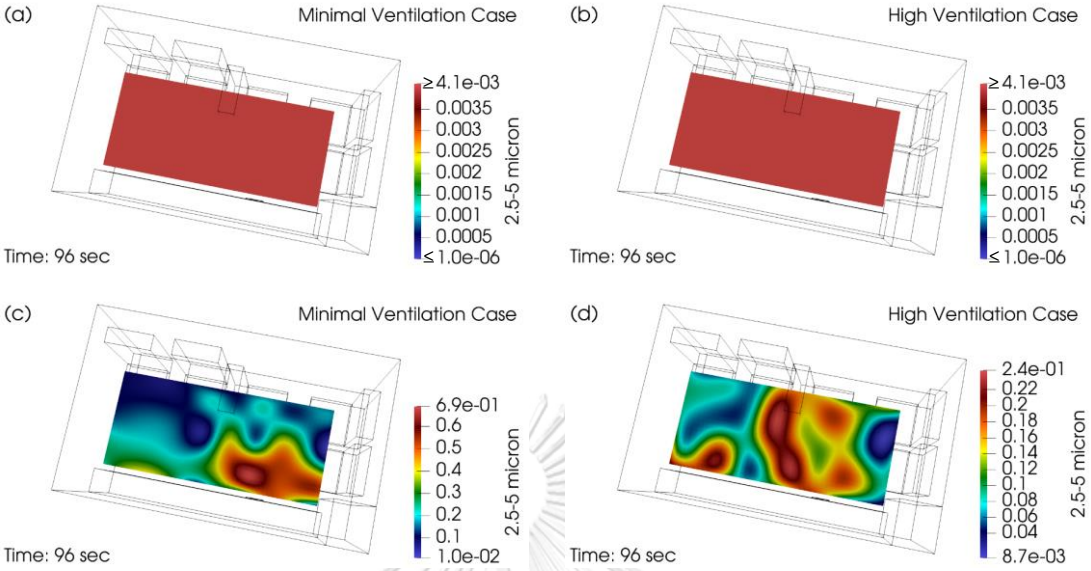

Figure 129 Contour Plane at EMS workers' Face Level at time = 96 second of Minimal Ventilation and High Ventilation with Different Colormap Ranges

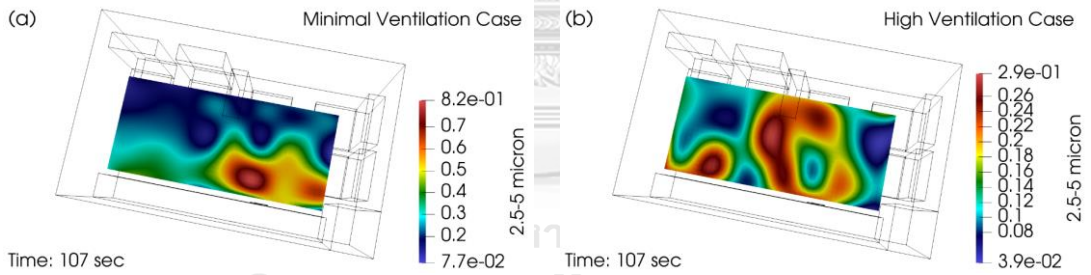

CHULALONGKORN UNIVERSITY

Figure 130 Contour Plane at EMS workers' Face Level at time = 107 second of Minimal Ventilation and High Ventilation

Until about 121st second, which is right after stopping particle injection, the peak concentration for MV and HV cases occurs (on the plane considered here) at this time. The areas of peak concentration in both cases are above the patient's face position, as shown in Figure 131. The peak concentration of the MV case is 0.848 μL/m^3 and the peak concentration for HV case is 0.606 μL/m^3. After that, at 137th second the significant reduction of concentration begins for both MV and HV cases.

MV case concentration reduces in the above patient's face area, including seat1, and in HV case, in the area above the patient's face, seat3, and the area opposite to seat5, as shown in Figure 132. Concentration continues to decline both cases as observed at the 180th second shown in Figure 133. As the time progresses to the 263rd second, as shown in Figure 134, HV case concentration begins to be visible with the background state colormap at the seat1 region. For the MV case concentration also continues to decline but none of the region on the plane reaches the background value. At 300th second, the HV case concentration area decreases to a wider area at the seat1 region, and there is also a decrease in the centre of the patient compartment, as shown in Figure 135. At the 350th second, HV case concentration continues to drop to the background state colormap in several regions which are seat1, seat2, and seat4, as shown in Figure 136. The concentration continues to decrease in both MV and HV cases which can be seen from Figure 137 which shows the contour of the 400th second. Until about 503rd second shown in Figure 138, the concentration of the HV case returns to the background state colormap. The concentration contour of the experiment end time of the HV case is shown in Figure 139.

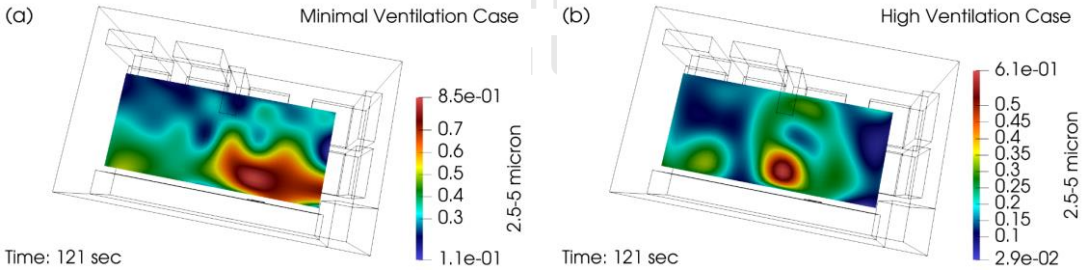

Figure 131 Contour Plane at EMS workers' Face Level at time = 121 second of Minimal Ventilation and High Ventilation

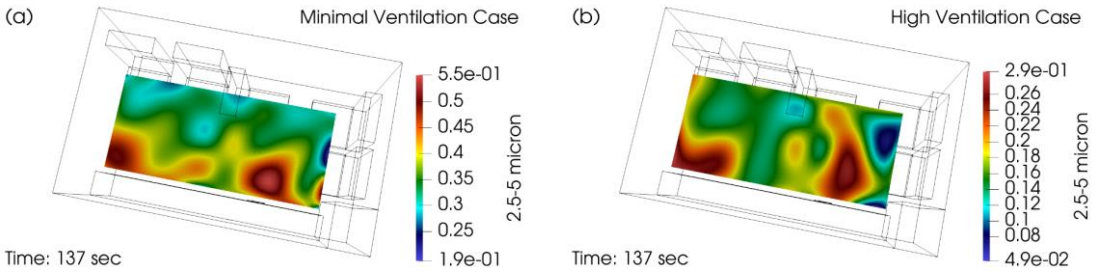

Figure 132 Contour Plane at EMS workers' Face Level at time = 137 second of Minimal Ventilation and High Ventilation

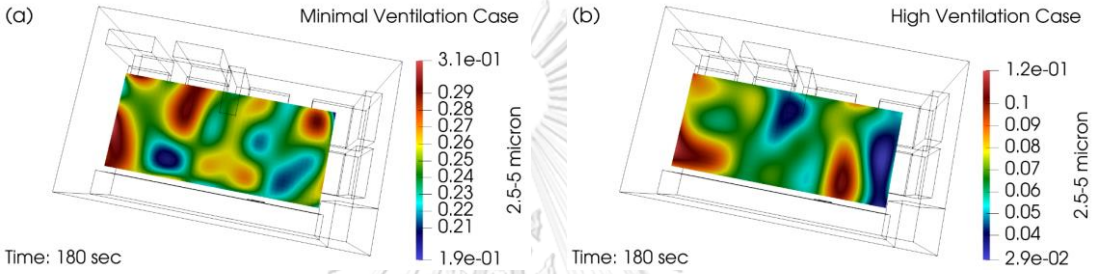

Figure 133 Contour Plane at EMS workers' Face Level at time = 180 second of Minimal Ventilation and High Ventilation

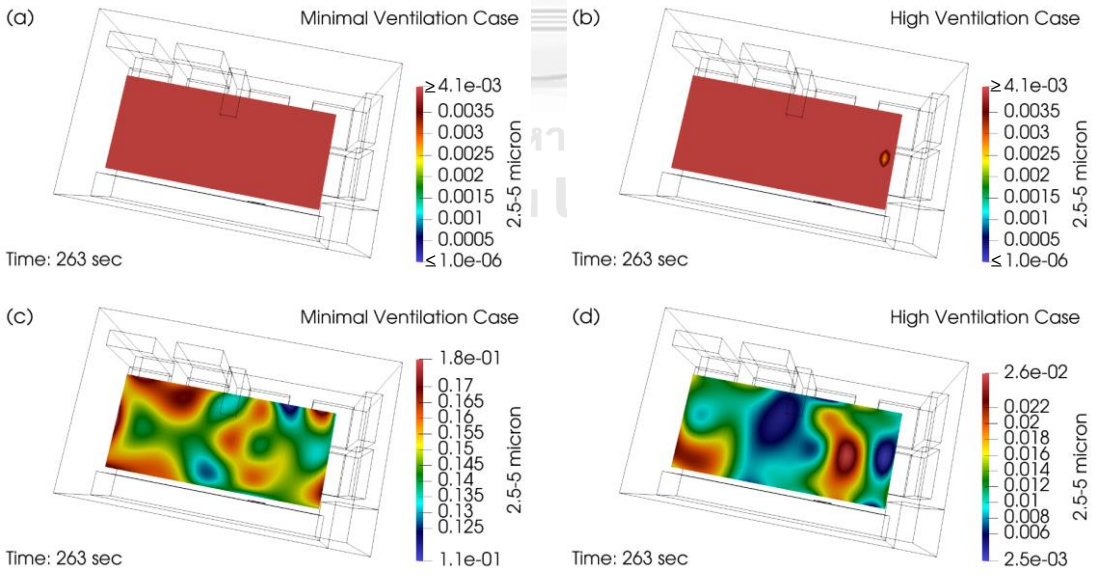

Figure 134 Contour Plane at EMS workers' Face Level at time = 263 second of Minimal Ventilation and High Ventilation with Different Colormap Ranges

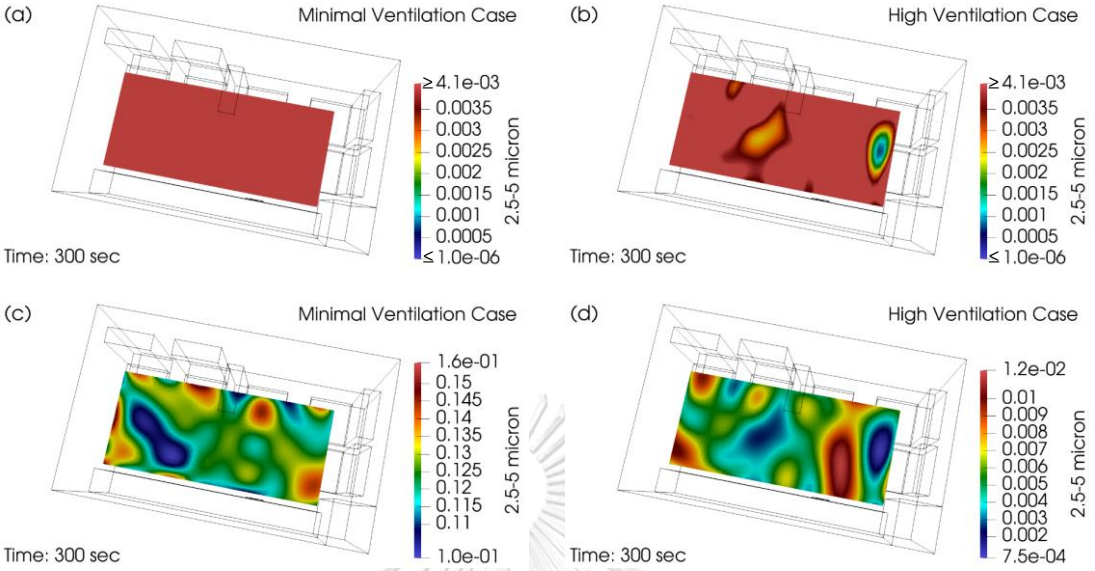

Figure 135 Contour Plane at EMS workers' Face Level at time = 300 second of Minimal Ventilation and High Ventilation with Different Colormap Ranges

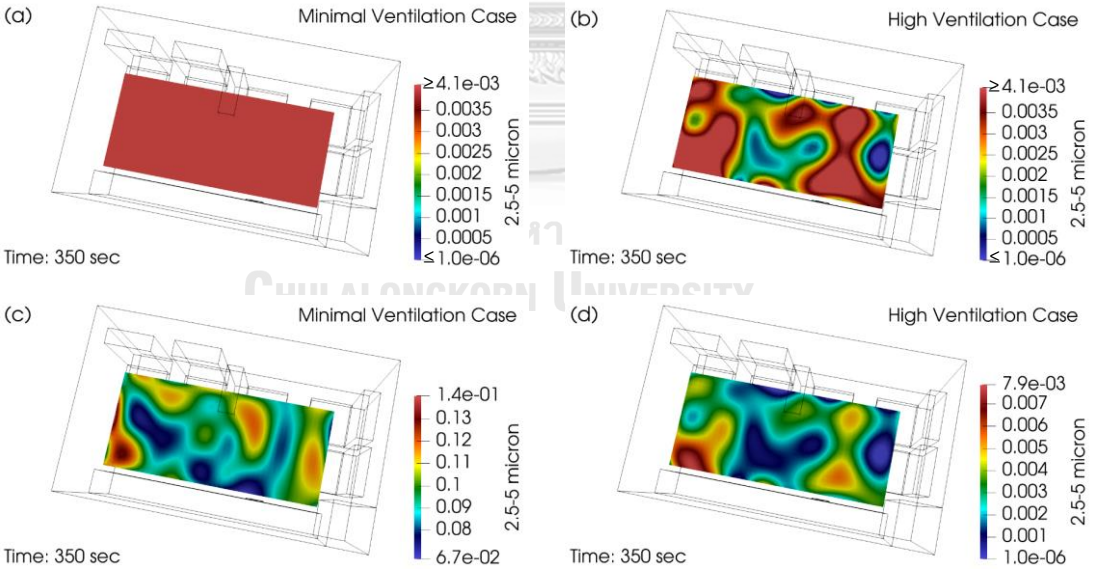

Figure 136 Contour Plane at EMS workers' Face Level at time = 350 second of Minimal Ventilation and High Ventilation with Different Colormap Ranges

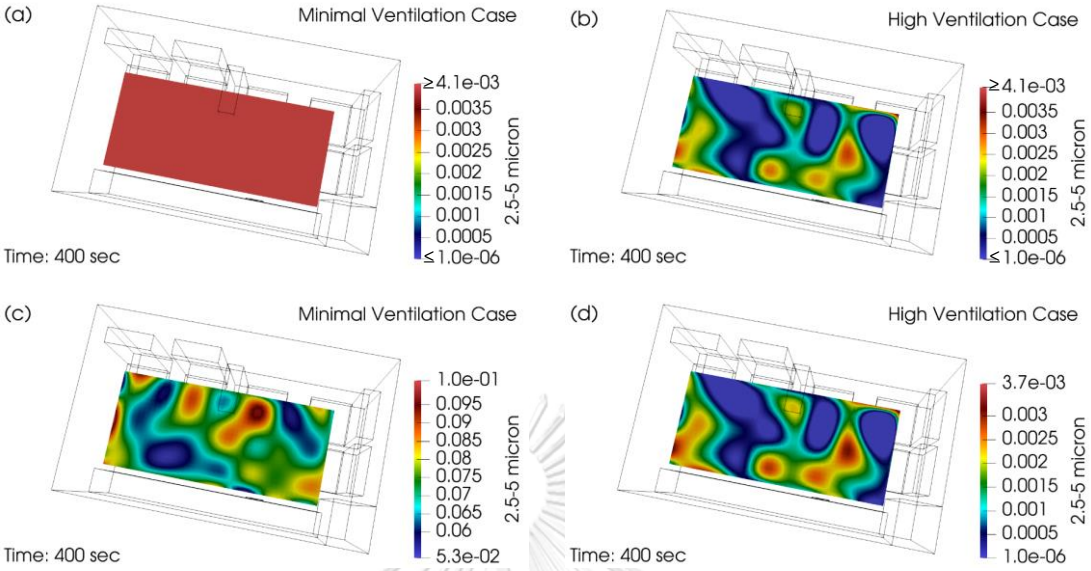

Figure 137 Contour Plane at EMS workers' Face Level at time = 400 second of Minimal Ventilation and High Ventilation with Different Colormap Ranges

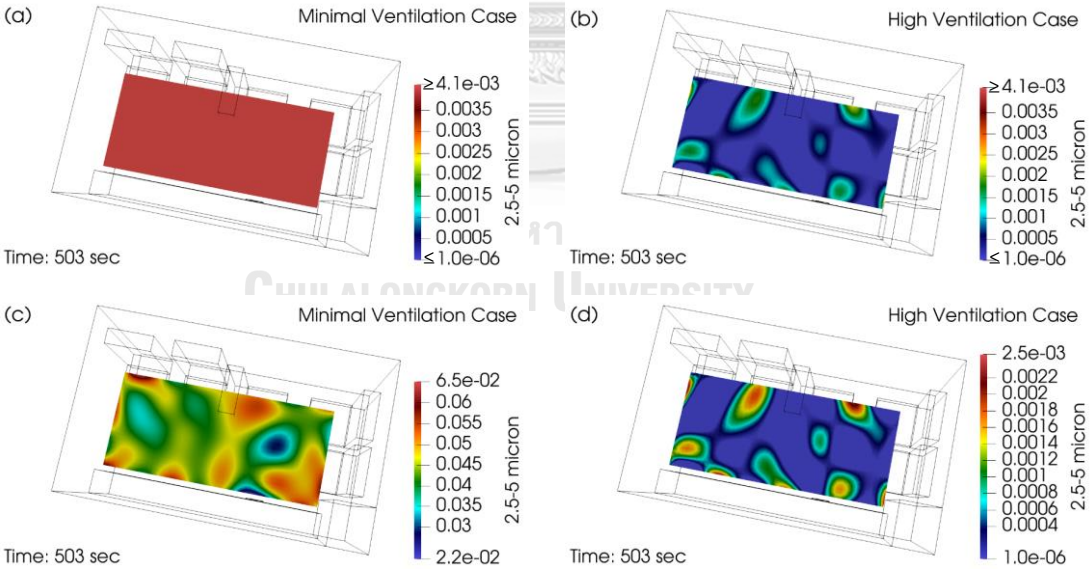

Figure 138 Contour Plane at EMS workers' Face Level at time = 503 second of Minimal Ventilation and High Ventilation with Different Colormap Ranges

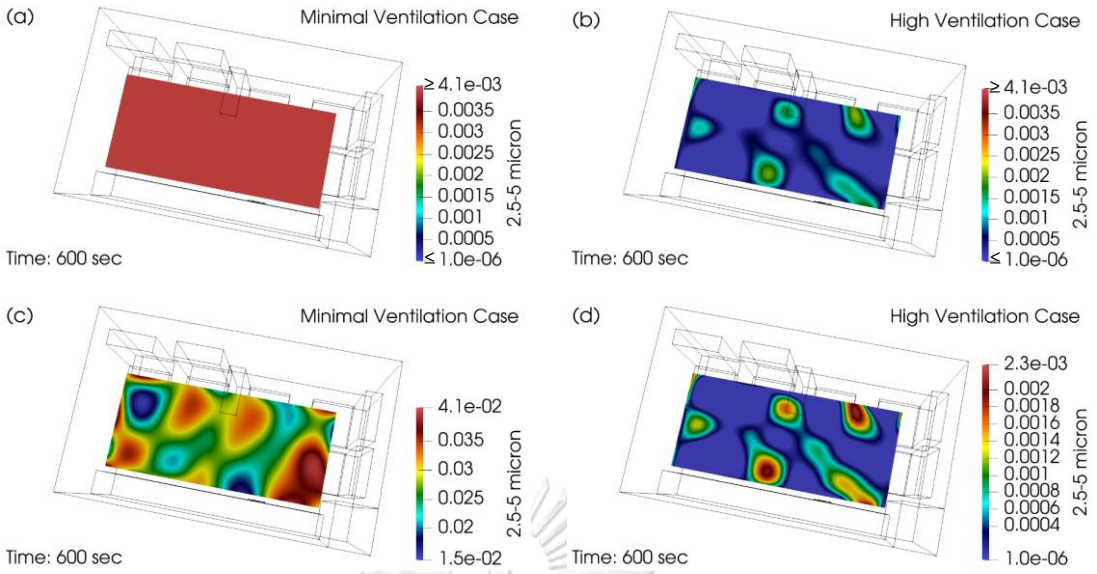

Figure 139 Contour Plane at EMS workers' Face Level at time = 600 second of Minimal Ventilation and High Ventilation with Different Colormap Ranges

Additional figures are added for the case of MV at further time. Although during the previous period the MV case concentration does not seem to decrease at all compared to the background state colormap; in fact, the concentration starts to decrease since about 121st second. Until about 861st second, the MV case concentration starts to decrease to the background state; the first area, where the reduction is observed, is at seat5, which can be seen in Figure 140. Considering the 950th second shown in Figure 141, the concentration area which decreased at 861st second is wider (more visible with background state colormap) and concentration begins to decline in several areas. At 1050th second, concentration begins to decline back to the background state colormap over a larger area, particularly at the end of the patient compartment and above the patient's face as shown in Figure 142 and continues to decline, which can be seen in Figure 143. Contour of the experiment end time is shown in Figure 144.

จุฬาลงกรณ์มหาวิทยาลัย
Chulalongkorn University

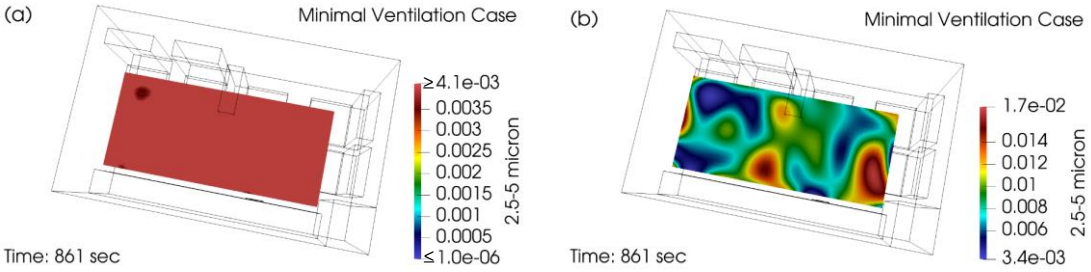

Figure 140 Contour Plane at EMS workers' Face Level at time = 861 second of Minimal Ventilation with Different Colormap Ranges

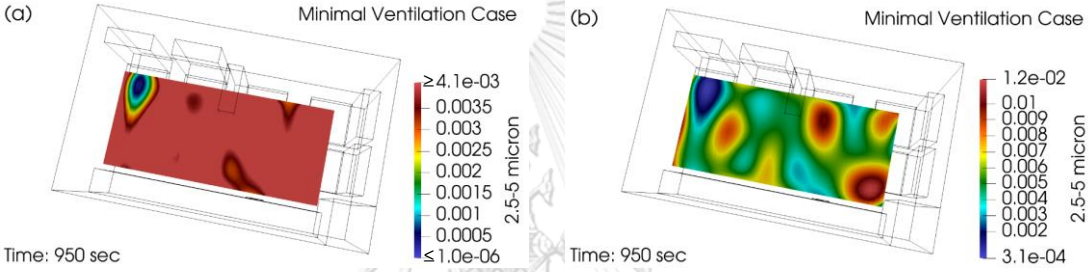

Figure 141 Contour Plane at EMS workers' Face Level at time = 950 second of Minimal Ventilation with Different Colormap Ranges

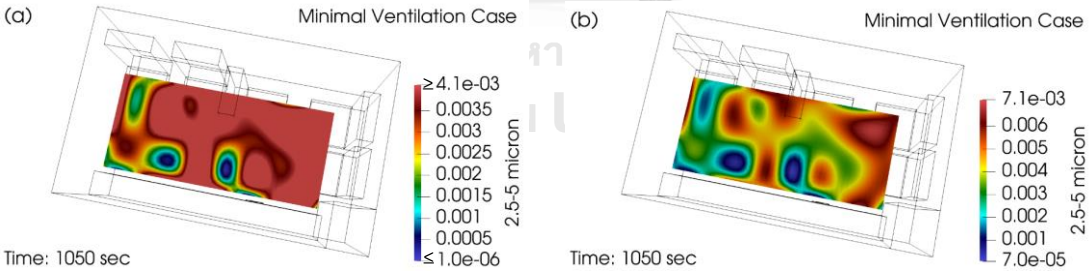

Figure 142 Contour Plane at EMS workers' Face Level at time = 1050 second of Minimal Ventilation with Different Colormap Ranges

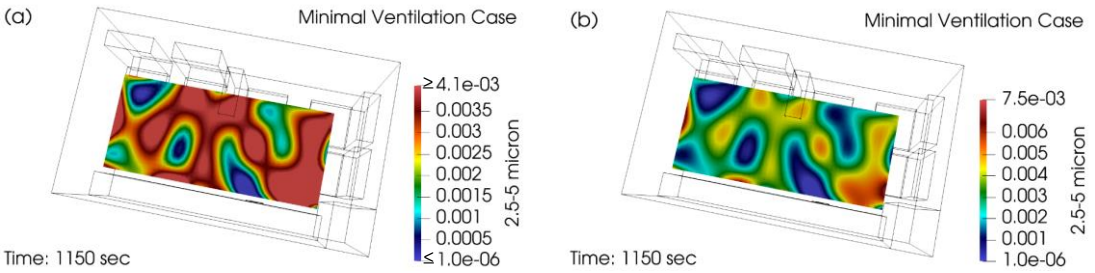

Figure 143 Contour Plane at EMS workers' Face Level at time = 1150 second of Minimal Ventilation with Different Colormap Ranges

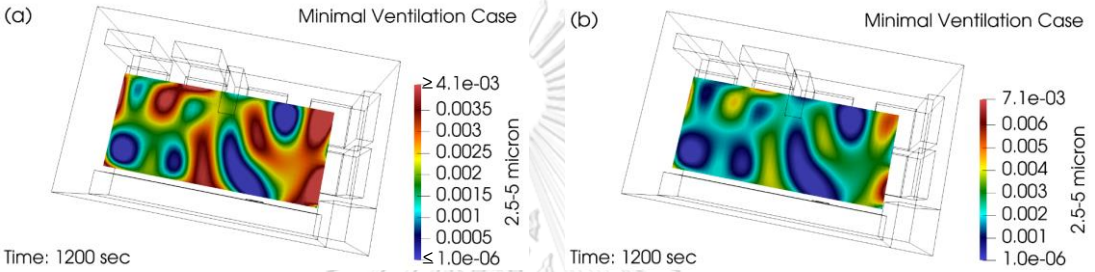

Figure 144 Contour Plane at EMS workers' Face Level at time = 1200 second of Minimal Ventilation with Different Colormap Ranges

To summarize, this section investigates the distribution of concentration of particles in the 2.5-5-micron size range. Right after the particle injection is initiated, detectable concentration (high concentration relative to background state colormap) is formed on the plane for both cases; the areas where these happen remain the same as previously mentioned size ranges. The resulting distribution area has the same distribution characteristics as in the previous two size ranges as well for both cases. the concentration across the horizontal planes (at face level) of both cases reach high value compared to the background state colormap at about 30 to 40 seconds after the injection is started. At about 120th second, the highest concentration over the experimental period is achieved on the plane for both cases. The concentration begins to decline until about three minutes, HV concentration begins to return to background, with the first region at seat 1, and returns to the background state all over the plane at about eighth minute of the experiment. For

จุฬาลงกรณ์มหาวิทยาลัย
Chulalongkorn University

the MV case, the concentration begins to decline to the background state in the region above seat 5 at about 13 minutes after the injection is commenced, but the concentration does not drop to the background state across the entire plane even after the experimental time has ended.

5.3 Vertical Contour Plane at Injection Position along Patient Cot

This section presents concentration contour on the vertical plane at injection position along patient cot at different times during the experiment period. The results are divided into three sections according to particles in the size range: 0.5-1 micron, 1-2.5 micron, and 2.5-5 micron.

5.3.1 Size range between 0.5 and 1 micron

Figure 145 to Figure 152 and Figure 158 to Figure 162 show the contours of the aerosol volume concentration for MV and HV cases at the injection position along patient cot in the ambulance at each time interval. Subfigure (a) and subfigure (b) show colormaps that compare with the background value at the start of the measurement or at the zeroth second, in order to investigate the change in the concentration in comparison to when it started. Subfigure (c) and (d) help indicate the location of high concentration at that time. The period of time when the change in concentration is not visible relative to the background state colormap is shown in Figure 153 to Figure 157. For contours at time intervals greater than 600th second, the time interval after the termination of the HV case, are shown in Figure 163 to Figure 167, where subfigure (a) shows a colormap relative to the background state and subfigure (b) is a visible range colormap for each time period of the MV case.

In the zeroth second which is the start time of the experiment, concentration and distribution for both MV and HV cases are shown in Figure 145. It is found that

the overall picture of concentration of the MV case is higher than those of the HV case, the reason being discussed in Section 5.2. After 60 seconds which is the time the particle injection is started; the concentration remains close to at zeroth second. The local peak concentration in the MV case remains at the same region but the HV local peak concentration shifts as shown in Figure 146. At the 62nd second, the MV case concentration is noticeably higher above the patient's face area (injection area) compared to the colormap of background state as observed in Figure 147. One second later, shown in Figure 148, HV case concentration begins to observable on the plane compared to background state colormap at the area above the patient's face. While during this time the distribution area of the MV case concentration expands to the top and the overall concentration value is also higher than the HV case. Figure 149, which shows the contour plane of 67th second, the relative high concentration of the MV case compared to the background state colormap almost distributes to a nearly full of the front part of the patient compartment. For the HV case, the area of relative high concentration distribution compared to the background colormap is larger than at 63rd second and there is a reversal of high concentration compared to background state after leaving the plane in the front of the patient compartment. At the 72nd second, the high concentration distribution relative to the background state colormap distributes almost across the entire plane for both MV and HV cases, which can be seen in Figure 150.

จุฬาลงกรณ์มหาวิทยาลัย
Chulalongkorn University

Until about 76th second, the concentration is relatively large (compared to the background state colormap) across the entire plane as shown in Figure 151, and the same is true for the HV case at the 81st second, as shown in Figure 152. Although the concentrations in both cases are higher across the plane compared to the MV visible range colormap at zeroth second, the concentrations continue to rise over time, as can be seen in Figure 153. Until about 116th second, which is 4 seconds before the stoppage of particle injection, the peak concentration of HV case occurs at seat1 region with a value of 0.082 $\mu L/m^3$, which can be seen in Figure 154.

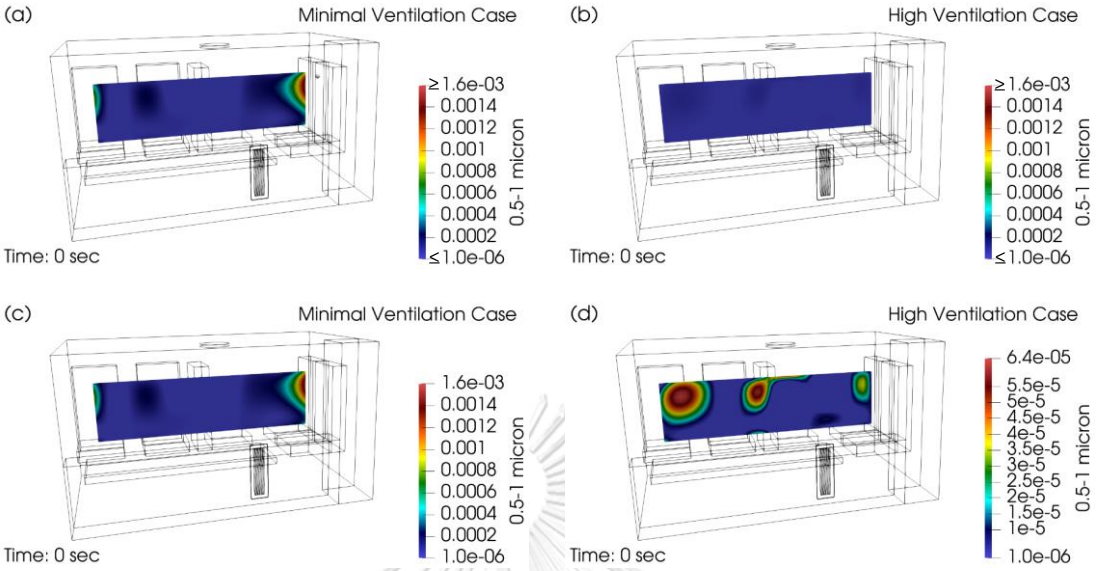

Figure 145 Contour Plane at Injection Position along Patient Cot at time = 0 second of Minimal Ventilation and High Ventilation with Different Colormap Ranges

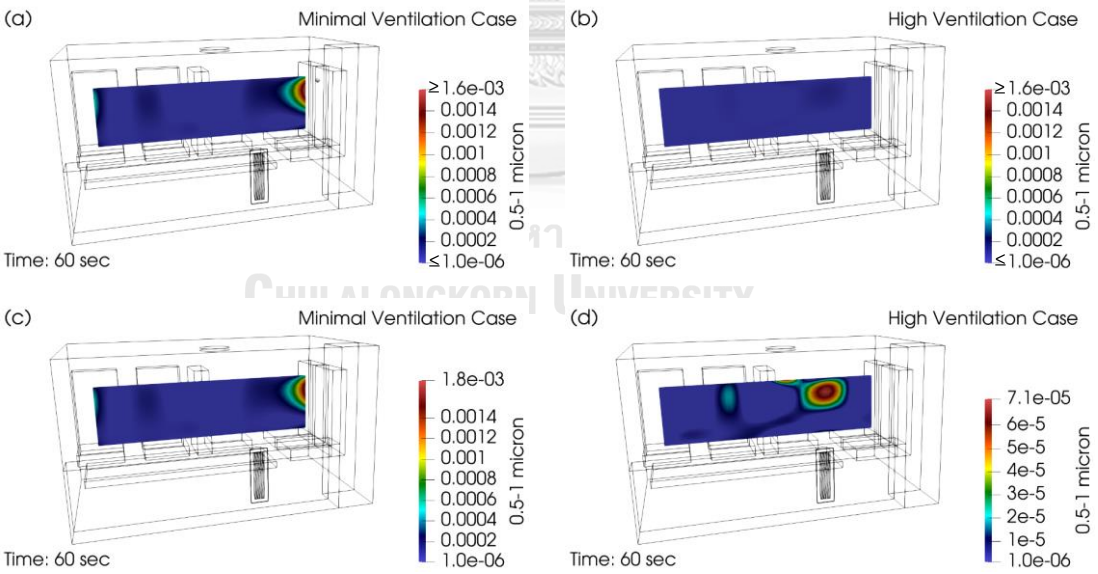

Figure 146 Contour Plane at Injection Position along Patient Cot at time = 60 second of Minimal Ventilation and High Ventilation with Different Colormap Ranges

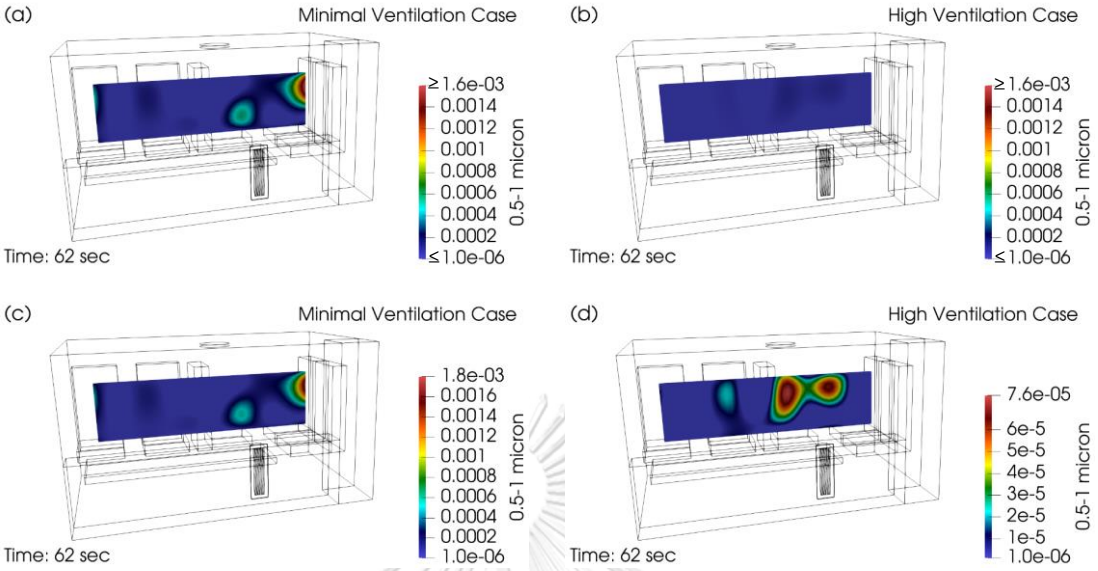

Figure 147 Contour Plane at Injection Position along Patient Cot at time = 62 second of Minimal Ventilation and High Ventilation with Different Colormap Ranges

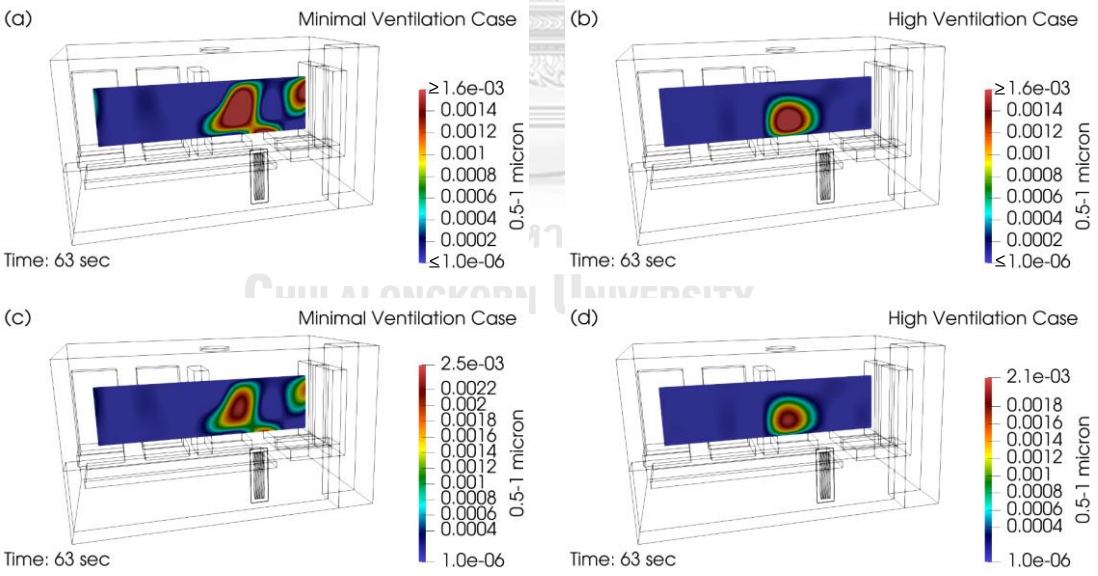

Figure 148 Contour Plane at Injection Position along Patient Cot at time = 63 second of Minimal Ventilation and High Ventilation with Different Colormap Ranges

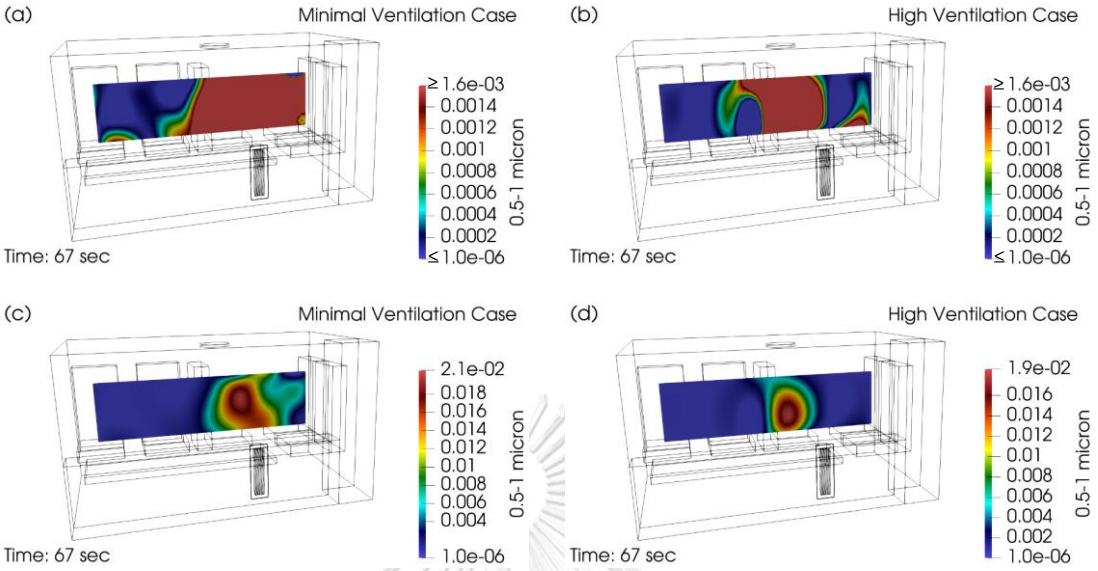

Figure 149 Contour Plane at Injection Position along Patient Cot at time = 67 second of Minimal Ventilation and High Ventilation with Different Colormap Ranges

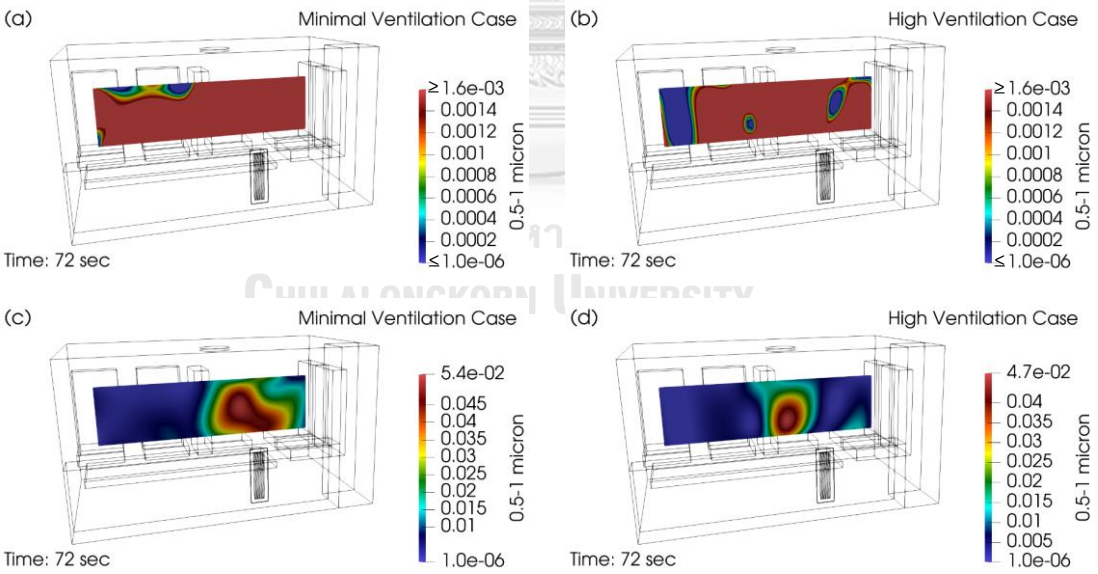

Figure 150 Contour Plane at Injection Position along Patient Cot at time = 72 second of Minimal Ventilation and High Ventilation with Different Colormap Ranges

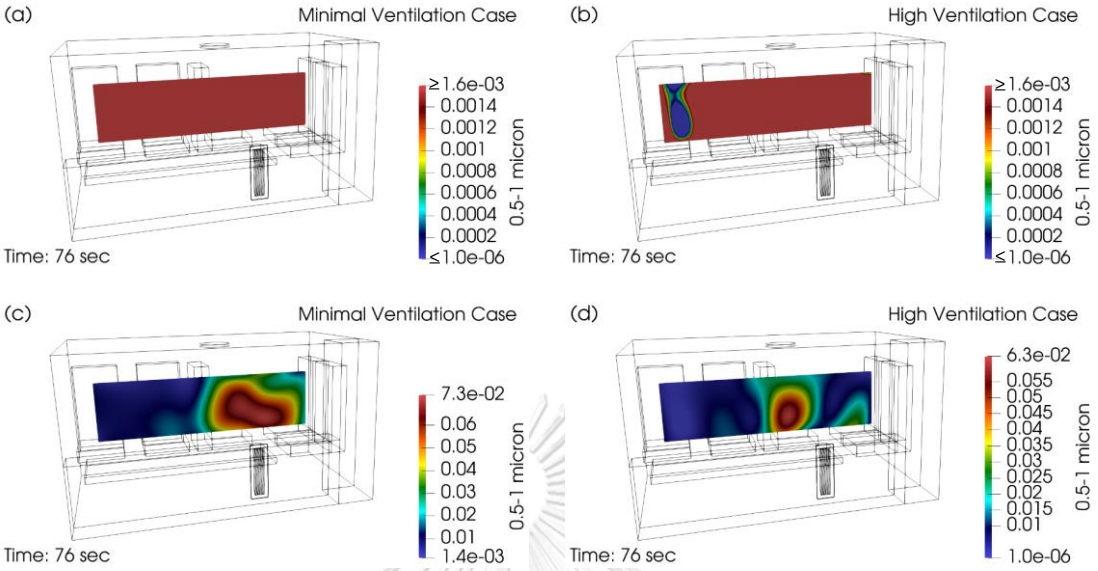

Figure 151 Contour Plane at Injection Position along Patient Cot at time = 76 second of Minimal Ventilation and High Ventilation with Different Colormap Ranges

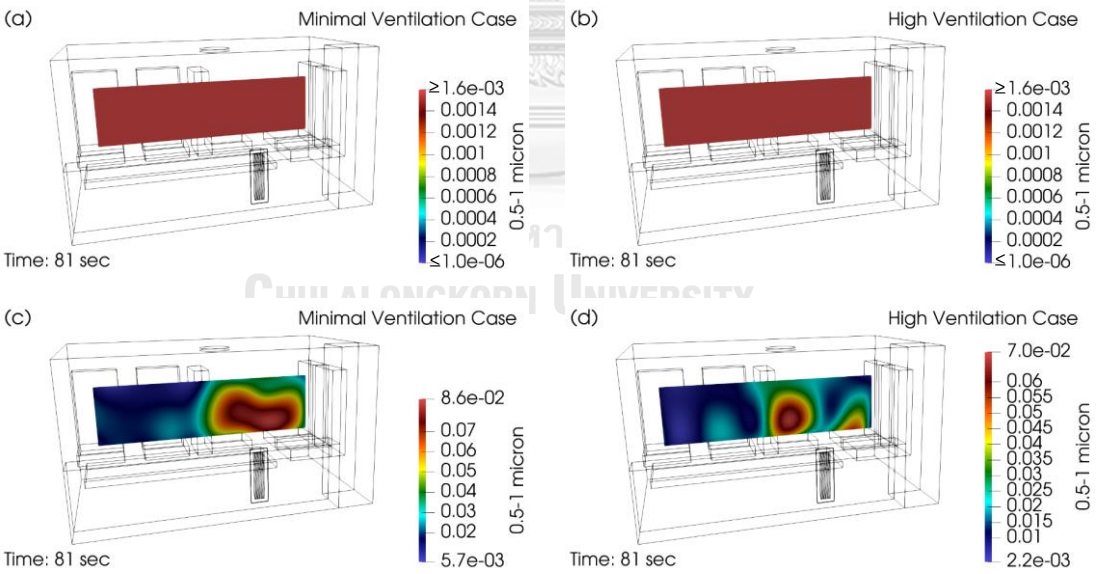

Figure 152 Contour Plane at Injection Position along Patient Cot at time = 81 second of Minimal Ventilation and High Ventilation with Different Colormap Ranges

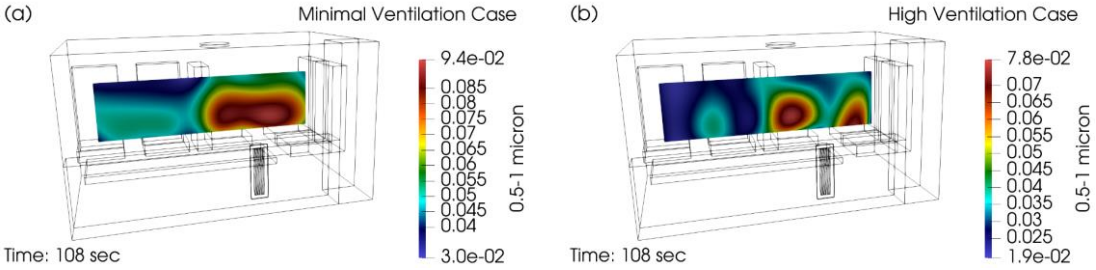

Figure 153 Contour Plane at Injection Position along Patient Cot at time = 108 second of Minimal Ventilation and High Ventilation

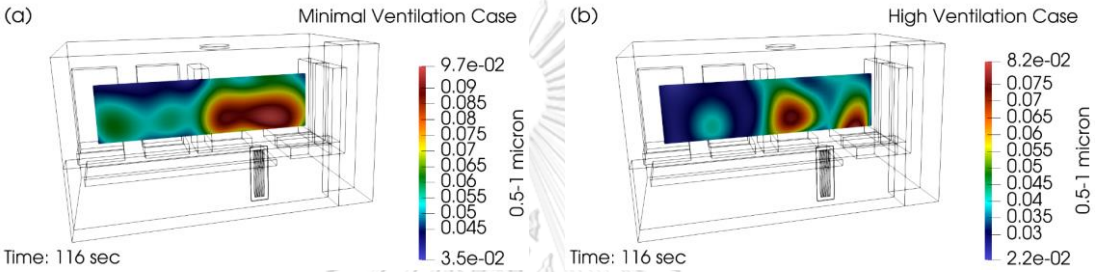

Figure 154 Contour Plane at Injection Position along Patient Cot at time = 116 second of Minimal Ventilation and High Ventilation

Particle injection is stopped at 120th second and 6 seconds later, shown in Figure 155, the peak concentration of the MV case occurs in the region between patient cot and seat1, with a value of 0.101 μL/m^3. From the inception of introducing particles into the patient compartment until the maximum concentration is reached, although the concentration and distribution of the concentration relative to the background state colormap change, the position of the local peak concentration at each time period is in same region as can be seen from Figure 147 to Figure 155. After the peak concentration achieves for both cases; concentration begins to decline at above the patient's face for both cases as observed in Figure 156 and concentration continues to decline across the plane, as observed in Figure 157, which shows the concentration contour at the 200th second. Until about 235th second, HV case concentration begins to be visible with the background state colormap in the area above the centre of the patient cot, which can be seen in

จุฬาลงกรณ์มหาวิทยาลัย
Chulalongkorn University

Figure 158. After that, at 300th second, HV high concentration compared to background state colormap begins to decline in many regions, especially in the area above the patient cot as shown in Figure 159. The HV concentration continues to decline until there are only two regions of high concentration compared to the background state colormap as shown in Figure 160. Until about 395th second, the HV case concentration returns to the background value across the entire plane, where the contour is shown in Figure 161. The final period of the HV case experiment can be seen in Figure 162.

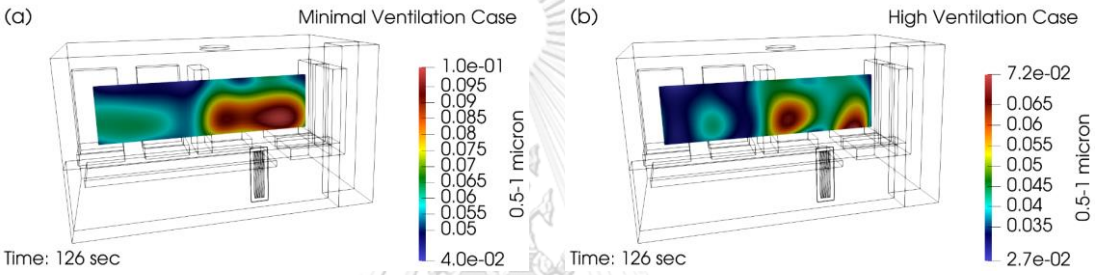

Figure 155 Contour Plane at Injection Position along Patient Cot at time = 126 second of Minimal Ventilation and High Ventilation

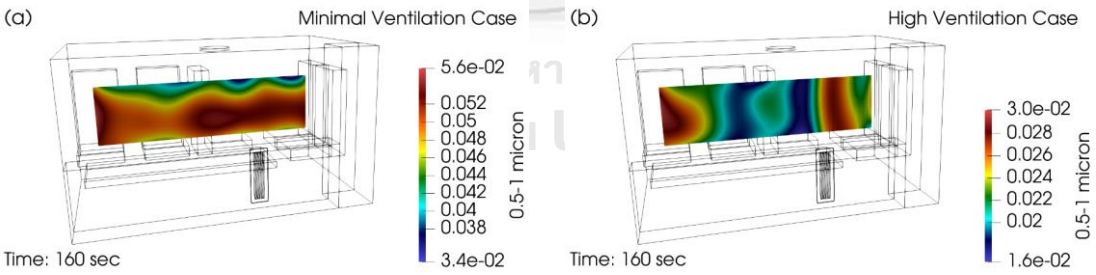

Figure 156 Contour Plane at Injection Position along Patient Cot at time = 160 second of Minimal Ventilation and High Ventilation

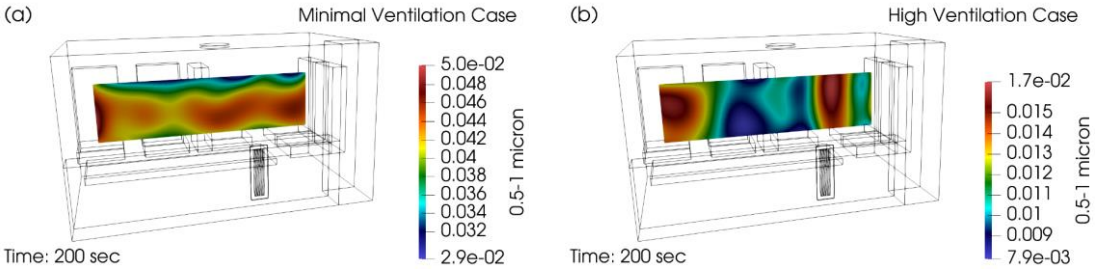

Figure 157 Contour Plane at Injection Position along Patient Cot at time = 200 second of Minimal Ventilation and High Ventilation

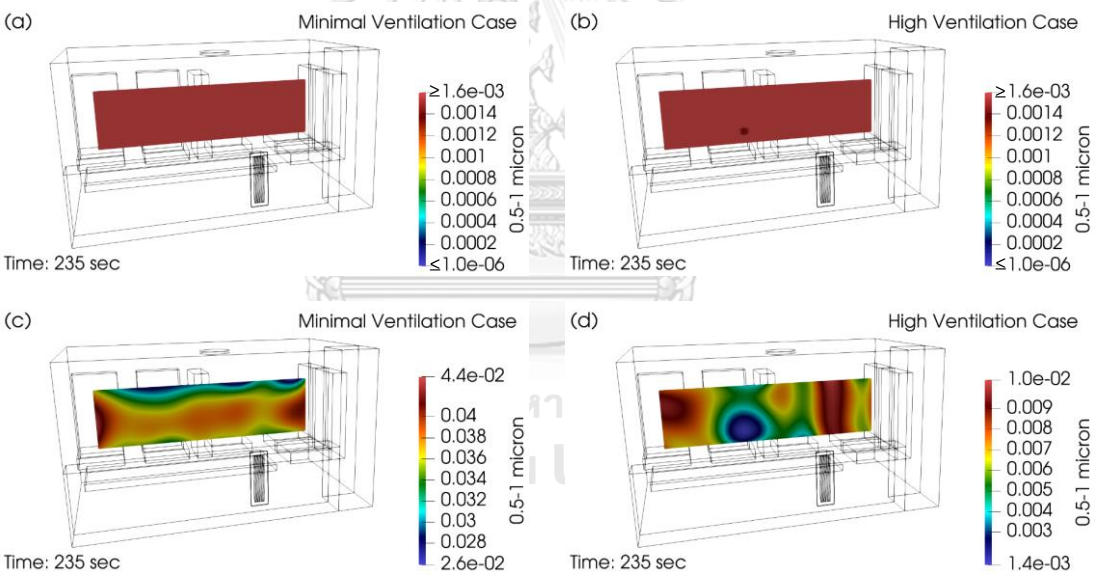

Figure 158 Contour Plane at Injection Position along Patient Cot at time = 235 second of Minimal Ventilation and High Ventilation with Different Colormap Ranges

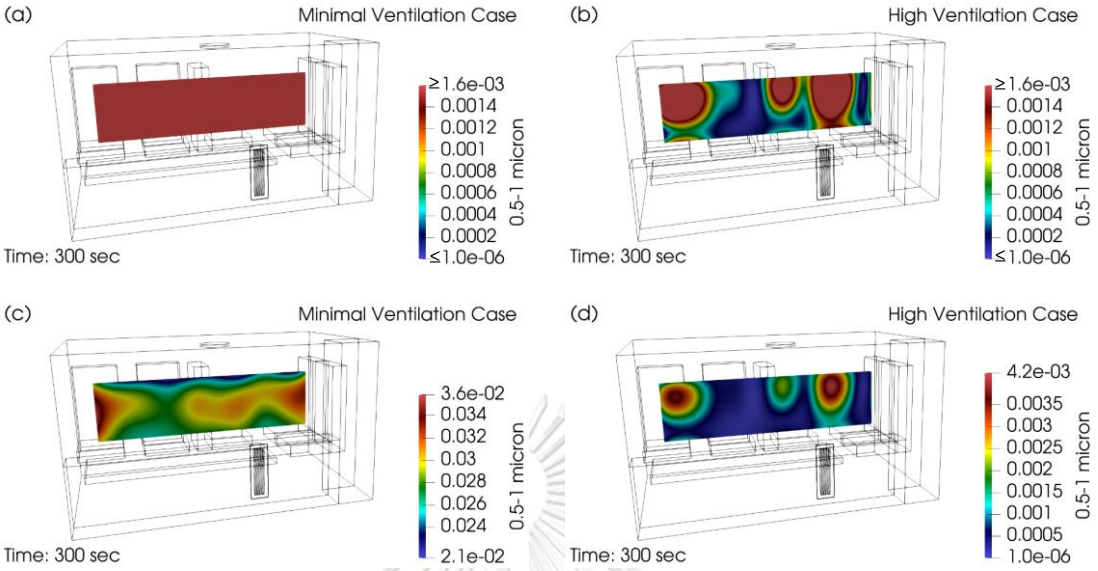

Figure 159 Contour Plane at Injection Position along Patient Cot at time = 300 second of Minimal Ventilation and High Ventilation with Different Colormap Ranges

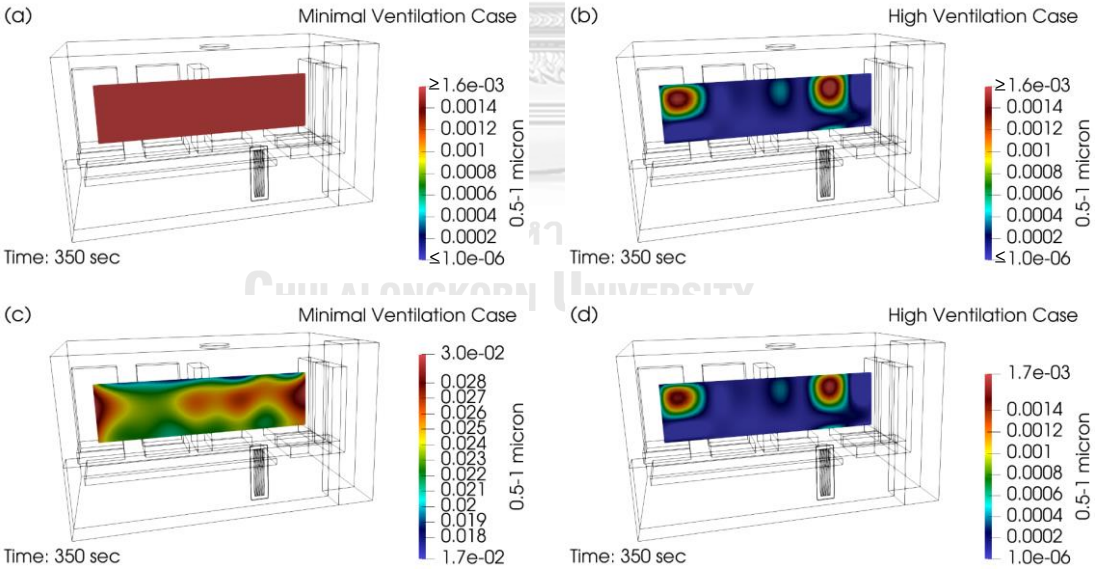

Figure 160 Contour Plane at Injection Position along Patient Cot at time = 350 second of Minimal Ventilation and High Ventilation with Different Colormap Ranges

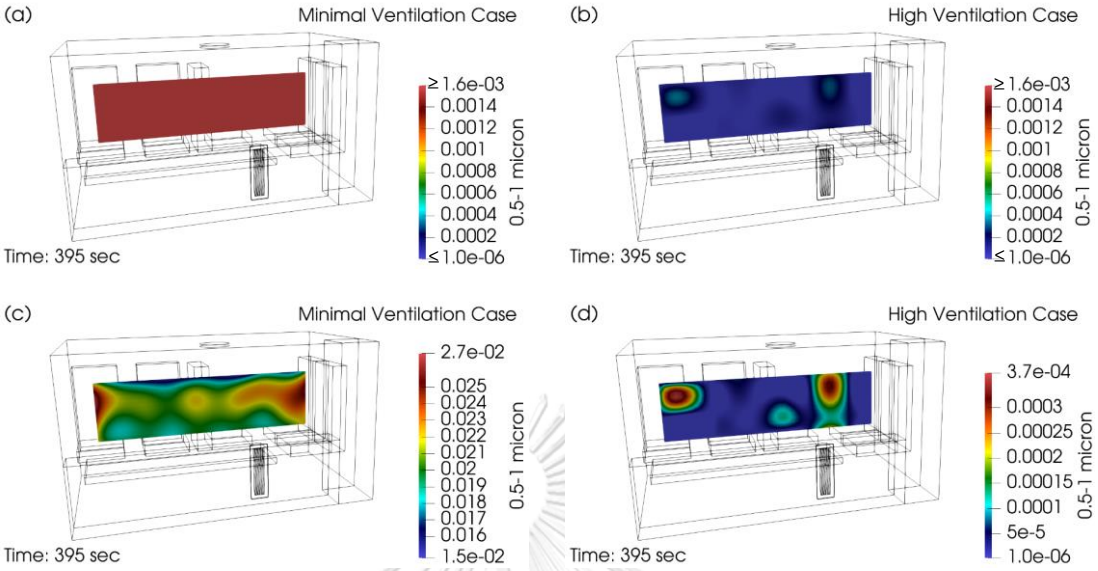

Figure 161 Contour Plane at Injection Position along Patient Cot at time = 395 second of Minimal Ventilation and High Ventilation with Different Colormap Ranges

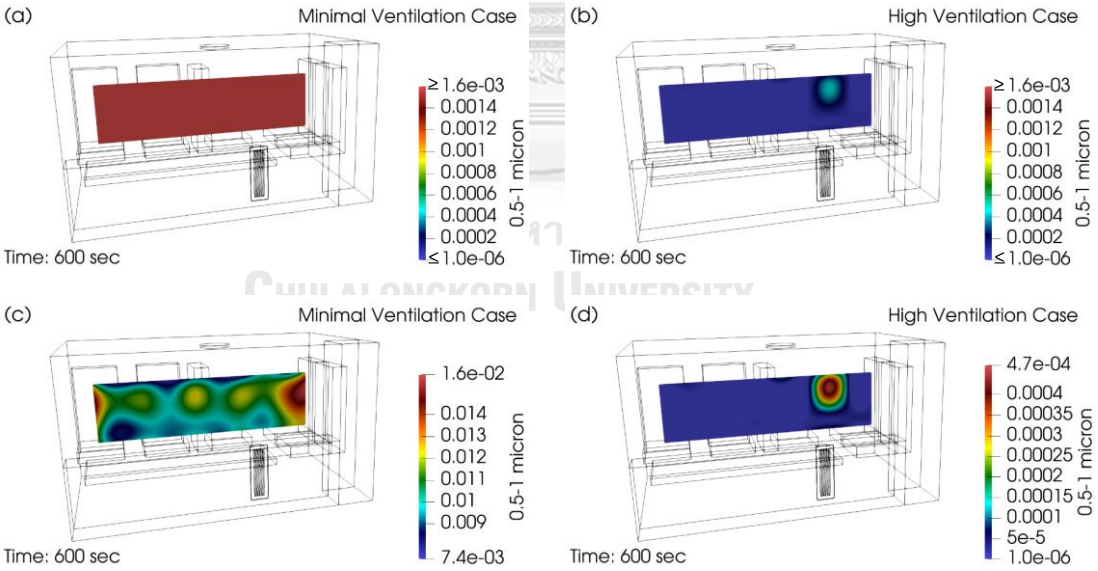

Figure 162 Contour Plane at Injection Position along Patient Cot at time = 600 second of Minimal Ventilation and High Ventilation with Different Colormap Ranges

Additional figures are added for the case of MV at further time. Although HV case concentration declines back to the background state across the entire plane at

395th second, the MV case concentration is not visible with the background state colormap. However, if we look at the visible range at each time period, it is found that the concentration of MV case starts to decrease since the peak concentration occurs, which can be observed from Figure 155 to Figure 162. Until about 807th second, the concentration of MV case compared to the background state colormap begins to decline, with the decreasing area at the foot of the patient cot as shown in Figure 163. Looking at Figure 164, the reduced concentration region relative to the background state is wider than the previous time, especially above the patient cot. The MV case concentration continues to decline over a larger area compared to the background state colormap, which can be seen from Figure 165 and Figure 166. The experimental end time of the MV case is shown in Figure 167.

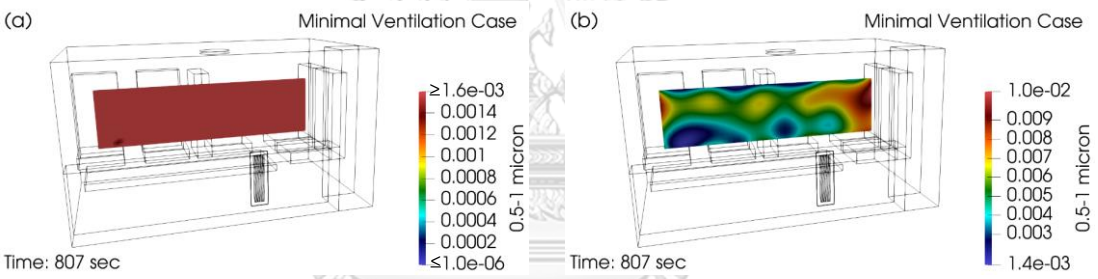

Figure 163 Contour Plane at Injection Position along Patient Cot at time = 807 second of Minimal Ventilation with Different Colormap Ranges

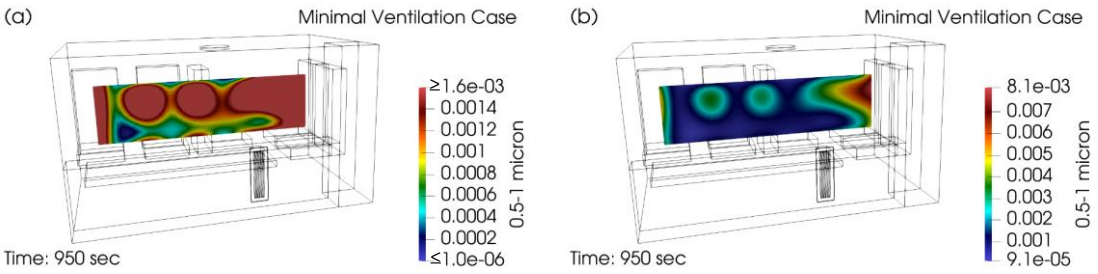

Figure 164 Contour Plane at Injection Position along Patient Cot at time = 950 second of Minimal Ventilation with Different Colormap Ranges

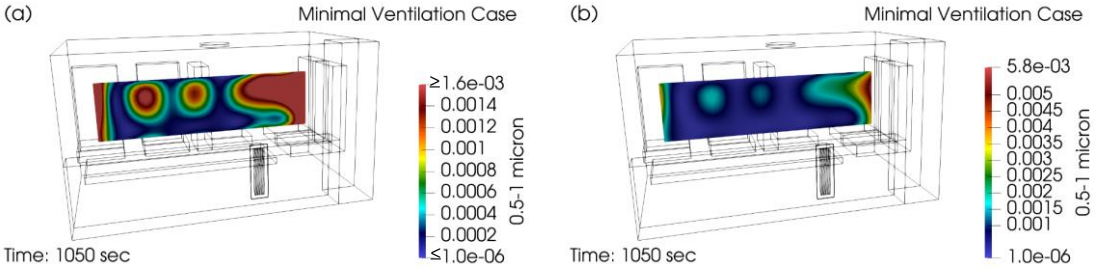

Figure 165 Contour Plane at Injection Position along Patient Cot at time = 1050 second of Minimal Ventilation with Different Colormap Ranges

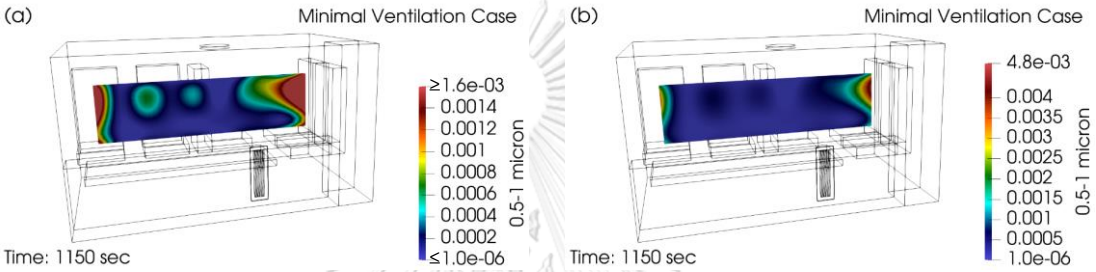

Figure 166 Contour Plane at Injection Position along Patient Cot at time = 1150 second of Minimal Ventilation with Different Colormap Ranges

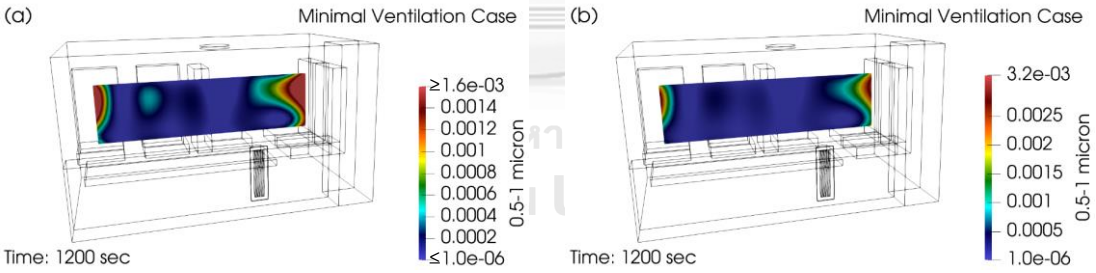

Figure 167 Contour Plane at Injection Position along Patient Cot at time = 1200 second of Minimal Ventilation with Different Colormap Ranges

To summarize, this section investigates the distribution of concentration of particles in the 0.5-1-micron size range. A high concentration occurs on the plane above the patient's face right after the particle injection is initiated (t = 60 sec) for both cases. In the first phase after the event mentioned above, the MV concentration distribution area is mainly at the anterior part of the patient

compartment while the HV concentration distribution area is mainly at the upper half of the patient cot. The concentration across the vertical planes (at the injection position) of both cases reach high value compared to the background state colormap at about 20 seconds after the injection. The highest concentration of all experiments is achieved on the plane at about second minute for both cases which is at when the injection is stopped. HV concentration begins to drop to the background state at about three minutes after the particle injection is started at the area above the middle of the patient cot and HV concentration is lower until it returns to the background state across the whole plane at about 395th second. For the MV case, the concentration begins to decline back to the background state at about 13 minutes (after the injection is initiated) in the area above the foot of the patient cot. However, the concentration of MV case does not drop back to background state across the plane even after the experimental period has ended.

5.3.2 Size range between 1 and 2.5 micron

Figure 168 to Figure 175 and Figure 181 to Figure 185 show the contours of the aerosol volume concentration for MV and HV cases at the injection position along patient cot in the ambulance at each time interval. Subfigure (a) and Subfigure (b) show colormaps that compare with the background value at the start of the measurement or at the zeroth second, in order to investigate the change in the concentration in comparison to when it started. Subfigure (c) and (d) help indicate the location of high concentration at that time. The period of time when the change in concentration is not visible relative to the background state colormap is shown in Figure 176 to Figure 180. For contours at time intervals greater than 600th second, the time interval after the termination of the HV case, are shown in Figure 186 to Figure 190, where subfigure (a) shows a colormap relative to the background state and subfigure (b) is a visible range colormap for each time period of the MV case.

The concentrations and distributions of HV and MV cases at the time of initiation of the experiment, are shown in Figure 168. The concentration on the contour plane for both cases is slightly different, with the MV case concentration being higher, and the location of the local peak concentration is different as well. At the time the particle injection is started; the concentration values remain close to the start of the experiment. The local peak concentration in the MV case remains at the same site but the HV local peak concentration shifts similarly in the 0.5-1-micron size range as shown in Figure 169. MV case concentration begins to increase, which is compared to the colormap of zeroth second, at 62nd second, with this higher concentration occurring in the region above the patient's face as observed in Figure 170. At 63rd second, shown in Figure 171, HV case concentration begins to rise above the patient's face area. For the MV case, the concentration distribution area spreads over a larger area to the top and the front of the patient compartment.

At 67th second, the high concentration compared to the background state colormap of the MV case begins to spread wider in the front of patient compartment and at the foot of the patient cot, which can be seen in Figure 172. For the HV case during the same period, the distribution area of the high concentration relative to the background state colormap is wider and observed a reversal of high concentration after leaving the plane in the front of the patient compartment same as in the size range of 0.5-1 micron (section 5.3.1).

At the 72nd second, the high concentration relative to the background state colormap in both cases almost distributes across the plane. In the case of MV, only the upper part of the patient compartment at the midpoint of the patient cot is not relatively large compared to the background state colormap whereas for the HV case, it is only at the end of the patient compartment, which can be seen in Figure 173. MV case concentration is relatively large (compared to the background state colormap) across the entire plane at about 77th second, as shown in Figure 174. Three seconds later, HV case concentrations are large across the plane compared to

the background state colormap, which can be seen in Figure 175. Although the concentration in both MV and HV cases is relatively large across the plane compared to the background state colormap, the concentration continues to increase over time, which can be observed from Figure 176. Until 112nd second, the highest concentration of HV case occurs at the seat1 region, with a value of 0.239 μL/m^3, which can be seen in Figure 177.

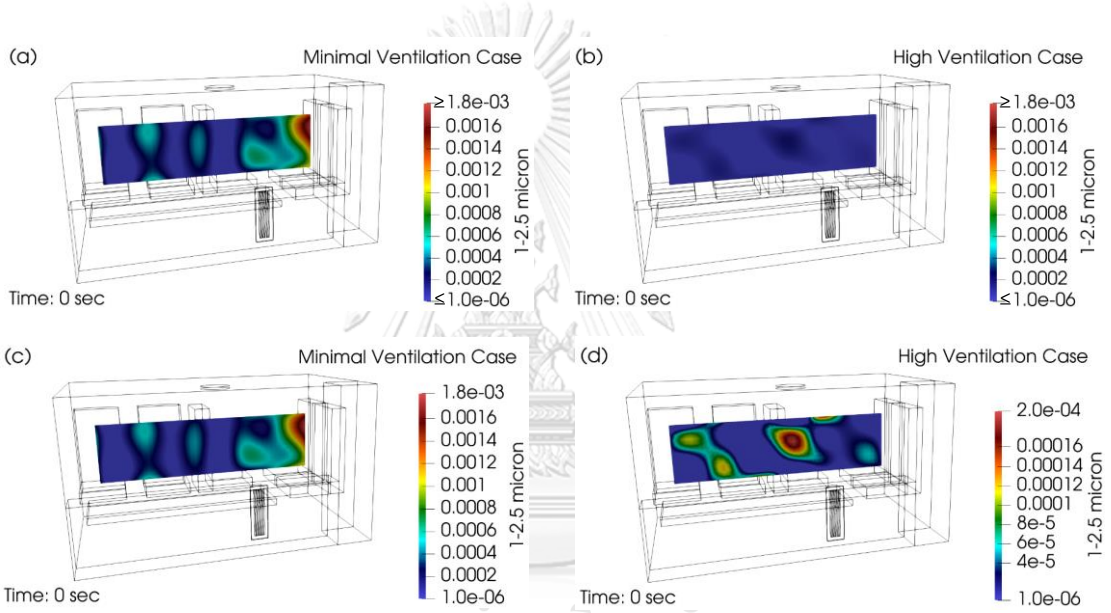

จุฬาลงกรณ์มหาวิทยาลัย
Chulalongkorn University

Figure 168 Contour Plane at Injection Position along Patient Cot at time = 0 second of Minimal Ventilation and High Ventilation with Different Colormap Ranges

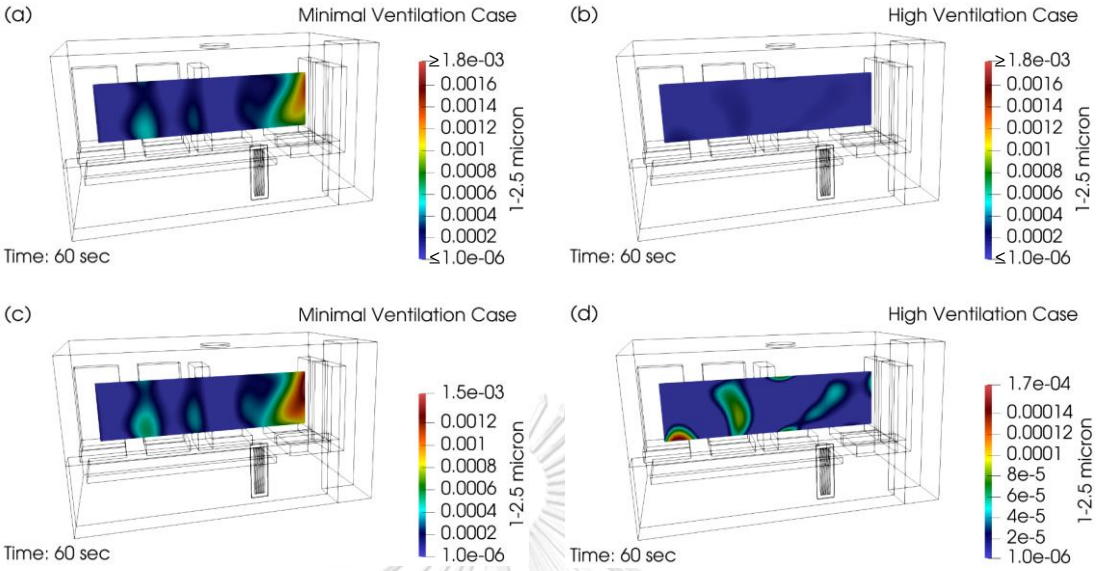

Figure 169 Contour Plane at Injection Position along Patient Cot at time = 60 second of Minimal Ventilation and High Ventilation with Different Colormap Ranges

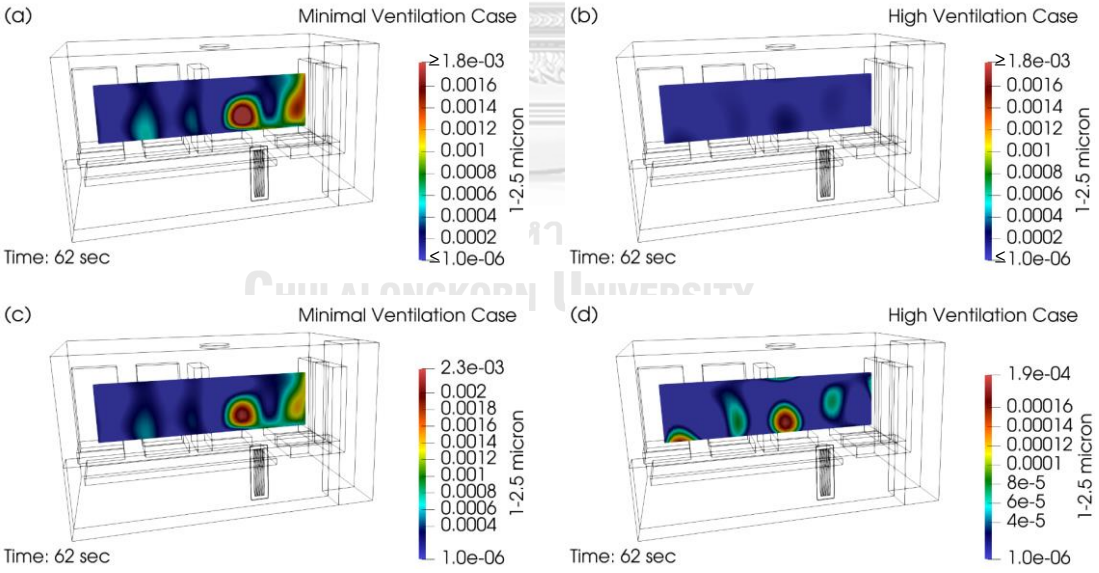

Figure 170 Contour Plane at Injection Position along Patient Cot at time = 62 second of Minimal Ventilation and High Ventilation with Different Colormap Ranges

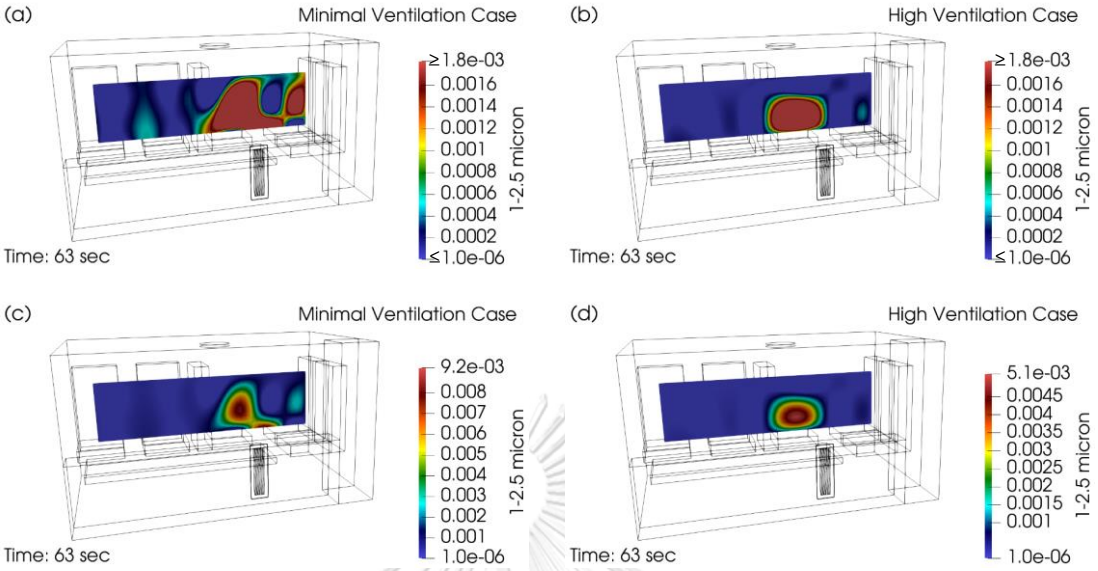

Figure 171 Contour Plane at Injection Position along Patient Cot at time = 63 second of Minimal Ventilation and High Ventilation with Different Colormap Ranges

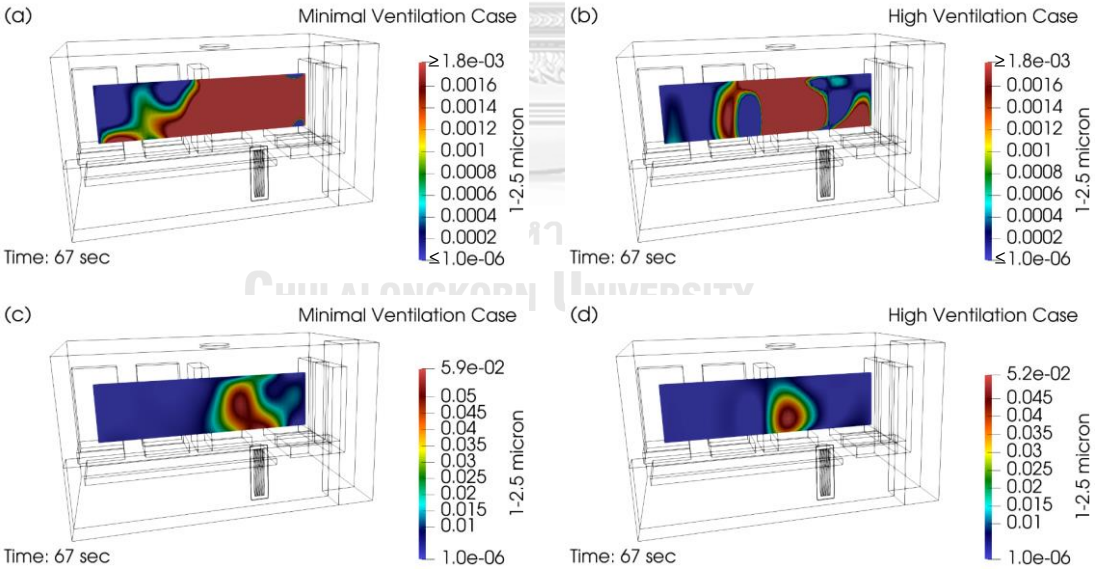

Figure 172 Contour Plane at Injection Position along Patient Cot at time = 67 second of Minimal Ventilation and High Ventilation with Different Colormap Ranges

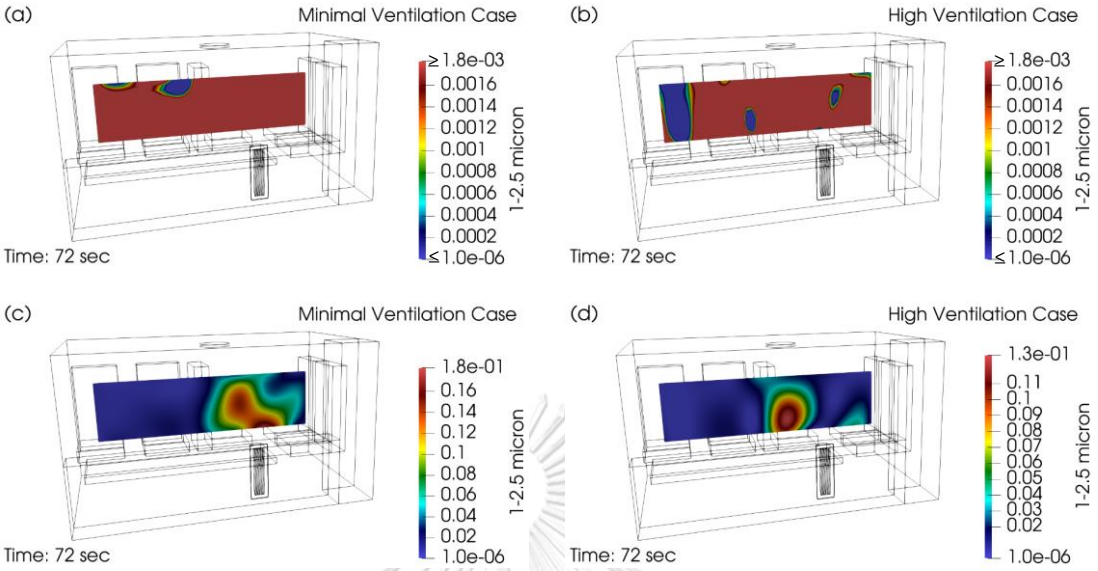

Figure 173 Contour Plane at Injection Position along Patient Cot at time = 72 second of Minimal Ventilation and High Ventilation with Different Colormap Ranges

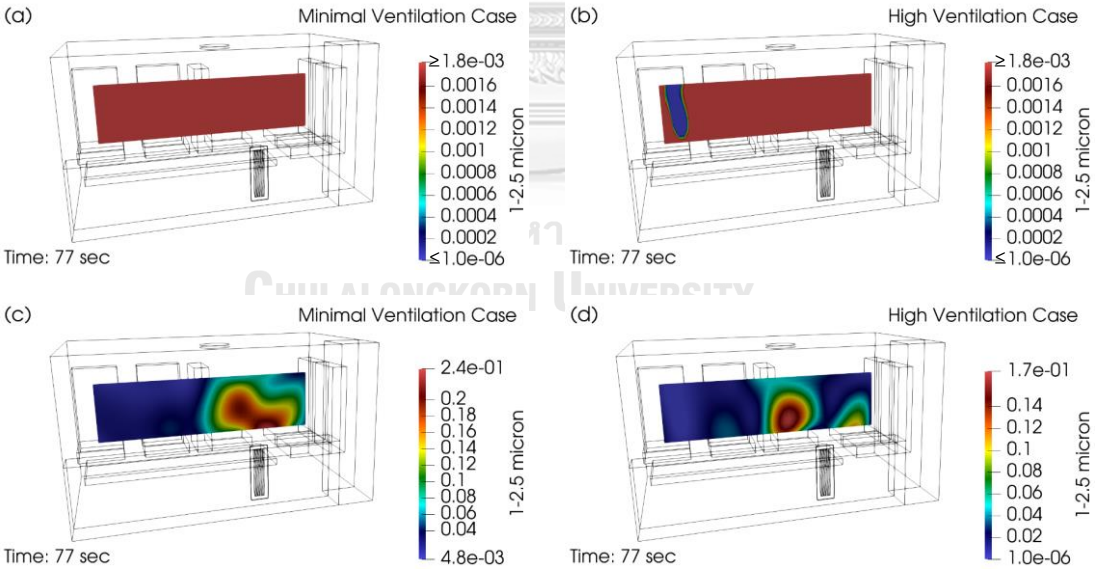

Figure 174 Contour Plane at Injection Position along Patient Cot at time = 77 second of Minimal Ventilation and High Ventilation with Different Colormap Ranges

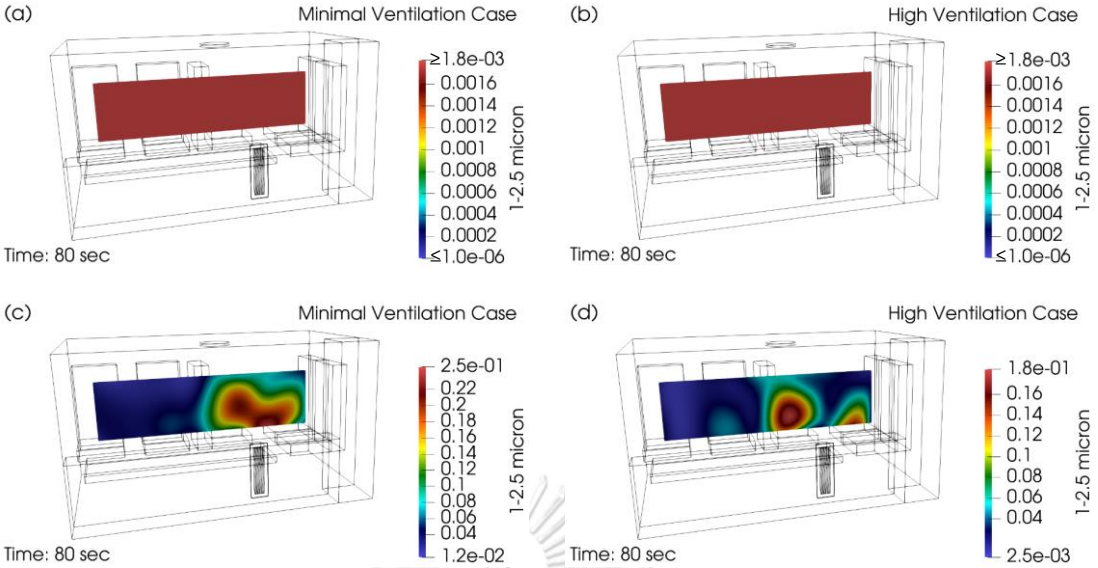

Figure 175 Contour Plane at Injection Position along Patient Cot at time = 80 second of Minimal Ventilation and High Ventilation with Different Colormap Ranges

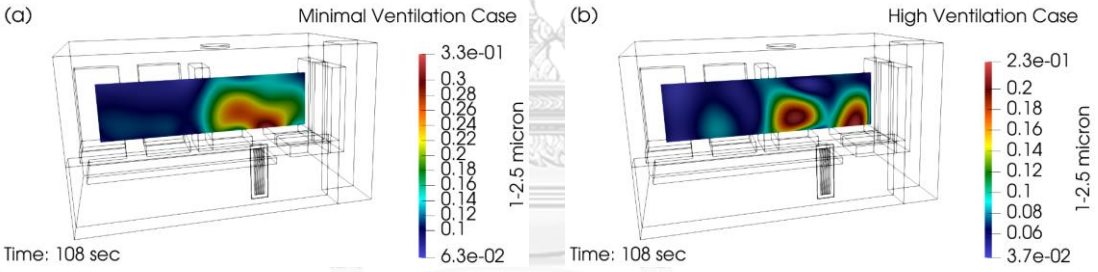

จุฬาลงกรณ์มหาวิทยาลัย
CHULALONGKORN UNIVERSITY

Figure 176 Contour Plane at Injection Position along Patient Cot at time = 108 second of Minimal Ventilation and High Ventilation

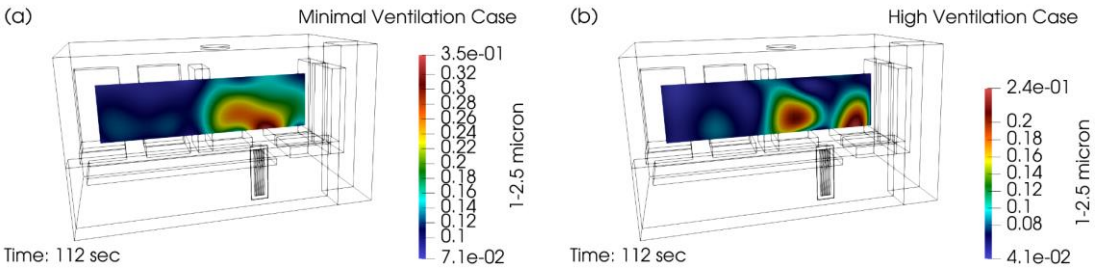

Figure 177 Contour Plane at Injection Position along Patient Cot at time = 112 second of Minimal Ventilation and High Ventilation

After stopping the particle injection into the patient compartment at the 120th second, four seconds later, the highest concentration of the MV case occurs in the region between patient cot and seat1, which can be seen in Figure 178, with a value of 0.350 μL/m^3. From the period after the initiation of particle injection until 124th second, we can observe that the local peak concentration at each time period occurs in close proximity for both MV and HV cases (above the top of the patient cot); this can be seen in Figure 170 to Figure 178. After the peak concentration is achieved for both cases; concentration begins to decline with the first noticeable area is above the patient's face to the seat1 area for MV case and above the patient's face for HV case, which can be observed in Figure 178 and Figure 179. At the 200th second, which is shown in Figure 180, the concentration continues to decline across the plane.

Figure 181 shows the concentration contour of the time at 277th second; it can be seen that HV case concentration begins to be visible with the background state colormap in the above of the middle of patient cot area, while MV case concentration does not start to return back to the background state colormap in any area. At 300th second, the HV high concentration relative to the background state colormap begins to decline in a wider area, particularly in the centre of the patient cot, as shown in Figure 182. At 350th second, the concentration continues to decline and left a region of high concentration relative to the background state colormap only in the vertical region between patient cot and seat1, which can be seen in Figure 183. Until about 470th second, shown in Figure 184, the HV case concentration returns to the background state across the entire plane. Figure 185 shows the contour plane of the 600th second, which is the end time of the HV case experiment.

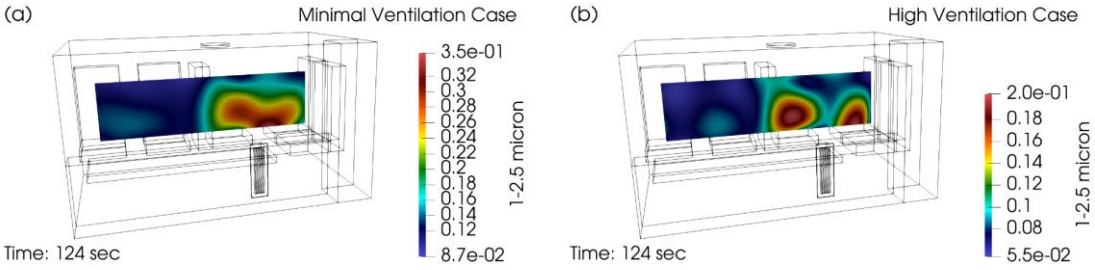

Figure 178 Contour Plane at Injection Position along Patient Cot at time = 124 second of Minimal Ventilation and High Ventilation

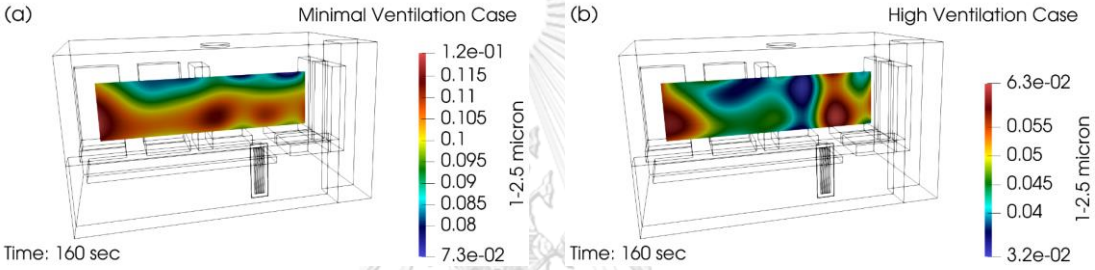

Figure 179 Contour Plane at Injection Position along Patient Cot at time = 160 second of Minimal Ventilation and High Ventilation

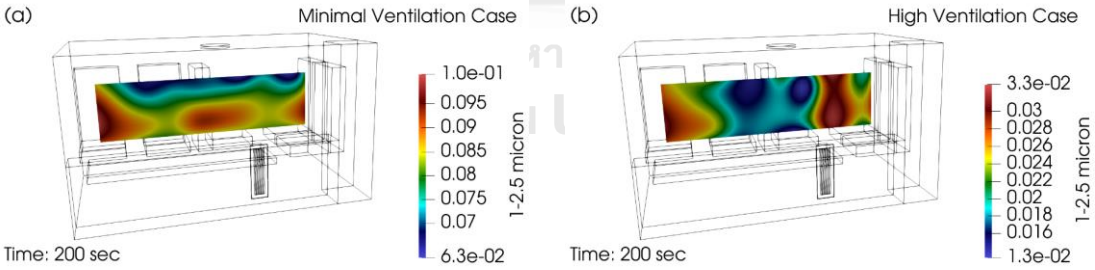

Figure 180 Contour Plane at Injection Position along Patient Cot at time = 200 second of Minimal Ventilation and High Ventilation

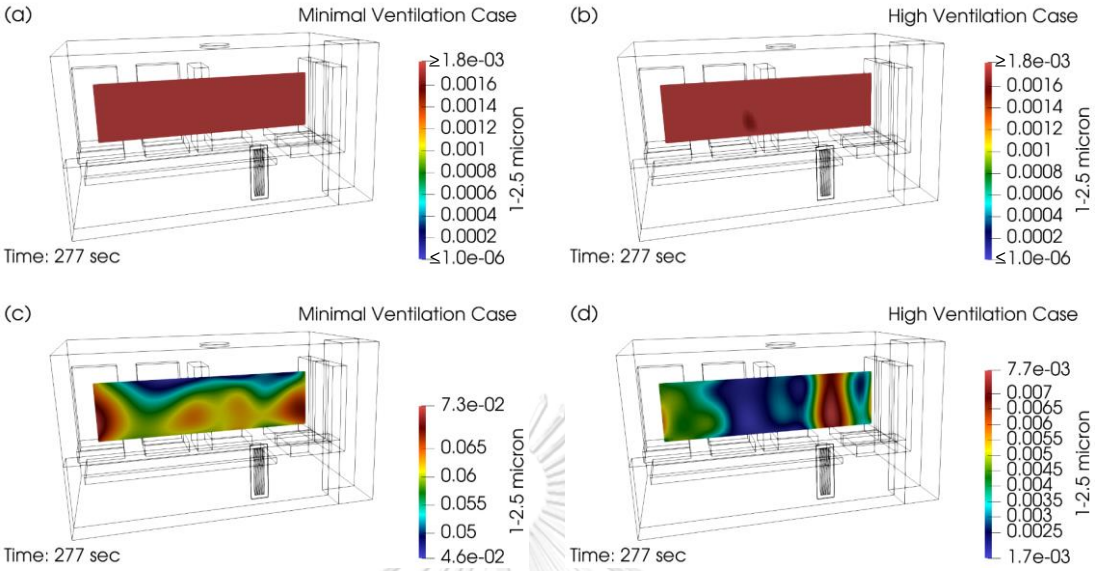

Figure 181 Contour Plane at Injection Position along Patient Cot at time = 277 second of Minimal Ventilation and High Ventilation with Different Colormap Ranges

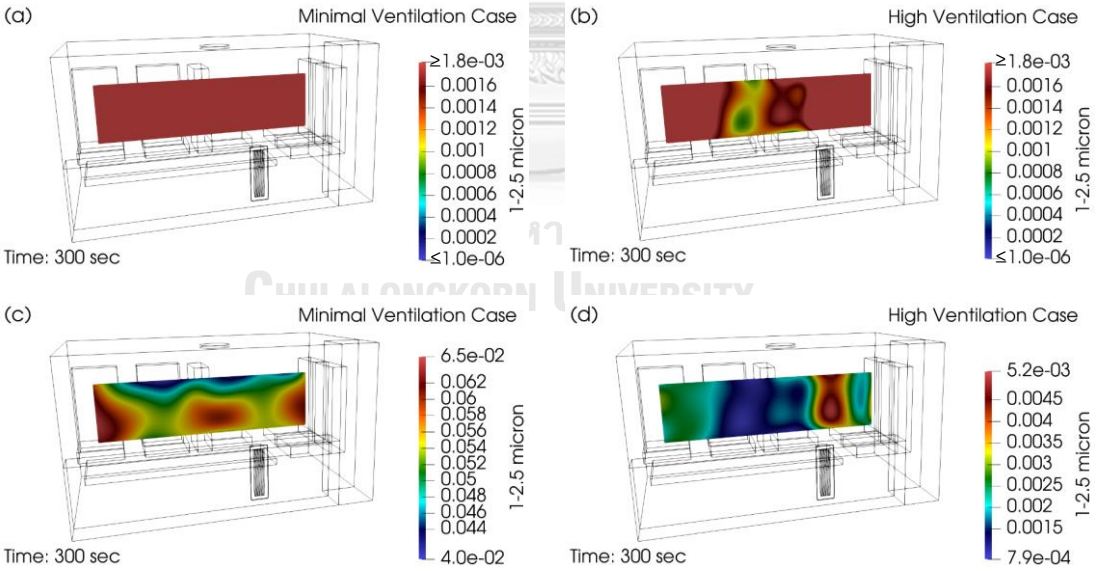

Figure 182 Contour Plane at Injection Position along Patient Cot at time = 300 second of Minimal Ventilation and High Ventilation with Different Colormap Ranges

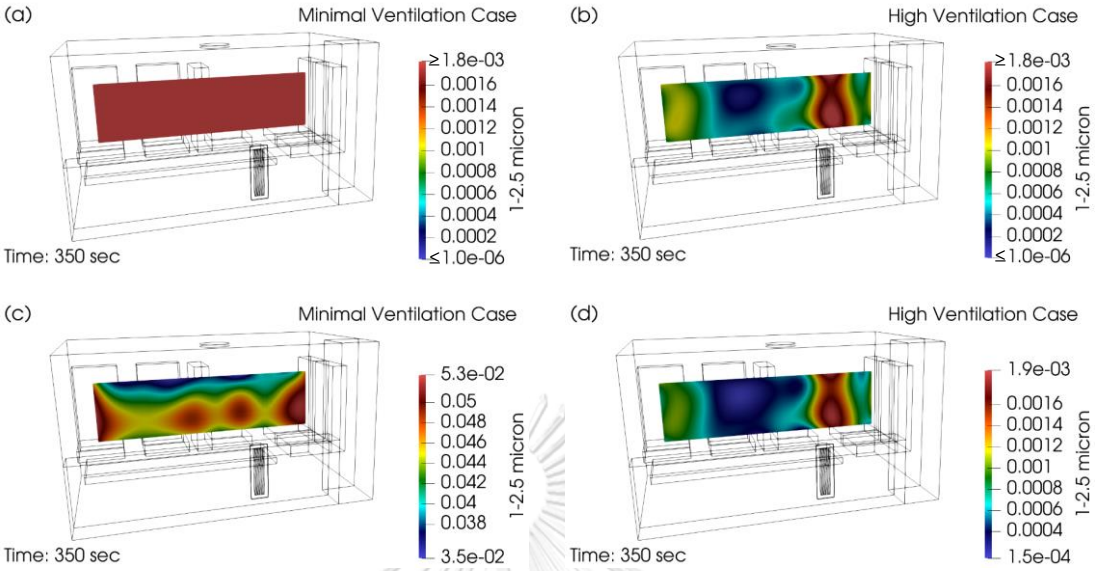

Figure 183 Contour Plane at Injection Position along Patient Cot at time = 350 second of Minimal Ventilation and High Ventilation with Different Colormap Ranges

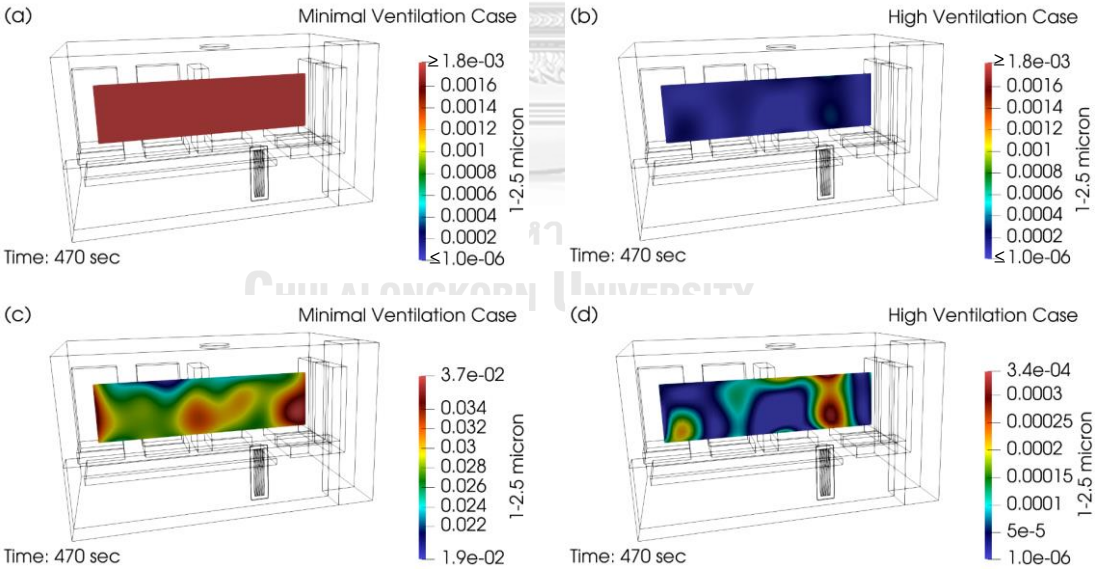

Figure 184 Contour Plane at Injection Position along Patient Cot at time = 470 second of Minimal Ventilation and High Ventilation with Different Colormap Ranges

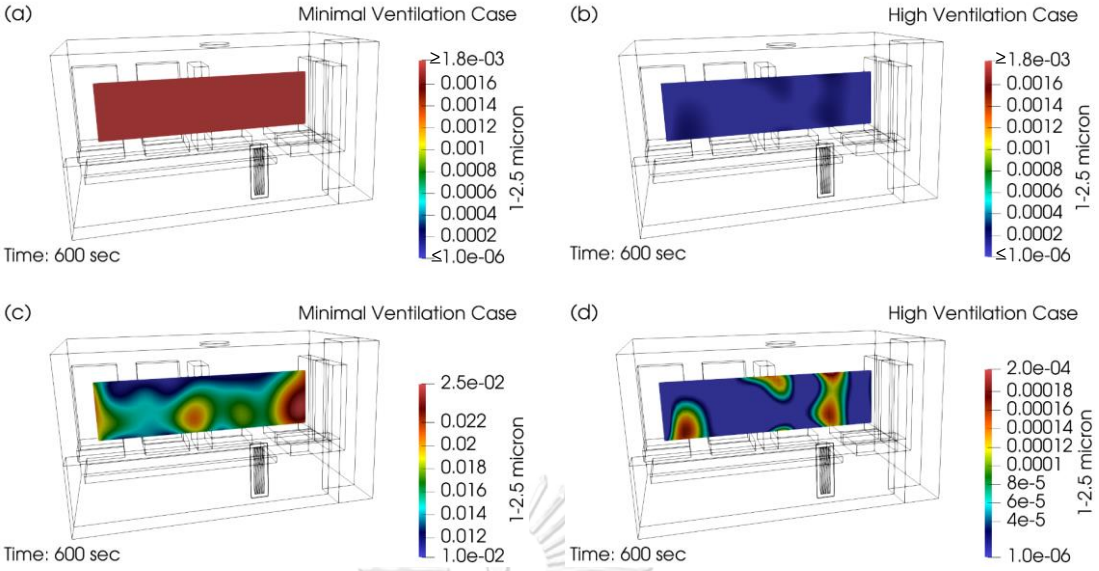

Figure 185 Contour Plane at Injection Position along Patient Cot at time = 600 second of Minimal Ventilation and High Ventilation with Different Colormap Ranges

Although at 470th second, the concentration compared to the background state colormap of the HV case returns to the background state, the MV case concentration does not decrease when considering the background state colormap. Additional figures are added for the case of MV at further time. When looking at the visible range colormap of each time, there is a decrease of MV case concentration as observed in Figure 178 to Figure 185. Until 930th second, shown in Figure 186, the concentration of MV case compared to the background state colormap begins to be visible in several regions. Thereafter, at 950th second, the areas of decreasing concentration in the previous period have a larger reduction area, particularly at the foot of the patient cot, which can be seen in Figure 187. The MV case concentration continues to decrease and decreases over a larger area compared to the background state colormap, which can be seen in Figure 188 and Figure 189. Figure 190 shows the contour of the end time of the MV case experiment.

จุฬาลงกรณ์มหาวิทยาลัย
Chulalongkorn University

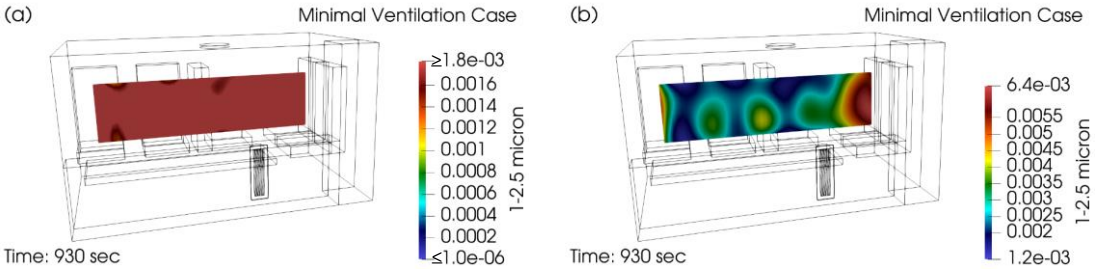

Figure 186 Contour Plane at Injection Position along Patient Cot at time = 930 second of Minimal Ventilation with Different Colormap Ranges

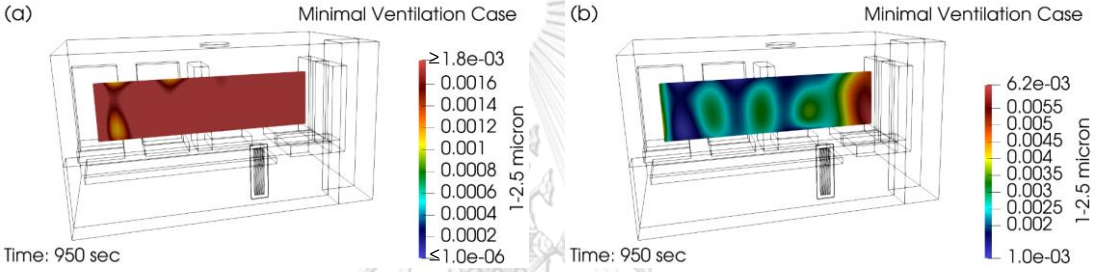

Figure 187 Contour Plane at Injection Position along Patient Cot at time = 950 second of Minimal Ventilation with Different Colormap Ranges

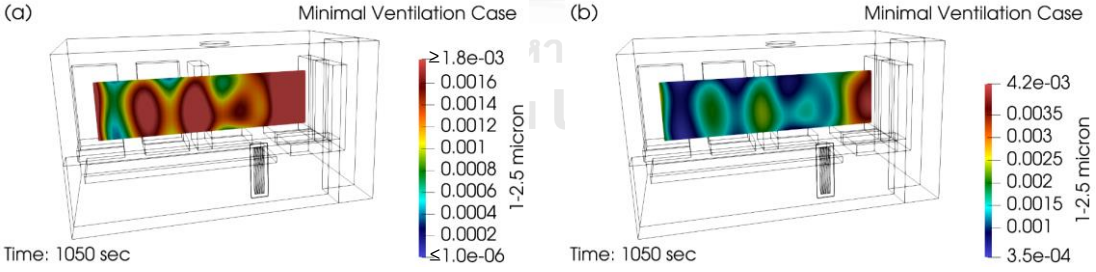

Figure 188 Contour Plane at Injection Position along Patient Cot at time = 1050 second of Minimal Ventilation with Different Colormap Ranges

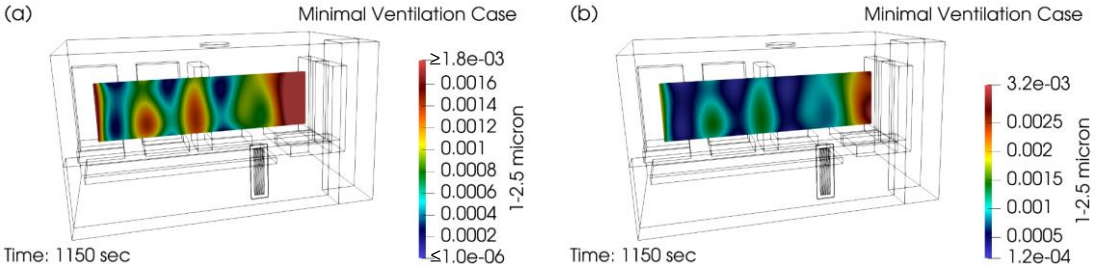

Figure 189 Contour Plane at Injection Position along Patient Cot at time = 1150 second of Minimal Ventilation with Different Colormap Ranges

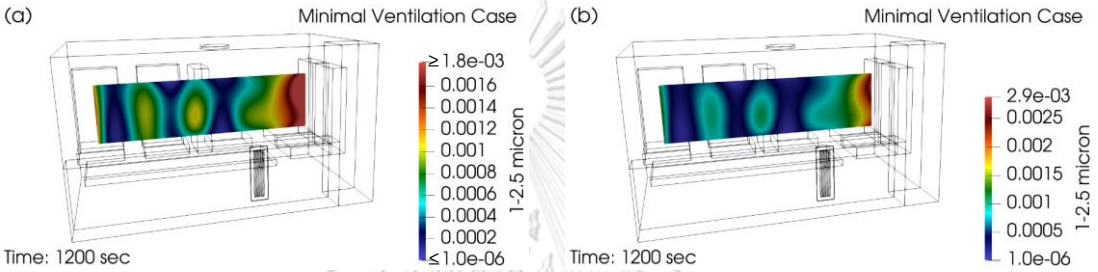

Figure 190 Contour Plane at Injection Position along Patient Cot at time = 1200 second of Minimal Ventilation with Different Colormap Ranges

To summarize, this section investigates the distribution of concentration of particles in the 1-2.5-micron size range. High concentration of particles is found just after the start of injection period in the area above the patient's face for both cases. At first, concentration distribution area of MV case is mainly in the front of the patient compartment. For the HV case, the distribution area of concentration is mainly at the upper half of the patient cot. Concentration on the plane continues to rise until it is relatively large across the plane compared to the background state colormap at about 20 seconds after the particle injection is begun for both cases. The peak concentration values across all experiments of both cases occur on the planes at about 120th second. HV concentration begins to fall back to the background state in the area above the middle of the patient cot at about four minutes after the start of injection and returns to the background across the entire plane at about 470th second. For the MV case, the concentration begins to decline

back to the background in multiple regions at about 15 minutes after the injection but does not drop to the background across the entire plane even after the end of the experiment.

5.3.3 Size range between 2.5 and 5 micron

Figure 191 to Figure 198 and Figure 204 to Figure 208 show the contours of the aerosol volume concentration for MV and HV cases at the injection position along patient cot in the ambulance at each time interval. Subfigure (a) and subfigure (b) show colormaps that compare with the background value at the start of the measurement or at the zeroth second, in order to investigate the change in the concentration in comparison to when it started. Subfigure (c) and (d) help indicate the location of high concentration at that time. The period of time when the change in concentration is not visible relative to the background state colormap is shown in Figure 199 to Figure 203. For contours at time intervals greater than 600th second, the time interval after the termination of the HV case, are shown in Figure 209 to Figure 213, where subfigure (a) shows a colormap relative to the background state and subfigure (b) is a visible range colormap for each time period of the MV case.

จุฬาลงกรณ์มหาวิทยาลัย
Chulalongkorn University

At the start of the experiment, the concentration and distribution for both HV and MV cases are shown in Figure 191, with the concentration in the MV case being slightly higher. By the time the particle injection is started; the concentration in both cases remains close to the start of the experiment, which can be seen in Figure 192. The concentration of MV and HV cases begin to rise abruptly compared to the background state colormap in the area above patient's face only few seconds after the particle injection is started as shown in Figure 193 and Figure 194. For the MV case, at 63rd second, the high concentration distribution relative to the background state colormap is more extensive to the seat1 region. Figure 195 shows the concentration contour of 67th second; the MV case begins to have a high concentration distribution compared to background state colormap in the front part

of the patient compartment and the concentration also distributes to the end of the patient cot. For the HV case, the area of high concentration distribution relative to the background state colormap is wider and can be observed a reversal of particles after leaving the plane in the front region of the patient compartment. At the 72nd second, the high concentration relative to the background state colormap distributes almost across the plane in both cases; for the case of MV, background state concentration is only left in the upper part of the middle of the patient cot. For the HV case, there are several areas left. These can be seen in Figure 196.

Until about 78th second, the MV concentration is relatively large (compared to the background state colormap) across the entire plane, while the HV case is left with background state concentration at above the foot of the patient cot as shown in Figure 197. After 3 seconds, HV case concentration value is high across the plane compared to the background state colormap, as shown in Figure 198. Although the concentration in both cases is relatively large across the plane compared to the background state, the concentration still decreases, which can be observed in the snapshot at 108th second, as shown in Figure 199. At 112nd second, the highest concentration of the HV case occurs on the contour plane in seat1 region, with a value of 1.023 μL/m^3, which can be observed in Figure 200. The highest concentration value of the MV case occurs at 117th second between patient cot and seat1, with a value of 2.529 μL/m^3,which can be seen in Figure 201.

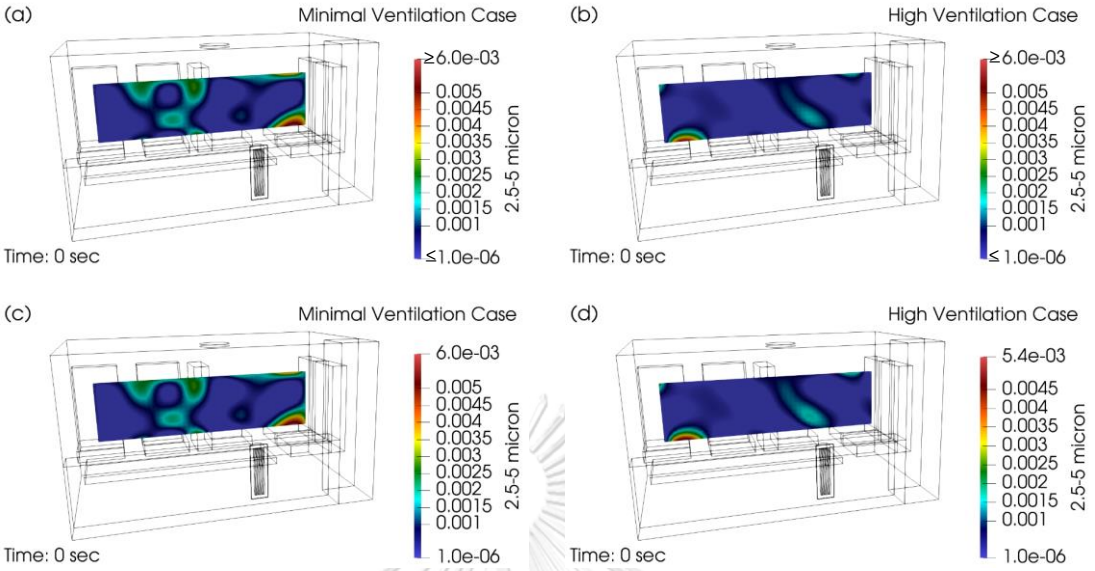

Figure 191 Contour Plane at Injection Position along Patient Cot at time = 0 second of Minimal Ventilation and High Ventilation with Different Colormap Ranges

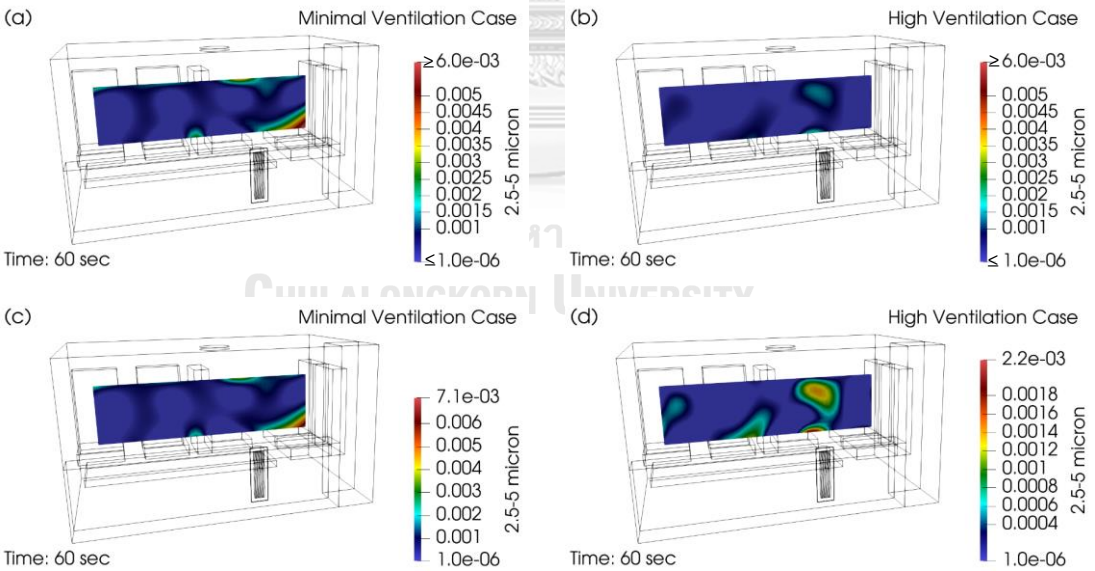

Figure 192 Contour Plane at Injection Position along Patient Cot at time = 60 second of Minimal Ventilation and High Ventilation with Different Colormap Ranges

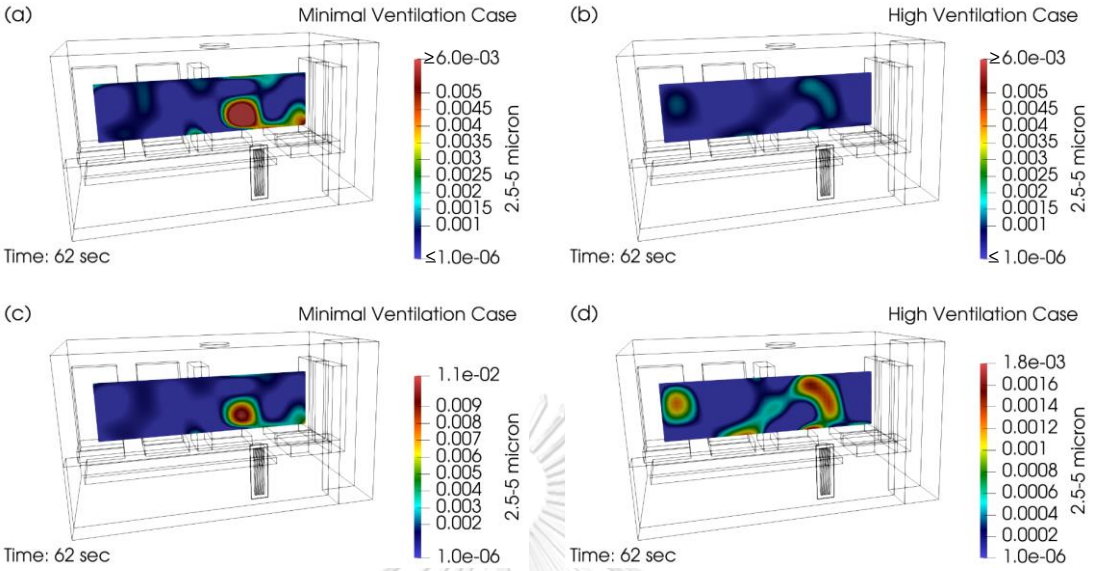

Figure 193 Contour Plane at Injection Position along Patient Cot at time = 62 second of Minimal Ventilation and High Ventilation with Different Colormap Ranges

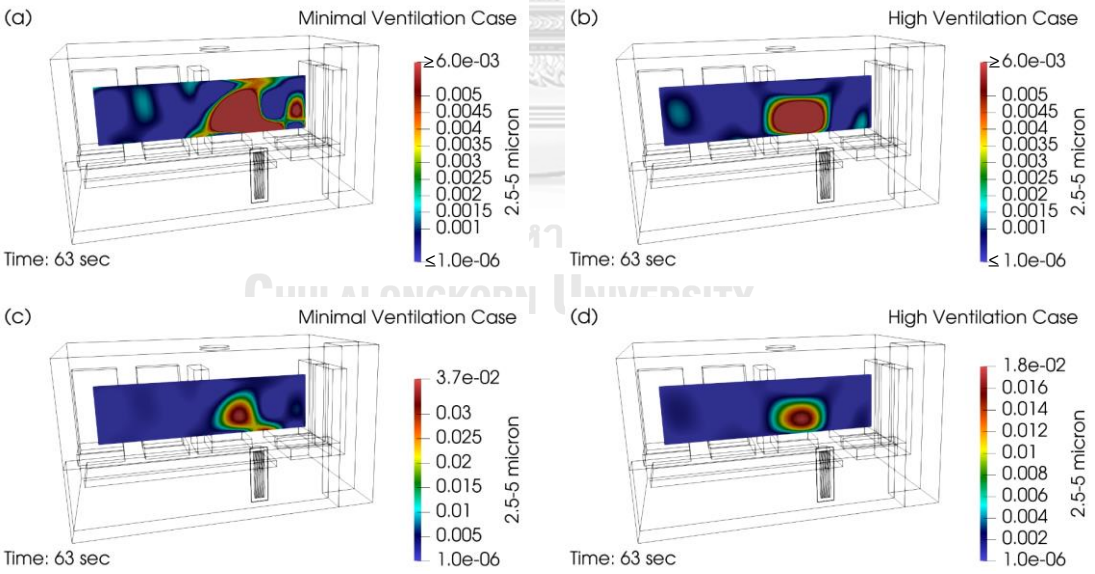

Figure 194 Contour Plane at Injection Position along Patient Cot at time = 63 second of Minimal Ventilation and High Ventilation with Different Colormap Ranges

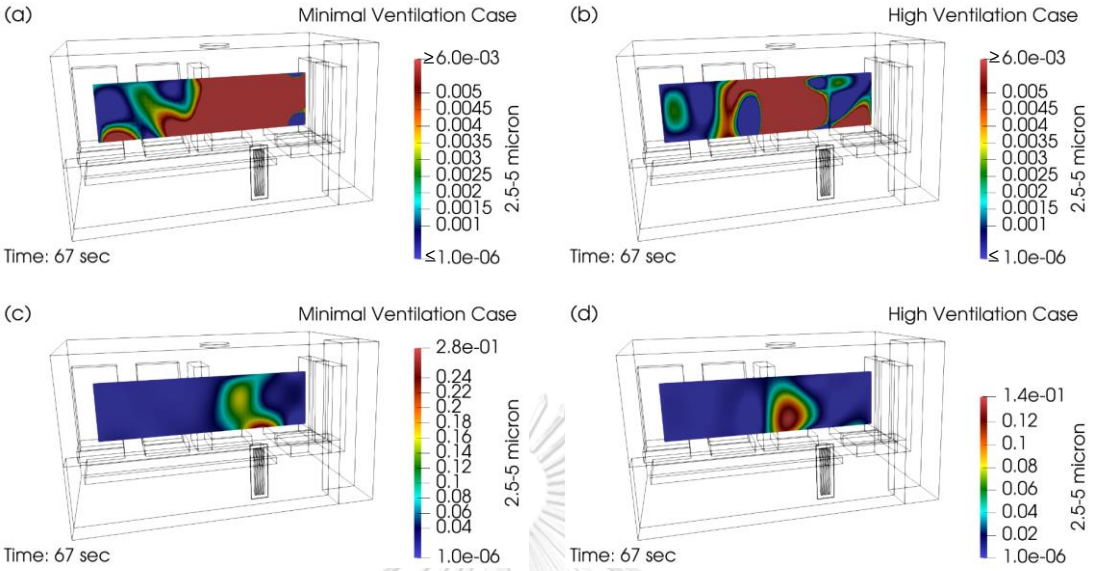

Figure 195 Contour Plane at Injection Position along Patient Cot at time = 67 second of Minimal Ventilation and High Ventilation with Different Colormap Ranges

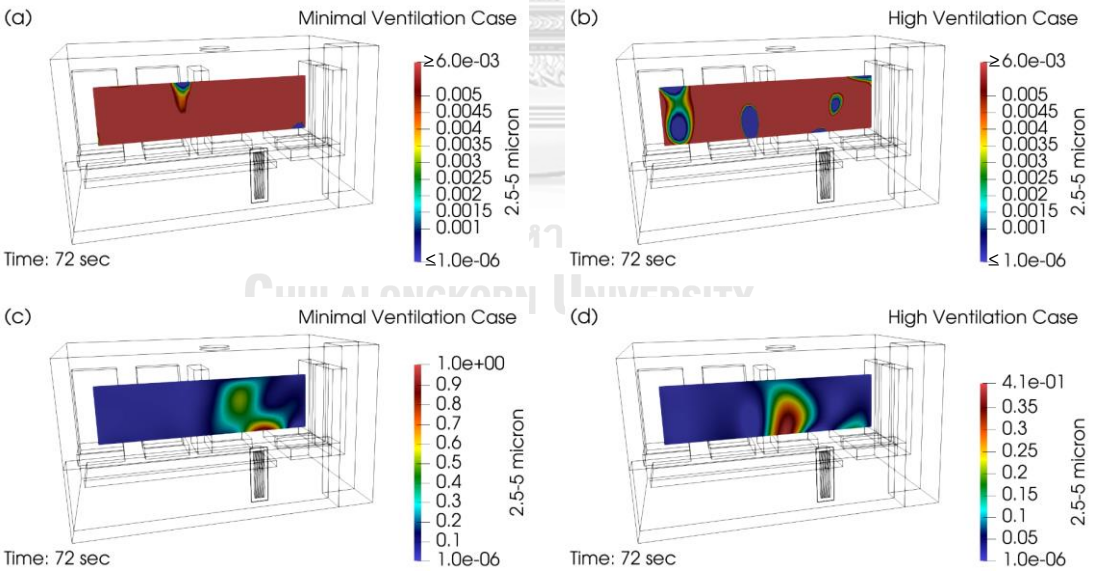

Figure 196 Contour Plane at Injection Position along Patient Cot at time = 72 second of Minimal Ventilation and High Ventilation with Different Colormap Ranges

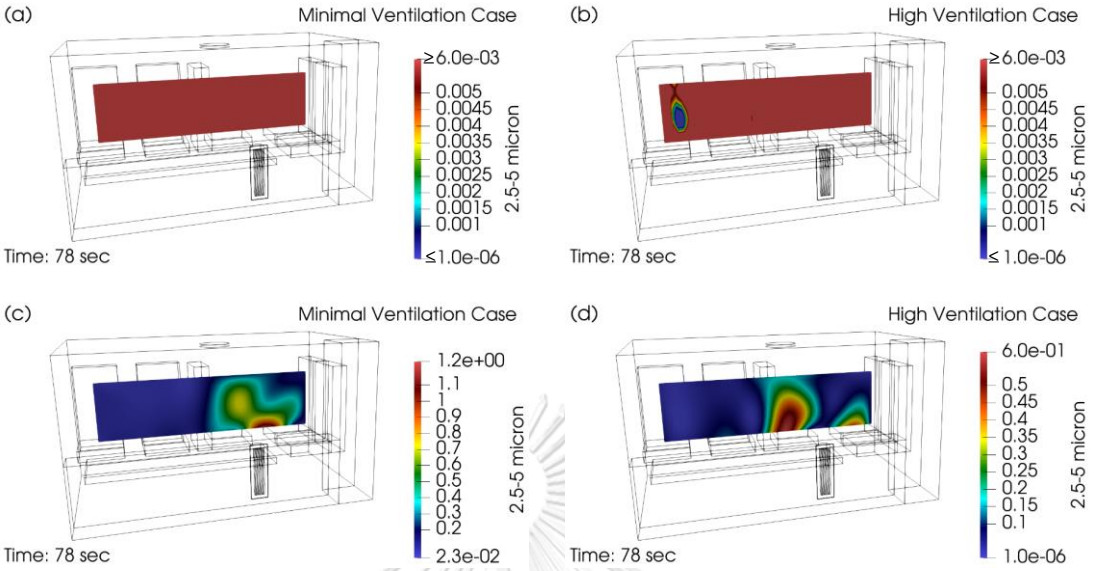

Figure 197 Contour Plane at Injection Position along Patient Cot at time = 78 second of Minimal Ventilation and High Ventilation with Different Colormap Ranges

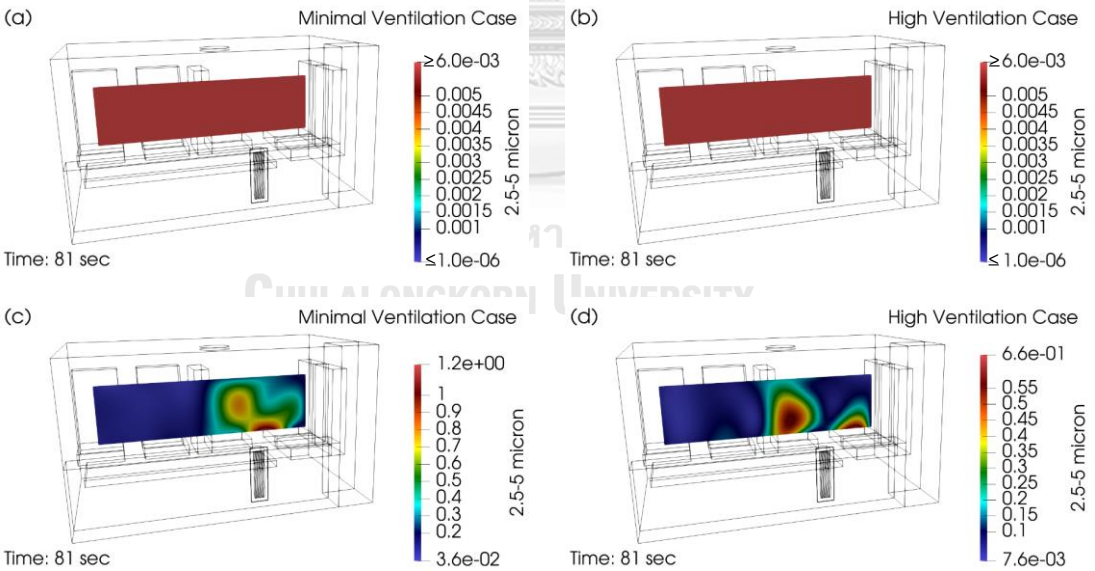

Figure 198 Contour Plane at Injection Position along Patient Cot at time = 81 second of Minimal Ventilation and High Ventilation with Different Colormap Ranges

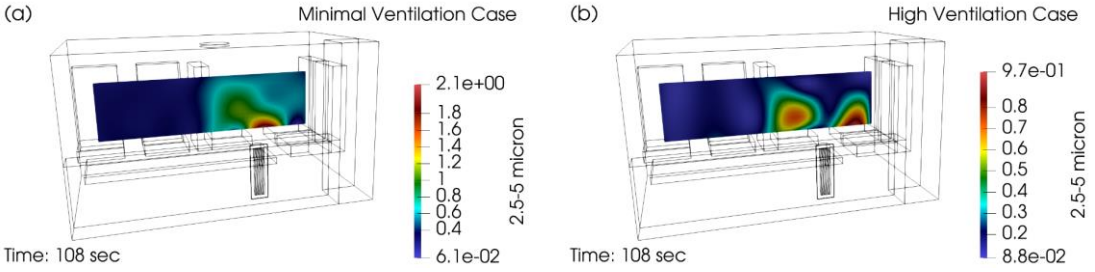

Figure 199 Contour Plane at Injection Position along Patient Cot at time = 108 second of Minimal Ventilation and High Ventilation

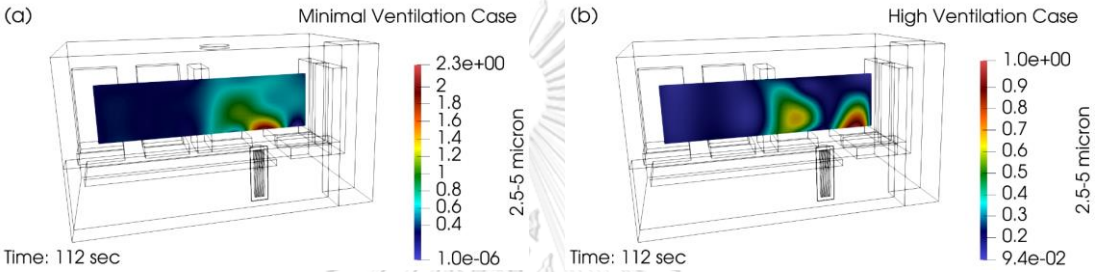

Figure 200 Contour Plane at Injection Position along Patient Cot at time = 112 second of Minimal Ventilation and High Ventilation

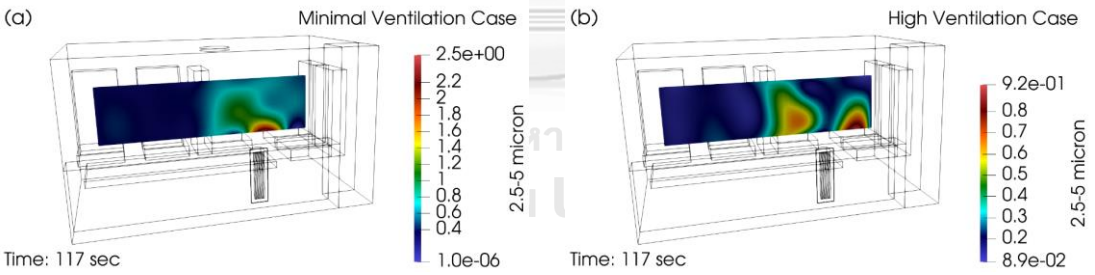

Figure 201 Contour Plane at Injection Position along Patient Cot at time = 117 second of Minimal Ventilation and High Ventilation

After peak concentration throughout the experiment has occurred in both cases, particle injection is stopped at 120th second. Concentration on the contour plane for both cases starts to decline after the above-mentioned peak concentration occurs as observed from Figure 200 to Figure 202. At 160th second, for the MV case, the concentration decline during this time significantly reduces in the front of the

patient compartment as well as at the foot area of the patient cot. For the case of HV, the areas where concentration significantly reduces are above the patient's face and seat1, as observed in Figure 202. Concentration continues to decline across the plane as shown in Figure 203. From Figure 193 to Figure 201, we can observe that the concentration and distribution from initiation of particle injection to peak concentration on the contour plane varies over time, but the local peak concentration still occurs in the same area every period. The HV case concentration on the plane begins to be visible with the background state colormap at about 254th second in the area above the centre of the patient cot. While there is no region on the contour plane of the MV case where the concentration begins to decline to background state, which can be observed in Figure 204. At 300th second, the high concentration region relative to the background state colormap of the HV case decreases to a larger region, while the MV case remains unchanged from the previous period as can be seen in Figure 205. At 350th second, as shown in Figure 206, HV case concentration declines back to the background state colormap almost across the plane and the entire plane returns to the background state at 500th second, as shown in Figure 207. The contour plane of the experiment end time of the HV case can be seen in Figure 208.

จุฬาลงกรณ์มหาวิทยาลัย
Chulalongkorn University

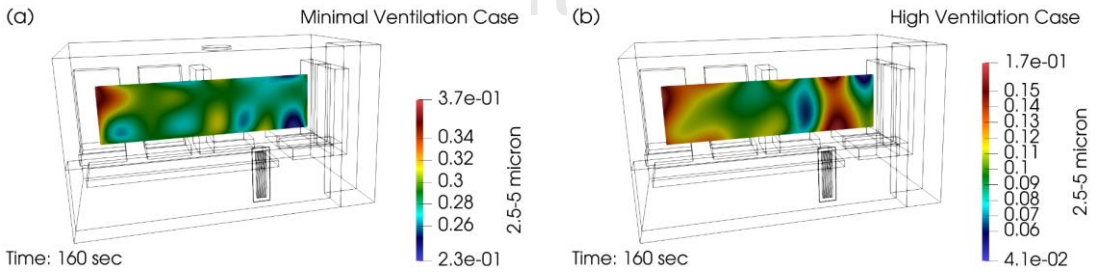

Figure 202 Contour Plane at Injection Position along Patient Cot at time = 160 second of Minimal Ventilation and High Ventilation

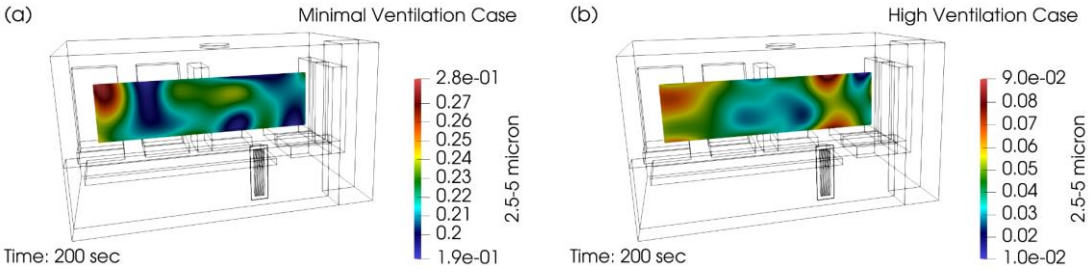

Figure 203 Contour Plane at Injection Position along Patient Cot at time = 200 second of Minimal Ventilation and High Ventilation

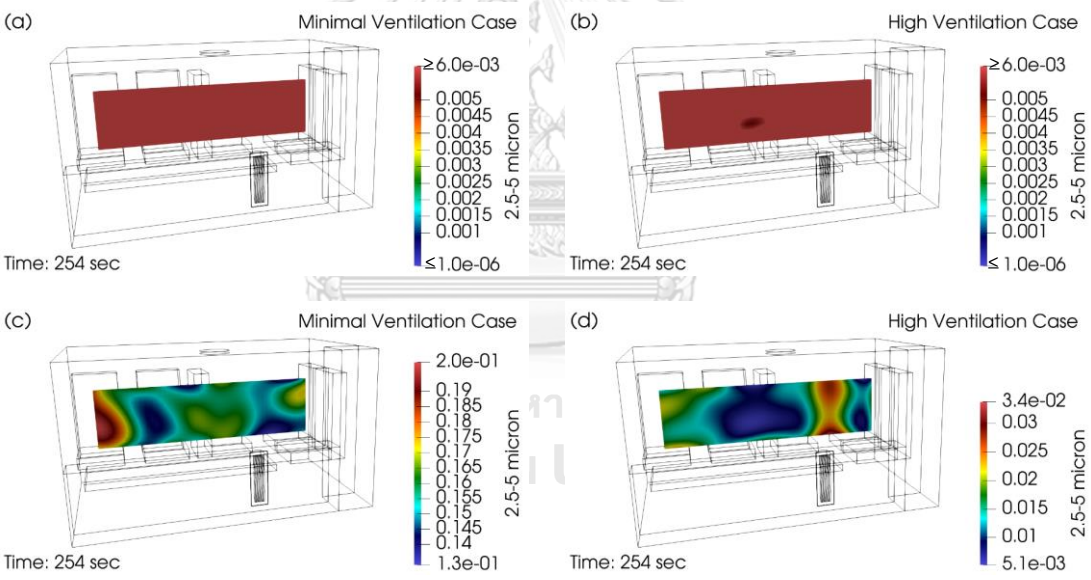

Figure 204 Contour Plane at Injection Position along Patient Cot at time = 254 second of Minimal Ventilation and High Ventilation with Different Colormap Ranges

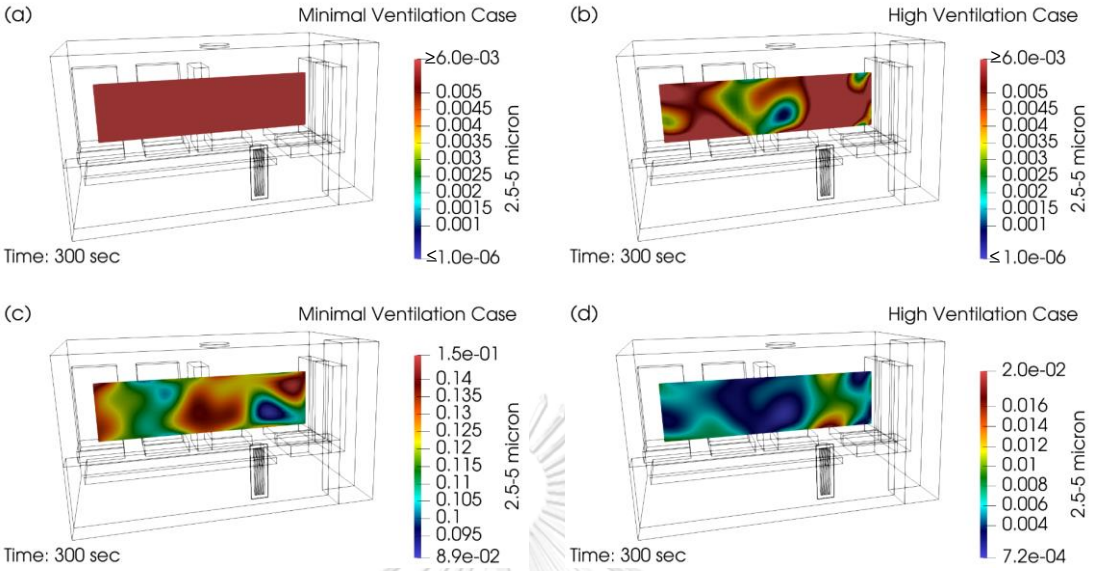

Figure 205 Contour Plane at Injection Position along Patient Cot at time = 300 second of Minimal Ventilation and High Ventilation with Different Colormap Ranges

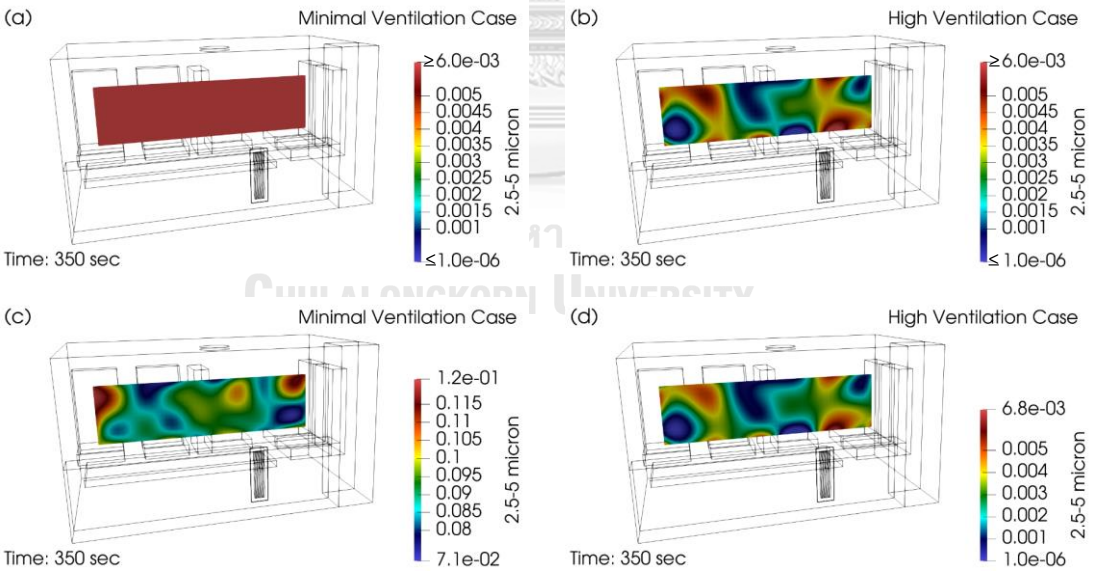

Figure 206 Contour Plane at Injection Position along Patient Cot at time = 350 second of Minimal Ventilation and High Ventilation with Different Colormap Ranges

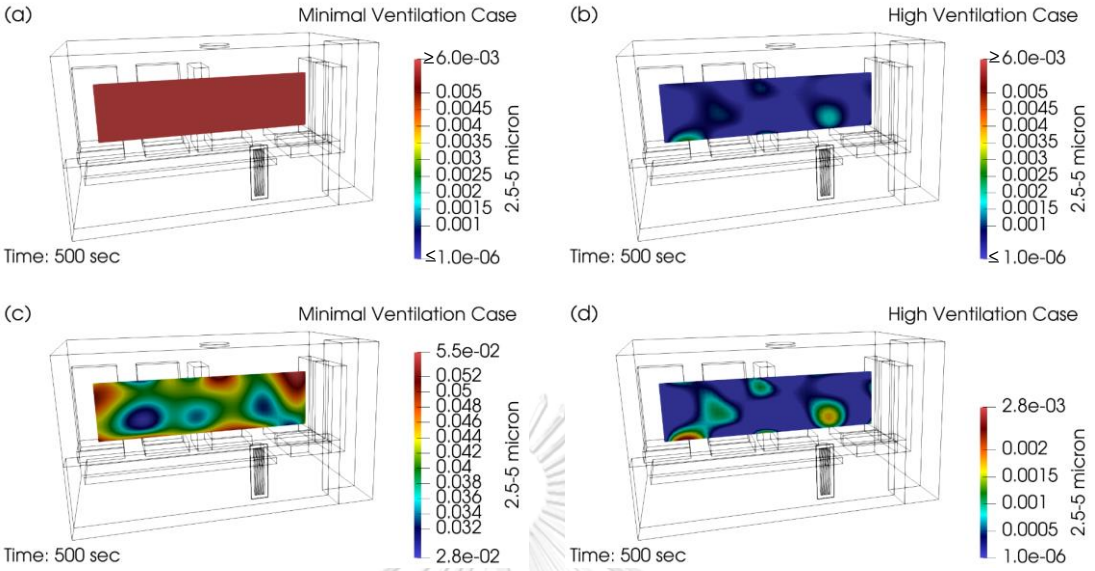

Figure 207 Contour Plane at Injection Position along Patient Cot at time = 500 second of Minimal Ventilation and High Ventilation with Different Colormap Ranges

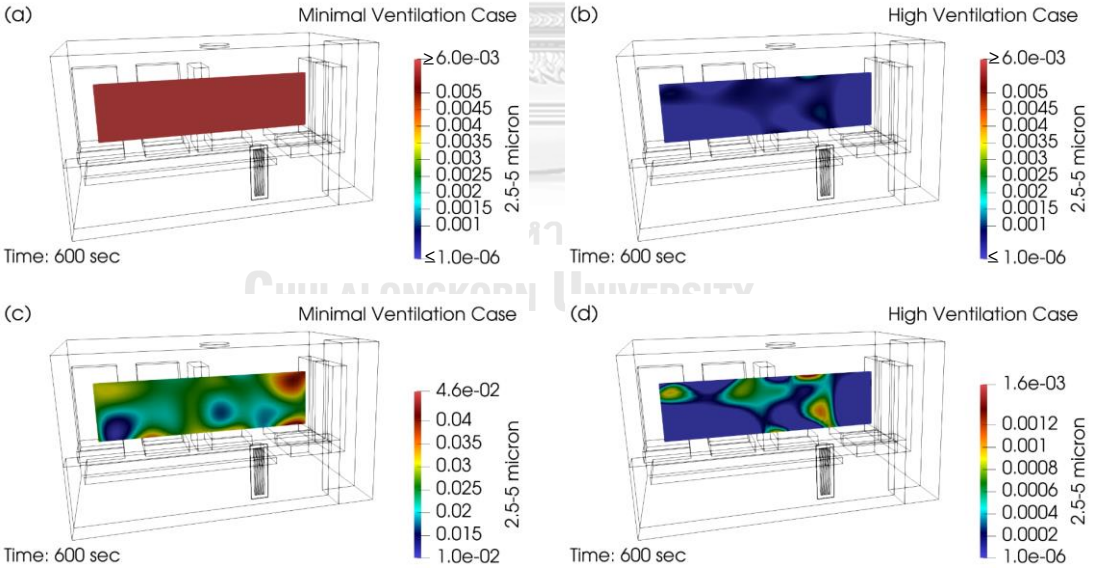

Figure 208 Contour Plane at Injection Position along Patient Cot at time = 600 second of Minimal Ventilation and High Ventilation with Different Colormap Ranges

Although the HV case experiment is terminated at 600th second, the MV case concentration does not begin to be visible with the background state colormap at all. Additional figures are added for the case of MV at further time. At about 745th second, MV case concentration begins to decline to the background state colormap in the area above the end of the patient cot as shown in Figure 209. Concentration gradually declines towards the background state colormap to a larger area, particularly above the patient's face region, as seen in Figure 210. Concentration continues to decline and fall back to the background state colormap over a larger area which can be seen in Figure 211 and Figure 212. Figure 213 shows the contour plane at 1200th second, which is the end of the MV case experiment.

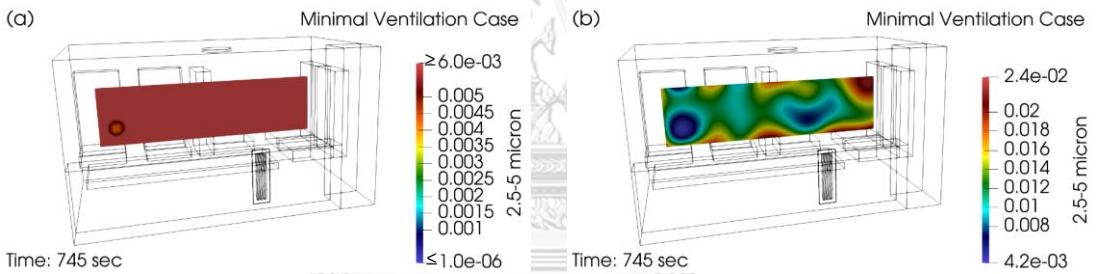

Figure 209 Contour Plane at Injection Position along Patient Cot at time = 745 second of Minimal Ventilation with Different Colormap Ranges

จุฬาลงกรณ์มหาวิทยาลัย
CHULALONGKORN UNIVERSITY

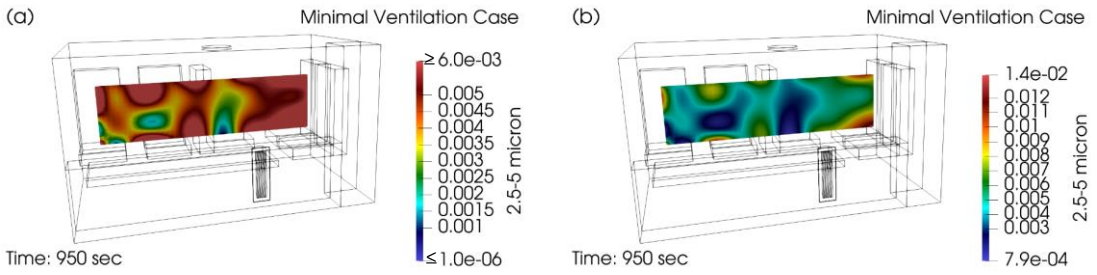

Figure 210 Contour Plane at Injection Position along Patient Cot at time = 950 second of Minimal Ventilation with Different Colormap Ranges

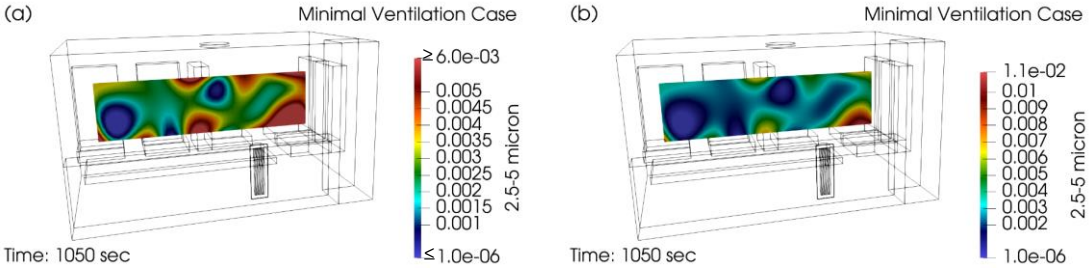

Figure 211 Contour Plane at Injection Position along Patient Cot at time = 1050 second of Minimal Ventilation with Different Colormap Ranges

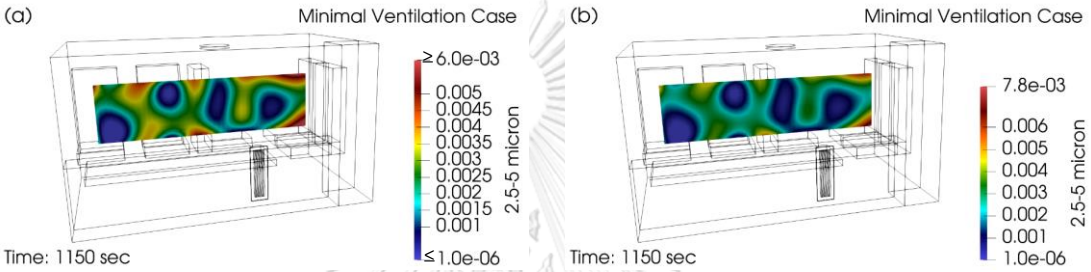

Figure 212 Contour Plane at Injection Position along Patient Cot at time = 1150 second of Minimal Ventilation with Different Colormap Ranges

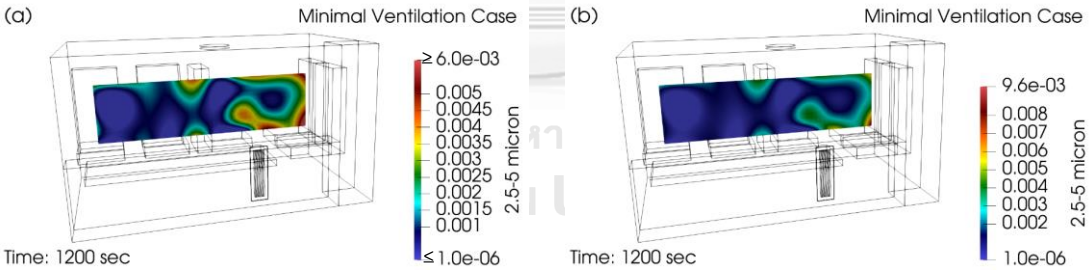

Figure 213 Contour Plane at Injection Position along Patient Cot at time = 1200 second of Minimal Ventilation with Different Colormap Ranges

To summarize, this section investigates the distribution of concentration of particles in the 2.5-5-micron size range. Concentration value of both cases becomes high compared to the background state colormap in the above patient's face region right after the particle injection. The initial distribution characteristics of the concentration on the plane remain the same as in the 0.5-1-micron and 1-2.5-micron

size ranges; the MV concentration distribution area is at the front part of the patient compartment while the HV concentration distribution area is mainly at above the upper half of the patient cot. The concentration is high across the whole plane compared to the background state colormap at about 20 seconds after the start of the particle injection for both cases. Concentration continues to rise until the peak concentration of all experiments occurs on the plane at about 115th second in both cases. After that, the high concentration on the plane starts to decline; until about three minutes after the injection, the HV case concentration begins to decline back to the background state colormap in the area above the middle of the patient cot and returns to background state across the plane at 500th second. For the MV case, the concentration begins to decline to the background state colormap at the foot of the patient cot about 11 minutes after the injection is commenced and continues to decline but does not return to the background across the plane at the end of the experiment.

5.4 Spatial-Averaged Aerosol Volume Concentration over Time

Spatial-averaged, that is averaging on the entire test section volume occupying all the nodes (a fraction of cabin volume), aerosol volume concentration over time is considered in this subsection. It is found simply by multiplying the volume concentration by the small "box" volume engulfing each node and taking summation from every node, then this box volume is measured $0.04 \times 0.04 \times 0.04 = 6.4\times10^{-5}$ m^3. After that, the average is calculated by dividing by the entire test section volume (6.4×10^{-5} m^3 multiplied by the number of nodes, which is 12558). The results in this section are divided into two parts. The first part compares with respect to particle sizes the temporal evolution in their concentration changes on the same rate of ventilation. The second part focuses rather on the

effect of ventilation rate on the temporal evolution of particle concentration at that same particle size range.

For part 1, consider Figure 214 and Figure 215. Figure 214 shows the spatial-averaged aerosol volume concentration of the case MV. Volume concentration value increases rapidly after the start of the aerosol injection at the 60th second and, continue to increase until 120th second signifying the inability in removing the particles at these influx and outflux rates. Thereafter, the concentration decreases exponentially after the injection is stopped at 120th second. For particles of different sizes, the volume concentration of particles in the large size range is not only higher than that of particles in the smaller size range but also larger in reduction rates (decay faster when normalized with their respective sizes, not shown). While the first is highly dependent on the injection in which initial particle size distribution differ from case to case, the latter is not: i.e. the reduction rate is directly proportional to particle size. The return-to-background times for all size ranges are approximately the same about 1000 seconds or approximately 16 minutes after the start of particle injection into the patient compartment.

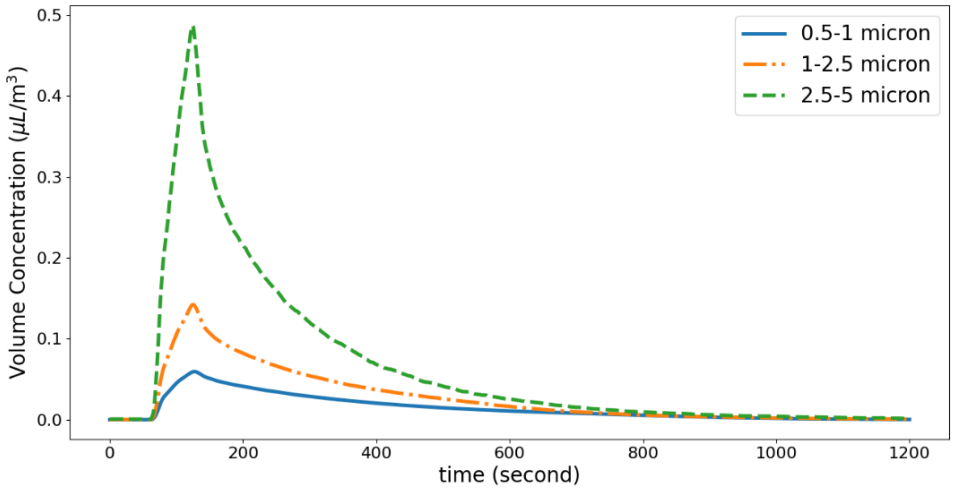

Figure 214 Spatial-Averaged Aerosol Volume Concentration over Time in the Case of Minimal Ventilation (MV)

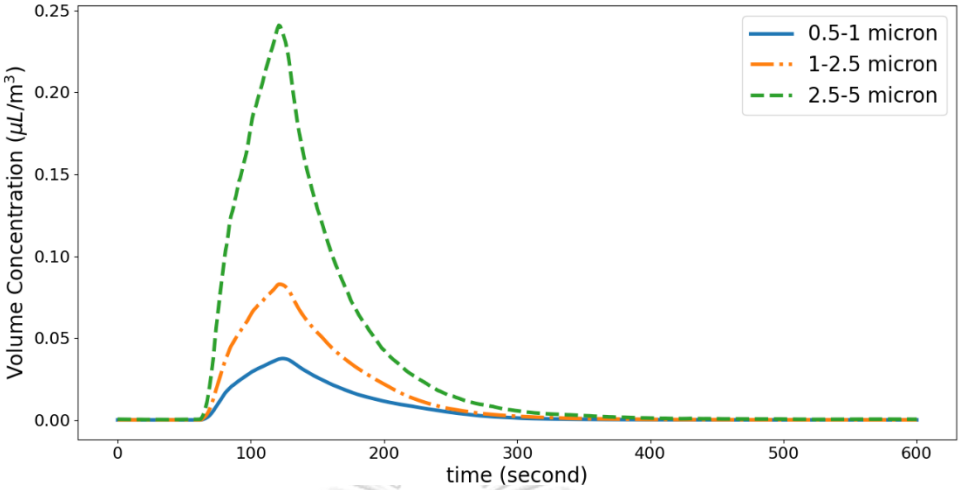

Figure 215 Spatial-Averaged Aerosol Volume Concentration over Time in the Case of High Ventilation (HV)

For the case of HV, which is shown in Figure 215, the increase when the particle injection is started and the decrease after the particle injection is stopped tends to be in the same direction as the MV case but the return-to-background time of HV case is cut to only about 5 minutes after the particle injection is initiated, indicating the effectiveness of the air exhaust system with the HV setting.

For part 2, from Figure 216, it is obvious that increasing ventilation rate reduces return-to-background time and also reduces peak concentration in every size range. The peak concentration in the HV case is approximately twice lower than the MV case for all size of particles.

จุฬาลงกรณ์มหาวิทยาลัย
CHULALONGKORN UNIVERSITY

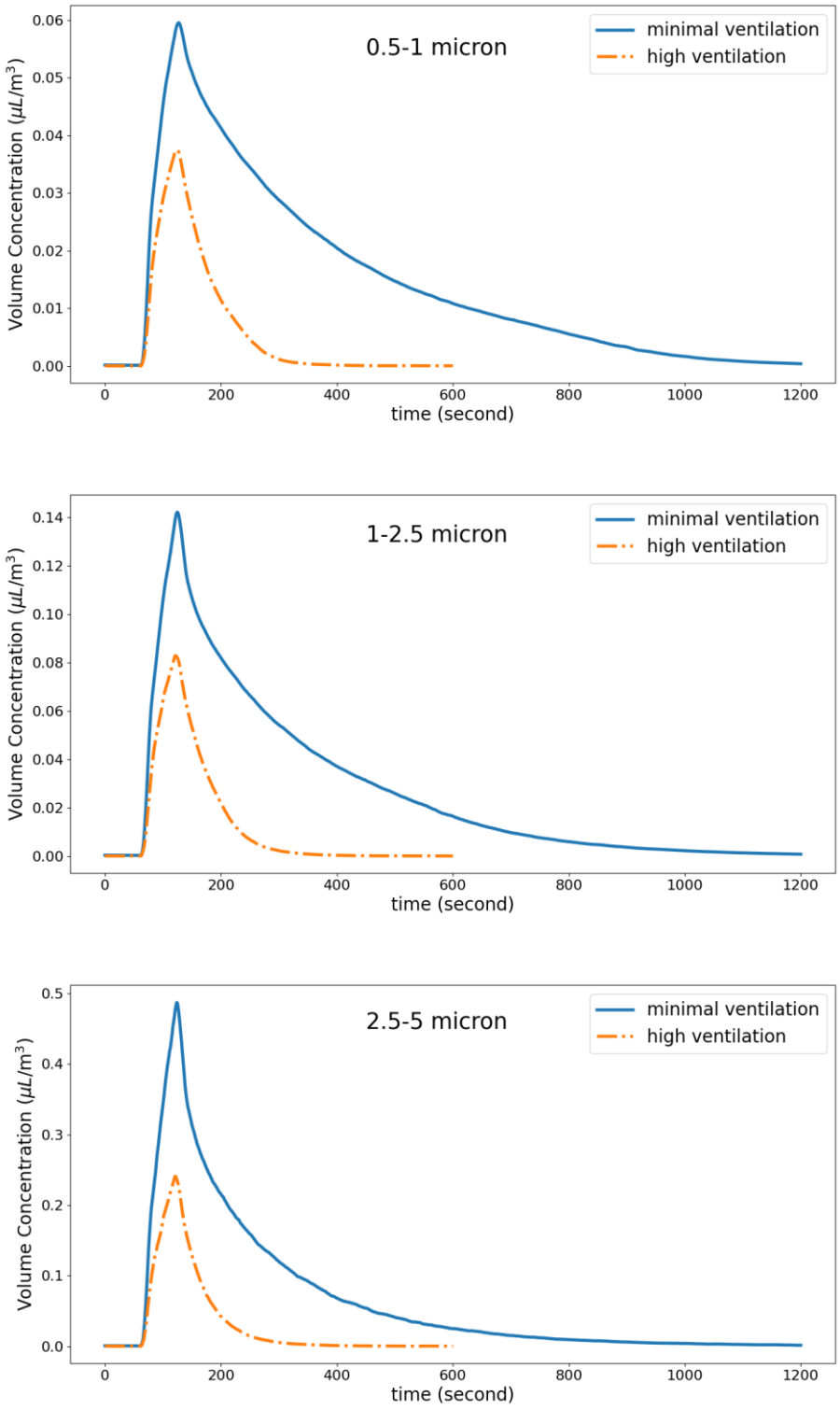

Figure 216 Spatial-Averaged Aerosol Volume Concentration over Time in each Size Bin

5.5 Aerosol Volume Concentration over Time at EMS Workers' Face

Aerosol volume concentration at EMS workers' face positions over time is considered. Note that this is the averaged value from the three experiments (ensemble-averaged). There are five positions based on the seating positions in the patient compartment as shown in Figure 67.

Figure 217 to Figure 222 show aerosol volume concentration over time of three experiments for each seat position: three different size ranges, and two different ventilation rates. From these figures, the time to return to the background-state concentration after starting the particles injection can be summarized as shown in Table 5 to Table 9. Note that the background state value is the average concentration values in the period before the injection is started and the return-to-background time is the time when the concentration returns to the background state value.

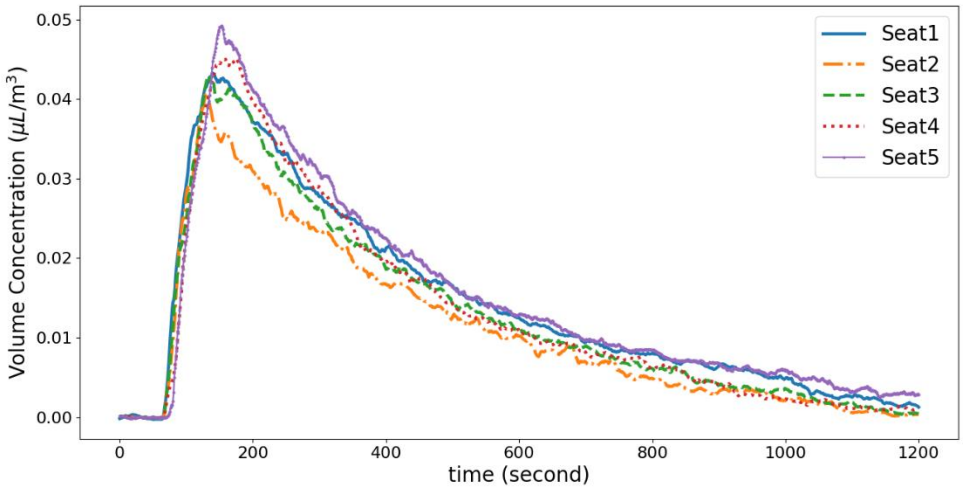

Figure 217 Aerosol Volume Concentration over Time at Five Different Seat Positions with Aerosol Particles in the Range between 0.5 and 1 Micron for Minimal Ventilation Case (MV)

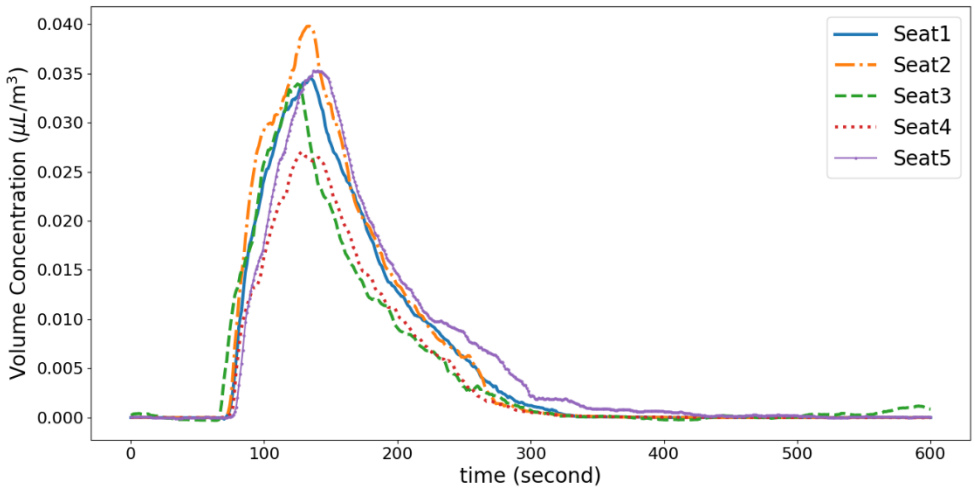

Figure 218 Aerosol Volume Concentration over Time at Five Different Seat Positions with Aerosol Particles in the Range between 0.5 and 1 Micron for High Ventilation Case (HV)

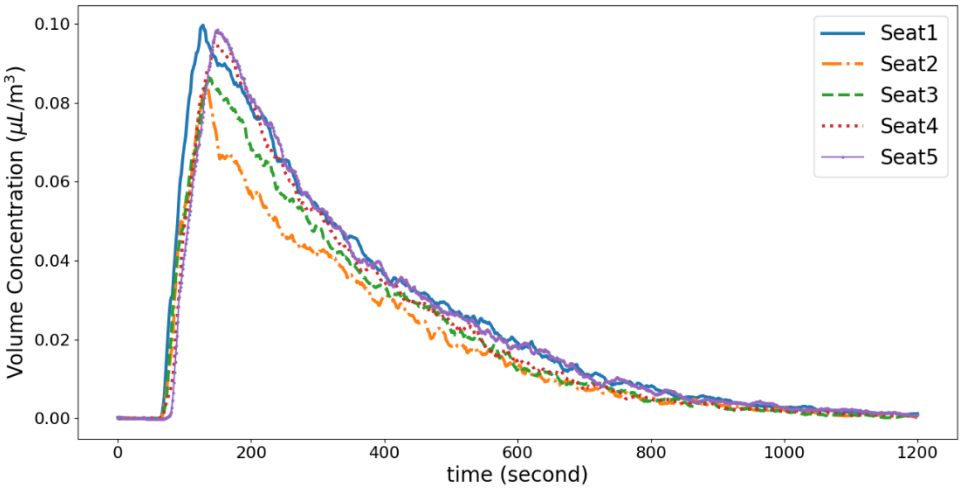

Figure 219 Aerosol Volume Concentration over Time at Five Different Seat Positions with Aerosol Particles in the Range between 1 and 2.5 Microns for Minimal Ventilation Case (MV)

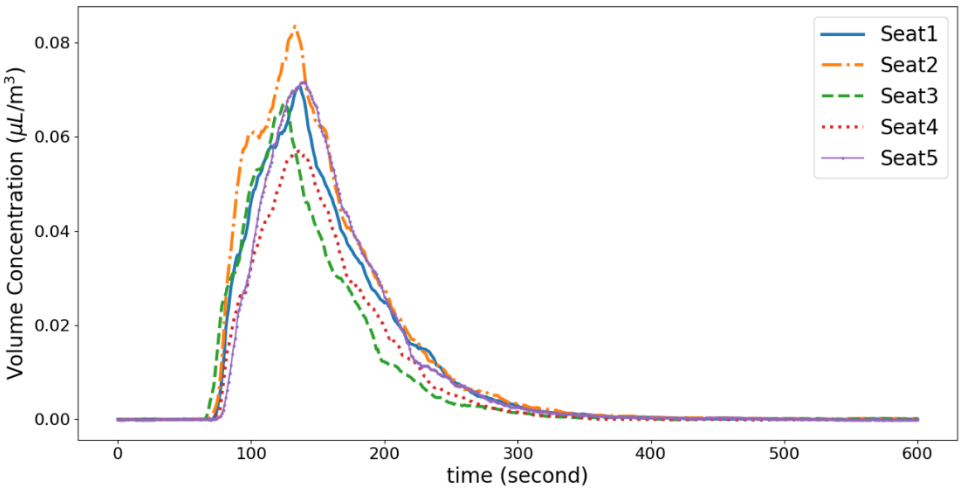

Figure 220 Aerosol Volume Concentration over Time at Five Different Seat Positions with Aerosol Particles in the Range between 1 and 2.5 Microns for High Ventilation Case (HV)

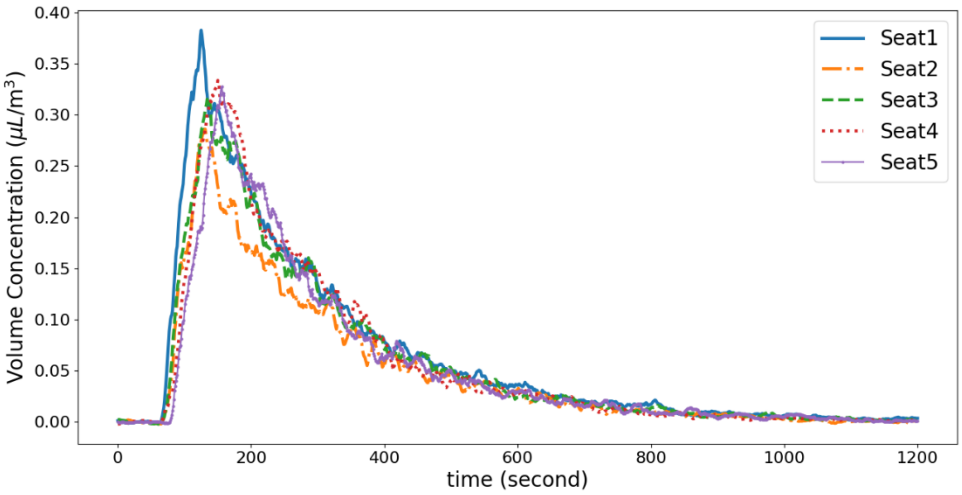

Figure 221 Aerosol Volume Concentration over Time at Five Different Seat Positions with Aerosol Particles in the Range between 2.5 and 5 Microns for Minimal Ventilation Case (MV)

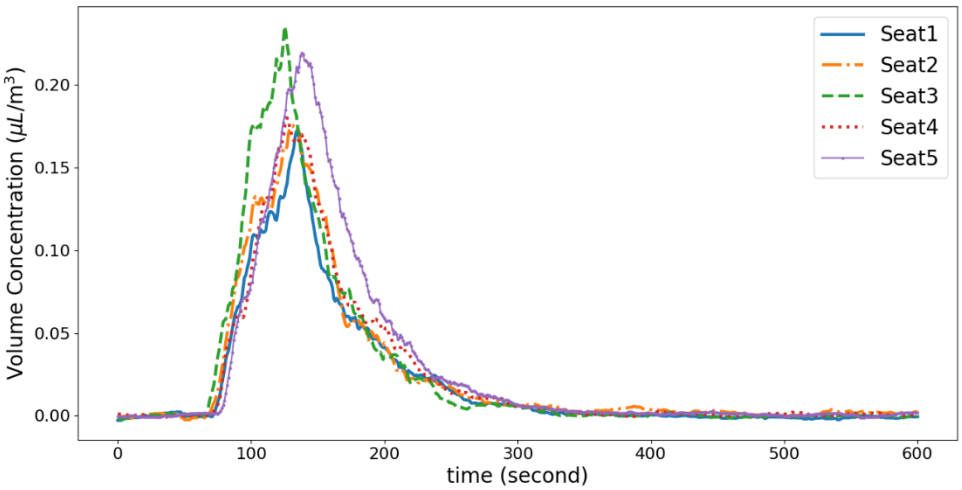

Figure 222 Aerosol Volume Concentration over Time at Five Different Seat Positions with Aerosol Particles in the Range between 2.5 and 5 Microns for High Ventilation Case (HV)

Table 5 Time to Return to the Background-State Concentration in Second at Seat 1

Seat 1		
Size Range (micron) \ Ventilation Rate	MV	HV
0.5-1	-	290
1-2.5	-	340
2.5-5	1040	260

จุฬาลงกรณ์มหาวิทยาลัย
Chulalongkorn University

Table 6 Time to Return to the Background-State Concentration in Second at Seat 2

Seat 2		
Size Range (micron) \ Ventilation Rate	MV	HV
0.5-1	1100	290
1-2.5	1140	350
2.5-5	960	420

Table 7 Time to Return to the Background-State Concentration in Second at Seat 3

Seat 3		
Size Range (micron) \ Ventilation Rate	MV	HV
0.5-1	-	280
1-2.5	1120	340
2.5-5	1120	290

จุฬาลงกรณ์มหาวิทยาลัย
Chulalongkorn University

Table 8 Time to Return to the Background-State Concentration in Second at Seat 4

Seat 4		
Size Range (micron) \ Ventilation Rate	MV	HV
0.5-1	-	290
1-2.5	1140	300
2.5-5	1120	290

Table 9 Time to Return to the Background-State Concentration in Second at Seat 5

Seat 5		
Size Range (micron) \ Ventilation Rate	MV	HV
0.5-1	-	350
1-2.5	-	340
2.5-5	1120	330

Table 5 to Table 9 indicates that the ventilation rate plays an important role that alters the return-to-background period. Concentrations of some seating positions and size ranges do not reduce to background values at the end of the experimental period. However, in Figure 217 to Figure 222, concentration at the end of the experiment in those seating positions and size ranges are low and close to the initial concentration. It can be concluded that the results for all positions and all size ranges combined show that it takes roughly 18 minutes (1100 seconds) at minimal ventilation rate and about 5 minutes (320 seconds) at maximum ventilation rate to reduce the concentration to the background state.

จุฬาลงกรณ์มหาวิทยาลัย
Chulalongkorn University

For part 2, from Figure 223 to Figure 227, apart from the evidence explained previously turning on the air exhaust system results in significant reductions in peak concentration. Except at the seat 2 in the size range 0.5-1 micron and 1-2.5 micron, the peak concentrations only slightly decrease. In addition, the reduction rates of the concentration of MV and HV cases also vary, with the HV case having greater slope reduction across all seating positions and all particle size ranges.

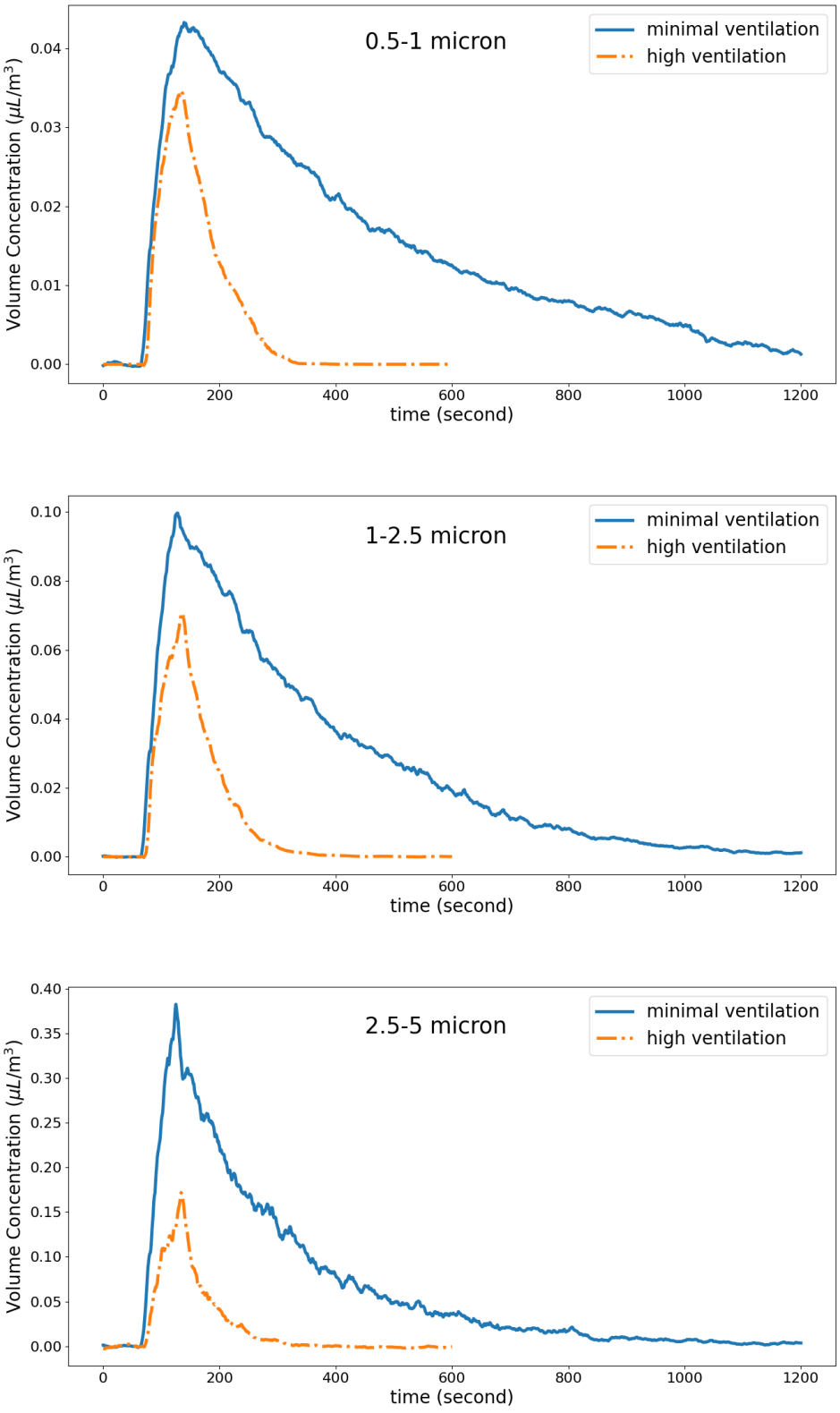

Figure 223 Aerosol Volume Concentration over Time in each Size Bin of Seat1

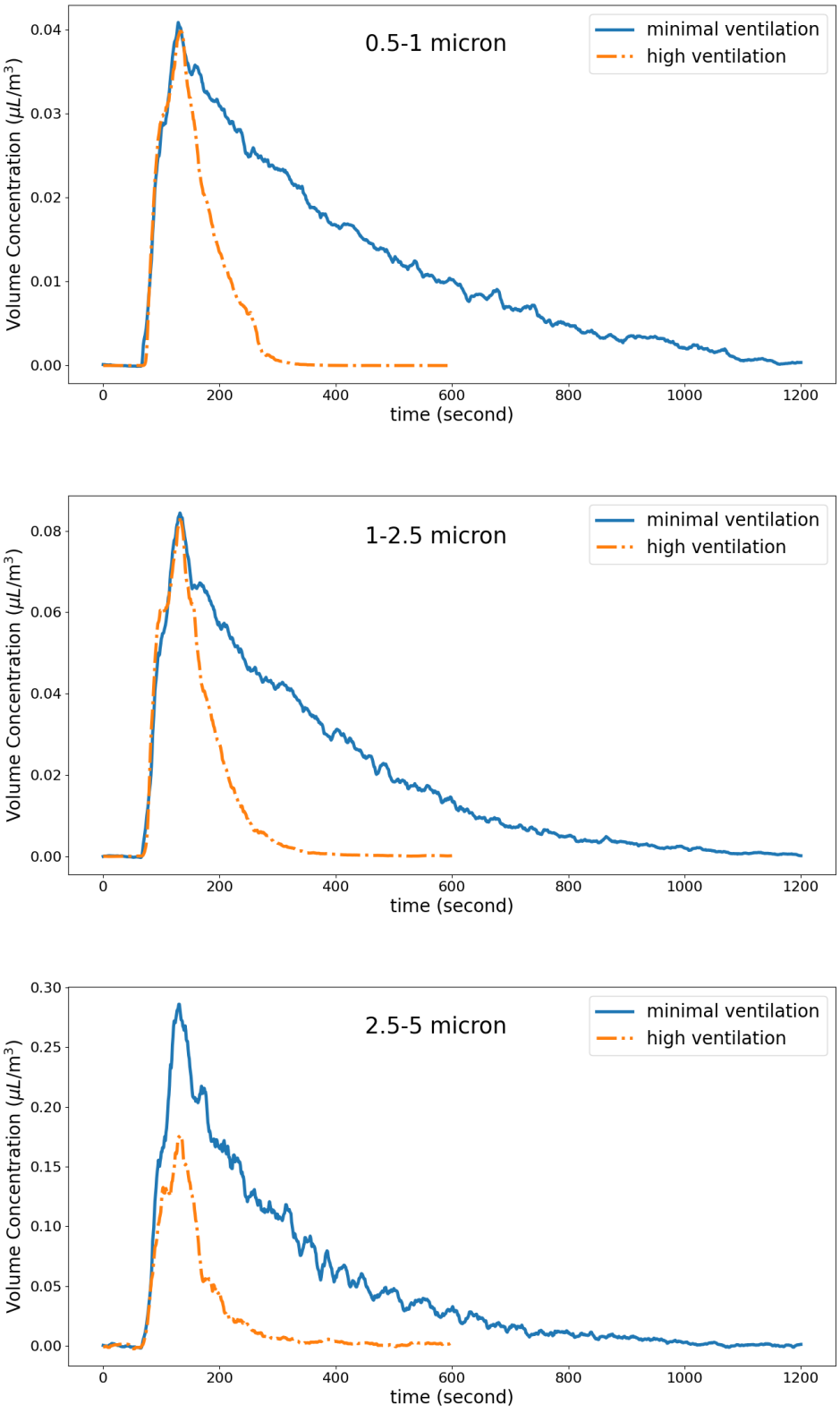

Figure 224 Aerosol Volume Concentration over Time in each Size Bin of Seat2

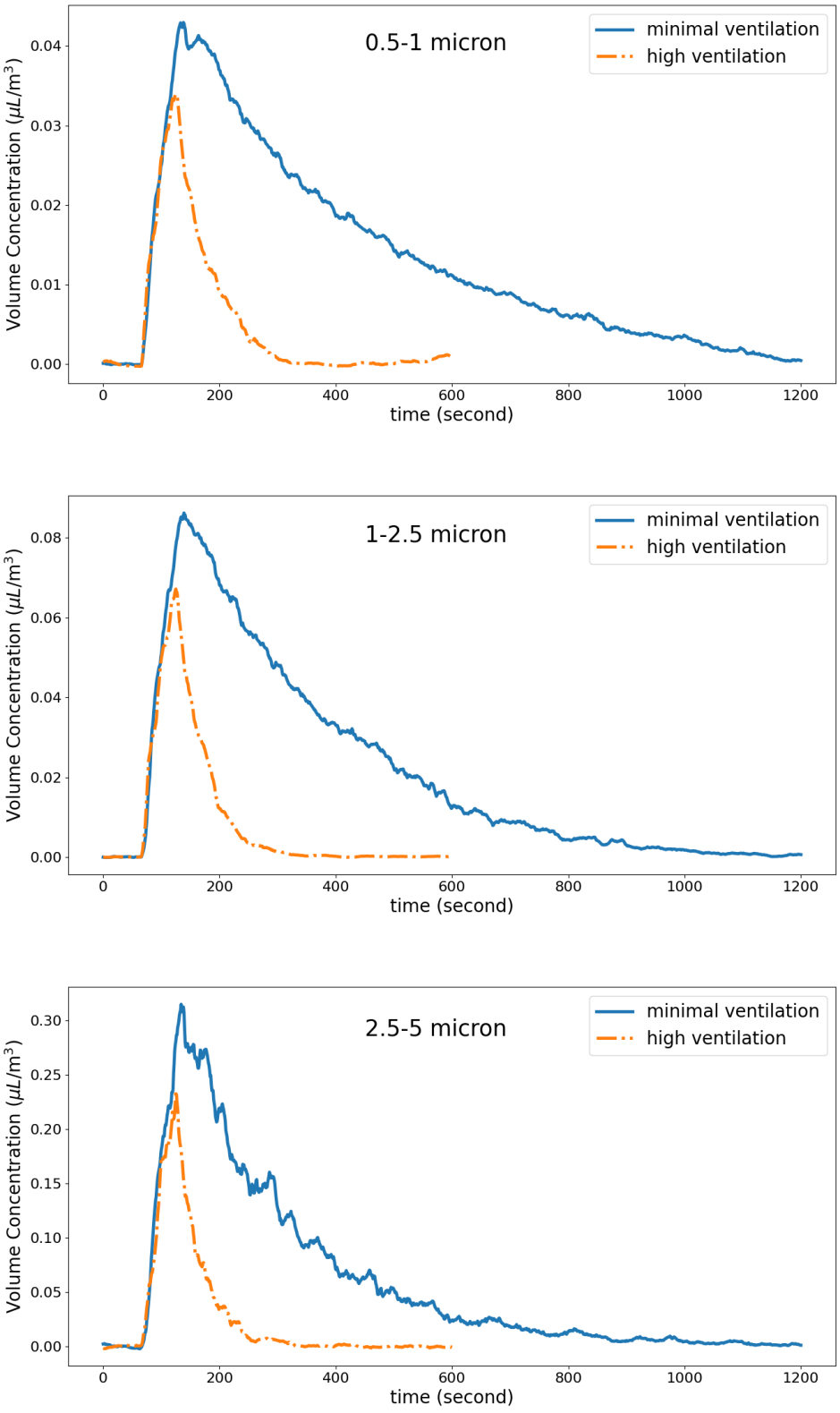

Figure 225 Aerosol Volume Concentration over Time in each Size Bin of Seat3

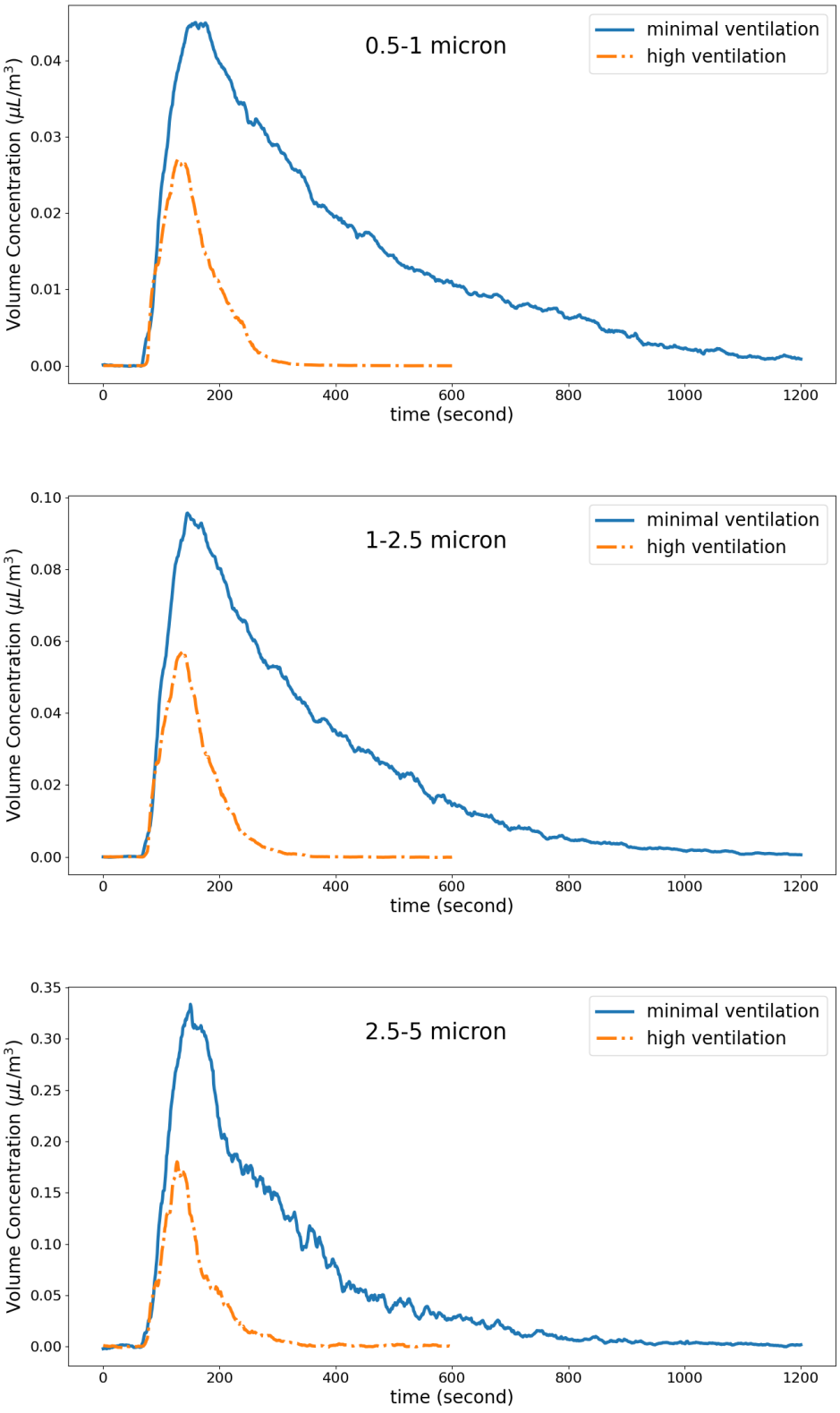

Figure 226 Aerosol Volume Concentration over Time in each Size Bin of Seat4

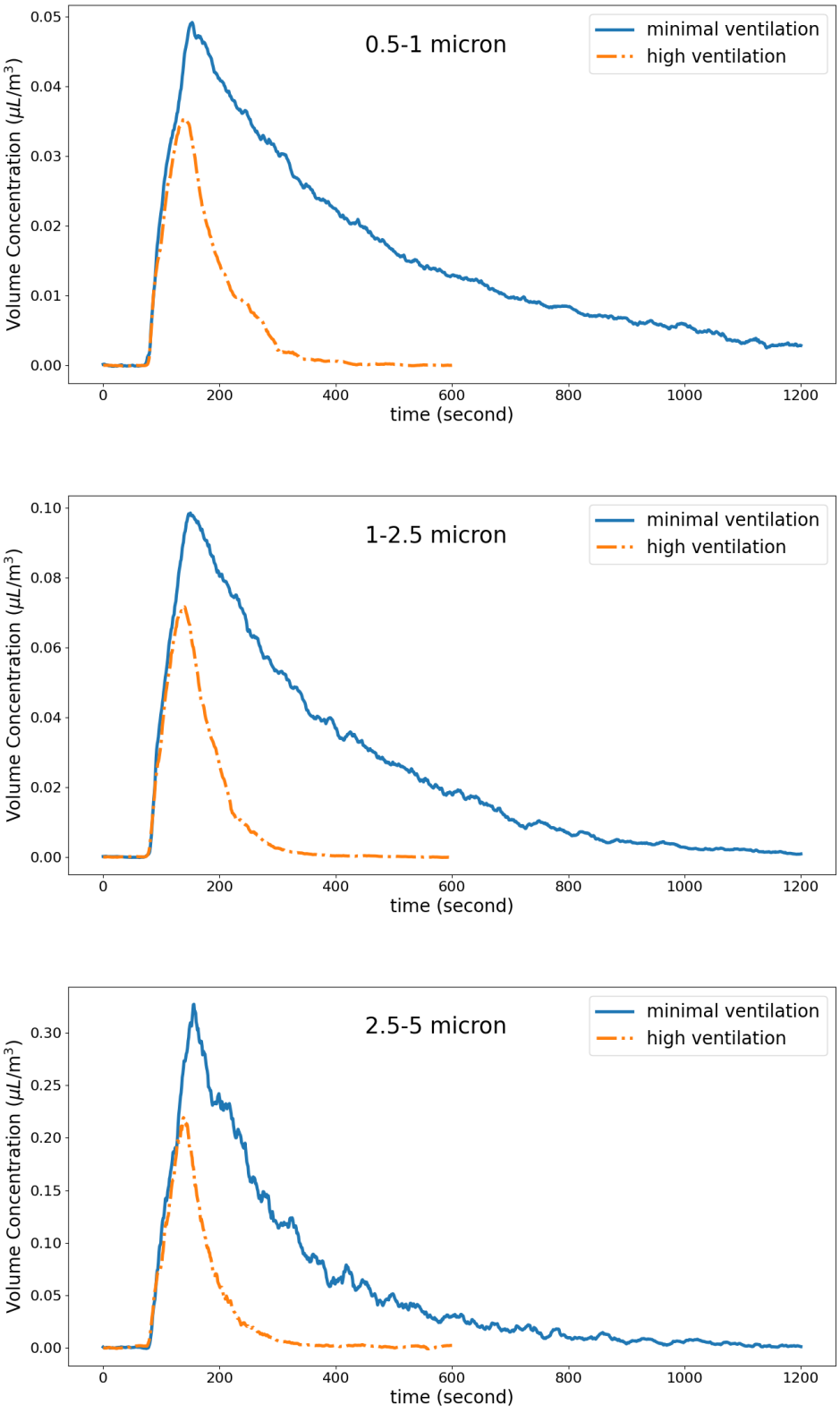

Figure 227 Aerosol Volume Concentration over Time in each Size Bin of Seat5

5.6 Maximum Aerosol Volume Concentration at EMS Workers' Face

Maximum aerosol volume concentration is obtained by averaging the maximum values from the three experiments during experimental period. The values were measured at EMS workers' face location for five seat positions in the patient compartment as shown in Figure 67.

5.6.1 Size range between 0.5 and 1 micron

Table 10 Maximum Volume concentration in 0.5-1-micron size range at all positions

Maximum Volume Concentration (μL/m^3): 0.5-1 micron		
Positions	Minimal Ventilation (MV)	High Ventilation (HV)
Seat 1	0.0432	0.0346
Seat 2	0.0408	0.0398
Seat 3	0.0429	0.0339
Seat 4	0.0449	0.0270
Seat 5	0.0492	0.0353

จุฬาลงกรณ์มหาวิทยาลัย
Chulalongkorn University

For the 0.5-1-micron size range, the highest maximum concentration throughout the experiment of MV case is found at seat 5 which can be observed concentration distribution in the subfigure (a) of Figure 82, Figure 83, and Figure 84 in section 5.2.1; concentration begins to rise from above the patient's face and begins to spread towards the end of the patient compartment until the highest concentration throughout the experiment in this seat 5 position occurs at 153 second as shown in subfigure (a) of Figure 228. However, this is not the highest concentration value on the contour plane at the current EMS workers' face level. The lowest maximum concentration is at seat 2 for the MV case. In the HV case, the highest maximum concentration during the experiment occurs at seat 2 which can be observed concentration distribution of the subfigure (b) of Figure 82, Figure 83, and Figure 84 in section 5.2.1, the high concentration relative to other regions on the

contour plane (the area above the patient's face) distributes to various seating positions, especially seat 2, and the concentration is highest throughout the experiment at this seat position at 134th as shown in subfigure (b) of Figure 228. The lowest maximum concentration for HV case occurs at seat 4. When the air exhaust system is turned on (changing from MV to HV), it is found that the area with the highest maximum concentration reduction in terms of concentration value occurs at seat 4 with a decrease of 0.0179 μL/m^3 or 39.87% compared to the MV case. The position with the least reduction in terms of decrease in concentration value is seat 2, with a decrease of 0.001 μL/m^3 or 2.45% compared to the maximum concentration value of MV case.

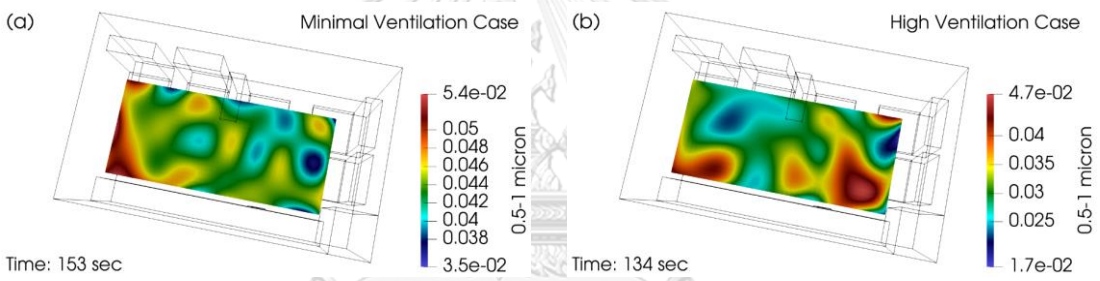

Figure 228 Contour Plot of Highest Maximum Concentration at EMS Workers' Face Position

จุฬาลงกรณ์มหาวิทยาลัย
Chulalongkorn University

5.6.2 Size range between 1 and 2.5 micron

Table 11 Maximum Volume concentration in 1-2.5-micron size range in all positions

Maximum Volume Concentration (μL/m^3): 1-2.5 micron		
Positions	Minimal Ventilation (MV)	High Ventilation (HV)
Seat 1	0.0997	0.0707
Seat 2	0.0844	0.0834
Seat 3	0.0862	0.0672
Seat 4	0.0957	0.0569
Seat 5	0.0985	0.0716

Maximum volume concentration value throughout the experiment for particles in the 1-2.5-micron size range of the MV case has the highest maximum concentration value at seat 1 which can be observed from the distribution of concentration in the subfigure (a) of Figure 106, Figure 107, and Figure 108 in section 5.2.2; it can be seen that the high concentration on the plane relative to other regions located above the patient's face mainly distributes to seat 1, resulting in the highest concentration throughout the experiment in this case occurring at the seat 1 position at 128th second as shown in subfigure (a) of Figure 229. The lowest maximum concentration of MV case is at seat 2. Whereas the highest maximum concentration in HV case occurs at seat 2 in contrast to that of the MV case. From subfigure (b) of Figure 107 and Figure 108 in section 5.2.2, it can be seen that the high concentration relative to the rest of the plane spreads mostly to seat 2 and creates the highest maximum concentration at this seat position in 133rd second as shown in subfigure (b) of Figure 229 and the lowest maximum concentration occurs at seat 4. Thus, the maximum for both MV and HV cases occur at about the same time (10 seconds after the injection has stopped).

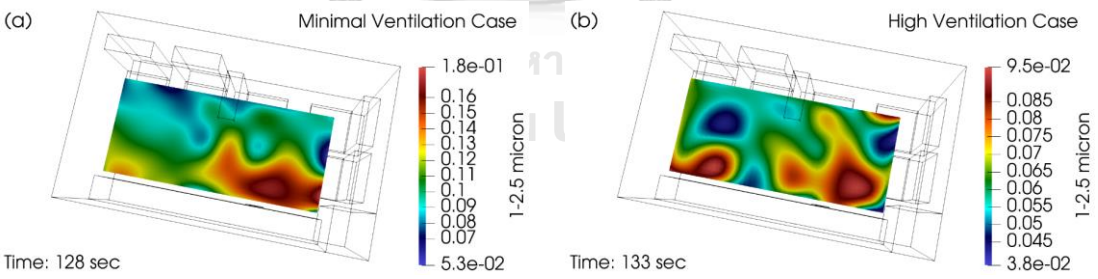

Figure 229 Contour Plot of Highest Maximum Concentration at EMS Workers' Face Position

Additionally, it is found that the position with the highest reduction, when the air exhaust system is on (changing from MV to HV), in maximum concentration value occurs at seat 4 with a value of 0.0388 μL/m^3 which is 40.54% compared to the MV case. The position with the least reduction in terms of decrease in concentration

value is seat 2, with a value of 0.001 μL/m^3 or 1.18% compared to the value of the MV case.

5.6.3 Size range between 2.5 and 5 micron

Table 12 Maximum Volume concentration in 2.5-5-micron size range in all positions

Maximum Volume Concentration (μL/m^3): 2.5-5 micron		
Positions	Minimal Ventilation (MV)	High Ventilation (HV)
Seat 1	0.3824	0.1719
Seat 2	0.2859	0.1763
Seat 3	0.3151	0.2355
Seat 4	0.3336	0.1801
Seat 5	0.3274	0.2193

Observing from Figure 130, Figure 131, and Figure 132 in section 5.2.3, it can be seen that the high concentration of the MV case compared to other regions on the plane mainly distributes to seat 1, resulting in highest maximum concentration throughout the experiment of particles in the 2.5-5-micron size range occurring at seat 1 in 125th second as shown in subfigure (a) of Figure 230. The lowest maximum concentration is at seat 2 for the MV case. In the HV case, it can be seen from Figure 130, Figure 131, and Figure 132 in section 5.2.3, which distribution of high concentration compared to other areas on the plane spreads to seat 3 more than other seat positions, resulting in the highest maximum concentration occurring at seat 3 at 125th second as shown in subfigure (b) of Figure 230. Thus, the maximum for both MV and HV cases occur at the exact time (5 seconds after the injection has stopped). The lowest maximum concentration in this case occurs at seat 1.

จุฬาลงกรณ์มหาวิทยาลัย
Chulalongkorn University

It is found that the position with the greatest reduction in maximum concentration value when the air exhaust system is on (changing from MV to HV) occurs at seat 1 with a value of 0.2105 μL/m^3 or 55.05% compared to the value of

the MV case and the position with the least reduction in concentration value is seat 3, with a value of 0.0796 μL/m^3 which is 25.26% compared to the MV case.

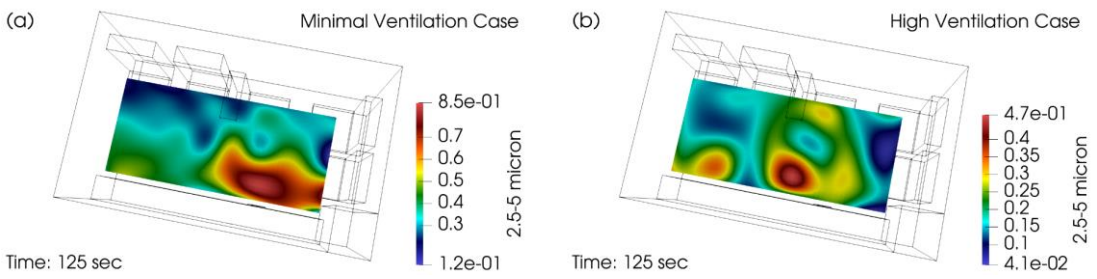

Figure 230 Contour Plot of Highest Maximum Concentration at EMS Workers' Face Position

The exponential decreases of particle concentration seen in the previous section, reflecting one criterion in measuring the effectiveness of the air exhaust system, do not however infer to the amount of concentration in which EMS workers are exposed to a cloud of the particles. The amounts can remain close to their corresponding maximum values for up to several seconds, a sufficiently-long period for the intaking by inhalation.

A set of histograms comparing the maximum volume concentration at all seat locations and size bins is shown in Figure 231. It is clear that increasing the ventilation rate decreases the maximum aerosol volume concentration for all size ranges and all seat positions.

When considering the particle size range, the concentration of MV case is peak at the seat position 1 for 1-2.5-micron and 2.5-5-micron particles, peak at seat 5 in the smallest size range of particle, and lowest at seat 2 for all size ranges. What is interesting is that although the lowest value when the air exhaust system is not turned on occurs at the seat 2 in all particle size ranges, when the air exhaust system is turned on, the concentration values noticeably reduce in all the particle size ranges and all seating positions except at seat 2 in the 0.5-1-micron and 1-2.5-micron

จุฬาลงกรณ์มหาวิทยาลัย
Chulalongkorn University

size ranges, with only a slight reduction which can be seen from the top and middle histograms of Figure 231. However, when observing the seat 2 location in Figure 67, it is likely that the seat 2 location is far from the outlet and because in the MV case the concentration in the seat 2 is already low which may cause the volume of concentration that can be reduced and the safest position in the two size ranges mentioned above in the case of HV is seat 4. For the largest size range, the position at the greatest risk with the air exhaust system on is seat 3, and seat 1 is safest.

จุฬาลงกรณ์มหาวิทยาลัย
Chulalongkorn University

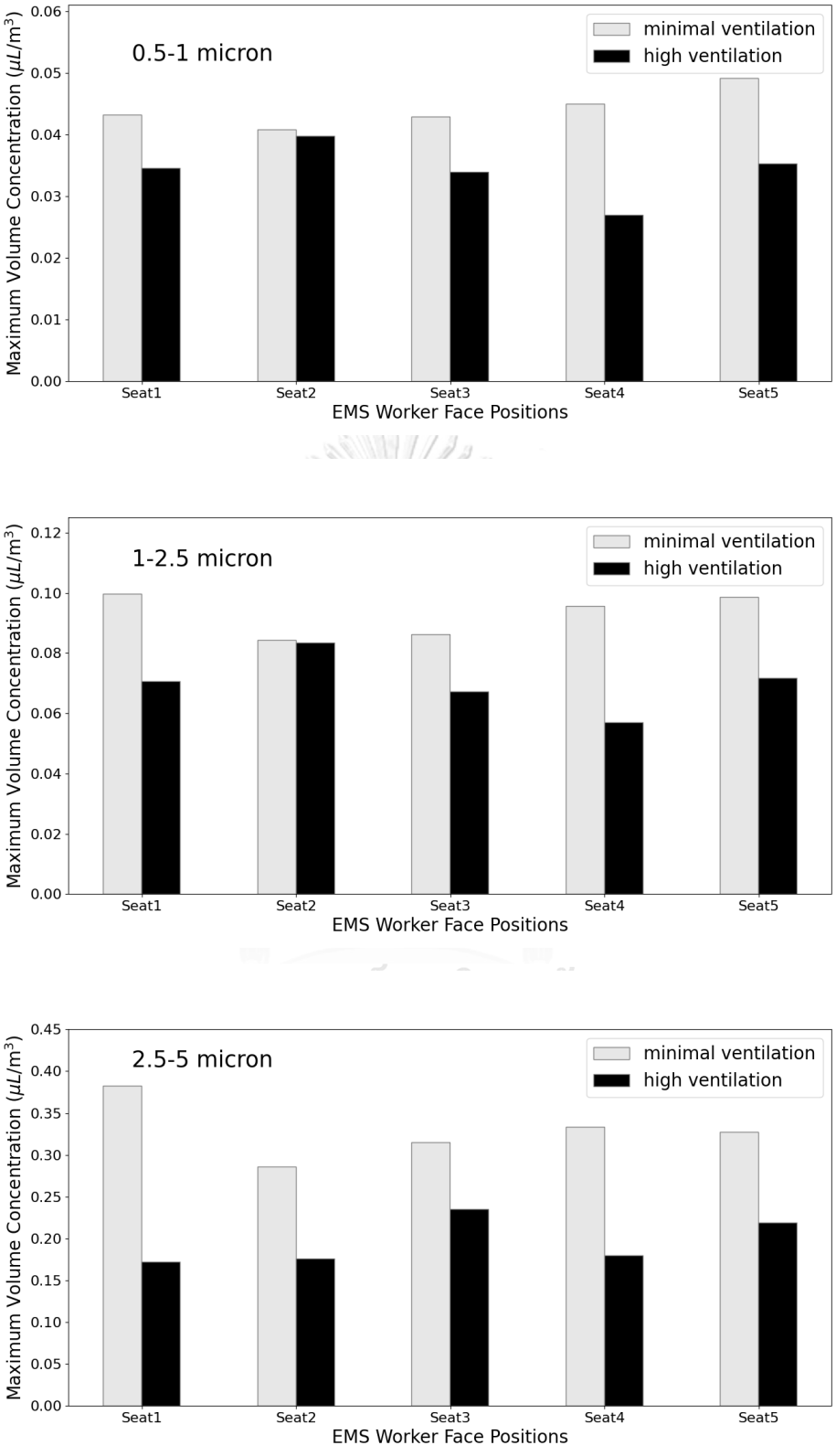

Figure 231 Maximum Volume Concentration at Five Different Locations in each Size Bin

5.7 Temporal-Averaged Aerosol Volume Concentration at EMS Workers' Face

Lastly, we consider the temporal-averaged volume concentration, shown as a set of histograms in Figure 232. Temporal-averaged volume concentration is determined by summing the aerosol volume concentration in each size bin and then averaging the total volume concentration over 10 minutes (measured one minute before introducing particle into patient compartment) for both minimal ventilation (MV) and high ventilation (HV) case at EMS workers' face in every seat position as shown in Figure 67.

5.7.1 Size range between 0.5 and 1 micron

Table 13 Temporal-Averaged Volume concentration in 0.5-1-micron size range in all positions

Temporal-Averaged Volume Concentration ($\mu L/m^3$): 0.5-1 micron		
Positions	Minimal Ventilation (MV)	High Ventilation (HV)
Seat 1	0.0224	0.0059
Seat 2	0.0186	0.00642
Seat 3	0.0209	0.0051
Seat 4	0.0215	0.0045
Seat 5	0.0231	0.00639

จุฬาลงกรณ์มหาวิทยาลัย
Chulalongkorn University

The temporal-averaged volume concentration in the 0.5-1-micron size range has the highest concentration at seat 5 and the lowest concentration at seat 2 for the MV case; in the HV case, the highest concentration occurs at seat 2 and the lowest concentration occurs at seat 4. When the air exhaust system is switched on, it is found that the position with greatest reduction (when changing from MV to HV) in terms of temporal-averaged concentration value occurs at seat 4 with a value of 0.017 $\mu L/m^3$ or 79.06% compared to the value of the MV case. The position with the

smallest reduction in temporal-averaged concentration value is seat 2, with a decrease of 0.01218 μL/m^3 or 65.48% compared to the MV case.

5.7.2 Size range between 1 and 2.5 micron

Table 14 Temporal-Averaged Volume concentration in 1-2.5-micron size range in all positions

Temporal-Averaged Volume Concentration (μL/m^3): 1-2.5 micron		
Positions	Minimal Ventilation (MV)	High Ventilation (HV)
Seat 1	0.0443	0.0112
Seat 2	0.0337	0.0132
Seat 3	0.0381	0.0092
Seat 4	0.0405	0.0087
Seat 5	0.0419	0.0111

The temporal-averaged volume concentration in the 1-2.5-micron size range has the highest concentration value at seat 1 and the lowest concentration at seat 2 for the MV case, while for the HV case the highest concentration is at seat 2 and the lowest concentration occurs at seat 4. A decrease in temporal-averaged concentration value occurs when the air exhaust system is turned on (changing from MV to HV); the location with the highest reduction is at seat 1, with a decrease of 0.0331 μL/m^3 or 74.72% compared to concentration value of the MV case. The position with the smallest reduction in concentration value is at seat 2, with a value of 0.0205 μL/m^3 or 60.83% compared to concentration value of the MV case.

จุฬาลงกรณ์มหาวิทยาลัย
Chulalongkorn University

5.7.3 Size range between 2.5 and 5 micron

Table 15 Temporal-Averaged Volume concentration in 2.5-5-micron size range in all positions

Temporal-Averaged Volume Concentration ($\mu L/m^3$): 2.5-5 micron		
Positions	Minimal Ventilation (MV)	High Ventilation (HV)
Seat 1	0.1191	0.0212
Seat 2	0.0912	0.0252
Seat 3	0.1072	0.0272
Seat 4	0.1092	0.0249
Seat 5	0.1018	0.0300

The temporal-averaged volume concentration in the 2.5-5-micron size range is highest at seat 1 and lowest at seat 2 for the MV case. In the HV case, the highest concentration occurs at seat 5 and the lowest concentration occurs at seat 1. When the air exhaust system is turned on (changing from MV to HV), it is found that the position of greatest reduction in terms of temporal-averaged concentration value occurs at seat 1 with a value of 0.0979 $\mu L/m^3$ or 82.20% compared to the concentration value of MV case. The position with the least reduction in concentration value is seat 2, with a decrease of 0.066 $\mu L/m^3$, which is 72.37% compared to the MV case.

Reflecting the overall particle exposure, the set of temporal-averaged values in Figure 232 looks similar to that seen in the previously section of the maximum values data. For MV case, the location of the highest and lowest temporal-averaged concentration in each size range remains the same as the previous section, with trend of concentration of other seating positions likely similar to the maximum volume concentration as well. In the HV case, the highest and lowest temporal-averaged concentration still occurs in the same locations as the maximum volume concentration case in the 0.5-1-micron and 1-2.5-micron size ranges; in the 2.5-5-

micron size range, the lowest concentration position remains at the same position as maximum volume concentration, but the highest concentration position changes as shown in Figure 231 and Figure 232.

To conclude, turning on the air exhaust system results in a huge decrease in temporal-averaged concentration in every seat position and in every size range (reduce with a greater proportion compared to the maximum concentration in section 5.6). However, the most secure location when the air exhaust system is off occurs in the seat 2 position across all size ranges and the high-risk positions compared to other seating positions are the seat 1 for 1-2.5-micron and 2.5-5-micron size ranges and seat 5 for 0.5-1-micron size range. On the contrary when the air exhaust is turned on, seat 2 is the position that is most at risk of exposure to the aerosol volume concentration in the 0.5-1-micron and 1-2.5-micron size ranges and the riskiest position for the 2.5-5-micron size range is the seat 5. The safest positions compared to other seat locations in this scenario for the 0.5-1-micron and 1-2.5-micron size ranges are at seat 4 and at seat 1 for the 2.5-5-micron size range.

จุฬาลงกรณ์มหาวิทยาลัย
CHULALONGKORN UNIVERSITY

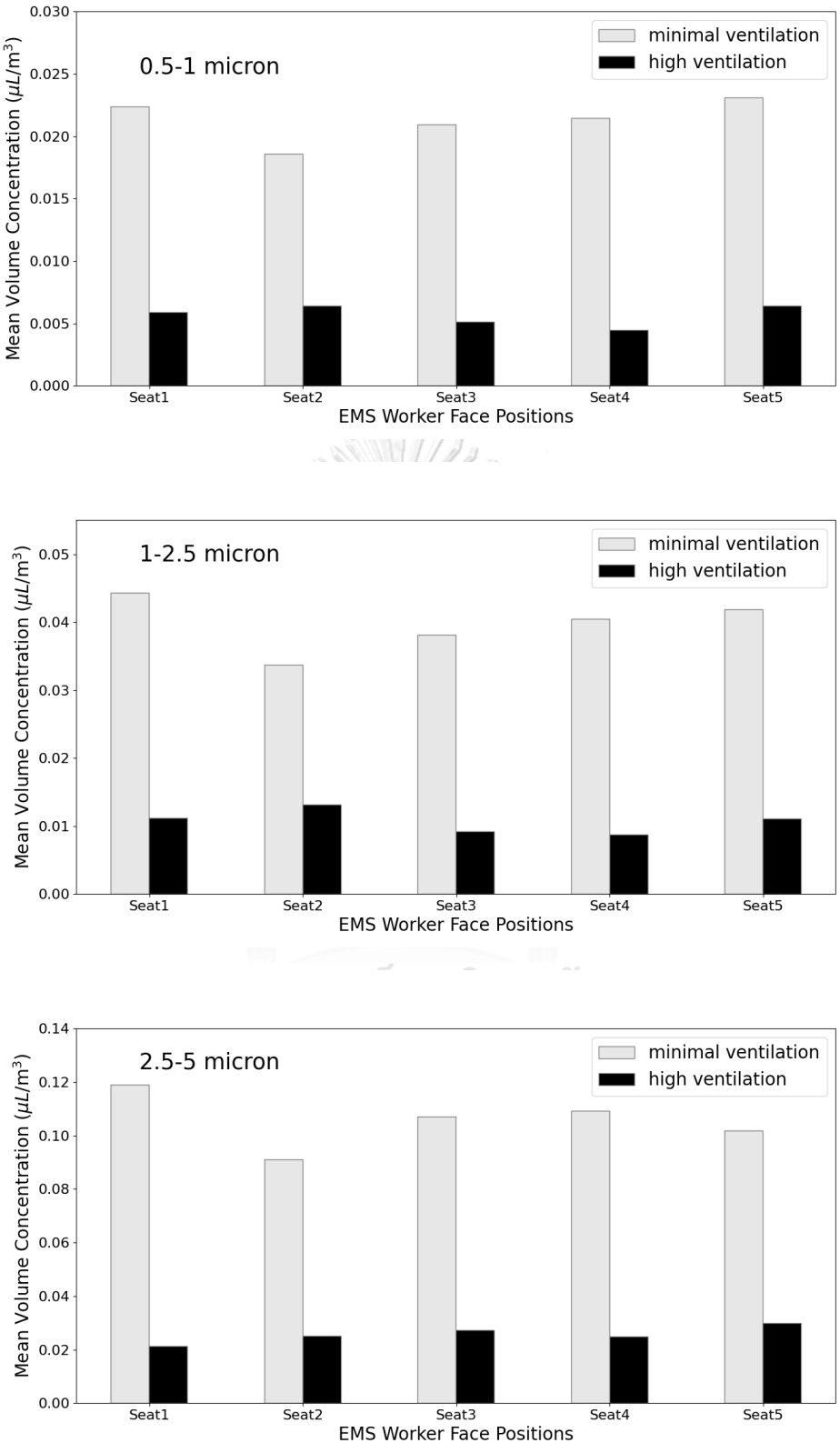

Figure 232 Temporal-Averaged Aerosol Volume Concentration at Five Different Locations in each Size Bin

CHAPTER 6
DISCUSSION

We successfully determine the effectiveness of the ambulance air exhaust system particularly in reducing the aerosol in the cabin. It should be emphasized that within the scopes of the thesis, it is the volume concentration that we are interested in. However, what posts the risk for respiratory infection is the number of viruses that are being carried by a cloud of aerosol rather than aerosols themselves. Although it seems sensible for the number of viruses to be directly correlated with the aerosol volume in which they are carried, we do not have concrete evidence of such claim. The following is merely an attempt in determining the infection probability.

Since we cannot directly estimate the risk of respiratory infection from the aerosol volume concentration, we need to convert the aerosol volume concentration to quanta generation rate which can be used to assess the probability of infection from Wells-Riley Equation (Dai & Zhao, 2020) as follows.

$$P = \frac{C}{S} = 1 - e^{-\frac{Iqpt}{Q}}$$

จุฬาลงกรณ์มหาวิทยาลัย
CHULALONGKORN UNIVERSITY

where P is the probability of infection

C is the number of new infection cases

S is the number of susceptible individuals

I is the number of infected people

q is the quanta generation rate (1/hr)

p is the breathing volume flow rate of a person (m^3/hr)

t is the exposure time (hr)

Q is the room ventilation rate with clean air (m^3/hr)

Based on a study by Eiche and Kuster (2020), we can convert aerosol volume concentration (μL/m^3) per time period to quanta generation rate (1/hr) by multiplying by 10^6 to 10^{11} (1/mL) and then multiplying by the volume engulfing this aerosol volume concentration.

Since the values used to convert from aerosol volume concentration to quanta are in a wide range. In this chapter, the value 10^8 (1/mL) is chosen and selected aerosol volume concentration data from spatial-averaged aerosol volume concentration over time from section 5.4 by using the 0.5-1-micron size range for the calculation.

In the case of high ventilation, the quanta generation rate can be calculated as follows:

$$q = 3.763 \ \frac{\mu L}{m^3 hr} \times \frac{1 \ mL}{1000 \ \mu L} \times \frac{10^8}{mL} \times 6.4\times10^{-5} \ m^3 = 24.08 \ \frac{1}{hr}$$

In the case of minimal ventilation, the quanta generation rate can be calculated as follows:

จุฬาลงกรณ์มหาวิทยาลัย
Chulalongkorn University

$$q = 18.214 \ \frac{\mu L}{m^3 hr} \times \frac{1 \ mL}{1000 \ \mu L} \times \frac{10^8}{mL} \times 6.4\times10^{-5} \ m^3 = 116.60 \ \frac{1}{hr}$$

For the calculation, assume that within the patient compartment there is one patient and five EMS workers, each has a respiratory rate of 16 breaths per minute (usually 12-20 breaths per minute for adult) and tidal volume of 500 mL per breath, which is a breathing volume flow rate of 0.48 m^3/hr. The ventilation rate when the air exhaust system is turned on at the maximum rate is roughly 80 ACH and the patient compartment has a volume of 5.733 m^3.

Probability of infection of EMS workers who are in the patient compartment with the patient for 15 minutes when the maximum ventilation rate is on can be calculated from the Wells-Riley Equation as follows:

$$P = 1 - e^{-\frac{(1)(24.08)(0.48)(0.25)}{(80)(5.733)}}$$

$$P = 0.0063 \text{ or } 0.63\%$$

A risk factor of 0.63% means that when five EMS workers are inside the patient compartment with one patient for 15 minutes, there is a risk of infection of 0.0315 people.

Besides, when considering when the air exhaust system is closed (minimal ventilation), it can be seen that the quanta value is higher than in the case of high ventilation. In addition, the air change rate is very low compared to the case of high ventilation as well. If we assume that the air change rate for the case of the minimal ventilation is about 5 ACH, which may in fact be much lower. The probability of infection can be calculated as follows:

$$P = 1 - e^{-\frac{(1)(116.60)(0.48)(0.25)}{(1)(5.733)}}$$

จุฬาลงกรณ์มหาวิทยาลัย
CHULALONGKORN UNIVERSITY

$$P = 0.3861 \text{ or } 38.61\%$$

A risk factor of 38.61% means that when five EMS workers are inside the patient compartment with one patient for 15 minutes, there is a risk of infection of 1.93 people.

It can be seen that when the air exhaust system is turned off and turned on at the maximum rate, there is difference in aerosol volume concentration values which directly affect the quanta generation rate. In addition, from the above data, we found that turning on the air exhaust system at maximum rate significantly reduces the risk of infection among healthcare workers.

CHAPTER 7
SUMMARY AND CONCLUSION

Airborne disease transmission has increasingly been prevalent on a global scale, particularly due to the COVID-19 pandemic. Medical sectors take different measures in suppressing the contagious virus, e.g., revising their ventilation systems in hospitals and ambulances. The objective of this work is to assess the effectiveness of a newly installed ambulance air exhaust system in reducing the volume density of airborne particles. The so-called recovery test is done by diffusing aerosols into the ambulance cabin at the patient's face position for a short period and measuring the aerosol concentration inside the cabin over time.

The experiment is conducted inside Toyota Ventury (ER-1) from King Chulalongkorn Memorial Hospital that is equipped with the Camfil® model CC410-concealed air exhaust system. The measurement is done using a particle counter (PMS5003) attached to an Arduino board that is connected to a computer laptop. Pulses of artificially-injected-aerosol particles (0.9% NaCl solution) are created by nebulizer (Aeroneb® Professional Nebulizer), connected with a portable ventilator (Oxylog® 3000 plus). The experiment begins with preconditioning to establish an identical initial state for the set of experiments. The cloud of particle is injected for one minute. Concentration is measured throughout the entire period of experiment that ends after the background state is reached or sufficiently-long time. The measurement, repeated three times for each case, is done for 200 positions (a cartesian grid of 10 x 5 x 4). The measured numbers of particle per unit volume of air is then converted into volume concentration. The resulting volume concentration is investigated by means of 1) Three-dimensional visualization, 2) Concentration on the horizontal plane positioned at EMS workers' face level (3 cm. from top of the patient compartment), 3) Concentration on the vertical plane at injection position along

จุฬาลงกรณ์มหาวิทยาลัย
Chulalongkorn University

patient cot (55 cm. from the right of the patient compartment), 4) Spatial-averaged (entire cabin volume) aerosol volume concentration over time, 5) Aerosol volume concentration over time at EMS workers' face, 6) Maximum aerosol volume concentration at EMS workers' face, and 7) Temporal-averaged aerosol volume concentration at EMS workers' face are summarized as follows.

When considering three-dimensional visualization, immediately after the 1-minute injection period (to be referred to as IP onward), the aerosol concentration is largest above the injected nozzle (the patient face). The aerosol is advected toward the cabin's frontal part, covering seat 1, and then disperses across the control volume. The concentration continues to rise until it reaches its maximum value adjacent to the outlet soon after the IP ends. Though it remains uniformly dense around the diffuser. Later time concentration drops and then the entire cabin is found to contain almost uniform concentration about 8 minutes following IP for the MV case and only about 1 minute after IP for HV case for all size ranges. The MV concentration of larger-size particles is found to decay relatively faster, with the order of concentration magnitude decreases and then becomes comparable to that of the background state at about 9 minutes for 2.5-5 microns, 12 minutes for 1-2.5 microns, and 16 minutes for 0.5-1 microns particles. The air exhaust system is able to reduce the time required in bring the aerosol concentration down close to the background state, about 3 minutes for 2.5-5 microns, 3 minutes for 1-2.5 microns, and 4 minutes for 0.5-1 microns particles. Again, in this context, time is measured 'from' the end of IP.

Investigation via horizontal contours at the EMS workers' face level shows that the early distribution of concentration in MV case has multiple concentration peaks appear in the cabin frontal region, that is seat 1-4 experience high exposure relative to the rear end. The HV aerosol distributes itself largely to seat 4 from this horizontal plane perspective.

From the horizontal and vertical contour point-of-view reveals multiple local concentration peaks throughout the decaying period. MV case takes about 12 minutes for the aerosol concentration to decay and reach relatively-low value (order of background state) only for a few seat positions. The air exhaust system is able to shorten the decaying period (from IP to background state order of concentration magnitude) by 10 minutes. It is important to emphasize that the background state order of concentration magnitude is not exactly of value at background state, but merely at when the field is visible using the background state colormap.

Consider the average concentration across the control volume (the entire cabin) at each period: it rises quickly when the IP begins and then falls off exponentially once the IP ends. Reduction rate is directly proportional to particle size, large particles decay relatively faster than small particles. The MV concentration returns to the background about 16 minutes after the IP is initiated and the HV takes 5 minutes.

Consider each EMS workers' face positions. When the air exhaust system is disabled, seat 5's peak concentration is highest among peaks of other positions and its temporal-averaged value is also highest among the temporal-averaged values of others for the smallest size range. For other size ranges, the largest appears to be at seat 1. This risky exposure at both seats (5 and 1) occurs approximately 15 seconds after the end of the IP. The lowest exposure to the aerosol is at seat 2 for all size ranges. When the air exhaust system is on, seat 2 is exposed to largest concentration both of its peak and temporal-averaged value for the 0.5-1 micron and 1-2.5 micron size ranges. But for 2.5-5 micron size range, seat 3's peak concentration is highest among peaks of others, while the highest temporal-averaged concentration is at seat 5. The highest peak concentration occurs at about 10 seconds after the end of IP. Seat 4 in the 0.5-1 micron and 1-2.5 micron size ranges, and seat 1 in the 2.5-5 micron size range, are the safest locations for both peak and temporal-averaged concentration. Regardless of seat position and size of particles, the `return-to-

จุฬาลงกรณ์มหาวิทยาลัย
Chulalongkorn University

background' duration measures about 18 minutes after starting of injection for MV case and approximately 5 minutes for HV case. It can generally be said that, averaging among seats and particle sizes, the air exhaust system is able to reduce maximum concentration by approximately 25% and temporal-averaged concentration by 70%.

จุฬาลงกรณ์มหาวิทยาลัย
Chulalongkorn University

REFERENCES

Aerogen®. (2015). *Aeroneb® Pro Micropump Nebulizer Instruction Manual*. Retrieved October 22, 2020, from https://www.yumpu.com/en/document/read/37524572/aeroneb-pro-instruction-manual-aerogen

Aleandri, S., Vaccaro, A., Armenta, R., Völker, A. C., & Kuentz, M. (2018). Dynamic Light Scattering of Biopharmaceutics—Can Analytical Performance Be Enhanced by Laser Power? *Pharmaceutics*, *10*(3), 94. https://doi.org/10.3390/pharmaceutics10030094

Alford, R. H., Kasel, J. A., Gerone, P. J., & Knight, V. (1966). Human Influenza Resulting from Aerosol Inhalation. *Experimental Biology and Medicine*, *122*(3), 800-804. https://doi.org/10.3181/00379727-122-31255

American Society for Microbiology. (2020, August 19). *COVID-19 Testing FAQs*. Retrieved November 15, 2020, from https://asm.org/Articles/2020/April/COVID-19-Testing-FAQs

ASHRAE, S. (2017). Standard 170-2017-Ventilation of Health Care Facilities 1 (ANSI/ASHRAE/ASHE Approved), in. *ASHRAE 170-2017*.

Autech. (2020). *[AUTECH Solati (H-350)]*. Retrieved February 20, 2021, from http://www.autech.co.kr/english/products/medical/Eumab_ambulance.asp

Baixardoc. (n.d.). *[Turbulent Mixed Flow Cleanroom]*. Retrieved March 26, 2021, from https://baixardoc.com/preview/4--5c97e8cab856e

Belkin, N. L. (1997). The evolution of the surgical mask: filtering efficiency versus effectiveness. *Infection Control & Hospital Epidemiology*, *18*(1), 49-57. https://doi.org/10.2307/30141964

Bhagat, R. K., Wykes, M. D., Dalziel, S. B., & Linden, P. (2020). Effects of ventilation on the indoor spread of COVID-19. *Journal of Fluid Mechanics*, *903*. https://doi.org/10.1017/jfm.2020.720

Bielawska-Drózd, A., Cieslik, P., Bohacz, J., Kornitłowicz-Kowalska, T., Zakowska, D., Bartoszcze, M., Wlizło-Skowronek, B., Winnicka, I., Brytan, M., & Kubiak, L. (2018).

จุฬาลงกรณ์มหาวิทยาลัย
Chulalongkorn University

Microbiological analysis of bioaerosols collected from Hospital Emergency Departments and ambulances. *Ann Agric Environ Med*, *25*(2), 274-279. https://doi.org/10.26444/aaem/80711

Bielawska-Drózd, A., Cieslik, P., Wlizło-Skowronek, B., Winnicka, I., Kubiak, L., Jaroszuk-sciseł, J., Depczynska, D., Bohacz, J., Kornitłowicz-Kowalska, T., & Skopinska-Rózewska, E. (2017). Identification and characteristics of biological agents in work environment of medical emergency services in selected ambulances. *Int. J. Occup. Med. Environ. Health*, *30*(4), 617-627. https://doi.org/10.13075/ijomeh.1896.00816

Camfil. (2021a). *30/30*. Camfil.

Camfil. (2021b). *Absolute CE*. Camfil.

Centers for Disease Control and Prevention. (2017, October 5). *[COVID-19 Specimen Collection]*. Retrieved February 11, 2021, from https://www.cdc.gov/flu/pdf/professionals/flu-specimen-collection-poster.pdf

Centers for Disease Control and Prevention. (2020, February 11). *Coronavirus Disease 2019 (COVID-19)*. Retrieved December 22, 2020, from https://www.cdc.gov/coronavirus/2019-ncov/more/scientific-brief-sars-cov-2.html

Dai, H., & Zhao, B. (2020). Association of infected probability of COVID-19 with ventilation rates in confined spaces: a Wells-Riley equation based investigation. *MedRxiv*. https://doi.org/10.1101/2020.04.21.20072397

Doroszkowski, A. (1999). Particle size and size measurement. In *Paint and Surface Coatings* (pp. 243-285). Woodhead Publishing. https://doi.org/10.1533/9781855737006.243

Dräger. (2020a, April 1). *[Dräger Oxylog® 3000 plus]*. Retrieved March 16, 2021, from https://www.draeger.com/Products/Media/Draeger-Oxylog-3000-plus.jpg?imwidth=1280

Dräger. (2020b, November 7). *Dräger Oxylog® 3000 plus Emergency & Transport Ventilation*. Retrieved December 14, 2020, from https://www.draeger.com/Products/Content/oxylog-3000-plus-pi-9066205-en-master-1604-4.pdf

จุฬาลงกรณ์มหาวิทยาลัย
Chulalongkorn University

Eiche, T., & Kuster, M. (2020). Aerosol release by healthy people during speaking: possible contribution to the transmission of SARS-CoV-2. *International Journal of Environmental Research and Public Health*, *17*(23), 9088. https://doi.org/10.3390/ijerph17239088

Escombe, A. R., Oeser, C. C., Gilman, R. H., Navincopa, M., Ticona, E., Pan, W., Martínez, C., Chacaltana, J., Rodríguez, R., & Moore, D. A. (2007). Natural ventilation for the prevention of airborne contagion. *PLoS Med*, *4*(2), e68. https://doi.org/10.1371/journal.pmed.0040068

Fernstrom, A., & Goldblatt, M. (2013). Aerobiology and its role in the transmission of infectious diseases. *J Pathog*, *2013*, 493960. https://doi.org/10.1155/2013/493960

Gibson, C. V. (2019). Emergency medical services oxygen equipment: a fomite for transmission of MRSA? *Emergency medicine journal*, *36*(2), 89-91. https://doi.org/10.1136/emermed-2018-207758

Gralton, J., Tovey, E., McLaws, M. L., & Rawlinson, W. D. (2011). The role of particle size in aerosolised pathogen transmission: a review. *J Infect*, *62*(1), 1-13. https://doi.org/10.1016/j.jinf.2010.11.010

Gralton, J., Tovey, E. R., McLaws, M. L., & Rawlinson, W. D. (2013). Respiratory virus RNA is detectable in airborne and droplet particles. *J Med Virol*, *85*(12), 2151-2159. https://doi.org/10.1002/jmv.23698

Gupta, J. K., Lin, C. H., & Chen, Q. (2010). Characterizing exhaled airflow from breathing and talking. *International Journal of Indoor Environment and Health*, *20*(1), 31-39. https://doi.org/10.1111/j.1600-0668.2009.00623.x

Herrmann, H., Wiesen, P., Zellner, R., & Zetzsch, C. (2020). Covid-19 and the Role of Particles - Statement of the Working Committee Particulate Matter (AAF) of DECHEMA/ProcessNet, GDCh and KRdL.

Hudson, A. J., Glaister, G. D., & Wieden, H.-J. (2018). The emergency medical service microbiome. *Applied and environmental microbiology*, *84*(5). https://doi.org/10.1128/AEM.02098-17

Jeju Tourism Organization. (2020, October 28). *[Isolation Tent]*. Retrieved February 10, 2021, from https://jejutourism.wordpress.com/2020/10/28/notice-6-new-negative-pressure-ambulances-take-to-jejus-streets/

จุฬาลงกรณ์มหาวิทยาลัย
Chulalongkorn University

Jurelionis, A., Gagyte, L., Prasauskas, T., Čiužas, D., Krugly, E., Šeduikyte, L., & Martuzevičius, D. (2015). The impact of the air distribution method in ventilated rooms on the aerosol particle dispersion and removal: The experimental approach. *Energy and Buildings*, *86*, 305-313. https://doi.org/10.1016/j.enbuild.2014.10.014

King, J. (2020, March 26). *[Finger Prick]*. Retrieved January 12, 2021, from https://www.thetimes.co.uk/article/home-coronavirus-antibody-test-for-millions-through-amazon-mvxwpxplf

Knight, V. (1980). Viruses as agents of airborne contagion. *Annals of the New York Academy of Sciences*, *353*(1), 147-156. https://doi.org/10.1111/j.1749-6632.1980.tb18917.x

Kutter, J. S., Spronken, M. I., Fraaij, P. L., Fouchier, R. A., & Herfst, S. (2018). Transmission routes of respiratory viruses among humans. *Current Opinion in Virology*, *28*, 142-151. https://doi.org/10.1016/j.coviro.2018.01.001

Kwon, S., Lim, K., Jung, J., Bae, G., & Lee, K. (2003). Design and calibration of a 5-stage cascade impactor (K-JIST cascade impactor). *Journal of aerosol science*, *34*(3), 289-300. https://doi.org/10.1016/S0021-8502(02)00177-5

Le, V., Thi, T. H., Robins, E., & Flament, M. P. (2012). Dry powder inhalers: study of the parameters influencing adhesion and dispersion of fluticasone propionate. *Aaps Pharmscitech*, *13*(2), 477-484. https://doi.org/10.1208/s12249-012-9765-8

Lighthouse Worldwide Solutions. (2018, November 7). *Technical Datasheet Handheld Particle Counters*. Retrieved December 14, 2020, from https://www.golighthouse.com/media/files/product/Handheld_Datasheet_2016_3016_3016IAQ_5016.pdf

Lighthouse Worldwide Solutions. (2019, March 15). *[Handheld 3016]*. Retrieved March 16, 2021, from https://www.golighthouse.com/media/cache/b_HandHeld-3016.jpg

Lindsley, W. G., Blachere, F. M., McClelland, T. L., Neu, D. T., Mnatsakanova, A., Martin Jr, S. B., Mead, K. R., & Noti, J. D. (2019). Efficacy of an ambulance ventilation system in reducing EMS worker exposure to airborne particles from a patient cough aerosol simulator. *Journal of occupational and environmental hygiene*,

จุฬาลงกรณ์มหาวิทยาลัย
Chulalongkorn University

16(12), 804-816. https://doi.org/10.1080/15459624.2019.1674858

Lindsley, W. G., Noti, J. D., Blachere, F. M., Szalajda, J. V., & Beezhold, D. H. (2014). Efficacy of face shields against cough aerosol droplets from a cough simulator. *Journal of occupational and environmental hygiene*, *11*(8), 509-518. https://doi.org/10.1080/15459624.2013.877591

Lindsley, W. G., Reynolds, J. S., Szalajda, J. V., Noti, J. D., & Beezhold, D. H. (2013). A cough aerosol simulator for the study of disease transmission by human cough-generated aerosols. *Aerosol Science and Technology*, *47*(8), 937-944. https://doi.org/10.1080/02786826.2013.803019

Liu, L., Li, Y., Nielsen, P. V., Wei, J., & Jensen, R. L. (2017). Short-range airborne transmission of expiratory droplets between two people. *International Journal of Indoor Environment and Health*, *27*(2), 452-462. https://doi.org/10.1111/ina.12314

Liu, L., Wei, J., Li, Y., & Ooi, A. (2017). Evaporation and dispersion of respiratory droplets from coughing. *International Journal of Indoor Environment and Health*, *27*(1), 179-190. https://doi.org/10.1111/ina.12297

Magyc Now. (2019, October 12). *Arduino Uno SMD Rev3* Retrieved December 14, 2020, from https://docs.rs-online.com/d7b4/0900766b811af13a.pdf

Medplan. (2021, March 16). *[Aeroneb Pro nebulizer]*. Retrieved March 16, 2021, from http://www.medplan.hu/en/AeronebProEN

Merkus, H. G. (2009). Sedimentation Techniques. In *Particle Size Measurements* (pp. 319-348). Springer.

National Direct Network. (2020, January 24). *[Vertical Laminar Flow Cleanroom]*. Retrieved March 26, 2021, from http://ndn.co.th/image/clean_room/Clean%20room%20vertical%20flow.gif

Neoteryx. (2020, August 17). *[Blood Draw]*. Retrieved December 15, 2020, from https://www.neoteryx.com/hs-fs/hubfs/blood%20draw%20for%20an%20immunosuppressive%20therapy%20blood%20test.jpg?width=1800&name=blood%20draw%20for%20an%20immunosuppressive%20therapy%20blood%20test.jpg

Pipitsangjan, S., Luksamijarulkul, P., Sujirarat, D., & Vatanasomboon, P. (2011). Risk

จุฬาลงกรณ์มหาวิทยาลัย
Chulalongkorn University

assessment towards droplet and airborne infections among ambulance personnel in a province of northeastern Thailand. *Asia J Public Health*, *2*(1), 20-26.

Plane Boi. (2019, December 5). *[Ambulance]*. Retrieved March 26, 2021, from https://www.flickr.com/photos/164597013@N04/49172241048

Plantower. (2017, September 15). *Digital universal particle concentration sensor PMS5003 series data manual*. Retrieved December 14, 2020, from https://www.aqmd.gov/docs/default-source/aq-spec/resources-page/plantower-pms5003-manual_v2-3.pdf

Ruvii Vehicle. (2020). *[Negative Pressure Ambulance]*. Retrieved February 20, 2021, from http://www.ruviivehicle.com/products/negative-pressure-ambulance/

Sayed, M. E., Kue, R., McNeil, C., & Dyer, K. S. (2011). A descriptive analysis of occupational health exposures in an urban emergency medical services system: 2007–2009. *Prehospital emergency care*, *15*(4), 506-510. https://doi.org/10.3109/10903127.2011.598608

Siegel, J. D., Rhinehart, E., Jackson, M., & Chiarello, L. (2007). 2007 guideline for isolation precautions: preventing transmission of infectious agents in health care settings. *American journal of infection control*, *35*(10), S65-S164.

Sympatec GmbH. (2017, May 24). *[Laser Diffraction]*. Retrieved January 17, 2021, from https://www.sympatec.com/fileadmin/_processed_/8/8/csm_Laserbeugung_OptischerAufbau_EN_362fa170f5.png

Thomas, R. J. (2013). Particle size and pathogenicity in the respiratory tract. *Virulence*, *4*(8), 847-858. https://doi.org/10.4161/viru.27172

Variddhi Ungbhakorn. (2012). *Cleanroom design manual*. The Engineering Institute of Thailand under H.M. the King's Patronage.

Verras, M. (2021, January 17). *[3D illustration of the size comparison of giant viruses to other common viruses and bacteria]*. Retrieved March 15, 2021, from https://www.shutterstock.com/th/image-illustration/3d-illustration-size-comparison-giant-viruses-720441124

Visual Capitalist. (2020, October 10). *The Relative Size of Particles*. Retrieved March 16, 2021, from https://www.visualcapitalist.com/visualizing-relative-size-of-particles/

จุฬาลงกรณ์มหาวิทยาลัย
Chulalongkorn University

Willeke, K., Qian, Y., Donnelly, J., Grinshpun, S., & Ulevicius, V. (1996). Penetration of airborne microorganisms through a surgical mask and a dust/mist respirator. *American Industrial Hygiene Association Journal*, *57*(4), 348-355. https://doi.org/10.1080/15428119691014882

Wonderlich, E. R., Swan, Z. D., Bissel, S. J., Hartman, A. L., Carney, J. P., O'Malley, K. J., Obadan, A. O., Santos, J., Walker, R., Sturgeon, T. J., Frye, L. J., Jr., Maiello, P., Scanga, C. A., Bowling, J. D., Bouwer, A. L., Duangkhae, P. A., Wiley, C. A., Flynn, J. L., Wang, J., Cole, K. S., Perez, D. R., Reed, D. S., & Barratt-Boyes, S. M. (2017). Widespread Virus Replication in Alveoli Drives Acute Respiratory Distress Syndrome in Aerosolized H5N1 Influenza Infection of Macaques. *J Immunol*, *198*(4), 1616-1626. https://doi.org/10.4049/jimmunol.1601770

World Health Organization. (2014). *Infection prevention and control of epidemic-and pandemic-prone acute respiratory infections in health care*. World Health Organization.

Worldometer. (2021a, March 15). *COVID-19 Coronavirus Pandemic*. Retrieved March 15, 2021, from https://www.worldometers.info/coronavirus/

Worldometer. (2021b, March 15). *COVID-19 Coronavirus Pandemic: United States*. Retrieved March 15, 2021, from https://www.worldometers.info/coronavirus/country/us/

Worldometer. (2021c, March 15). *COVID-19 Coronavirus Pandemic: China*. Retrieved March 15, 2021, from https://www.worldometers.info/coronavirus/country/china/

Worldometer. (2021d, March 15). *COVID-19 Coronavirus Pandemic: Thailand*. Retrieved March 15, 2021, from https://www.worldometers.info/coronavirus/country/thailand/

Xinhuanet. (2020, February 17). *[SAIC Motor Co., Ltd. Ambulances Construction]*. Retrieved February 20, 2021, from http://www.xinhuanet.com/english/2020-02/17/c_138789610_2.htm

Yali, R., Jiandong, M., Hu, Z., Chunyan, Z., Xin, G., Zhimin, R., Qiang, W., & Yi, Z. (2020). Prediction of aerosol particle size distribution based on neural network. *Advances in Meteorology*. https://doi.org/10.1155/2020/5074192

จุฬาลงกรณ์มหาวิทยาลัย
Chulalongkorn University

Yang, C., Yang, X., & Zhao, B. (2015). The ventilation needed to control thermal plume and particle dispersion from manikins in a unidirectional ventilated protective isolation room. *Building Simulation*, *8*(5), 551-565. https://doi.org/10.1007/s12273-014-0227-6

Zuo, Z., Kuehn, T. H., Verma, H., Kumar, S., Goyal, S. M., Appert, J., Raynor, P. C., Ge, S., & Pui, D. Y. (2013). Association of airborne virus infectivity and survivability with its carrier particle size. *Aerosol Science and Technology*, *47*(4), 373-382. https://doi.org/10.1080/02786826.2012.754841

จุฬาลงกรณ์มหาวิทยาลัย
CHULALONGKORN UNIVERSITY

APPENDICES

จุฬาลงกรณ์มหาวิทยาลัย
Chulalongkorn University

APPENDIX A

PMS5003 WIRING DIAGRAM FOR PRELIMINARY EXPERIMENT (ACTIVE MODE)

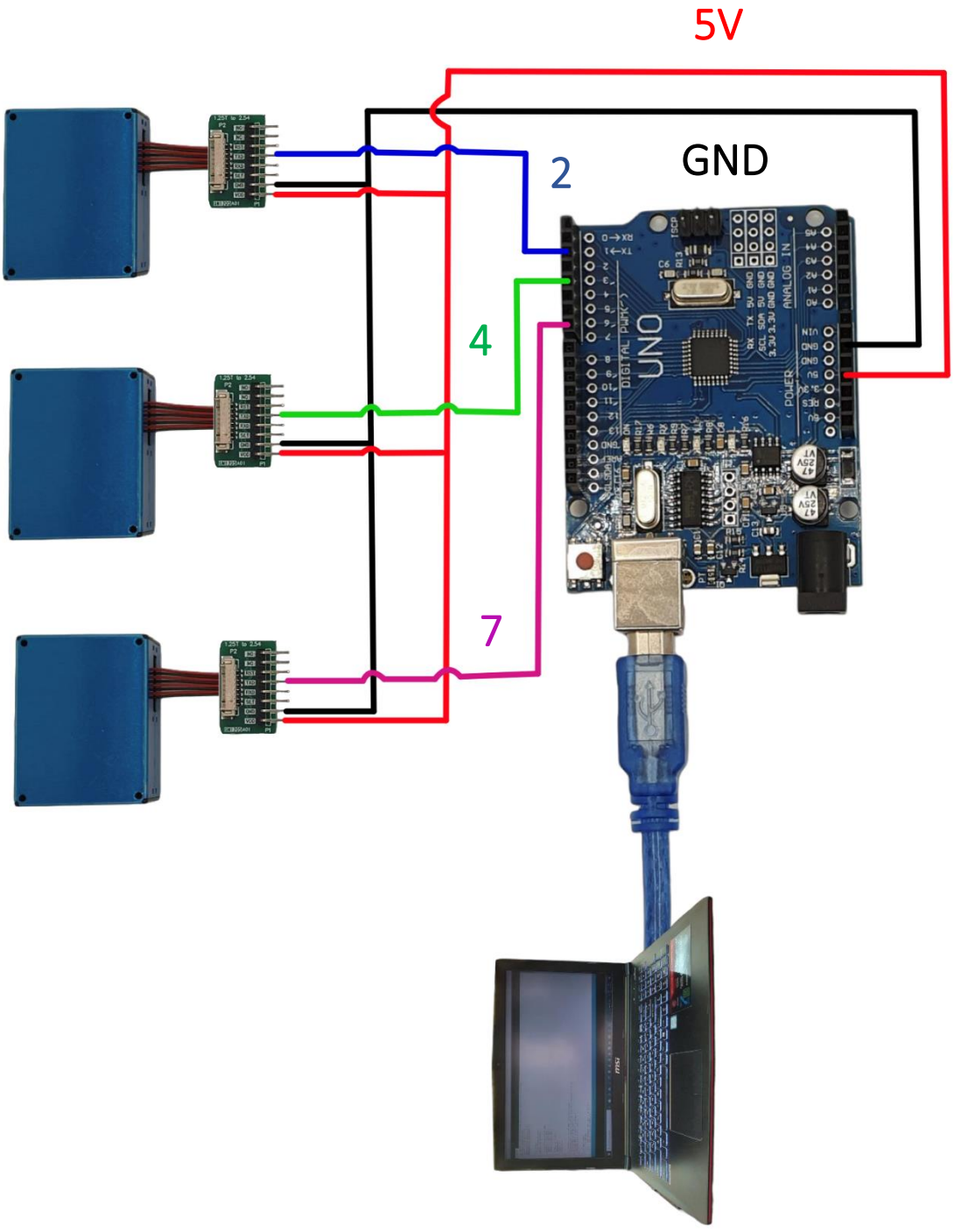

APPENDIX B

CODE FOR PMS5003 (ACTIVE MODE)

Line	Code
1	#include <SoftwareSerial.h>
2	SoftwareSerial pmsSerial0(2,3);
3	SoftwareSerial pmsSerial1(4,5);
4	SoftwareSerial pmsSerial2(7,6);
5	void setup() {
6	Serial.begin(115200);
7	pmsSerial0.begin(9600);
8	pmsSerial1.begin(9600);
9	pmsSerial2.begin(9600);
10	pinMode(11, OUTPUT);
11	beep(50,20);
12	beep(50,20);
13	delay(1000);
14	}
15	void beep(unsigned char delayms, unsigned char power) {
16	analogWrite(11, power);
17	delay(delayms);
18	analogWrite(11, 0);
19	}
20	struct pms5003data {
21	uint16_t framelen;
22	uint16_t pm10_standard, pm25_standard, pm100_standard;
23	uint16_t pm10_env, pm25_env, pm100_env;
24	uint16_t particles_03um, particles_05um, particles_10um,
25	particles_25um,particles_50um, particles_100um;
26	uint16_t unused;
27	uint16_t checksum;
28	};
29	struct pms5003data data;
30	void loop() {
31	pmsSerial0.listen();
32	delay(1000);
33	if (readPMSdata(&pmsSerial0)) {

จุฬาลงกรณ์มหาวิทยาลัย
Chulalongkorn University

```
34      long time = millis();
35      float HH03 = (data.particles_03um/0.1)*(1000/35.3147);
36      float HH05 = (data.particles_05um/0.1)*(1000/35.3147);
37      float HH10 = (data.particles_10um/0.1)*(1000/35.3147);
38      float HH25 = (data.particles_25um/0.1)*(1000/35.3147);
39      float HH50 = (data.particles_50um/0.1)*(1000/35.3147);
40      float HH100 = (data.particles_100um/0.1)*(1000/35.3147);
41      Serial.print("pmsSerial0 ");
42      Serial.print(time);Serial.print(" ");Serial.print(HH03,0);
43      Serial.print(" ");Serial.print(HH05,0);Serial.print(" ");
44      Serial.print(HH10,0);Serial.print(" ");Serial.print(HH25,0);
45      Serial.print(" ");Serial.print(HH50,0);Serial.print(" ");
46      Serial.print(HH100,0);Serial.print(" ");
47      if (data.particles_25um > 50)
48      {
49        if(data.particles_25um < 255)
50        {
51          beep(data.particles_25um,data.particles_25um);
52        }
53        else{
54          beep(255,255);
55        }
56      }
57    }
58
59    pmsSerial1.listen();
60    delay(1000);
61    if (readPMSdata(&pmsSerial1)) {
62      long time = millis();
63      float HH03 = (data.particles_03um/0.1)*(1000/35.3147);
64      float HH05 = (data.particles_05um/0.1)*(1000/35.3147);
65      float HH10 = (data.particles_10um/0.1)*(1000/35.3147);
66      float HH25 = (data.particles_25um/0.1)*(1000/35.3147);
67      float HH50 = (data.particles_50um/0.1)*(1000/35.3147);
68      float HH100 = (data.particles_100um/0.1)*(1000/35.3147);
69      Serial.print("pmsSerial1 ");
70      Serial.print(time);Serial.print(" ");Serial.print(HH03,0);
71      Serial.print(" ");Serial.print(HH05,0);Serial.print(" ");
```

จุฬาลงกรณ์มหาวิทยาลัย
Chulalongkorn University

```
72      Serial.print(HH10,0);Serial.print(" ");Serial.print(HH25,0);
73      Serial.print(" ");Serial.print(HH50,0);Serial.print(" ");
74      Serial.print(HH100,0);Serial.print(" ");
75      if (data.particles_25um > 50)
76      {
77        if(data.particles_25um < 255)
78        {
79          beep(data.particles_25um,data.particles_25um);
80        }
81        else{
82          beep(255,255);
83        }
84      }
85    }
86
87    pmsSerial2.listen();
88    delay(1000);
89    if (readPMSdata(&pmsSerial2)) {
90      long time = millis();
91      float HH03 = (data.particles_03um/0.1)*(1000/35.3147);
92      float HH05 = (data.particles_05um/0.1)*(1000/35.3147);
93      float HH10 = (data.particles_10um/0.1)*(1000/35.3147);
94      float HH25 = (data.particles_25um/0.1)*(1000/35.3147);
95      float HH50 = (data.particles_50um/0.1)*(1000/35.3147);
96      float HH100 = (data.particles_100um/0.1)*(1000/35.3147);
97      Serial.print("pmsSerial2 ");
98      Serial.print(time);Serial.print(" ");Serial.print(HH03,0);
99      Serial.print(" ");Serial.print(HH05,0);Serial.print(" ");
100     Serial.print(HH10,0);Serial.print(" ");Serial.print(HH25,0);
101     Serial.print(" ");Serial.print(HH50,0);Serial.print(" ");
102     Serial.println(HH100,0);
103     if (data.particles_25um > 50)
104     {
105       if(data.particles_25um < 255)
106       {
107         beep(data.particles_25um,data.particles_25um);
108       }
109       else{
```

จุฬาลงกรณ์มหาวิทยาลัย
Chulalongkorn University

```
110           beep(255,255);
111         }
112       }
113     }
114   }
115   boolean readPMSdata(Stream *s) {
116     if (! s->available()) {
117       return false;
118     }
119     if (s->peek() != 0x42) {
120       s->read();
121       return false;
122     }
123     if (s->available() < 32) {
124       return false;
125     }
126     uint8_t buffer[32];
127     uint16_t sum = 0;
128     s->readBytes(buffer, 32);
129     for (uint8_t i = 0; i < 30; i++) {
130       sum += buffer[i];
131     }
132     uint16_t buffer_u16[15];
133     for (uint8_t i = 0; i < 15; i++) {
134       buffer_u16[i] = buffer[2 + i * 2 + 1];
135       buffer_u16[i] += (buffer[2 + i * 2] << 8);
136     }
137     memcpy((void *)&data, (void *)buffer_u16, 30);
138     if (sum != data.checksum) {
139       Serial.println("Checksum failure");
140       return false;
141     }
142     return true;
143   }
```

จุฬาลงกรณ์มหาวิทยาลัย
Chulalongkorn University

APPENDIX C

PMS5003 WIRING DIAGRAM (PASSIVE MODE)

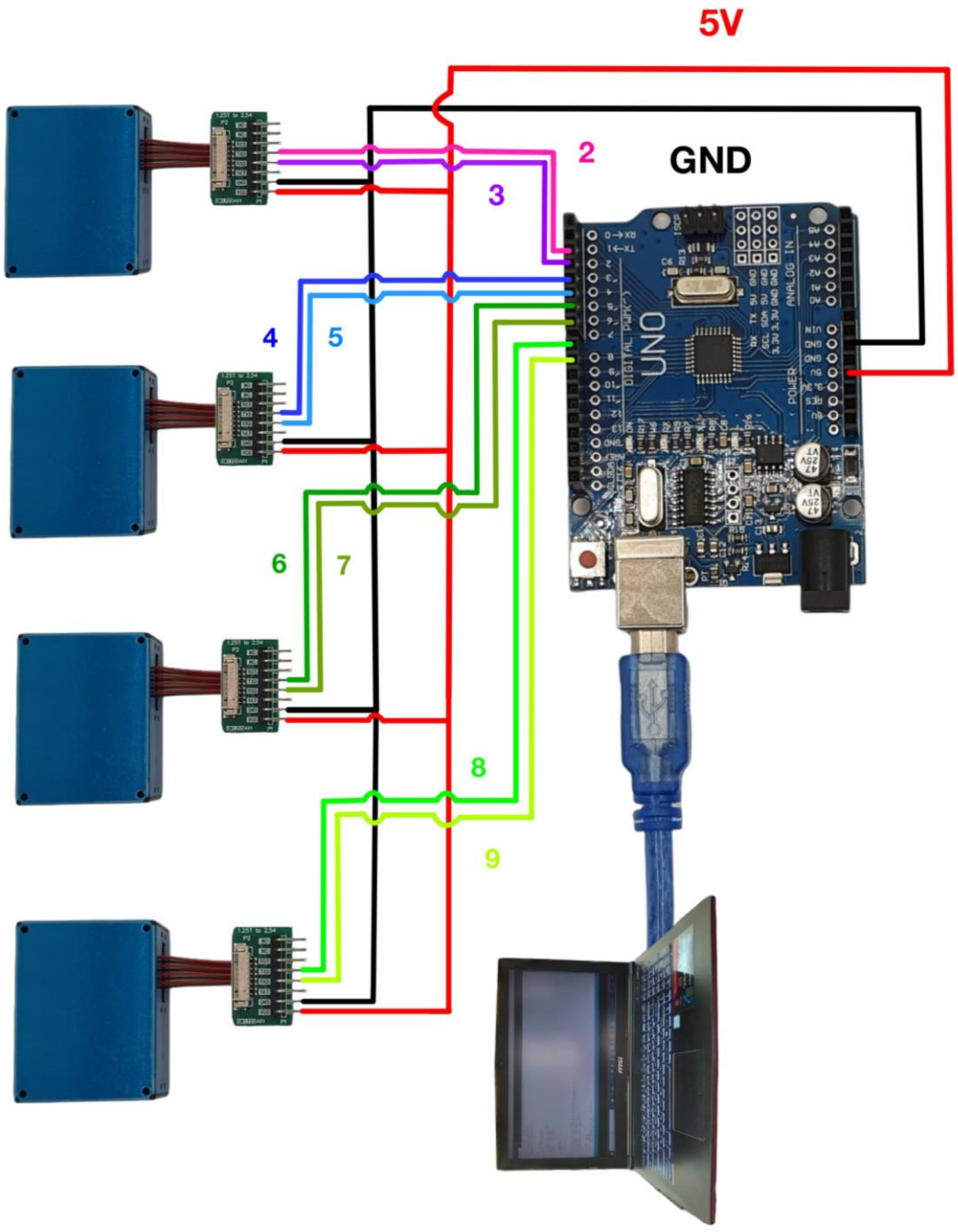

APPENDIX D

CODE FOR PMS5003 (PASSIVE MODE)

Line	Code
1	#include <SoftwareSerial.h>
2	SoftwareSerial pmsSerial1(2,3);
3	SoftwareSerial pmsSerial2(4,5);
4	SoftwareSerial pmsSerial3(6,7);
5	SoftwareSerial pmsSerial4(8,9);
6	int wait_for_sensor_read_ms = 50;
7	void set_passive_mode(Stream *s) {
8	uint8_t cmd[] = { 0x42, 0x4D, 0xE1, 0x00, 0x00, 0x01, 0x70 };
9	s->write(cmd, sizeof(cmd));
10	}
11	void init_sensor(SoftwareSerial *s) {
12	// sensor baud rate is 9600
13	s->begin(9600);
14	set_passive_mode(s);
15	}
16	void setup() {
17	Serial.begin(115200);
18	init_sensor(&pmsSerial1);
19	init_sensor(&pmsSerial2);
20	init_sensor(&pmsSerial3);
21	init_sensor(&pmsSerial4);
22	init_sensor(&pmsSerial5);
23	Serial.println("name,time,0.5-1micron,1-2.5micron,2.5-5micron");
24	delay(1000);
25	}
26	struct pms5003data {
27	uint16_t framelen;
28	uint16_t pm10_standard, pm25_standard, pm100_standard;
29	uint16_t pm10_env, pm25_env, pm100_env;
30	uint16_t particles_03um, particles_05um, particles_10um,
31	particles_25um, particles_50um, particles_100um;
32	uint16_t unused;
33	uint16_t checksum;

จุฬาลงกรณ์มหาวิทยาลัย
Chulalongkorn University

```
};
struct pms5003data data;
void loop() {
  readPMSdata(&pmsSerial1, "Sensor 1");
  readPMSdata(&pmsSerial2, "Sensor 2");
  readPMSdata(&pmsSerial3, "Sensor 3");
  readPMSdata(&pmsSerial4, "Sensor 4");
  Serial.println();
}
void send_passive_read_cmd(Stream *s) {
  uint8_t command[] = { 0x42, 0x4D, 0xE2, 0x00, 0x00, 0x01, 0x71 };
  s->write(command, sizeof(command));
}
boolean readPMSdata(SoftwareSerial *s, String name) {
  s->listen();
  send_passive_read_cmd(s);
  delay(wait_for_sensor_read_ms);
  bool is_err = false;
  if (! s->available()) {
    is_err = true;
  }
  if (!is_err && s->peek() != 0x42) {
    s->read();
    is_err = true;
  }
  if (!is_err && s->available() < 32) {
    is_err = true;
  }
  if (!is_err) {
    uint8_t buffer[32];
    uint16_t sum = 0;
    s->readBytes(buffer, 32);
    for (uint8_t i = 0; i < 30; i++) {
      sum += buffer[i];
    }
    uint16_t buffer_u16[15];
    for (uint8_t i = 0; i < 15; i++) {
      buffer_u16[i] = buffer[2 + i * 2 + 1];
```

จุฬาลงกรณ์มหาวิทยาลัย
Chulalongkorn University

```
72        buffer_u16[i] += (buffer[2 + i * 2] << 8);
73      }
74      size_t data_size = 30;
75      memcpy((void *)&data, (void *)buffer_u16, data_size);
76      if (sum != data.checksum) {
77        is_err = true;
78      }
79    }
80    if (is_err) {
81      logError(name);
82    } else {
83      logResult(name);
84    }
85  }
86  void logResult(String name) {
87      long time = millis()-1000;
88      float HH05 = (data.particles_05um/0.1)*(1000/35.3147);
89      float HH10 = (data.particles_10um/0.1)*(1000/35.3147);
90      float HH25 = (data.particles_25um/0.1)*(1000/35.3147);
91      float HH50 = (data.particles_50um/0.1)*(1000/35.3147);
92      float pms05_10 = HH05 - HH10;
93      float pms10_25 = HH10 - HH25;
94      float pms25_50 = HH25 - HH50;
95      float pms05_10_cal;
96      float pms10_25_cal;
97      float pms25_50_cal;
98      float pi = 3.14159265358979323846264338327 95;
99      Serial.print(name + ",");
100     Serial.print(time);Serial.print(",");
101     Serial.print(pms05_10,0);Serial.print(",");
102     Serial.print(pms10_25,0);Serial.print(",");
103     Serial.print(pms25_50,0);Serial.print(",");
104 }
105 void logError(String name) {
106     long time = millis()-1000;
107     Serial.print(name + ",");
108     Serial.print(time);Serial.print(",");
109     Serial.print("null,");
```

จุฬาลงกรณ์มหาวิทยาลัย
Chulalongkorn University

```
110         Serial.print("null,");
111         Serial.print("null,");
112     }
```


จุฬาลงกรณ์มหาวิทยาลัย
Chulalongkorn University

APPENDIX E

PYTHON CODE FOR CALIBRATION AND CONVERSION

Line	Code
1	import pandas as pd
2	import numpy as np
3	File1 = "Filename1"
4	File2 = "Filename1"
5	File3 = "Filename1"
6	df1 = pd.read_csv("Filepath/" + str(File1) + ".csv")
7	df2 = pd.read_csv("Filepath/" + str(File2) + ".csv")
8	df3 = pd.read_csv("Filepath/" + str(File3) + ".csv")
9	column_names = ['time','0.5-1micron','1-2.5micron','2.5-5micron']
10	df1.columns = column_names
11	df2.columns = column_names
12	df3.columns = column_names
13	for i in range(len(df1)):
14	if df1.loc[i, '0.5-1micron'] >= 258249:
15	df1.loc[i, '0.5-1micron'] = round(0.32908 * (df1.loc[i, '0.5-1micron']) ** 1.1734)
16	else:
17	df1.loc[i, '0.5-1micron'] = round(10**(-18) * (df1.loc[i, '0.5-1micron']) ** 4.4101)
18	if df1.loc[i, '1-2.5micron'] >= 172166:
19	df1.loc[i, '1-2.5micron'] = round(1.0491 * (df1.loc[i, '1-2.5micron']) ** 1.0239)
20	else:
21	df1.loc[i, '1-2.5micron'] = round(0.00017783 * (df1.loc[i, '1-2.5micron']) ** 1.7441)
22	if df1.loc[i, '2.5-5micron'] >= 5664:
23	df1.loc[i, '2.5-5micron'] = round(0.4794 * (df1.loc[i, '2.5-5micron']) ** 1.1733)
24	else:
25	df1.loc[i, '2.5-5micron'] = round(19.9526 * (df1.loc[i, '2.5-5micron']) ** 0.74185)
26	if df2.loc[i, '0.5-1micron'] >= 258249:
27	df2.loc[i, '0.5-1micron'] = round(0.32908 * (df2.loc[i, '0.5-1micron']) ** 1.1734)
28	else:
29	df2.loc[i, '0.5-1micron'] = round(10**(-18) * (df2.loc[i, '0.5-1micron']) ** 4.4101)
30	if df2.loc[i, '1-2.5micron'] >= 172166:
31	df2.loc[i, '1-2.5micron'] = round(1.0491 * (df2.loc[i, '1-2.5micron']) ** 1.0239)
32	else:
33	df2.loc[i, '1-2.5micron'] = round(0.00017783 * (df2.loc[i, '1-2.5micron']) ** 1.7441)

จุฬาลงกรณ์มหาวิทยาลัย
Chulalongkorn University

```
    if df2.loc[i, '2.5-5micron'] >= 5664:
        df2.loc[i, '2.5-5micron'] = round(0.4794 * (df2.loc[i, '2.5-5micron']) ** 1.1733)
    else:
        df2.loc[i, '2.5-5micron'] = round(19.9526 * (df2.loc[i, '2.5-5micron']) ** 0.74185)
    if df3.loc[i, '0.5-1micron'] >= 258249:
        df3.loc[i, '0.5-1micron'] = round(0.32908 * (df3.loc[i, '0.5-1micron']) ** 1.1734)
    else:
        df3.loc[i, '0.5-1micron'] = round(10**(-18) * (df3.loc[i, '0.5-1micron']) ** 4.4101)
    if df3.loc[i, '1-2.5micron'] >= 172166:
        df3.loc[i, '1-2.5micron'] = round(1.0491 * (df3.loc[i, '1-2.5micron']) ** 1.0239)
    else:
        df3.loc[i, '1-2.5micron'] = round(0.00017783 * (df3.loc[i, '1-2.5micron']) ** 1.7441)
    if df3.loc[i, '2.5-5micron'] >= 5664:
        df3.loc[i, '2.5-5micron'] = round(0.4794 * (df3.loc[i, '2.5-5micron']) ** 1.1733)
    else:
        df3.loc[i, '2.5-5micron'] = round(19.9526 * (df3.loc[i, '2.5-5micron']) ** 0.74185)
df1.to_csv("Filepath/" + str(File1) + "_cal.csv", index = False)
df2.to_csv("Filepath/" + str(File2) + "_cal.csv", index = False)
df3.to_csv("Filepath/" + str(File3) + "_cal.csv", index = False)
for i in range(len(df1)):
    df1.loc[i, '0.5-1micron_conc'] = 4.70859672 * 10**(-8) * df1.loc[i, '0.5-1micron'] * np.pi * (((0.5+1)/2)/2)**(3)
    df1.loc[i, '1-2.5micron_conc'] = 4.70859672 * 10**(-8) * df1.loc[i, '1-2.5micron'] * np.pi * (((1+2.5)/2)/2)**(3)
    df1.loc[i, '2.5-5micron_conc'] = 4.70859672 * 10**(-8) * df1.loc[i, '2.5-5micron'] * np.pi * (((2.5+5)/2)/2)**(3)
    df2.loc[i, '0.5-1micron_conc'] = 4.70859672 * 10**(-8) * df2.loc[i, '0.5-1micron'] * np.pi * (((0.5+1)/2)/2)**(3)
    df2.loc[i, '1-2.5micron_conc'] = 4.70859672 * 10**(-8) * df2.loc[i, '1-2.5micron'] * np.pi * (((1+2.5)/2)/2)**(3)
    df2.loc[i, '2.5-5micron_conc'] = 4.70859672 * 10**(-8) * df2.loc[i, '2.5-5micron'] * np.pi * (((2.5+5)/2)/2)**(3)
    df3.loc[i, '0.5-1micron_conc'] = 4.70859672 * 10**(-8) * df3.loc[i, '0.5-1micron'] * np.pi * (((0.5+1)/2)/2)**(3)
    df3.loc[i, '1-2.5micron_conc'] = 4.70859672 * 10**(-8) * df3.loc[i, '1-2.5micron'] * np.pi * (((1+2.5)/2)/2)**(3)
    df3.loc[i, '2.5-5micron_conc'] = 4.70859672 * 10**(-8) * df3.loc[i, '2.5-5micron'] * np.pi * (((2.5+5)/2)/2)**(3)
```

จุฬาลงกรณ์มหาวิทยาลัย
Chulalongkorn University

```
63  df1.to_csv("Filepath/" + str(File1) + "_cal_conc.csv", index = False)
64  df2.to_csv("Filepath/" + str(File2) + "_cal_conc.csv", index = False)
65  df3.to_csv("Filepath/" + str(File3) + "_cal_conc.csv", index = False)
```


จุฬาลงกรณ์มหาวิทยาลัย
Chulalongkorn University

APPENDIX F

PYTHON CODE FOR CUBIC SPLINE INTERPOLATION

Line	Code
1	from scipy.interpolate import interp1d
2	import pandas as pd
3	import numpy as np
4	Filename = "Filename"
5	df = pd.read_csv("Filepath/" + str(Filename) + "_avg_conc.csv")
6	w = np.array(df["time"])
7	x = np.array(df["0.5-1micron_conc"])
8	y = np.array(df["1-2.5micron_conc"])
9	z = np.array(df["2.5-5micron_conc"])
10	w = np.insert(w,0,0)
11	x = np.insert(x,0,x[0])
12	y = np.insert(y,0,y[0])
13	z = np.insert(z,0,z[0])
14	f1 = interp1d(w, x, kind='cubic')
15	f2 = interp1d(w, y, kind='cubic')
16	f3 = interp1d(w, z, kind='cubic')
17	w_new = np.arange(0, 1200250, 250) #for minimal ventilation
18	# w_new = np.arange(0, 600250, 250) #for high ventilation
19	rows = []
20	# for i in np.arange(0, 600250, 250): #for high ventilation
21	for i in np.arange(0, 1200250, 250): #for minimal ventilation
22	row = []
23	for j in range(1):
24	row.append(f1(i).tolist())
25	row.append(f2(i).tolist())
26	row.append(f3(i).tolist())
27	rows.append(row)
28	useful_cols = ['0.5-1micron_conc','1-2.5micron_conc','2.5-5micron_conc']
29	df_final = pd.DataFrame(rows, columns = useful_cols)
30	df_final['time'] = (w_new).tolist()
31	df_final = df_final[['time','0.5-1micron_conc','1-2.5micron_conc','2.5-5micron_conc']]
32	df_final.to_csv("Filepath/" + str(Filename) + "_avg_conc_cubic_spline.csv", index = False)

จุฬาลงกรณ์มหาวิทยาลัย
Chulalongkorn University

APPENDIX G

PYTHON CODE FOR WINDOW MOVING AVERAGE

Line	Code
1	import pandas as pd
2	Filename = "Filename"
3	df = pd.read_csv("Filepath/" + str(Filename) + ".csv")
4	wa_cols = ['time_wa', '0.5-1micron_conc_wa', '1-2.5micron_conc_wa', '2.5-5micron_conc_wa']
5	window = 5
6	for j in range(0,len(df.columns)):
7	for i in range(0,len(df)-(window-1)):
8	n = 0
9	lst = []
10	for x in range(0,window):
11	sum_ = 0
12	n = n + 1 if df.iloc[i+x, j] != 0 else n
13	lst.append(df.iloc[i+x, j])
14	if n == 0:
15	df.loc[df.index[i+(window-1)], wa_cols[j]] = 0
16	else:
17	sum_ += sum(lst)
18	df.loc[df.index[i+(window-1)], wa_cols[j]] = sum_/n
19	df = df.fillna(0)
20	df.iloc[df.index[window-1],df.index[4]] = 250*(window+1)/2-250
21	for z in range(int((window-1)/2),(window-1)):
22	df.iloc[z, 4] = df.iloc[z-int((window-1)/2), 0]
23	df.iloc[z, 5] = df.iloc[z, 1]
24	df.iloc[z, 6] = df.iloc[z, 2]
25	df.iloc[z, 7] = df.iloc[z, 3]
26	for v in range(len(df),len(df)+int((window-1)/2)):
27	df.loc[v, 'time_wa'] = df.iloc[v-int((window-1)/2), 0]
28	df.loc[v, '0.5-1micron_conc_wa'] = df.iloc[v-int((window-1)/2), 1]
29	df.loc[v, '1-2.5micron_conc_wa'] = df.iloc[v-int((window-1)/2), 2]
30	df.loc[v, '2.5-5micron_conc_wa'] = df.iloc[v-int((window-1)/2), 3]
31	df1 = df[wa_cols]
32	df1.iloc[int((window-1)/2):len(df)+int((window-1)/2)].to_csv("Filepath/" + str(Filename) + "_avg_conc_wa5.csv", index = False)

จุฬาลงกรณ์มหาวิทยาลัย
Chulalongkorn University

APPENDIX H

PYTHON CODE FOR WRITING VTK FILE

Line	Code
1	import os
2	import pandas as pd
3	# for i in range(601): #for high ventilation
4	for i in range(1201): #for minimal ventilation
5	file = open(os.path.join('Filepath/', 'Filename' + str(int(i)).zfill(4) + '.vtk'), 'w')
6	s = []
7	m = []
8	l = []
9	for ... : # Need to create the Loop For All File Names
10	Filename = "Filename"
11	File_Path = "Filepath"
12	df = pd.read_csv(str(File_Path) + "/" + str(Filename) + "_avg_conc_cubic_spline_wa5.csv")
13	s.append(df.loc[i, '0.5-1micron_conc_wa'])
14	m.append(df.loc[i, '1-2.5micron_conc_wa'])
15	l.append(df.loc[i, '2.5-5micron_conc_wa'])
16	lst_small = []
17	lst_medium = []
18	lst_large = []
19	for j in range(12558):
20	a = str(s[j]) + '\n'
21	lst_small.append(a)
22	b = str(m[j]) + '\n'
23	lst_medium.append(b)
24	c = str(l[j]) + '\n'
25	lst_large.append(c)
26	Header = ["# vtk DataFile Version 2.0\n", "FlowField\n", "ASCII\n", "DATASET STRUCTURED_GRID\n", "DIMENSIONS 46 21 13\n", "POINTS 12558 float\n"]
27	Coordiante = [...] # List of coordinates for using in ParaView ["0 0 0\n","4 0 0\n",..,"176 80 48\n","180 80 48\n"]
28	Small = ["SCALARS S float\n", "LOOKUP_TABLE default\n"]
29	Small_Value = lst_small
30	Medium = ["SCALARS M float\n", "LOOKUP_TABLE default\n"]
31	Medium_Value = lst_medium

จุฬาลงกรณ์มหาวิทยาลัย
Chulalongkorn University

```
32      Large = ["SCALARS L float\n", "LOOKUP_TABLE default\n"]
33      Large_Value = lst_large
34      file.writelines(Header)
35      file.writelines(Coordinate)
36      file.write("\n")
37      file.write("POINT_DATA 12558\n")
38      file.write("\n")
39      file.writelines(Small)
40      file.writelines(Small_Value)
41      file.write("\n")
42      file.writelines(Medium)
43      file.writelines(Medium_Value)
44      file.write("\n")
45      file.writelines(Large)
46      file.writelines(Large_Value)
47      file.close()
```

จุฬาลงกรณ์มหาวิทยาลัย
Chulalongkorn University

APPENDIX I

SUPPLEMENTAL MATERIALS FOR PRELIMINARY RESULTS

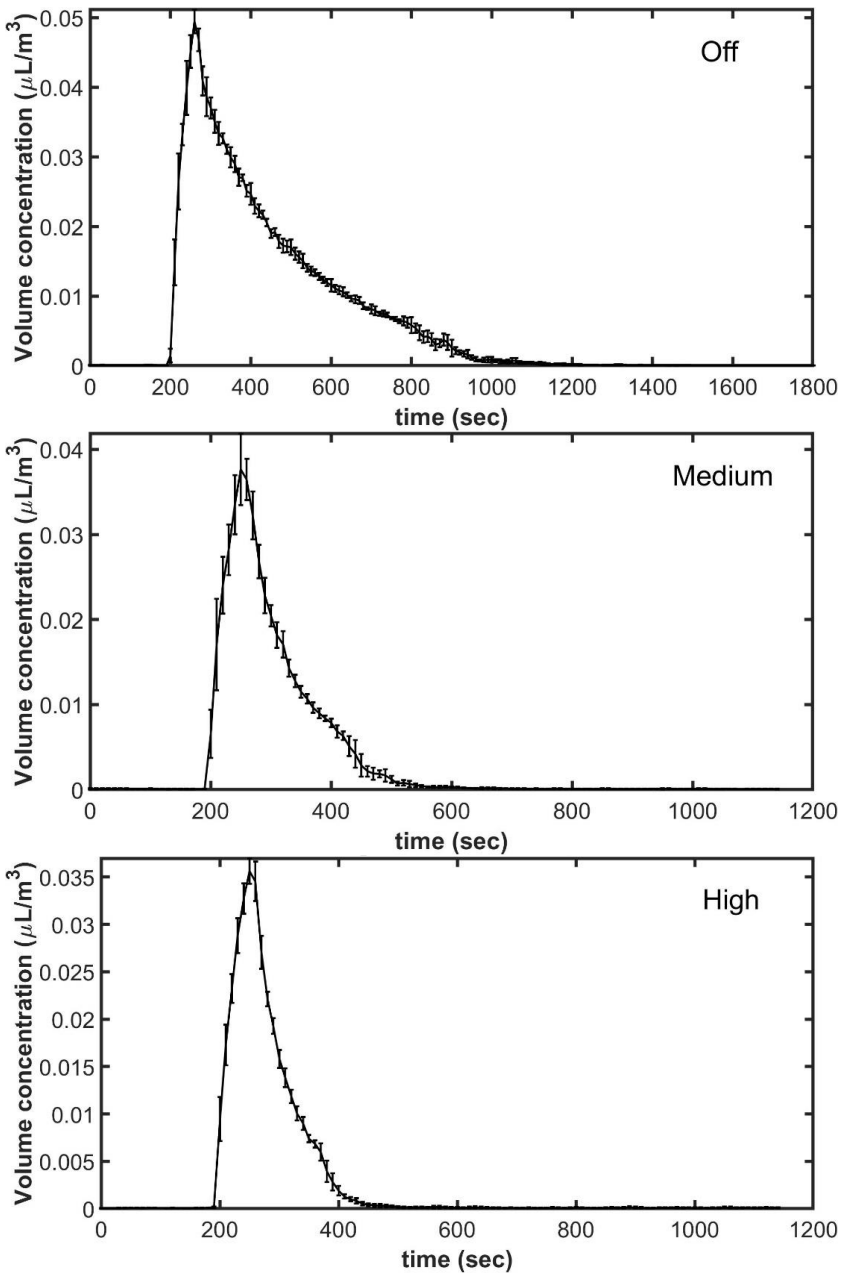

Figure 233 Aerosol Volume Concentration over Time with Three Different Ventilation Rate at Seat 1 with Aerosol Particles in the Range between 0.5 and 1 micron. Each Line Shows the Mean and Standard Deviation of Six Experiments.

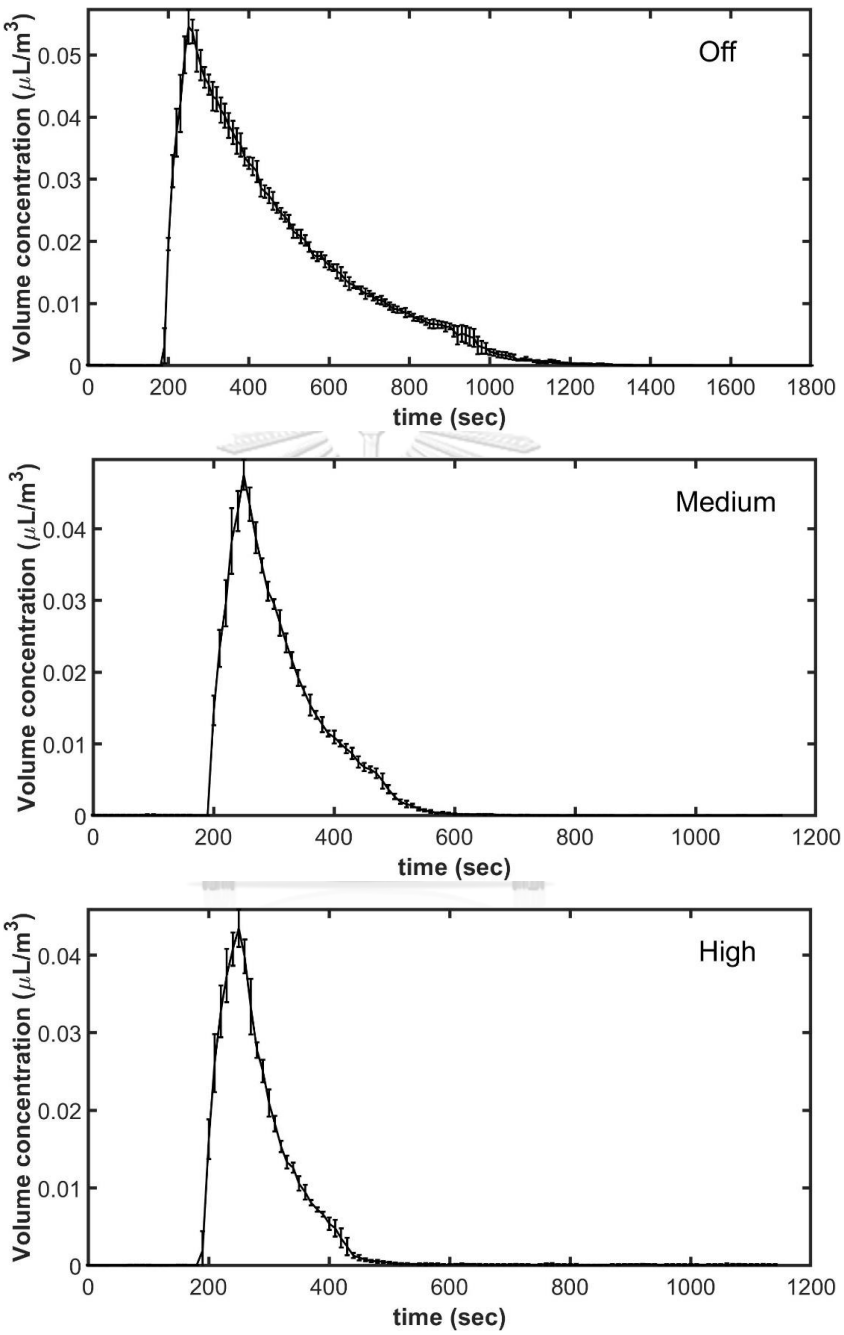

Figure 234 Aerosol Volume Concentration over Time with Three Different Ventilation Rate at Seat 2 with Aerosol Particles in the Range between 0.5 and 1 micron. Each Line Shows the Mean and Standard Deviation of Six Experiments

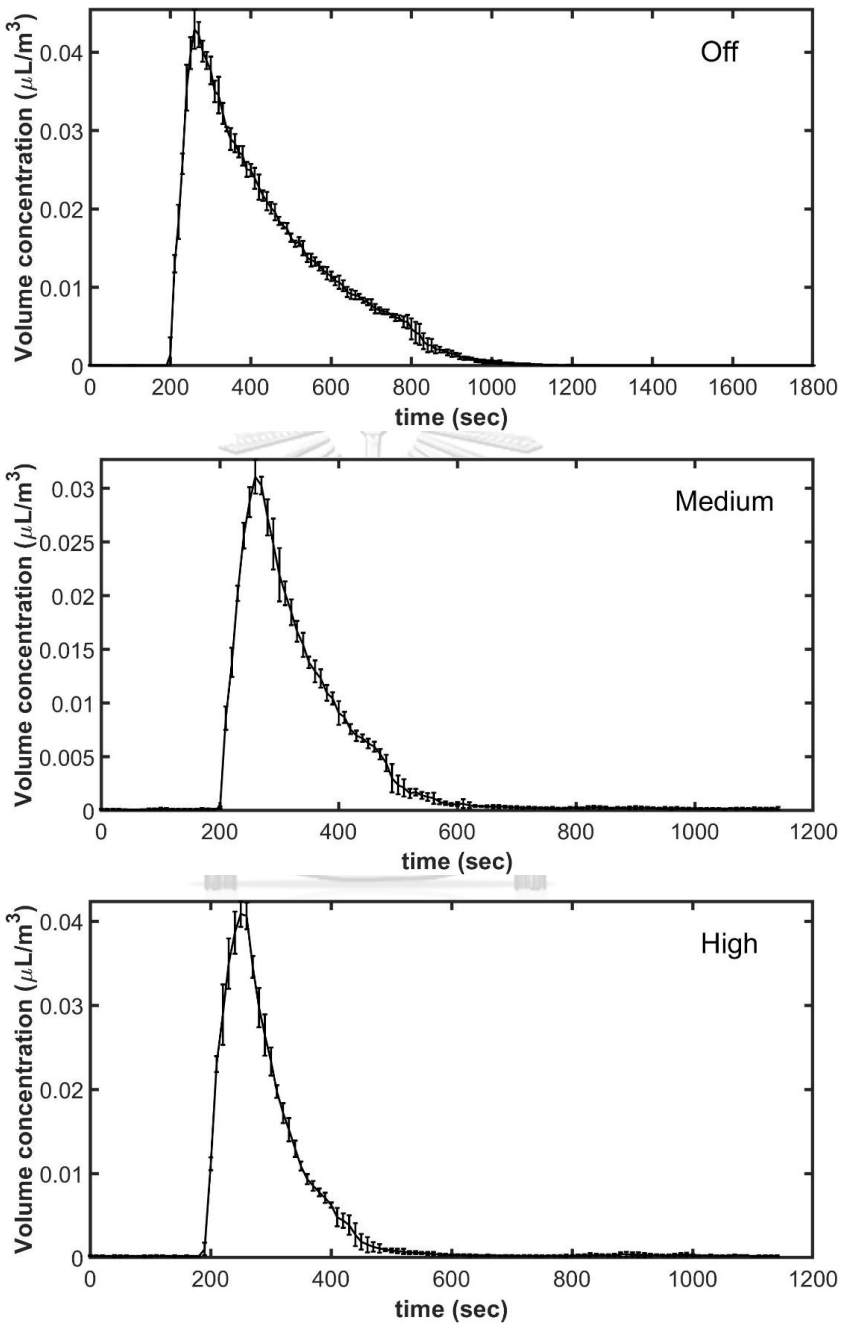

Figure 235 Aerosol Volume Concentration over Time with Three Different Ventilation Rate at Seat 3 with Aerosol Particles in the Range between 0.5 and 1 micron. Each Line Shows the Mean and Standard Deviation of Six Experiments

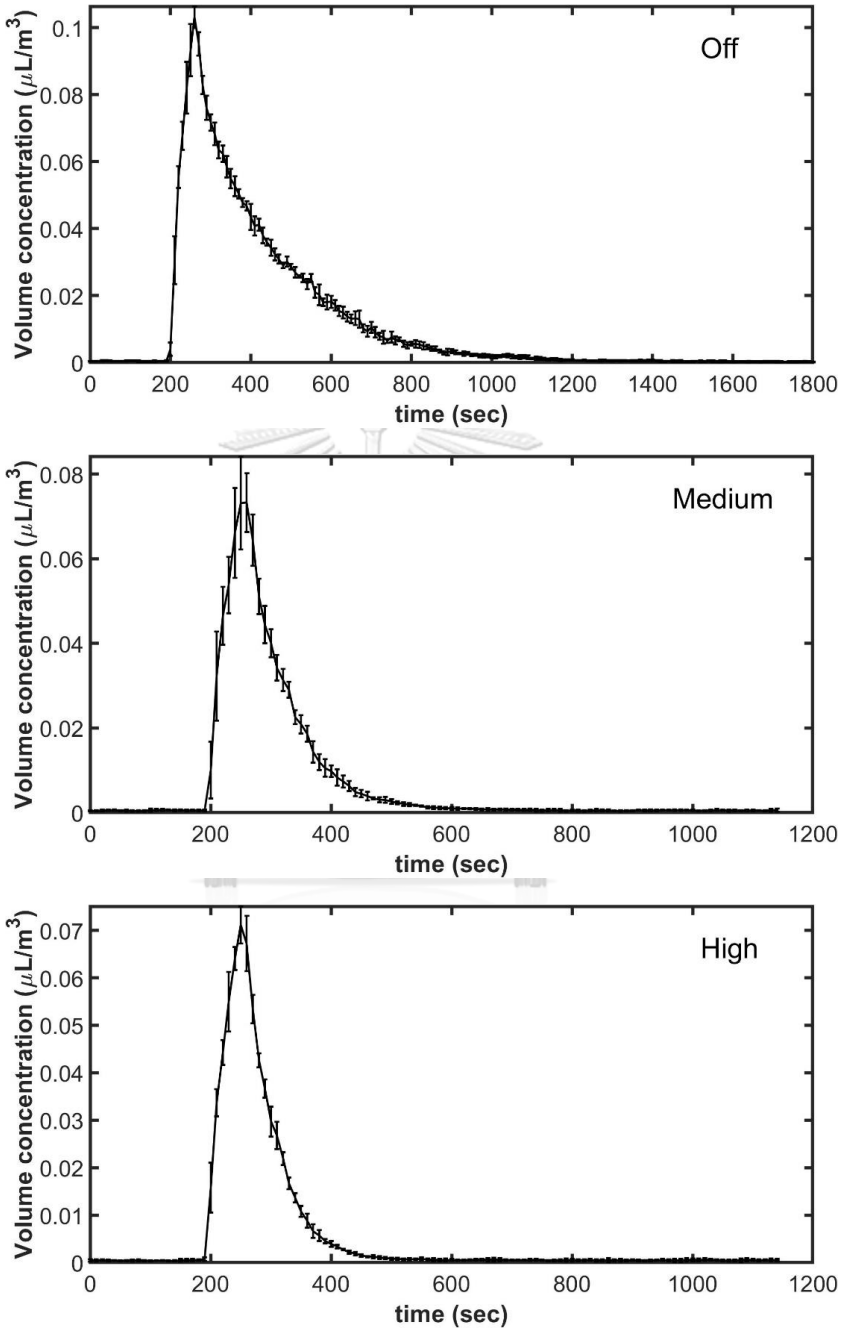

Figure 236 Aerosol Volume Concentration over Time with Three Different Ventilation Rate at Seat 1 with Aerosol Particles in the Range between 1 and 2.5 microns. Each Line Shows the Mean and Standard Deviation of Six Experiments

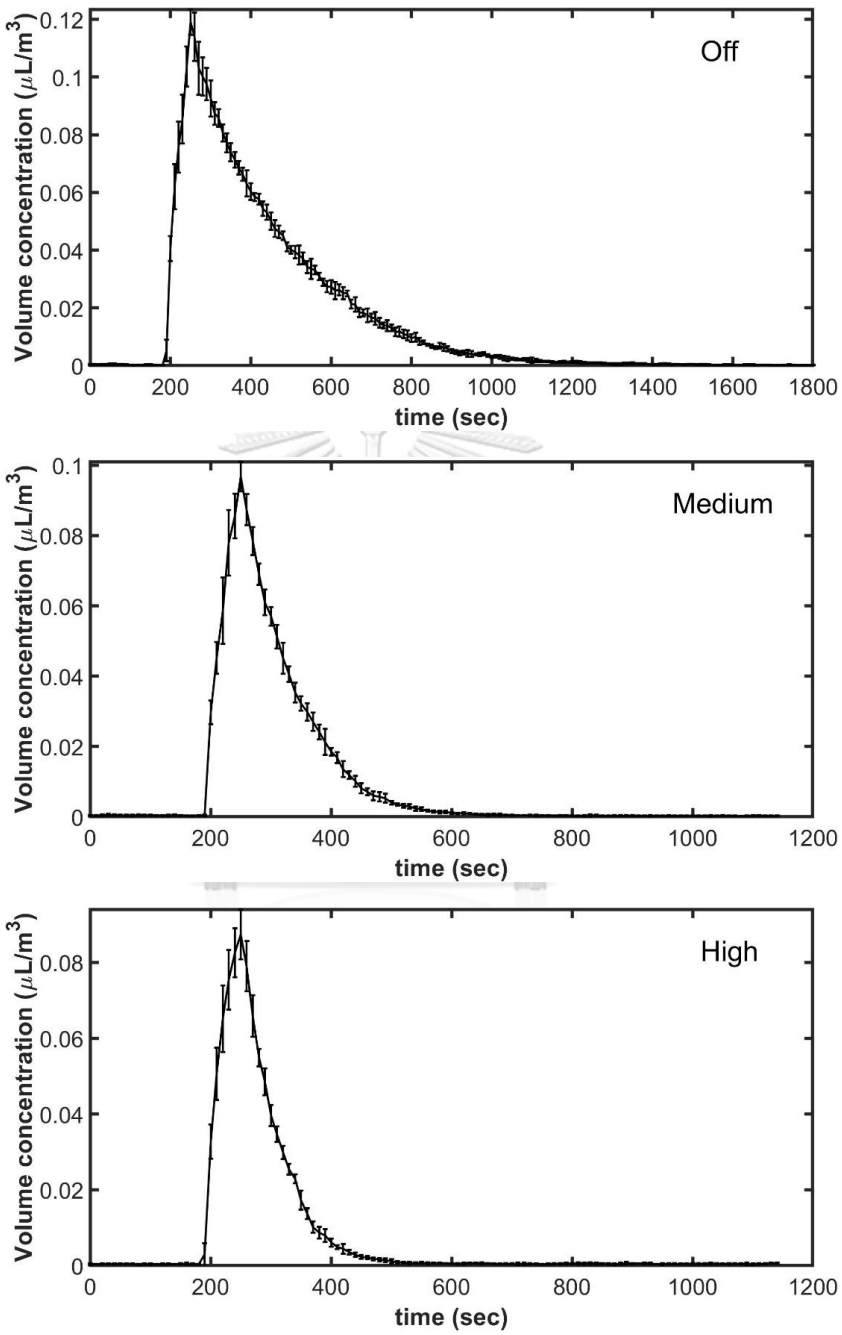

Figure 237 Aerosol Volume Concentration over Time with Three Different Ventilation Rate at Seat 2 with Aerosol Particles in the Range between 1 and 2.5 microns. Each Line Shows the Mean and Standard Deviation of Six Experiments

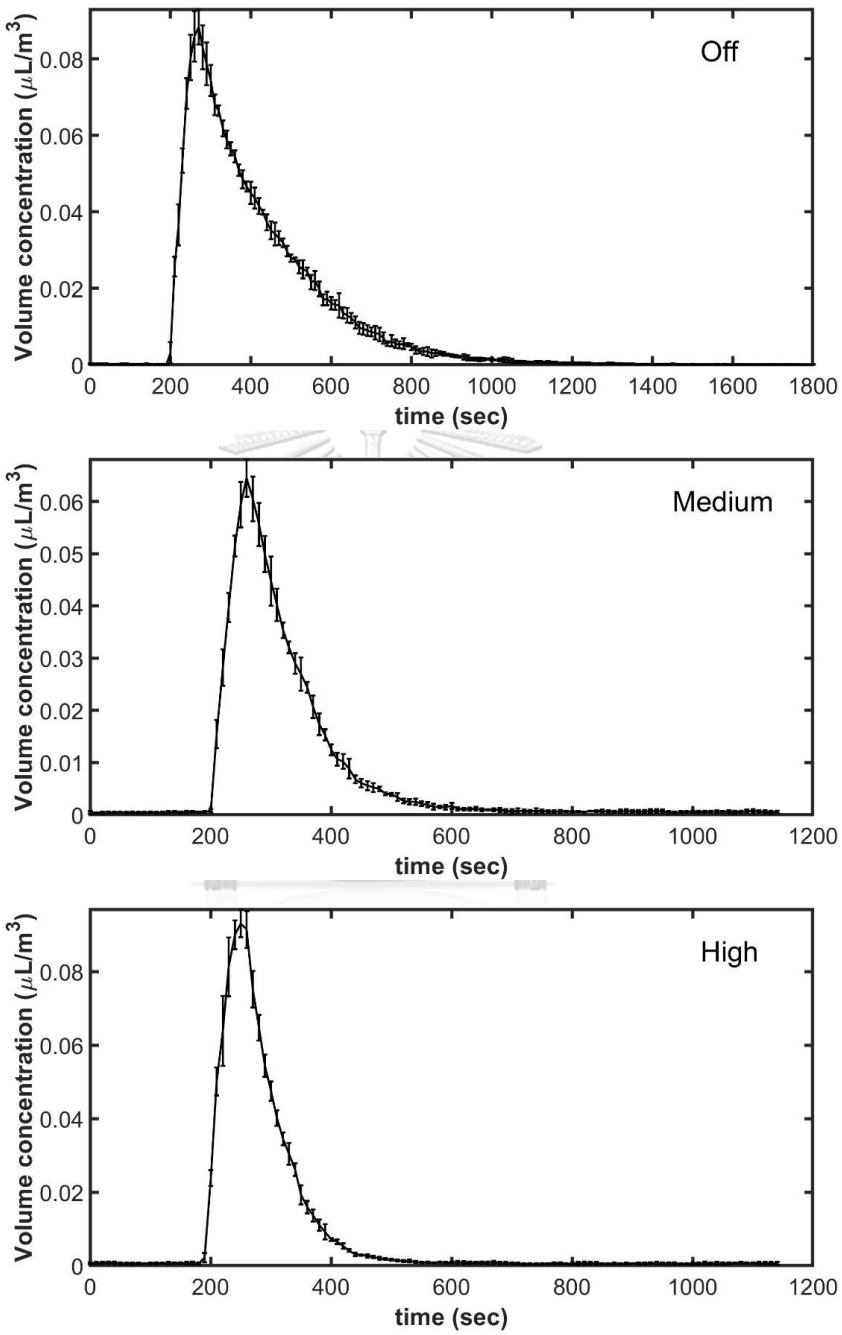

Figure 238 Aerosol Volume Concentration over Time with Three Different Ventilation Rate at Seat 3 with Aerosol Particles in the Range between 1 and 2.5 microns. Each Line Shows the Mean and Standard Deviation of Six Experiments

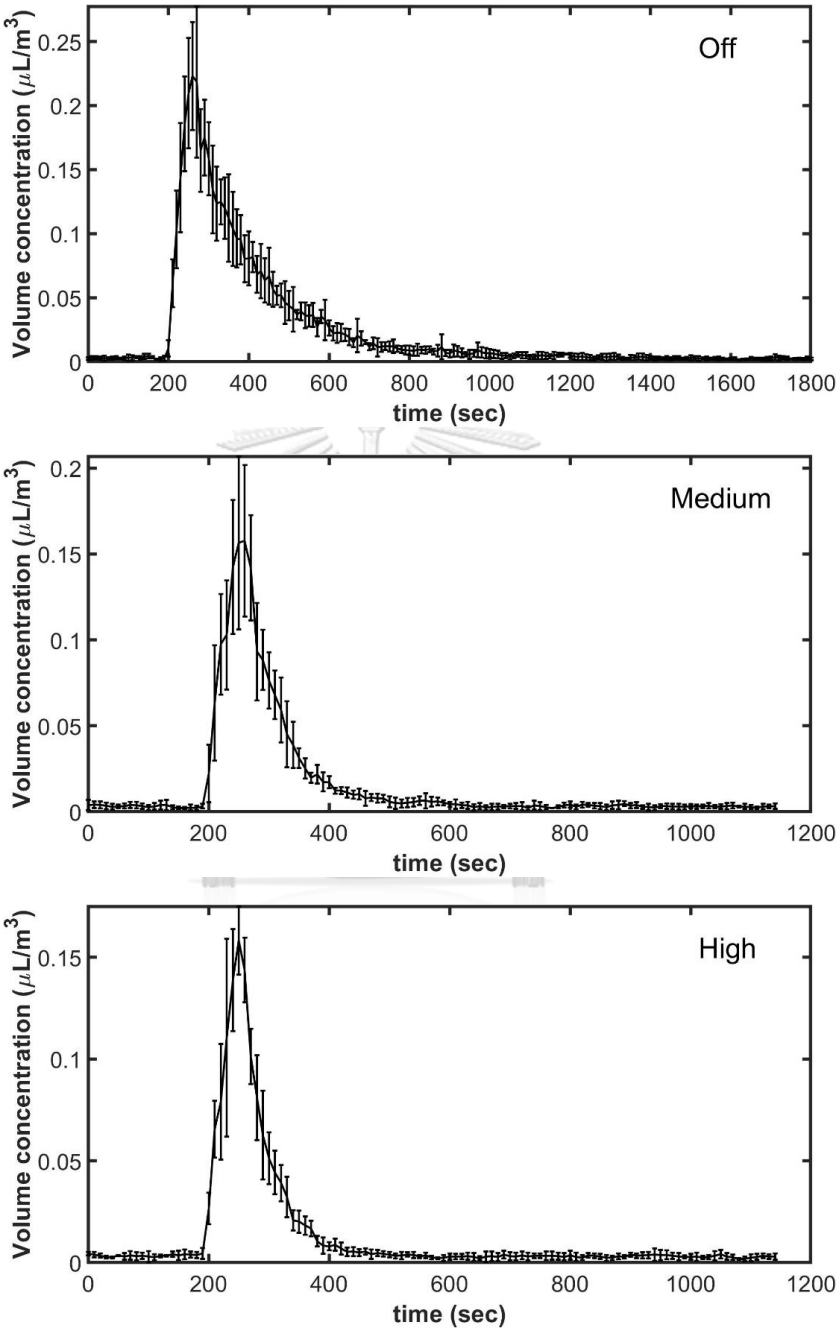

Figure 239 Aerosol Volume Concentration over Time with Three Different Ventilation Rate at Seat 1 with Aerosol Particles in the Range between 2.5 and 5 microns. Each Line Shows the Mean and Standard Deviation of Six Experiments

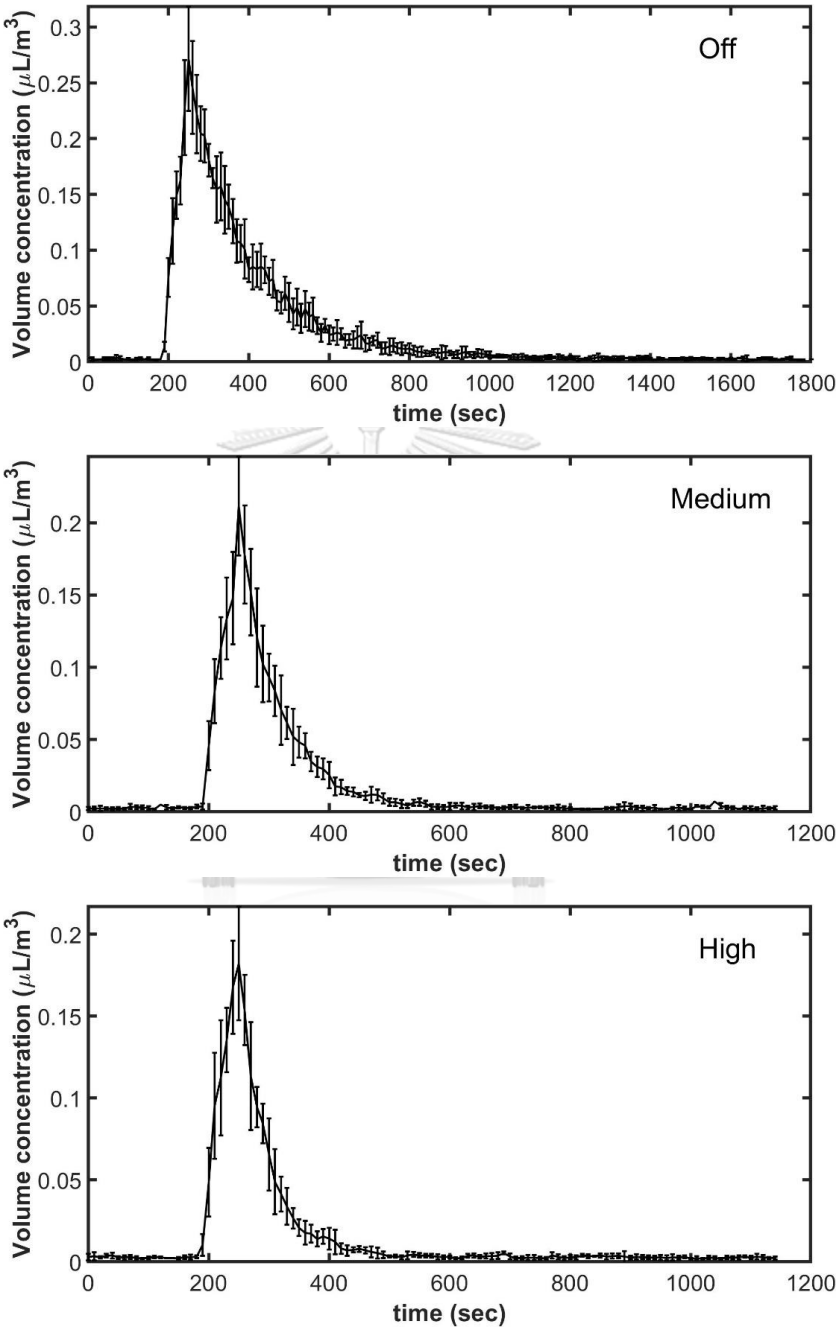

Figure 240 Aerosol Volume Concentration over Time with Three Different Ventilation Rate at Seat 2 with Aerosol Particles in the Range between 2.5 and 5 microns. Each Line Shows the Mean and Standard Deviation of Six Experiments

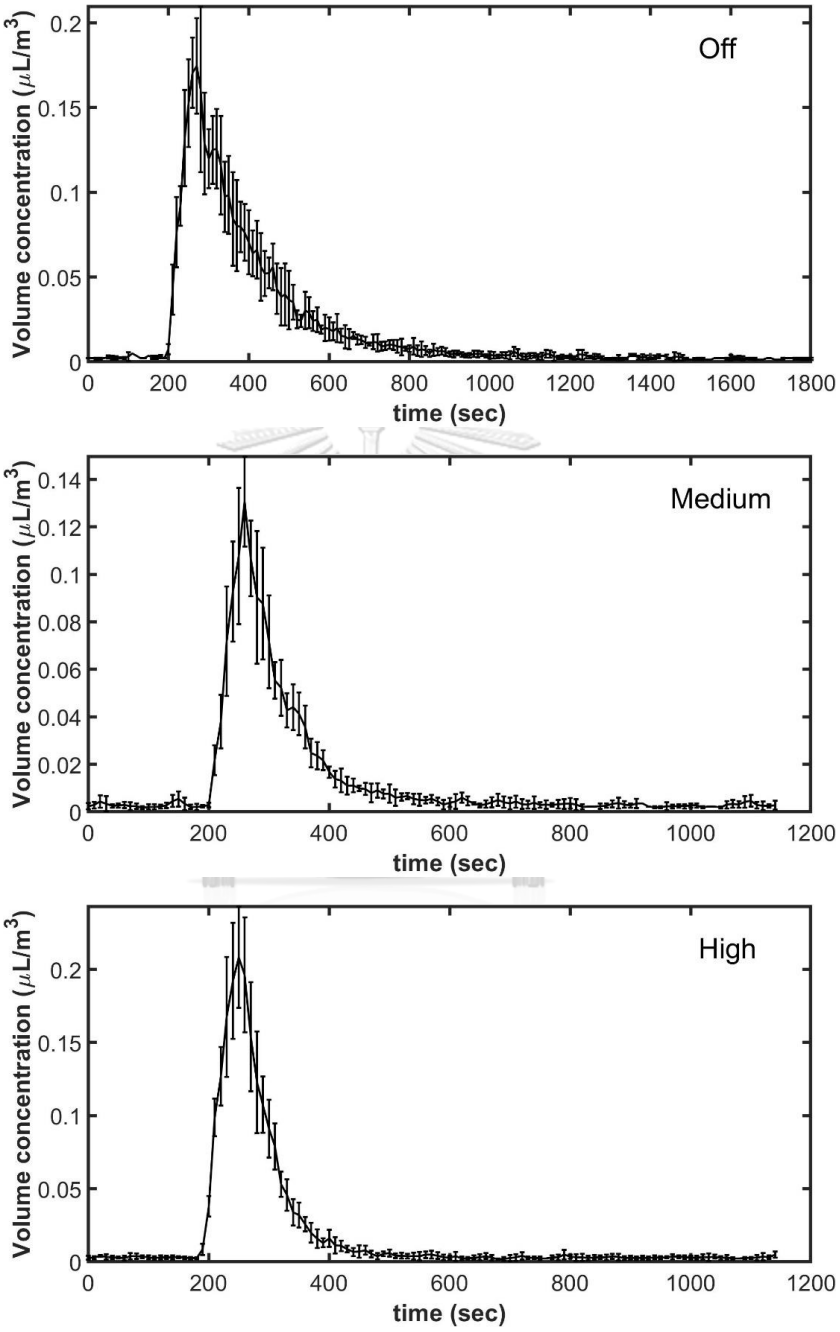

Figure 241 Aerosol Volume Concentration over Time with Three Different Ventilation Rate at Seat 3 with Aerosol Particles in the Range between 2.5 and 5 microns. Each Line Shows the Mean and Standard Deviation of Six Experiments

APPENDIX J

CONFERENCE PROCEEDING

Efficacy of the Ambulance Air Purifier System for Airborne Particle Reduction

Vasutorn Petrangsan[1], Thanadol Rojanasarntikul[2] and Karu Chongsiripinyo[1*]

[1]Department of Mechanical Engineering, Faculty of Engineering, Chulalongkorn University, Bangkok 10330, Thailand

[2]Emergency Department, King Chulalongkorn Memorial Hospital, Bangkok 10330, Thailand

[*]Corresponding Author: Karu.C@chula.ac.th

Abstract

The objective of this study is to assess the efficacy of an ambulance air purifier system in reducing the volume density of airborne particles via a process similar to what is called 'recovery test'. Aerosol particles of various sizes are introduced into the cabin via nebulizer injection at the patient's head position for one minute. The test is then accomplished by measuring the aerosol volume concentration of particles in 3 ranges of sizes at 0.5-1; 1-2.5; and 2.5-5 microns for 3 different ventilation rates (minimal, medium, and maximum), directly relating to 'air changes per hour (ACH)', and at 3 different seat positions (top; side; rear-end, relative to the patient cot). During the injection period, particle concentration sharply increases, then exponentially decays toward the background state. Larger ACH takes shorter time to decay but not necessarily suppresses peak concentration. Regardless of the seat position and size of particles, the 'return-to-background' duration measures 15 minutes for the minimal ventilation case, 7 minutes for the medium ventilation case, and 5 minutes for the maximum ventilation case. Peak concentration is found to be inversely proportional to ventilation rate for the two seat positions that are adjacent to the bed front portion (top and side). Interestingly, the rear-end position experiences the maximum concentration at the highest ventilation rate especially for larger particles. On average in time, the side position (seat 2) is, among the seats, practically exposed to the largest number of aerosol particles at any ventilation rate.

Keywords: Pandemic; airborne transmission; aerosol particle; ambulance; air purifier system

จุฬาลงกรณ์มหาวิทยาลัย
Chulalongkorn University

1 Introduction

Respiratory infections have unfortunately been increasingly prevalent in these recent days, in particular of viral types. The difficulty, in detecting these life-threatening viruses, that varies depending on their types along with the challenge in predicting whether which type of viruses will trigger the next epidemic post the global problem we are all confronting.

However due to the fact that one cause of the Coronavirus (COVID-19) spreading is from viruses that are airborne-transmitted, among other types of transmissions: direct transmission; fomite transmission; droplet transmission, what we can do is investigating the media itself in which those viruses are attached to.

Transmission ability of the COVID-19 disease depends on the size of media particles. Particles of size larger than 5 microns, such as droplets, are dominated by gravitational force and drop to ground within 6 feet from the source [1]. Droplet-type particles that are ejected from coughing or sneezing from one person can be deposited to another person especially in the upper respiratory tract [2] including nose, nasal cavity, pharynx, and larynx above vocal folds.

Particles smaller than or equal to 5 microns can however be easily inhaled and affect the lower respiratory tract [3, 4] whether it be larynx below vocal folds, trachea, bronchus, or lungs. This type of small particle tends to be airborne for extended periods [1, 5-7] and can travel to a greater distance than 6 feet from the source.

There are multiple ways to protect and shield ourselves from the disease such as using protection equipment, e.g., eye protection, gown, gloves, and surgical mask [8 ,9]. Negative pressure rooms and airborne infection isolation rooms can be designed and constructed in order to help reducing the risk of infection not only inside but outside of hospital areas.

While hospital airborne infection isolation room is important in controlling the transmission of patients to those around them, the risk of infection of frontline EMS workers [10-13] cannot be overlooked. EMS workers are constantly in proximity with patients while providing pre-hospital emergency medical care and transporting them to hospital.

One of the keys in reducing healthcare workers' exposure to aerosol particles is a good ventilation system. While studies on indoor ventilation have been done [14-16] and the standard [17] is set for the acceptable system, there are however much fewer studies on ambulance ventilation system, e.g. [18]. While not established in particular for ambulance, the standard [17] is often adopted in response to the pandemic so as to ensure reduction in the risk of medical personnel exposed to airborne viruses.

จุฬาลงกรณ์มหาวิทยาลัย
Chulalongkorn University

In Thailand at the time of conducting this study, almost all of the ambulances do not have a ventilation system that is suitable for such occurrence, risking medical workers for a high risk of contracting disease from the patient. For this reason, a ventilation system is installed in a few numbers of ambulances at the emergency department, King Chulalongkorn Memorial Hospital. Our goal is to determine the effectiveness of the equipment in reducing the risk of infection of medical workers in the ambulance.

The aim of this research is to study the efficiency of the newly installed ventilation system. In particular, how does a ventilation rate induced by the system affect the volume concentration of aerosol particle cloud that is emitted inside the cabin for each particle size ranging below 5 microns at different seat locations?

2 Experiment

2.1 Experimental procedure

A set of experimental studies is performed to assess the efficacy of Camfil® model CC410-concealed with pre filter; UVC; and HEPA filter H14, an ambulance air purifier system, in reducing the volume density of airborne particles by measuring the volume concentration of artificially-injected- aerosol particles for different size ranges at different seating locations when the ambulance is parked.

The ambulance is a Toyota Ventury van. The patient compartment is measured 1.5 m wide, 2.7 m long, and 1.4 m high. Particles are introduced into the patient compartment in the form of pulses by portable ventilator, Oxylog® 3000 plus, connected to the nebulizer, Aeroneb® Professional Nebulizer used for aerosolizing solutions. This process simulates the patient's breathing pattern. Throughout the process of introducing particles into the cabin, the number concentration of particles is measured over time by PMS5003, an affordable particle counter, at 3 different seat positions. The device is calibrated against a more-accurate, Handheld3016 particle counter.

Aerosol particle released in the cabin is nebulized from 0.9% sodium chloride solution, representing a combination of respiratory pathogens. Data are collected at 3 different seat positions and at 3 different ventilation rates. The rate is controlled by adjusting the ventilation system's fan speeds for the intake fan at the top of the patient compartment and an exhaust blower on the right side of the ambulance next to the patient cot. The exhaust blower adjustment is made of three levels: level 0 (turned-off), level 3 (medium), and level 6 (maximum). We use the term 'minimal' interchangeably with 'off' for the case when

จุฬาลงกรณ์มหาวิทยาลัย
Chulalongkorn University

blower adjustment is turned-off rather than ‘no ventilation’.

The medium and maximum ventilation rates used in this study yield very rough approximations of ‘air changes per hour (ACH)’ to be 40 and 80, respectively. The approximation is based on the exhaust blower specification sheet and an approximated volume of the cabin. The experiment setup is depicted as in Fig. 1.

The experiment begins with environment preconditioning: the ventilation system is turned on with the exhaust blower at maximum rate for 15 minutes, air flow is allowed to stabilize for an additional 10 minutes, and the particle counter is then activated to log data. After 3 minutes, the aerosol particles are released into the ambulance patient compartment for 1 minute by the nebulizer, placed on the patient cot as shown in Fig. 1. A transport ventilator supplies air flow to the nebulizer, replicating patient breathing pattern using the VC-CMV mode. This sets the tidal volume (VT) to 500 mL, ventilation time ratio (I:E) to 1:2 and adjusted respiratory rate (RR) at 12 breaths per minute for the inspiratory time (Ti) to be 1.7 second. Additional information on human breathing pattern can be found in [19].

Afterward, number of particles larger than 0.5 microns is measured for 26 minutes. For the second and the third cases (medium and maximum ventilation rate), the procedure is as aforementioned, but data is logged for 16 minutes after the particle injection. Six experiments are conducted for each case resulting in 18 experiments in total.

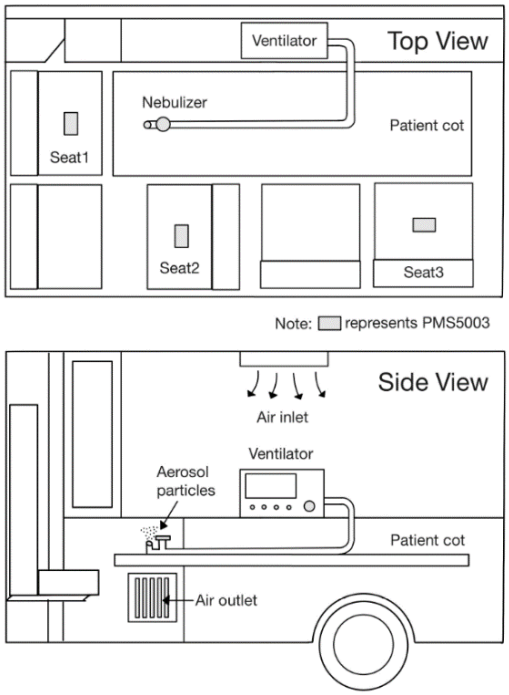

Fig. 1 Ambulance patient compartment with experimental equipment

2.2 Data analysis

The number of a transmission carrier (pathogens, viruses, or microorganisms) does not only depend on the number of aerosol particles but also on the size of particles [20]. Particle volume concentration is thus a more appropriate mean to quantitate the carrier amount.

Since PMS5003 reports the number of aerosol particles per cubic feet of air in each particle size bin, these data can simply be transformed into volume concentration ($\mu L/m^3$) with

จุฬาลงกรณ์มหาวิทยาลัย
Chulalongkorn University

$$\sigma = 4.7\times10^{-8}N\pi r^3$$

where σ is volume concentration ($\mu L/m^3$)

N is number of particles ($1/ft^3$)

r is mean radius in each size bin (μm)

3 PMS5003 calibration

PMS5003 is calibrated against a more-accurate, high-precision Handheld3016 particle counter. The process is done by comparing output values from the two devices, placed in adjacent positions inside the ambulance cabin during the entire period where the experimental procedure with the maximum exhaust blower mentioned previously is being conducted. The measurement is repeated 3 times.

Data at each particle size bin from the two devices are considered separately, i.e., in total of 3 calibration curves for the size bins of 0.5-1 micron, 1-2.5 microns and 2.5-5 microns. As an example, the scattered data along with its calibration curve for the size bin of 0.5-1 micron in the log-log scale is shown in Fig. 2.

According to the scattered data, two distinctive calibration curves are constructed. One for low particle concentration and the other for high particle concentration. Fig. 3 compares the ensemble-averaged (from the three experiments) volume concentrations between that from the Handheld3016 and from the PMS5003 after correction.

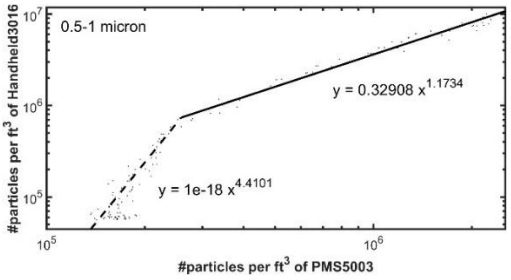

Fig. 2 Particle volume concentrations measured by Handheld3016 and PMS5003 and calibration curves

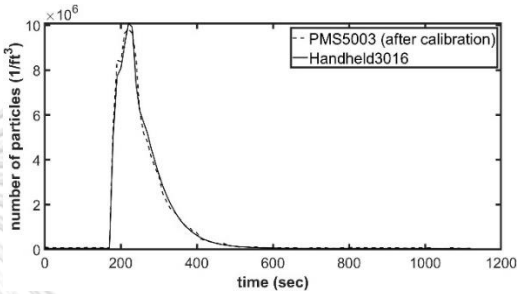

Fig. 3 Particle volume concentrations over time from Handheld3016 and PMS5003, with correction, for particles in the 0.5-1-micron size bin

4 Results

4.1 Aerosol volume concentration over time

The aerosol volume concentrations over time at each seat position are shown in Fig. 4 for the particle size bin of 0.5-1 micron. The concentrations start to sharply arise at about t = 180 seconds indicating an immediate response to the particle feeding system (the nebulizer and the transport ventilator) being turned on. Recall that at t = 180 seconds is where the nebulizer begins the diffusion. After 60 seconds, as the feeding lasts for that period, the concentration levels begin to decline from their peak values, with the decaying rate

จุฬาลงกรณ์มหาวิทยาลัย
Chulalongkorn University

depending on ventilation rate and seat position.

Consider the concentration at seat number 2 for minimal ventilation case, the volume concentration returns to the background state after about 15 minutes (900 seconds). This 'return-to-background' period, undoubtedly, is found to be inversely proportional to ACH, regardless of particle size range and seat position. This period takes about 7 minutes for medium ventilation case and about 5 minutes for high ventilation case.

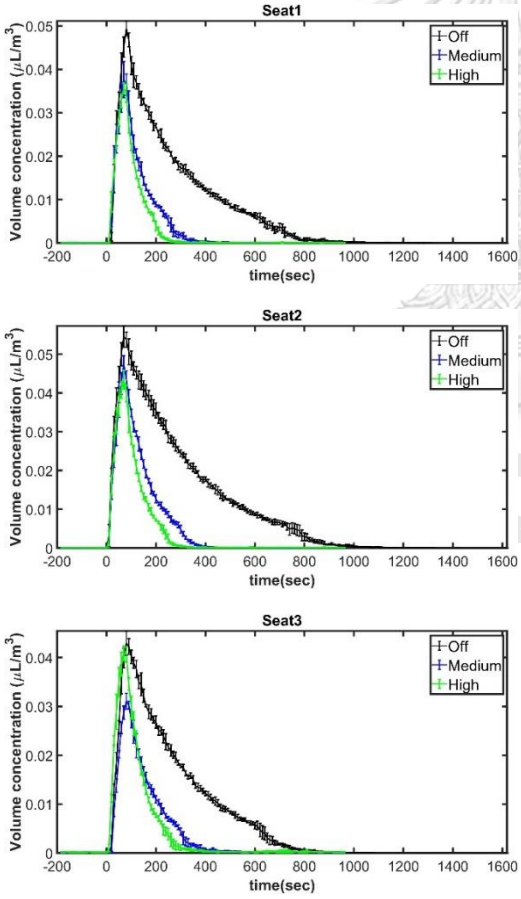

Fig. 4 Volume concentration for particles of size in the range 0.5-1 micron. Each line shows the ensemble mean of six experiments. A vertical line on top of the mean values represents standard deviation of the collected data at that point in time.

4.2 Maximum aerosol volume concentration

The exponential decreases of particle concentration seen in the previous section, reflecting one criterion in measuring the effectiveness of the ventilation system, do not however infer to the amount of concentration in which EMS workers are exposed to a cloud of the particles. The amounts can remain close to their corresponding maximum values for up to 30 seconds, a sufficiently-long period for the intaking by inhalation.

A set of histograms comparing the maximum volume concentration at all locations and size bins is shown in Fig. 5. It is clear that increasing the ventilation rate decreases the maximum aerosol volume concentration for all size ranges but only for the seat position 1 (especially for smaller particles) and for the seat position 2. However, this tendency does not hold for the seat position 3. At this rear-end location, the highest rate of ventilation yields a comparable concentration with that of minimal ventilation case for the two small particle size bins and surprisingly even a larger value for the 2.5-5-micron particles.

Regardless of particle size, the concentration is peaked at the seat position 2 for most scenarios, except those with high ventilation rate for 1-2.5- micron and 2.5-5-micron particles (see Fig. 5 in middle and

bottom, in green for seat 3) which, in fact, are not significantly larger than that of seat 2.

4.3 Mean Aerosol Volume Concentration

Lastly, we consider the temporal-averaged volume concentration, shown as a set of histograms in Fig. 6. The averaging is done for the entire duration of 1200 seconds (20 minutes).

Reflecting the overall particle exposure, the set of mean values looks similar to that seen in the previously section of the maximum values data. In particular, the seat number 2 remains the riskiest position, again except those with high ventilation rate for 1-2.5-micron and 2.5-5-micron particles.

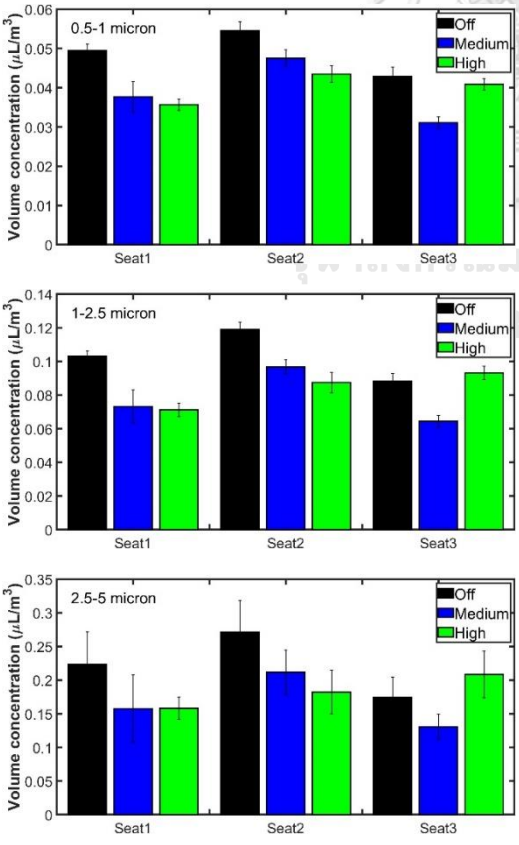

Fig. 5 Maximum volume concentration at three different seat locations in each particle size bin with standard deviation

5 Summary and Conclusions

Airborne disease transmission has increasingly been prevalent on a global scale, particularly due to the COVID-19 pandemic. Medical sectors take different measures in suppressing the contagious virus, e.g., revising their ventilation systems in hospitals and ambulances.

The objective of this study is to assess the efficacy of a newly installed ambulance air purifier system in reducing the volume density of airborne particles. This recovery test is done by diffusing nebulized 0.9% sodium chloride solution for one minute into the patient cabin and measuring its concentration at 3 different seat positions (top; side; rear-end, relative to the patient bed; with the three ventilation rates: off, medium, and high).

During the one-minute diffusion period, particle concentration sharply increases, then exponentially decays toward the background state. Particle concentration that experiences higher ventilation rate takes shorter time to decay. However, the higher rate does not necessarily reduce the peak concentration, depending on seat position.

Regardless of seat position and size of particles, the `return-to-background' duration measures about 15 minutes for minimal ventilation case, approximately 7

minutes for medium ventilation case, and close to 5 minutes for high ventilation case. Peak concentration is found to be inversely proportional to ventilation rate but only for the two seat positions that are adjacent to the bed front portion (top and side). It is found that the rear-end position experiences the peak concentration at the maximum ventilation rate especially for larger particles. On average in time, the side position (seat 2) is, among the seats, practically exposed to the largest number of aerosol particles at any ventilation rate.

Evidently, there is not a single ventilation rate that minimizes the exposure to peak aerosol particle concentration for every seat positions. We should, however, consider reallocating workers away from the cabin rear-end while utilizing the ventilation system at its maximum rate.

The newly installed air purifier is proven effective in its ability to shorten the duration, in which the amount of airborne particles reside in the cabin, by a factor of about 2 at the medium ventilation rate and about 3 at the peak ventilation rate. However, the largest air circulation rate, provided by the purifier, posts a concerning problem where an EMS worker at the particular seat position is over exposed, though short period, to the airborne particles.

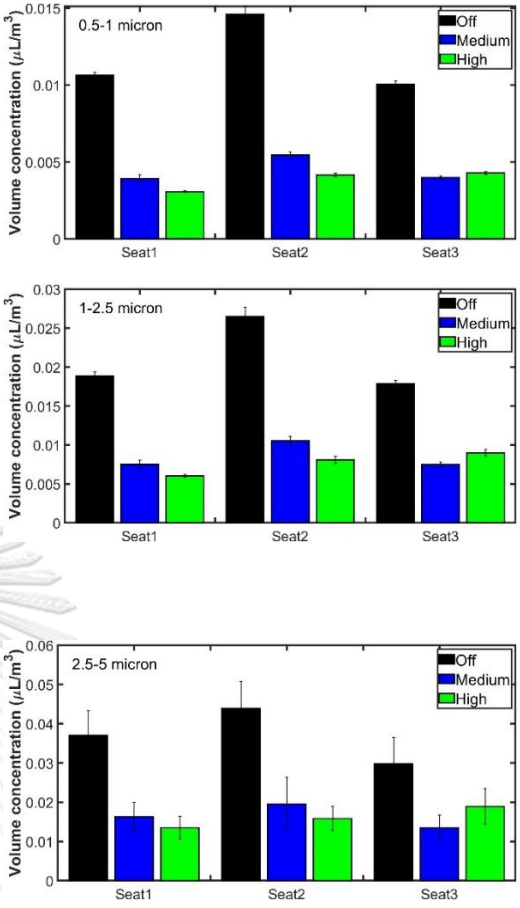

Fig. 6 Temporal mean volume concentration at three different seat locations in each particle size bin with standard deviation

จุฬาลงกรณ์มหาวิทยาลัย
Chulalongkorn University

6 Acknowledgement

The authors would like to thank the King Chulalongkorn Memorial Hospital for providing resources in conducting the experiments.

7 References

[1] Klompas, M., Baker, M. A., and Rhee, C. (2020). Airborne Transmission of SARS-CoV-2, JAMA, vol.324(5), July 2020, pp. 441 – 442.

[2] Harper, G., & Morton, J. (1953). The Respiratory Retention of Bacterial Aerosols:

Experiments with Radioactive Spores, Epidemiology & Infection, vol.51(3), September 1953, pp. 372 - 385.

[3] Siegel, J. D., Rhinehart, E., Jackson, M., & Chiarello, L. (2007). 2007 Guideline for Isolation Precautions: Preventing Transmission of Infectious Agents in Health Care Settings, American Journal of Infection Control, vol.35(10), December 2007, pp. S65 – S164.

[4] Brown, J. H., Cook, K. M., Ney, F. G., & Hatch, T. (1950). Influence of Particle Size upon the Retention of Particulate Matter in the Human Lung, American Journal of Public Health and the Nation's Health, vol.40(4), April 1950, pp. 450 – 480.

[5] Cowling, B. J., Ip, D. K. M., Fang, V. J., Suntarattiwong, P., Olsen, S. J., Levy, J., Uyeki, T. M., Leung, G. M., Malik Peiris, J. S., Chotpitayasunondh, T., Nishiura, H., & Mark Simmerman, J. (2013). Aerosol Transmission is an Important Mode of Influenza A Virus Spread, Nature Communication, vol.4(1), June 2013, pp. 1 – 6.

[6] Pica, N., & Bouvier, N. M. (2012). Environmental Factors Affecting the Transmission of Respiratory Viruses, Current Opinion in Virology, vol.2(1), February 2012, pp. 90 – 95.

[7] Fernstrom, A., & Goldblatt, M. (2013). Aerobiology and Its Role in the Transmission of Infectious Diseases, Journal of Pathogens, vol.2013, January 2013, pp. 1 – 13.

[8] Makison Booth, C., Clayton, M., Crook, B., & Gawn, J. M. (2013). Effectiveness of Surgical Masks against Influenza Bioaerosols, Journal of Hospital Infection, vol.84(1), May 2013, pp. 22 – 26.

[9] Smith, J. D., MacDougall, C. C., Johnstone, J., Copes, R. A., Schwartz, B., & Garber, G. E. (2016). Effectiveness of N95 Respirators versus Surgical Masks in Protecting Health Care Workers from Acute Respiratory Infection: a Systematic Review and Meta-Analysis, Canadian Medical Association Journal, vol.188(8), May 2016, pp. 567 – 574.

[10] Pipitsangjan, S., Luksamijarulkul, P., Sujirarat, D., & Vatanasomboon, P. (2011). Risk Assessment towards Droplet and Airborne Infections among Ambulance Personnel in a Province of Northeastern Thailand, Asia Journal of Public Health, vol.2(1), April 2011, pp. 20 – 26.

[11] Luksamijarulkul, P., & Pipitsangjan, S. (2015). Microbial Air Quality and Bacterial Surface Contamination in Ambulances During Patient Services, Oman Medical Journal, vol.30(2), March 2015, pp. 104 – 110.

[12] Roline, C. E., Crumpecker, C., & Dunn, T. M. (2007). Can Methicillin-Resistant Staphylococcus Aureus Be Found in an Ambulance Fleet?, Prehospital Emergency Care, vol.11(2), July 2009, pp. 241 – 244.

[13] Alves, D. W., & Bissell, R. A. (2008). Bacterial Pathogens in Ambulances: Results of Unannounced Sample Collection, Prehospital Emergency Care, vol.12(2), July 2009, pp. 218 – 224.

[14] Jurelionis, A., Gagyte, L., Prasauskas, T., Čiužas, D., Krugly, E., Šeduikyte, L., &

จุฬาลงกรณ์มหาวิทยาลัย
Chulalongkorn University

Martuzevičius, D. (2015). The Impact of the Air Distribution Method in Ventilated Rooms on the Aerosol Particle Dispersion and Removal: The Experimental Approach, Energy and Buildings, vol.86, January 2015, pp. 305 – 313.

[15] Quang, T. N., He, C., Morawska, L., & Knibbs, L. D. (2013). Influence of Ventilation and Filtration on Indoor Particle Concentrations in Urban Office Buildings, Atmospheric Environment, vol.79, November 2013, pp. 41 – 52.

[16] Lu, W., & Howarth, A. T. (1996). Numerical Analysis of Indoor Aerosol Particle Deposition and Distribution in Two-Zone Ventilation System, Building and Environment, vol.31(1), January 1996, pp. 41 – 50.

[17] American Society of Heating, Refrigerating and Air-Conditioning Engineers (2013). ANSI/ASHRAE/ASHE Standard 170–2013: Ventilation of Health Care Facilities, ASHRAE.

[18] Lindsley, W. G., Blachere, F. M., McClelland, T. L., Neu, D. T., Mnatsakanova, A., Martin, S. B., Mead, K. R., & Noti, J. D. (2019). Efficacy of an Ambulance Ventilation System in Reducing EMS Worker Exposure to Airborne Particles from a Patient Cough Aerosol Simulator, Journal of Occupational and Environmental Hygiene, vol.16(12), October 2019, pp. 804 – 816.

[19] Tobin, M. J., Chadha, T. S., Jenouri, G., Birch, S. J., Gazeroglu, H. B., & Sackner, M. A. (1983). Breathing Patterns, Chest, vol.84(2), August 1983, pp. 202 – 205.

[20] Zuo, Z., Kuehn, T. H., Verma, H., Kumar, S., Goyal, S. M., Appert, J., Raynor, P. C., Ge, S., & Pui, D. Y. H. (2013). Association of Airborne Virus Infectivity and Survivability with Its Carrier Particle Size, Aerosol Science and Technology, vol.47(4), December 2012, pp. 373 – 382.

จุฬาลงกรณ์มหาวิทยาลัย
Chulalongkorn University

APPENDIX K

PRESENTATION MATERIAL

EFFECTIVENESS OF THE NEW AMBULANCE AIR EXHAUST SYSTEM IN REDUCING AEROSOL PARTICLE CONCENTRATION

By Vasutorn Petrangsan

Associate Professor Alongkorn Pimpin, Ph.D. (chairman)

Karu Chongsiripinyo, Ph.D. (Thesis Advisor)

Assistant Professor Saran Salakij, Ph.D. (Examiner)

Associate Professor Vejapong Juttijudata, Ph.D. (External Examiner)

This work received financial support from Chulalongkorn University (CU-GR 63-34- 21-02), and Micro/Nano Electromechanical Integra ted Device Research Unit, Faculty of Engineering, Chulalongkorn University.

OBJECTIVE

To assess the effectiveness of an ambulance air exhaust system in reducing the volume density of airborne particles

SCOPES

AMBULANCE — The assessment is to be done experimentally inside a particular ambulance , currently deployed in the King Chulalongkorn Memorial Hospital . The experiments take place while the vehicle is parked .

POSITIONS — Aerosol concentration will be measured for 200 positions (10x5x4).

VENTILATION RATE — The air exhaust system is parameterized at 2 settings; turned off and maximum rate .

INJECTED PARTICLE — The size ranges of aerosol particles measurement are divided into three ranges: 0.5 to 1 micron , 1 to 2.5 microns and 2.5 to 5 microns. In place of real respiratory droplets, 0.9% sodium chloride solution diffused in aerosol form is utilized .

INTRODUCTION

- Pandemics & COVID-19 Current Situation
- Size of Particles and Viruses
- Transmission Pathway
- Particle Measurement Techniques
- Ventilation Types
- New Ambulances for Respiratory Disease

5

INTRODUCTION

- Pandemics & COVID-19 Current Situation
- Size of Particles and Viruses
- Transmission Pathway
- Particle Measurement Techniques
- Ventilation Types
- New Ambulances for Respiratory Disease

6

INTRODUCTION

- Pandemics & COVID-19 Current Situation
- Size of Particles and Viruses
- Transmission Pathway
- Particle Measurement Techniques
- Ventilation Types
- New Ambulances for Respiratory Disease

INTRODUCTION

- Pandemics & COVID-19 Current Situation
- Size of Particles and Viruses
- Transmission Pathway
- Particle Measurement Techniques
- Ventilation Types
- New Ambulances for Respiratory Disease

9

INDIRECT CONTACT TRANSMISSION

- Airborne Transmission
- Droplet Transmission
- Fomite Transmission

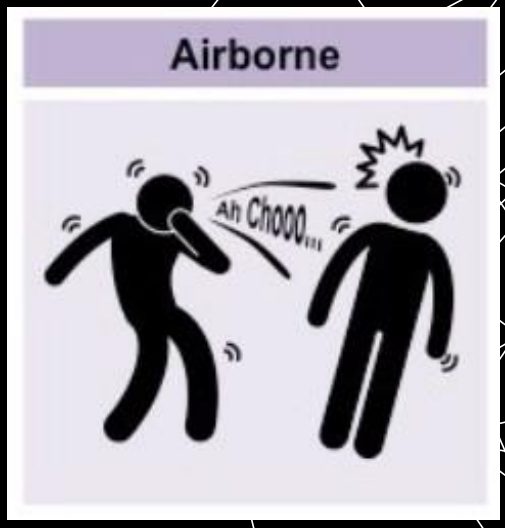

10

INTRODUCTION

- Pandemics & COVID-19 Current Situation
- Size of Particles and Viruses
- Transmission Pathway
- Particle Measurement Techniques
- Ventilation Types
- New Ambulances for Respiratory Disease

11

PARTICLE MEASUREMENT TECHNIQUES

Sieving Method

Particle Motion Inertia Method

Gravitational Sedimentation Method

Electrical Stream Sensing Zone Method

Dynamic Light Scattering

Static Light Scattering

12

STATIC LIGHT SCATTERING
(LASER DIFFRACTION)

- Fraunhofer Diffraction Theory
- MIE Scattering Theory

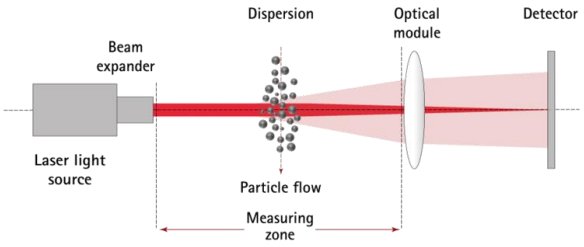

INTRODUCTION

- Pandemics & COVID-19 Current Situation
- Size of Particles and Viruses
- Transmission Pathway
- Particle Measurement Techniques
- Ventilation Types
- New Ambulances for Respiratory Disease

Mixing Ventilation

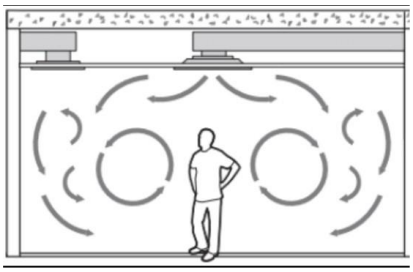

Displacement Ventilation

Natural Ventilation

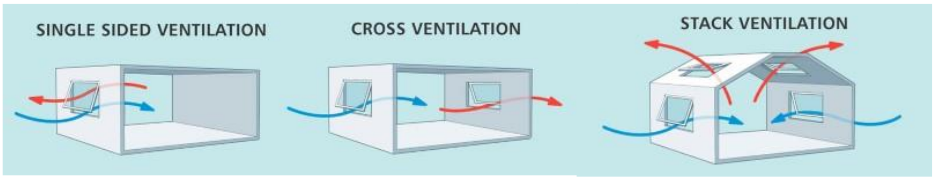

INTRODUCTION

- Pandemics & COVID-19 Current Situation
- Size of Particles and Viruses
- Transmission Pathway
- Particle Measurement Techniques
- Ventilation Types
- New Ambulances for Respiratory Disease

NEW AMBULANCES FOR RESPIRATORY DISEASE

- Negative Pressure Patient Compartment
- Ventilation System with Filter
- Isolation Tent

LITERATURE REVIEW

- Number and Size of Particles
- How far can particles spread and how long can they remain?
- Size and Severity of Infection
- Protection Equipment and Protection Method
- Risks of medical personnel working in an ambulance
- Ambulance Ventilation System

18

Breathing

Coughing

LITERATURE REVIEW

- Number and Size of Particles
  - Gupta et al. (2010)
  - Graton et al. (2011)
  - Fernstrom & Goldblatt (2013)

19

LITERATURE REVIEW

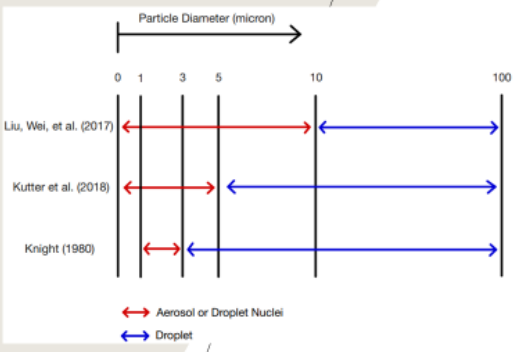

- How far can particles spread and how long can they remain?
  - Knight (1980)
  - Liu, Li et al. (2017)
  - Liu, Wei et al. (2017)
  - Kutter et al. (2018)

20

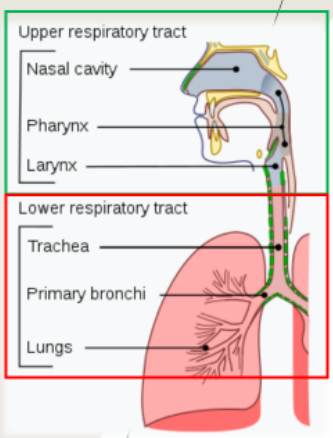

LITERATURE REVIEW

- Size and Severity of Infection
  - Alford et al. (1966)
  - Thomas (2013)
  - Wonderlich et al. (2017)
  - Kutter et al. (2018)

21

STANDARDS FOR AEROSOL PARTICLES AND DROPLETS

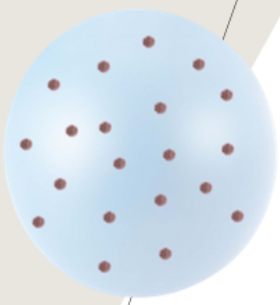

- Centers for Disease Control and Prevention (CDC)
- World Health Organization (WHO)

Droplet Particle > 5 microns

Aerosol Particle ≤ 5 microns

22

LITERATURE REVIEW

- Protection Equipment and Protection Method
  - Willeke et al. (1996)
  - Belkin (1997)
  - Escombe et al. (2007)
  - Lindsley et al. (2014)
  - Bhagat et al. (2020)

23

STANDARDS FOR BUILDING VENTILATION SYSTEM

- American Society of Heating, Refrigerating and Air-Conditioning Engineers (ASHRAE)

Function of Space (ee)	Pressure Relationship to Adjacent Areas (n)	Minimum Outdoor ach	Minimum Total ach	All Room Air Exhausted Directly to Outdoors (j)
NURSING UNITS AND OTHER PATIENT CARE AREAS				
AII anteroom (2.1–2.4.2.3) (u)	(e)	NR	10	Yes
AII room (2.1–2.4.2) (u)	Negative	2	12	Yes

24

LITERATURE REVIEW

- Risks of medical personnel working in an ambulance
  - Pipitsangjan et al. (2011)
  - Sayed et al. (2011)
  - Hudson et al. (2018)
  - Gibson (2019)

25

LITERATURE REVIEW

- Ambulance Ventilation System
  - Lindsley et al. (2019)

26

SUMMARY ON INTRODUCTION AND LITERATURE REVIEW

- The study looked at carrier particles, not viruses

RESEARCH INSTRUMENTS

Ambulance (Toyota Ventury)
CC 410-Concealed Air Purifier
Oxylog® 3000 plus
Aeroneb® Professional Nebulizer
0.9% Sodium Chloride Solution
PMS5003 G5 (with GM1705A01 pin adapter module)
Arduino UNO R3 SMD (CH340G)

AMBULANCE (TOYOTA VENTURY)

AMBULANCE (TOYOTA VENTURY)

Oxylog® 3000 plus

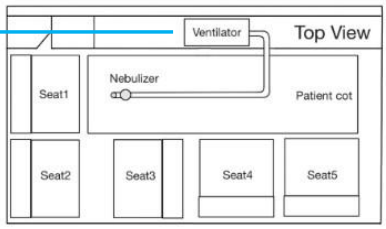

PMS5003 G5

Arduino UNO R3

Aeroneb® Professional Nebulizer

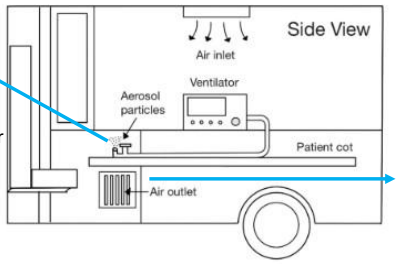

0.9% Sodium Chloride Solution

CC 410-Concealed Air Purifier

PMS5003 G5

Detect Liquid Particle

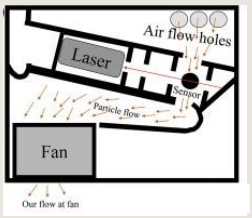

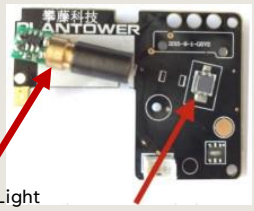

Laser Light Source

Photodiode Detector

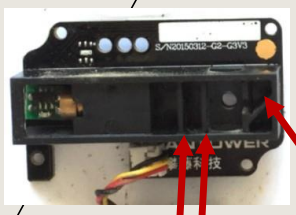

Light Baffles

Light Trap

PMS 5003 CALIBRATION

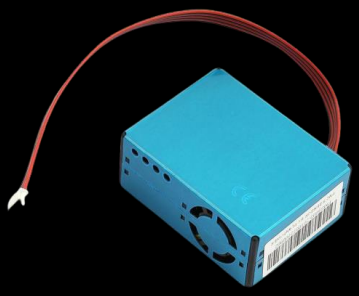

PMS 5003 G5

VS

HANDHELD 3016

Meets ISO 21501-4 calibration using NIST traceable PSL spheres

CALIBRATION PROCEDURE

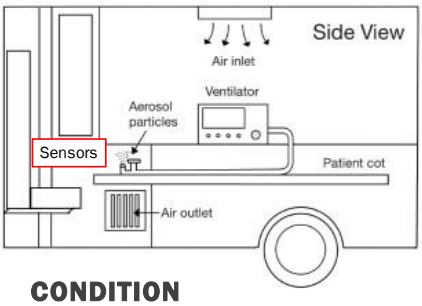

CONDITION

- Turn on air conditioner at 25 °C with all air grilles at the centre position

PRECONDITION

- Turn on ventilation system at maximum rate for 15 minutes for normalizing the number of particles in the patient compartment to the background level

PROCEDURES

- Turn on PMS5003 and Handheld3016 in adjacent to log data at the same time
- After 3 minute, turn on nebulizer to introduce particles into the ambulance for 1 minute
- Log data for 15 more minutes

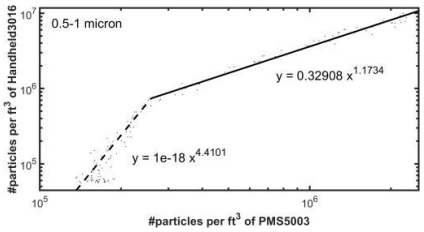

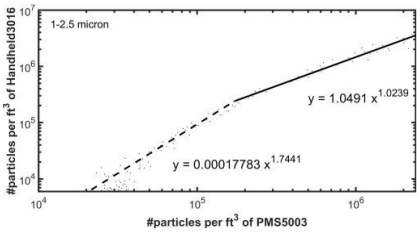

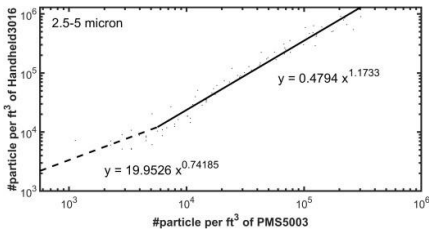

CALIBRATION CURVE

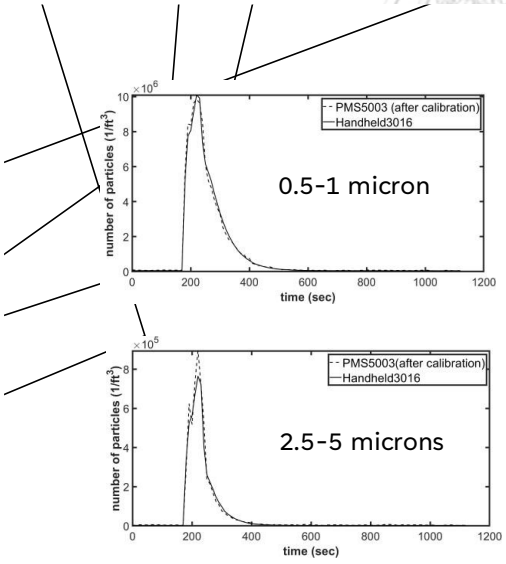

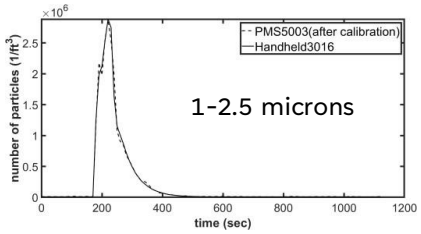

PMS5003 AFTER CALIBRATION

EXPERIMENTS

37

EXPERIMENT SETUP

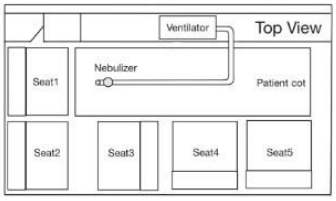

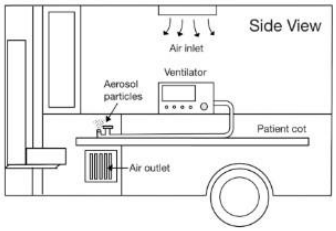

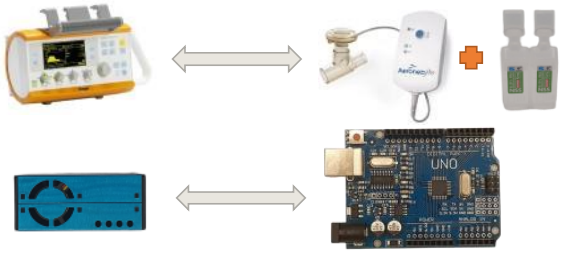

CONDITION

- Turn on air conditioner at 25 °C with all air grilles at the centre position
- Turn on oxylog 3000 plus, choose VC-CMV mode, set tidal volume (VT) to 500 mL, ventilation time ratio (I:E) to 1:2 and adjust respiratory rate (RR) to 12
- Inspiratory time (Ti) is 1.7 seconds

MEASURING POSITIONS

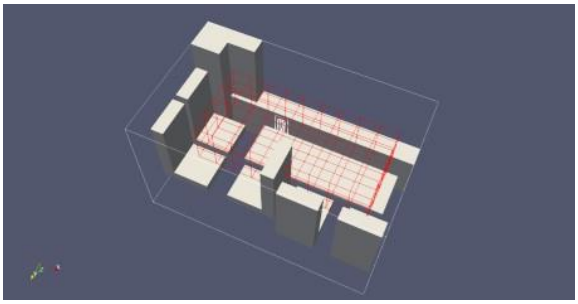

EXPERIMENTS

(PERFORMED THREE TIMES FOR EACH CASE)

MINIMAL

VERY LOW ACH

turning off the ventilation system

HIGH

80 ACH

turning on the ventilation system at level 6

TURNING OFF THE VENTILATION SYSTEM

CONDITION

- Turn on air conditioner at 25 °C with all air grilles at the centre position

PRECONDITION

- Turn on ventilation system at maximum rate (level 6) for 15 minutes to let the number of particles concentration in the patient compartment return to the background state
- Turn off the ventilation system and let the air in the patient compartment stabilize for 5 minutes

MEASUREMENT

- Turn on PMS5003 to log data
- After 1 minutes, turn on nebulizer to introduce particles into the patient compartment for 1 minute
- After that log data for 18 minutes

TURNING ON THE VENTILATION SYSTEM AT LEVEL 6 (HIGH)

CONDITION

- Turn on air conditioner at 25 °C with all air grilles at the centre position

PRECONDITION

- Turn on ventilation system at maximum rate (level6) for 15 minutes to let the number of particles concentration in the patient compartment return to the background state
- No need to let the air in the patient compartment stabilize

MEASUREMENT

- Turn on PMS5003 to log data
- After 1 minutes, turn on nebulizer to introduce particles into the patient compartment for 1 minute
- After that log data for 8 minutes

DATA ANALYSIS

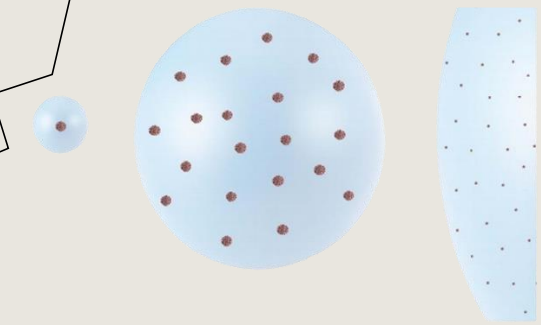

D = 0.5 μm D = 2 μm D = 100 μm

Herrmann et al. (2020)

- Zuo et al. (2013)
- Lindsley et al. (2019)

DATA ANALYSIS

$$\sigma = 4.71 \times 10^{-8} N \pi r^3$$

σ is volume concentration ($\mu L/m^3$)

N is number of particles ($1/ft^3$)

r is mean radius in each size bin (μm)

DATA ANALYSIS

Log-Normal Particle Size Distribution

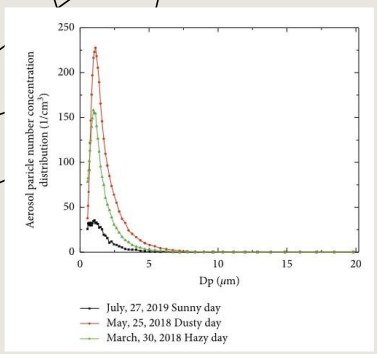

Yali et al. (2020)

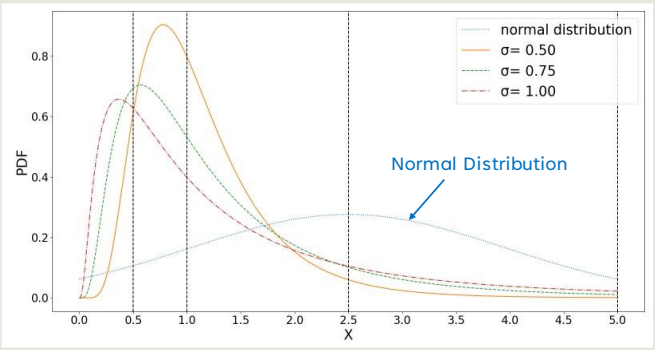

Log-Normal Distribution (Plot by Python)

DATA ANALYSIS

Average Number of Particles from Measurement → Particle Volume Concentration → Cubic Spline Interpolation in Time → Window Moving Average → Cubic Spline Interpolation in Space (3 dimension) → Remove Background Value

DATA ANALYSIS

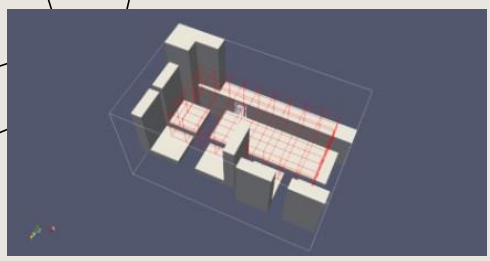

200 POINTS

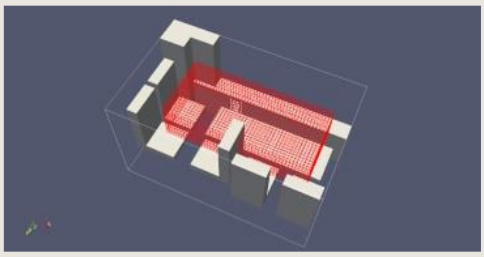

12558 POITNS

DATA ANALYSIS

ParaView

VTK

RESULTS

RESULTS

- THREE-DIMENSIONAL VISUALIZATION
- HORIZONTAL CONTOUR PLANE AT FACE LEVEL OF EMS WORKERS
- VERTICAL CONTOUR PLANE AT INJECTION POSITION ALONG PATIENT COT
- SPATIAL-AVERAGED AEROSOL VOLUME CONCENTRATION OVER TIME
- AEROSOL VOLUME CONCENTRATION OVER TIME AT EMS WORKERS' FACE
- MAXIMUM AEROSOL VOLUME CONCENTRATION AT EMS WORKERS' FACE
- TEMPORAL-AVERAGED AEROSOL VOLUME CONCENTRATION AT EMS WORKERS' FACE

MINIMAL VENTILATION CASE (MV: VERY LOW ACH)

HIGH VENTILATION CASE (HV: ROUGHLY 80 ACH)

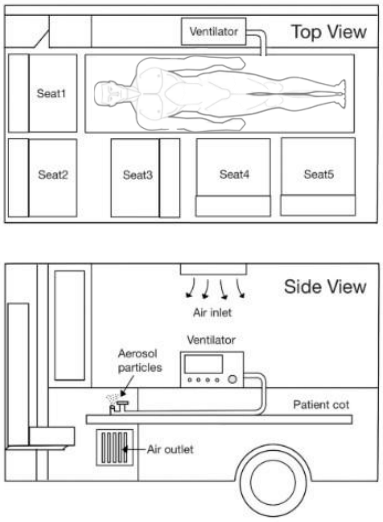

RESULTS

- ❖ THREE-DIMENSIONAL VISUALIZATION
- ❖ HORIZONTAL CONTOUR PLANE AT FACE LEVEL OF EMS WORKERS
- ❖ VERTICAL CONTOUR PLANE AT INJECTION POSITION ALONG PATIENT COT
- ❖ SPATIAL-AVERAGED AEROSOL VOLUME CONCENTRATION OVER TIME
- ❖ AEROSOL VOLUME CONCENTRATION OVER TIME AT EMS WORKERS' FACE
- ❖ MAXIMUM AEROSOL VOLUME CONCENTRATION AT EMS WORKERS' FACE
- ❖ TEMPORAL-AVERAGED AEROSOL VOLUME CONCENTRATION AT EMS WORKERS' FACE

Three-dimensional visualization

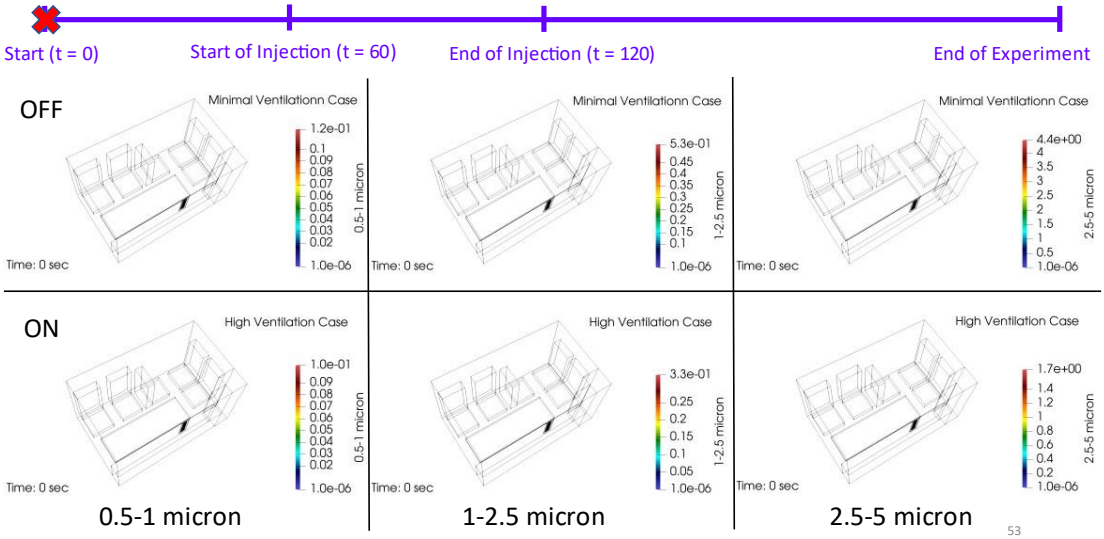

53

Three-dimensional visualization

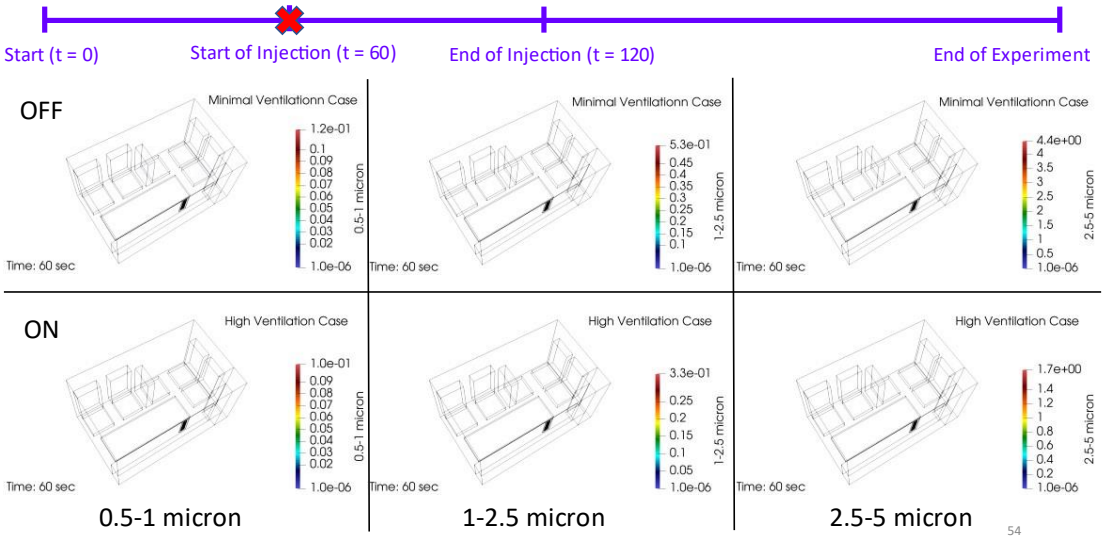

54

Three-dimensional visualization

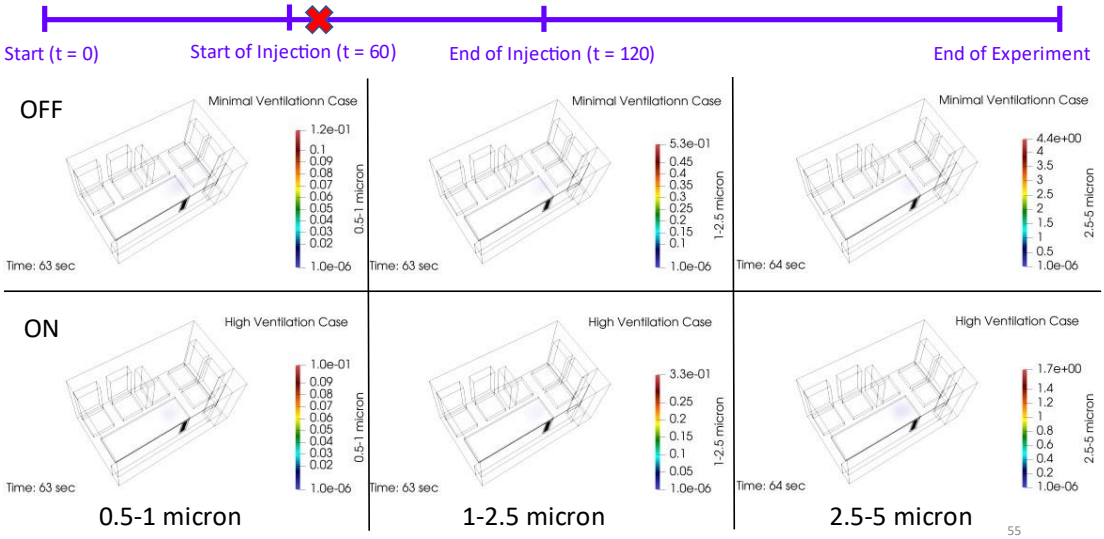

55

Three-dimensional visualization

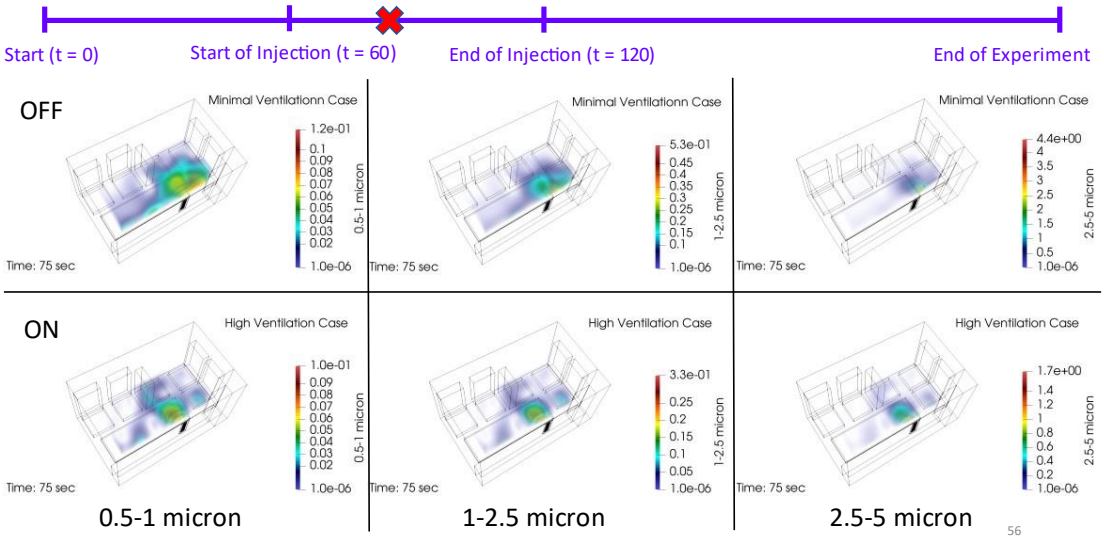

56

Three-dimensional visualization

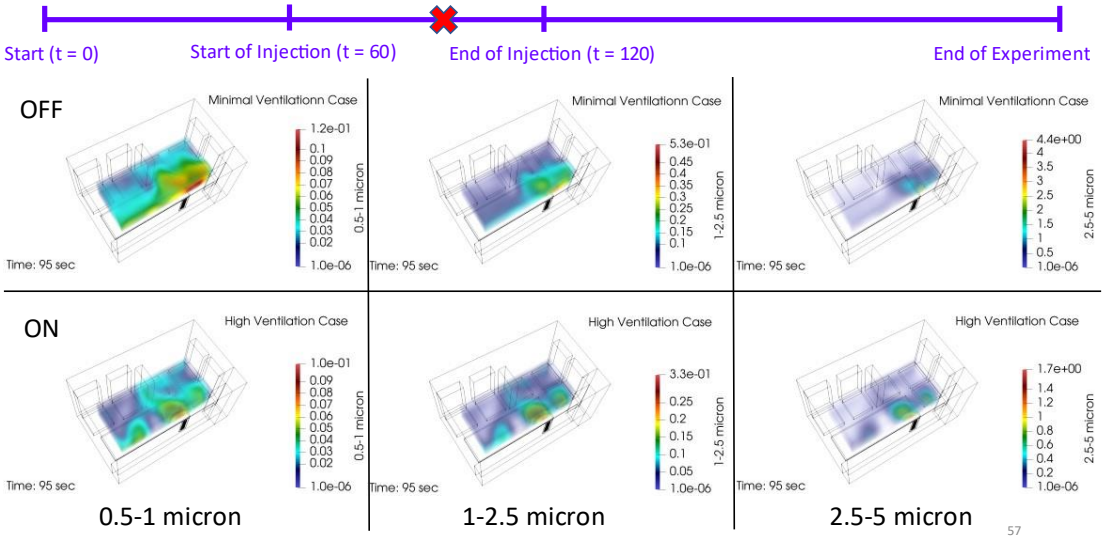

57

Three-dimensional visualization

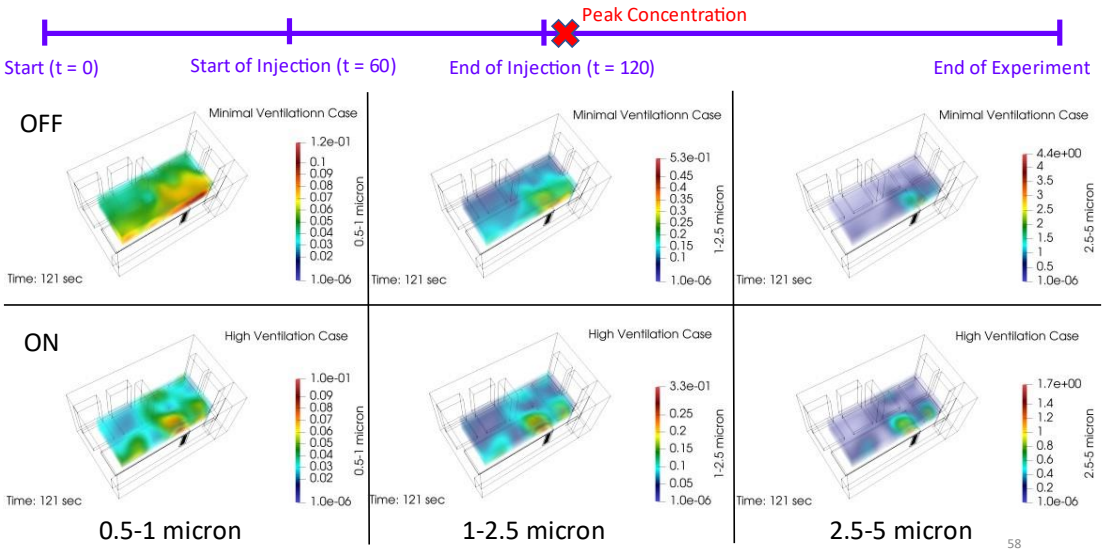

58

Three-dimensional visualization

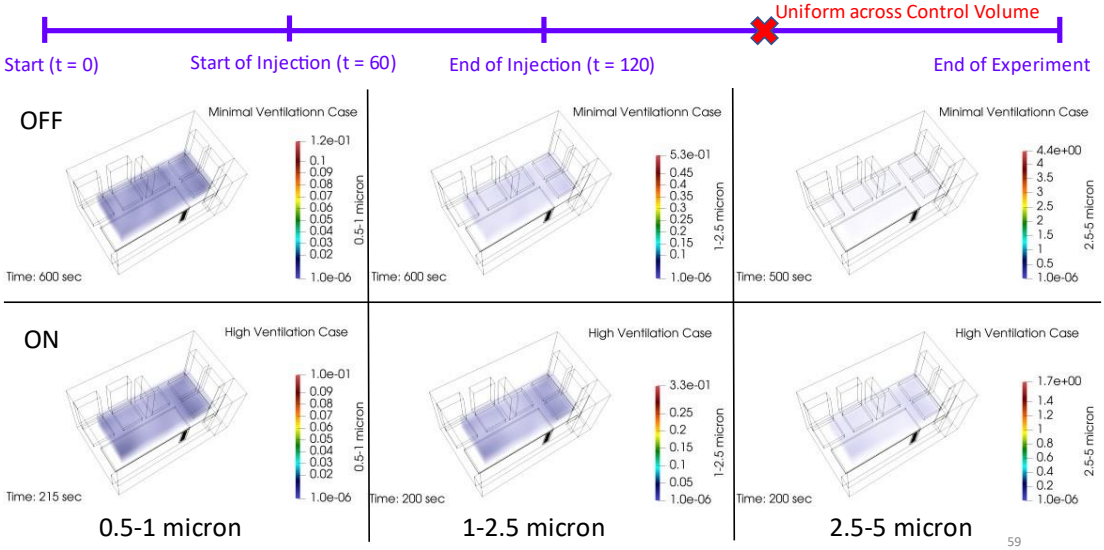

59

Three-dimensional visualization

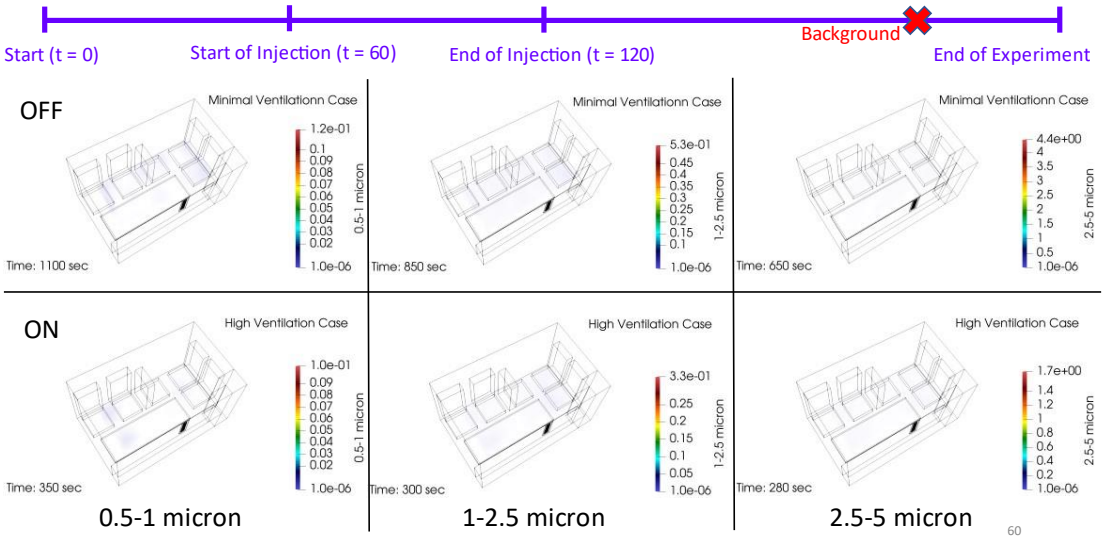

60

THREE-DIMENSIONAL VISUALIZATION

(summary)

➢ **Both Ventilation Rates**

- cloud of aerosols occurs at above patient face in control volume only a few seconds after the start of injection
- smaller-size particles have a relatively wider distribution area than larger particles (injection period)
- peak concentration throughout the experiment occurs immediately after the stop of injection

➢ **Minimal Ventilation:**

- local peak concentration is in the area above patient face and seat 1 (during injection period)
- larger-size particles is found to decay relatively faster
- it takes approximately 9 minutes for 2.5-5 microns, 12 minutes for 1-2.5 microns, and 16 minutes for 0.5-1 microns (after injection period is stopped) to become comparable to background state

➢ **High Ventilation:**

- local peak concentration is in the area adjacent to the exhaust outlet (during injection period)
- the return to background time is approximately 3 minutes for 2.5-5 microns, 3 minutes for 1-2.5 microns, and 4 minutes for 0.5-1 microns (after injection period is stopped)

RESULTS

- ❖ THREE-DIMENSIONAL VISUALIZATION
- ❖ HORIZONTAL CONTOUR PLANE AT FACE LEVEL OF EMS WORKERS
- ❖ VERTICAL CONTOUR PLANE AT INJECTION POSITION ALONG PATIENT COT
- ❖ SPATIAL-AVERAGED AEROSOL VOLUME CONCENTRATION OVER TIME
- ❖ AEROSOL VOLUME CONCENTRATION OVER TIME AT EMS WORKERS' FACE
- ❖ MAXIMUM AEROSOL VOLUME CONCENTRATION AT EMS WORKERS' FACE
- ❖ TEMPORAL-AVERAGED AEROSOL VOLUME CONCENTRATION AT EMS WORKERS' FACE

Horizontal Contour Plane at Face Level of EMS workers

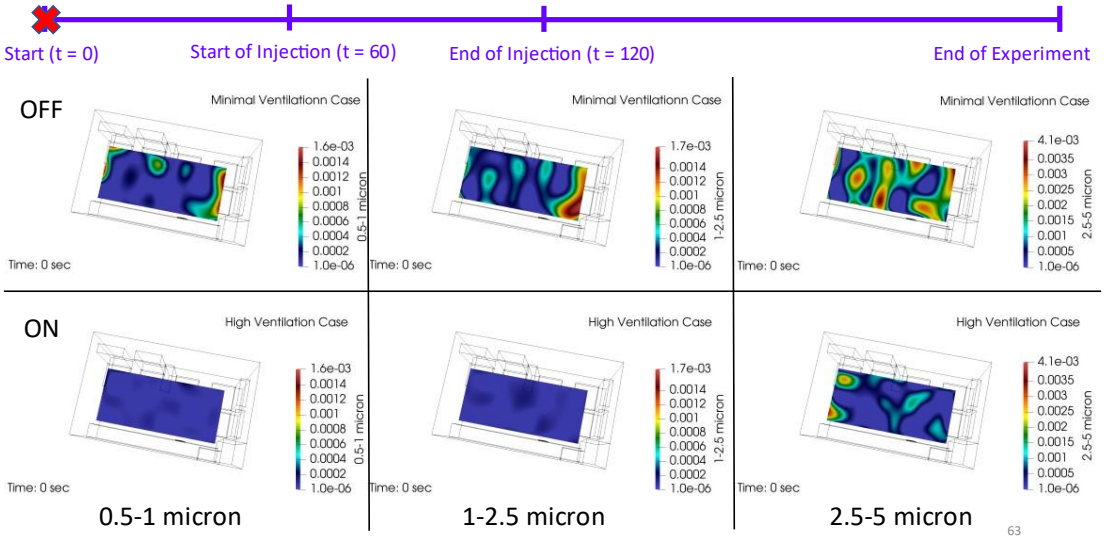

63

Horizontal Contour Plane at Face Level of EMS workers

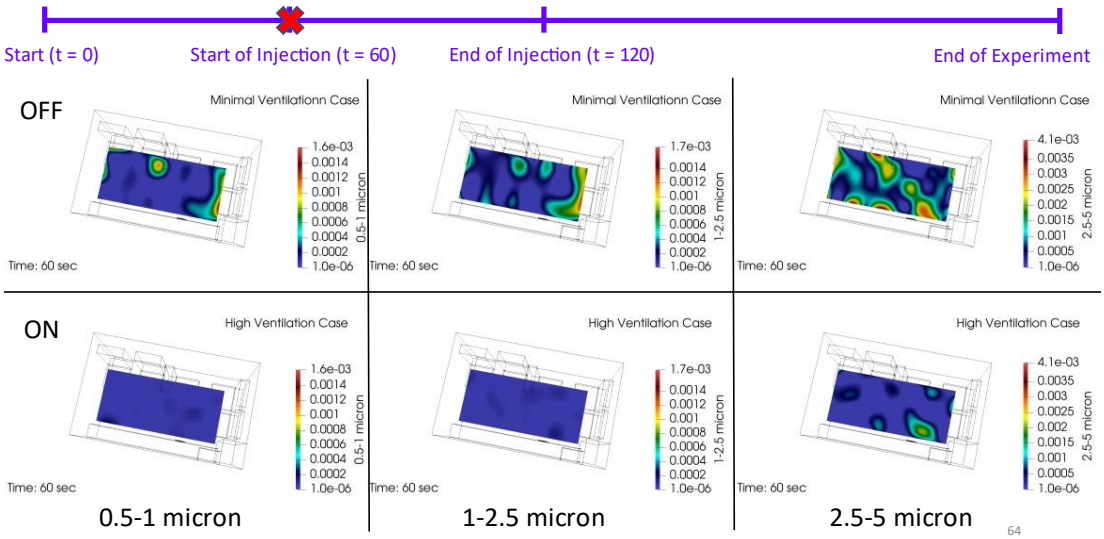

64

Horizontal Contour Plane at Face Level of EMS workers

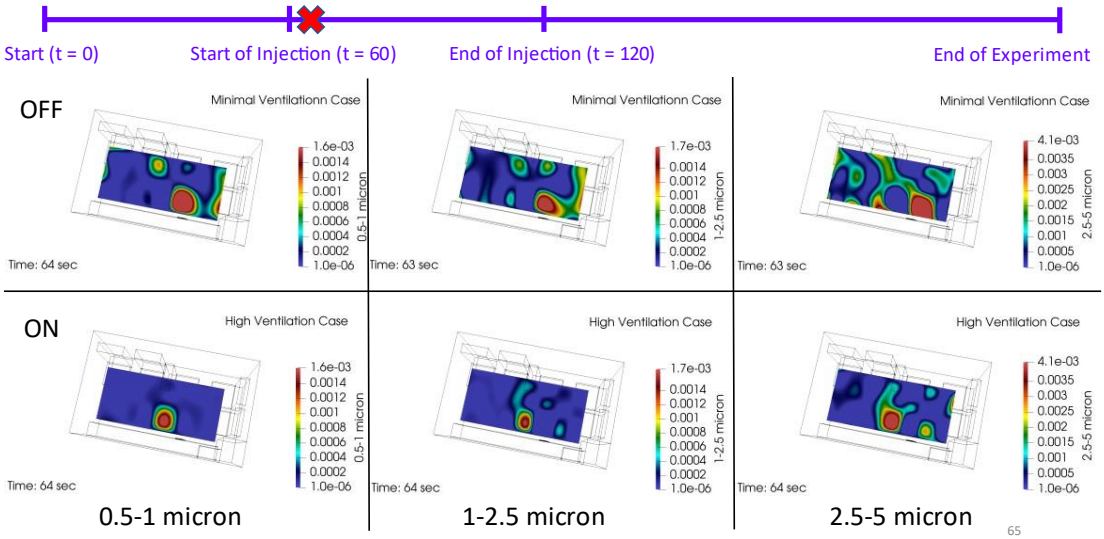

65

Horizontal Contour Plane at Face Level of EMS workers

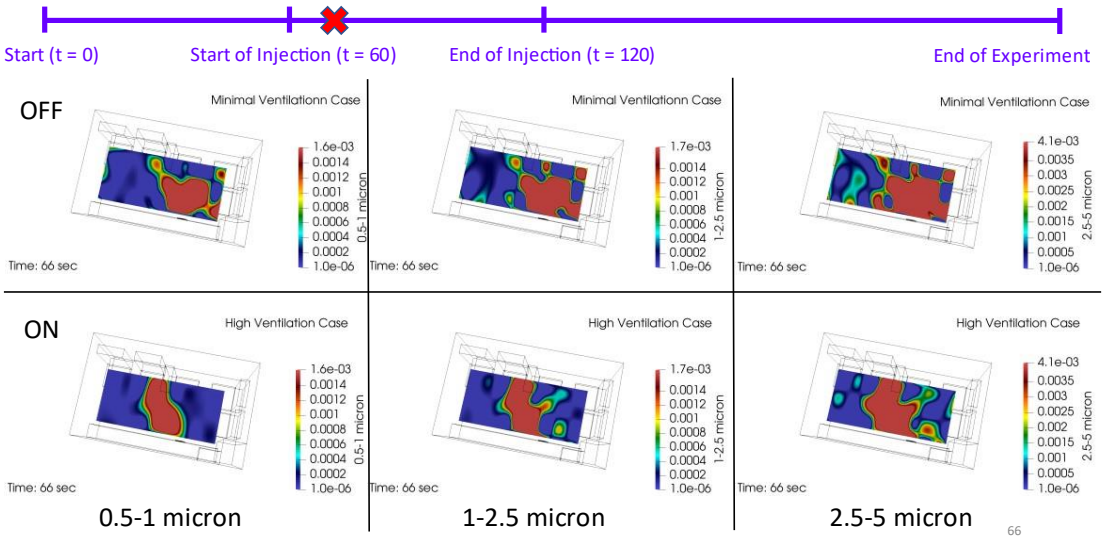

66

Horizontal Contour Plane at Face Level of EMS workers

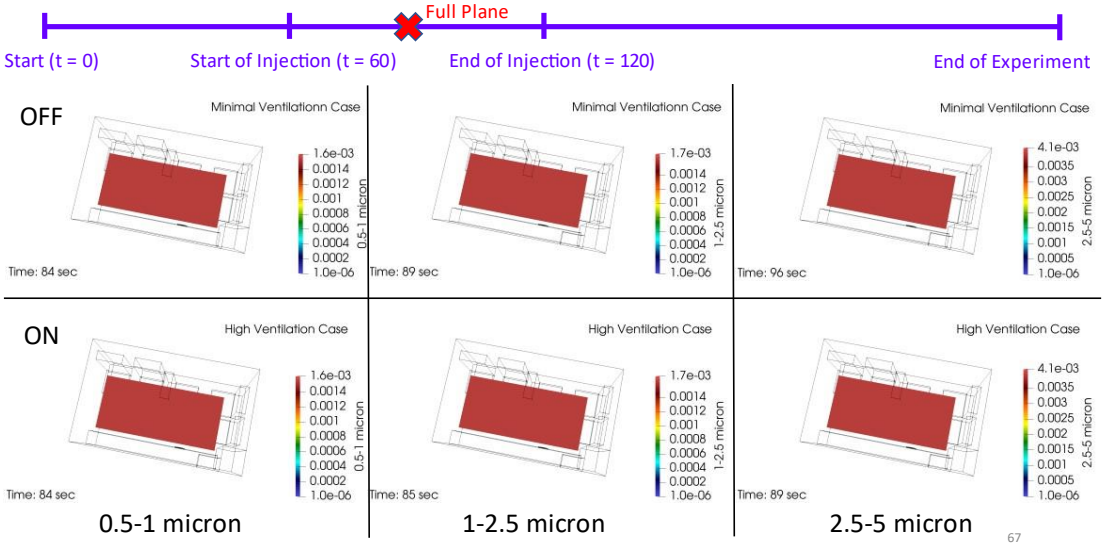

67

Horizontal Contour Plane at Face Level of EMS workers

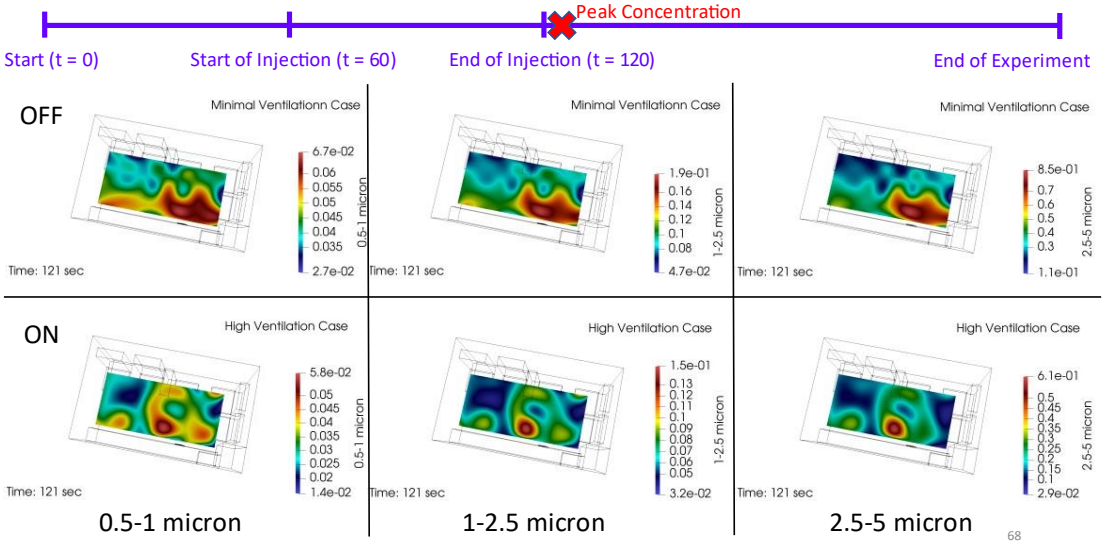

68

Horizontal Contour Plane at Face Level of EMS workers

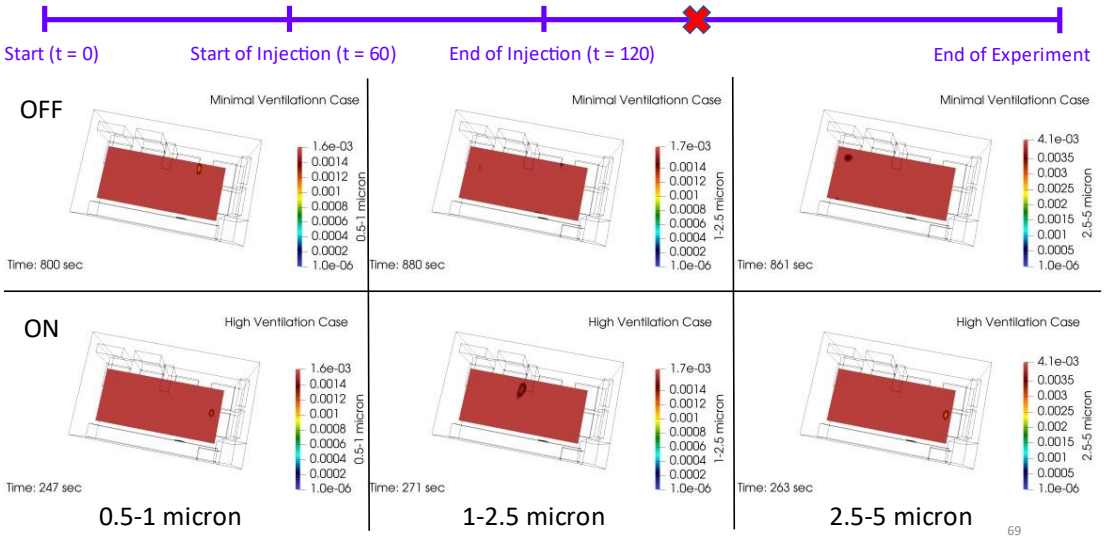

69

Horizontal Contour Plane at Face Level of EMS workers

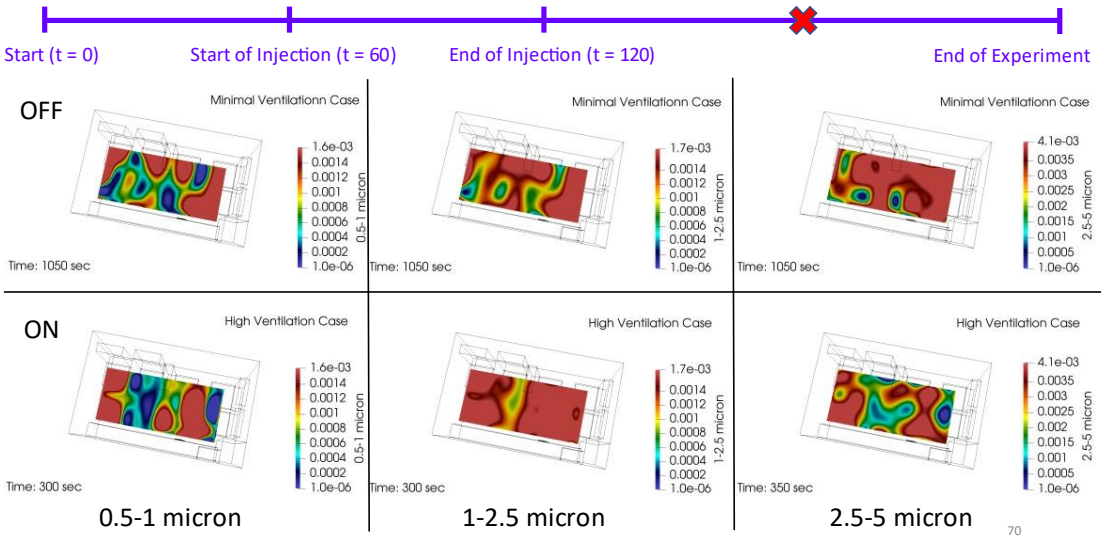

70

Horizontal Contour Plane at Face Level of EMS workers

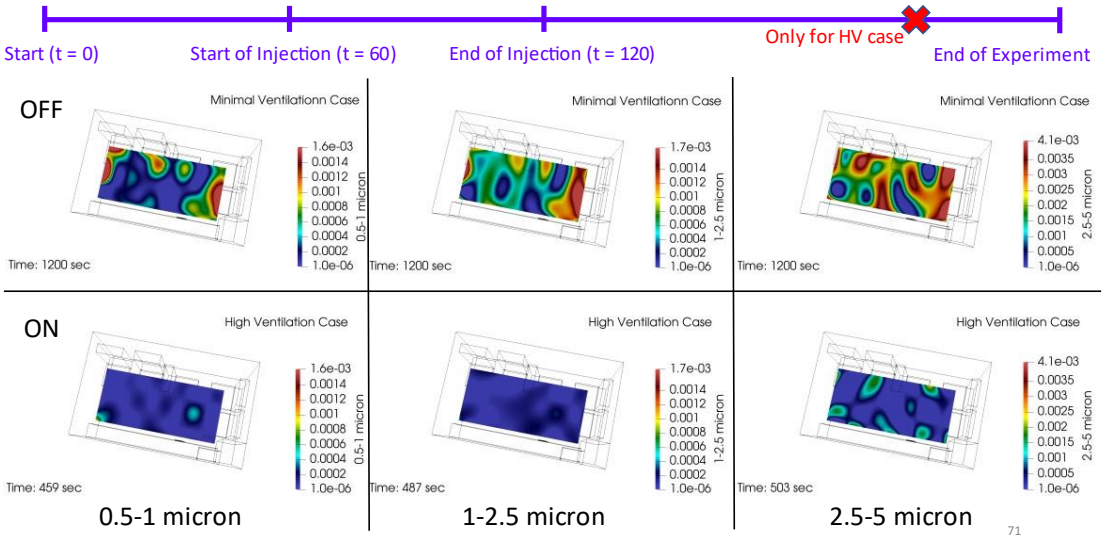

71

HORIZONTAL CONTOUR PLANE AT FACE LEVEL OF EMS WORKERS

(summary)

- **Both Ventilation Rates**
  - high concentration compared to other areas occurs on plane at above patient face only a few seconds after the start of injection
- **Minimal Ventilation:**
  - high concentration compared to other regions is at frontal part of the cabin (seat 1 to seat 4) (during injection period)
  - not return to background state the entire plane
- **High Ventilation:**
  - high concentration compared to other regions mainly distributes in the middle of the cabin (seat 4) (during injection period)
  - the return to background time is approximately 6 minutes for all size ranges (after injection period is stopped)

RESULTS

- THREE-DIMENSIONAL VISUALIZATION
- HORIZONTAL CONTOUR PLANE AT FACE LEVEL OF EMS WORKERS
- VERTICAL CONTOUR PLANE AT INJECTION POSITION ALONG PATIENT COT
- SPATIAL-AVERAGED AEROSOL VOLUME CONCENTRATION OVER TIME
- AEROSOL VOLUME CONCENTRATION OVER TIME AT EMS WORKERS' FACE
- MAXIMUM AEROSOL VOLUME CONCENTRATION AT EMS WORKERS' FACE
- TEMPORAL-AVERAGED AEROSOL VOLUME CONCENTRATION AT EMS WORKERS' FACE

Vertical Contour Plane at Injection Position along Patient Cot

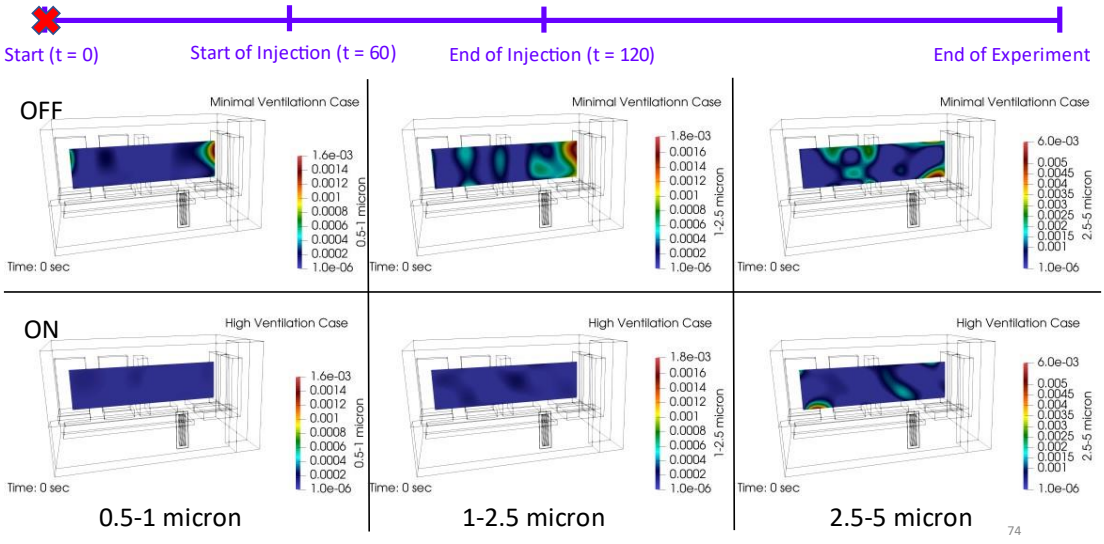

Vertical Contour Plane at Injection Positionalong Patient Cot

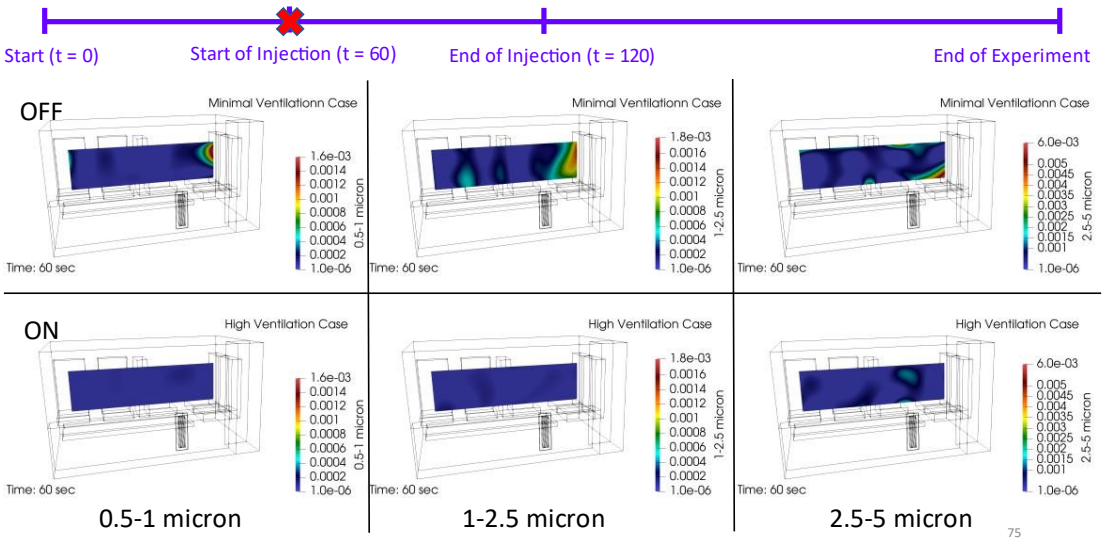

Vertical Contour Plane at Injection Positionalong Patient Cot

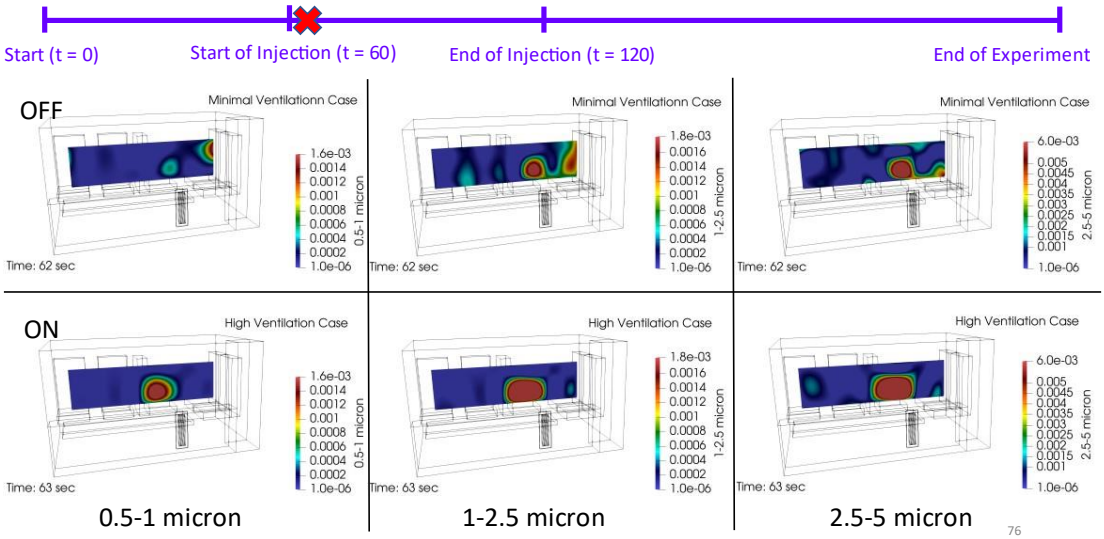

Vertical Contour Plane at Injection Positionalong Patient Cot

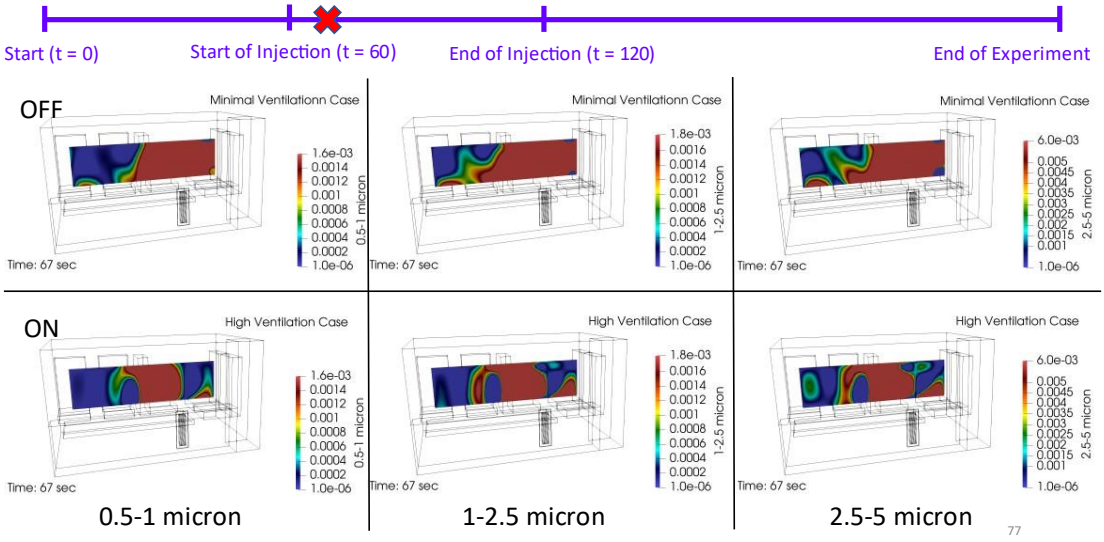

77

Vertical Contour Plane at Injection Positionalong Patient Cot

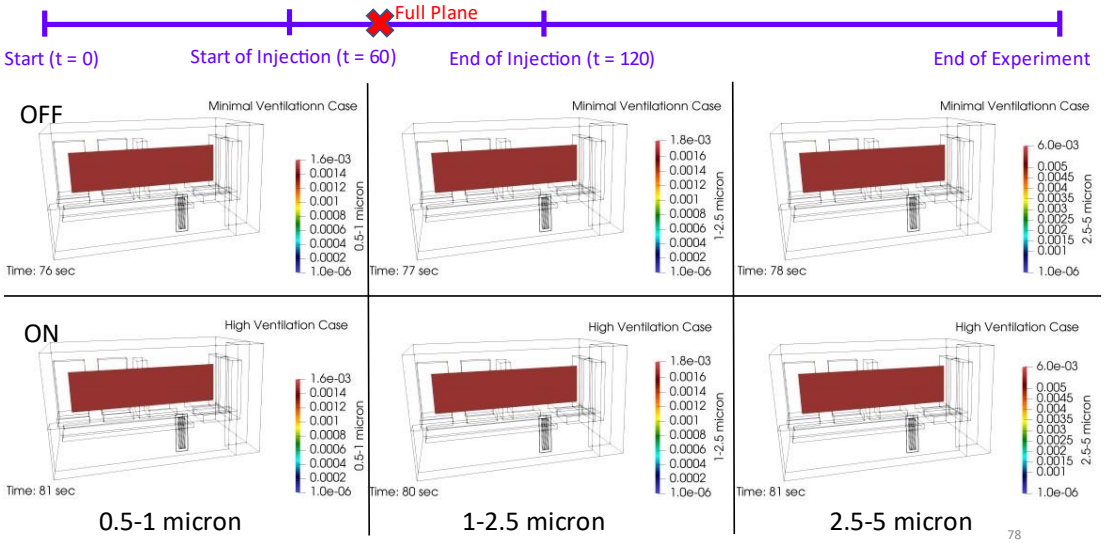

78

Vertical Contour Plane at Injection Positionalong Patient Cot

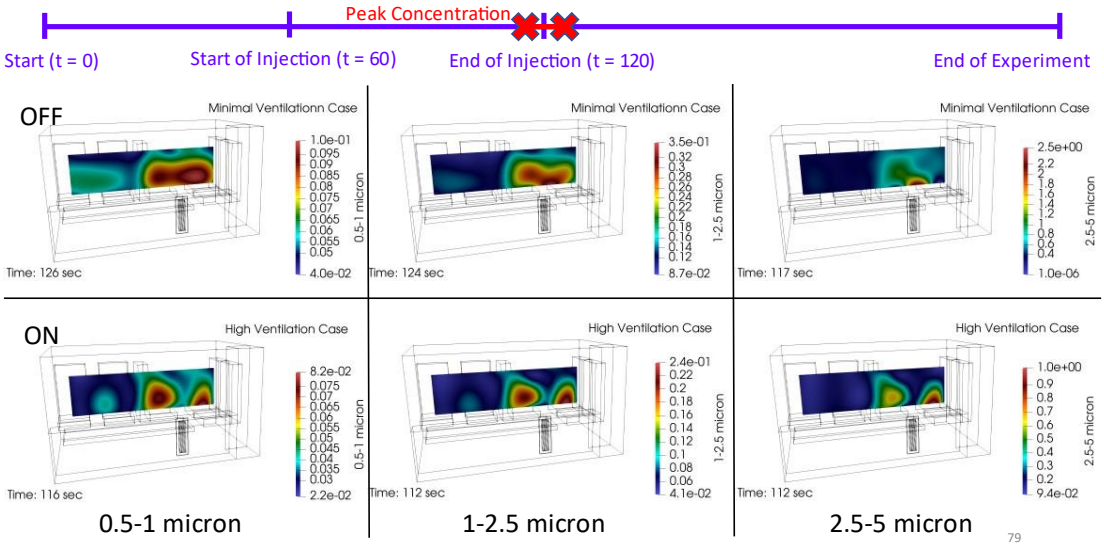

79

Vertical Contour Plane at Injection Positionalong Patient Cot

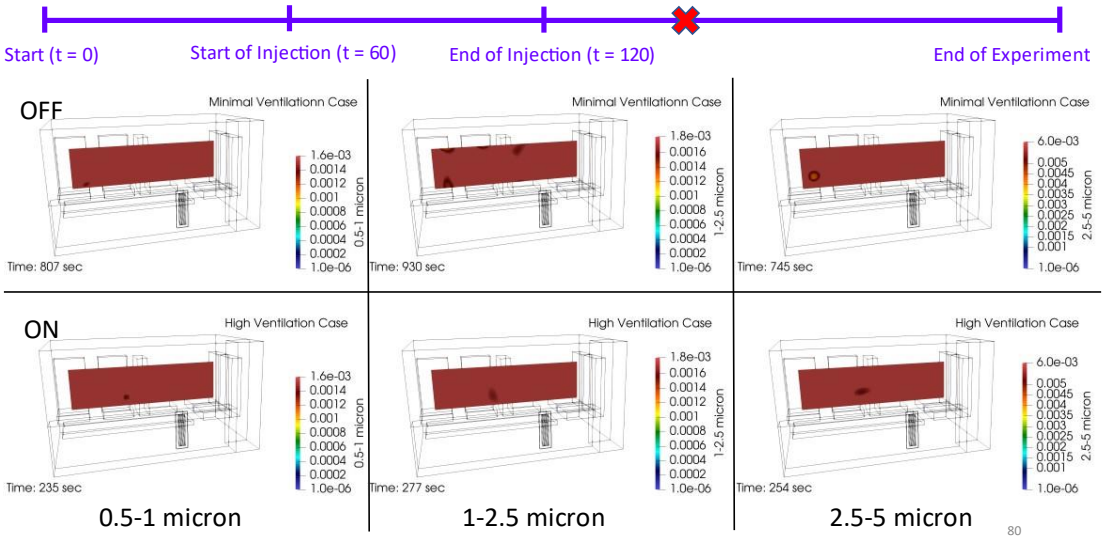

80

Vertical Contour Plane at Injection Positionalong Patient Cot

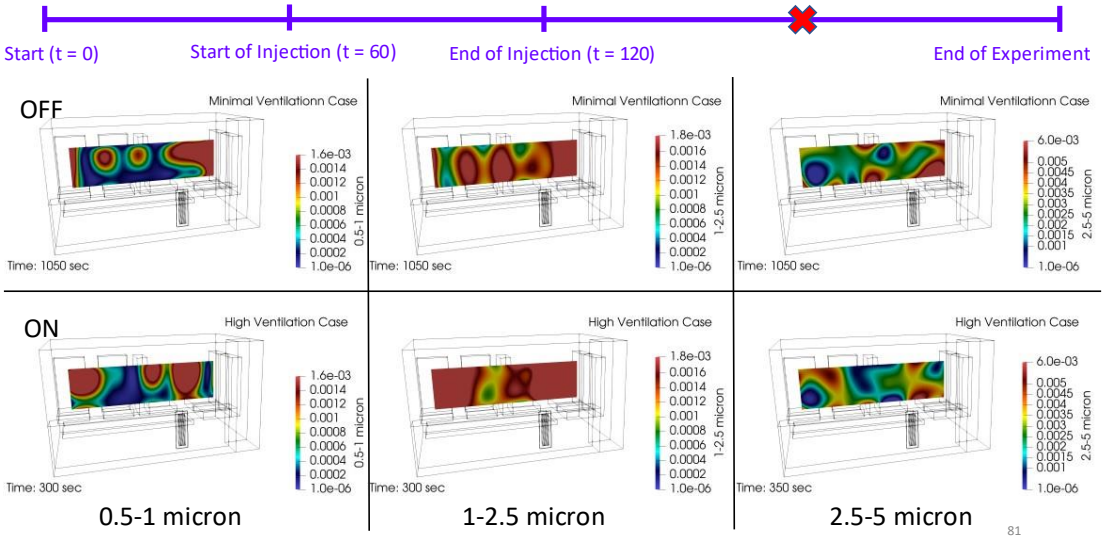

81

Vertical Contour Plane at Injection Positionalong Patient Cot

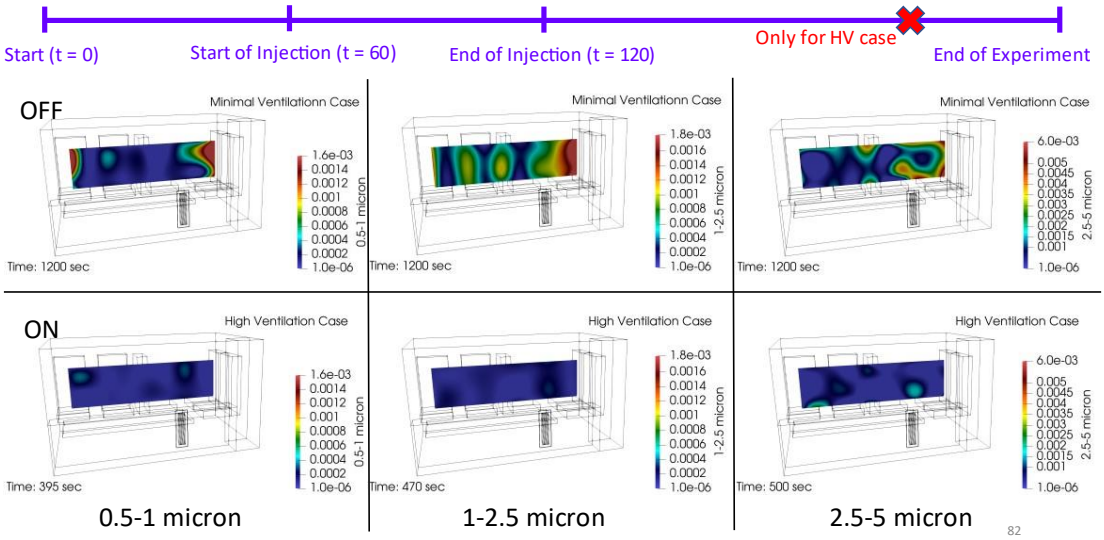

82

VERTICAL CONTOUR PLANE AT INJECTION POSITION ALONG PATIENT COT

(summary)

- **Both Ventilation Rates**
  - high concentration compared to other areas occurs on plane at above patient face only a few seconds after the start of injection
- **Minimal Ventilation:**
  - high concentration compared to other regions is at frontal part of the cabin (during injection period)
  - not return to background state the entire plane
- **High Ventilation:**
  - high concentration compared to other regions mainly distributes in the middle of the cabin (during injection period)
  - the return to background time is approximately 6 minutes for all size ranges (after injection period is stopped)

RESULTS

- THREE-DIMENSIONAL VISUALIZATION
- HORIZONTAL CONTOUR PLANE AT FACE LEVEL OF EMS WORKERS
- VERTICAL CONTOUR PLANE AT INJECTION POSITION ALONG PATIENT COT
- SPATIAL-AVERAGED AEROSOL VOLUME CONCENTRATION OVER TIME
- AEROSOL VOLUME CONCENTRATION OVER TIME AT EMS WORKERS' FACE
- MAXIMUM AEROSOL VOLUME CONCENTRATION AT EMS WORKERS' FACE
- TEMPORAL-AVERAGED AEROSOL VOLUME CONCENTRATION AT EMS WORKERS' FACE

SPATIAL-AVERAGED AEROSOL VOLUME CONCENTRATION OVER TIME

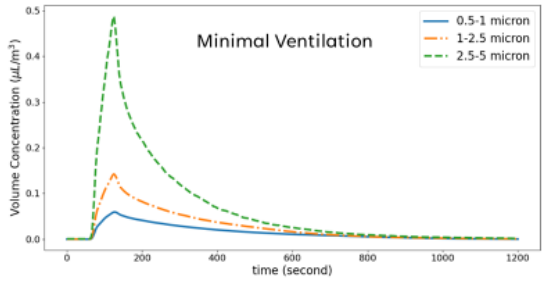

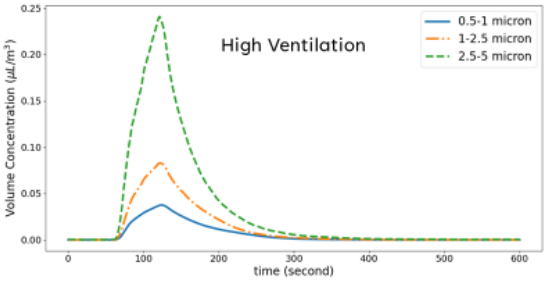

SPATIAL-AVERAGED AEROSOL VOLUME CONCENTRATION OVER TIME

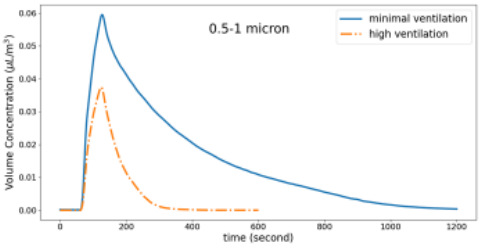

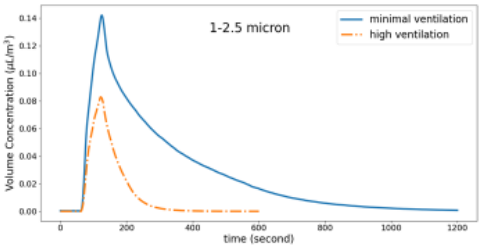

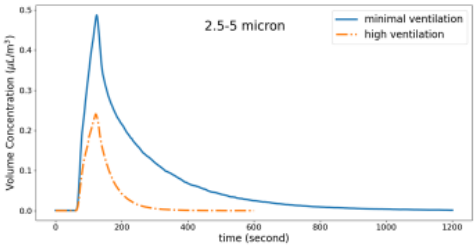

SPATIAL-AVERAGED AEROSOL VOLUME CONCENTRATION OVER TIME

(summary)

- the decay is exponential
- turning on the air exhaust system results in decreasing in peak aerosol volume concentration about 2 times
- reduction rate is directly proportional to particle size, larger-size particles is found to decay relatively faster
- the minimal ventilation case return to background time is approximately 15 minutes for all size ranges (after injection period is stopped)
- the high ventilation case return to background time is approximately 4 minutes for all size ranges (after injection period is stopped)

RESULTS

- THREE-DIMENSIONAL VISUALIZATION
- HORIZONTAL CONTOUR PLANE AT FACE LEVEL OF EMS WORKERS
- VERTICAL CONTOUR PLANE AT INJECTION POSITION ALONG PATIENT COT
- SPATIAL-AVERAGED AEROSOL VOLUME CONCENTRATION OVER TIME
- AEROSOL VOLUME CONCENTRATION OVER TIME AT EMS WORKERS' FACE
- MAXIMUM AEROSOL VOLUME CONCENTRATION AT EMS WORKERS' FACE
- TEMPORAL-AVERAGED AEROSOL VOLUME CONCENTRATION AT EMS WORKERS' FACE

AEROSOL VOLUME CONCENTRATION OVER TIME AT EMS WORKERS' FACE

SEAT 1

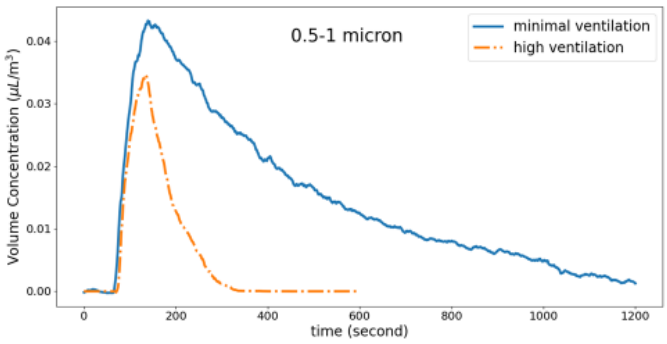

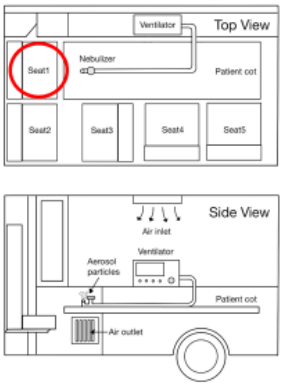

AEROSOL VOLUME CONCENTRATION OVER TIME AT EMS WORKERS' FACE

SEAT 2

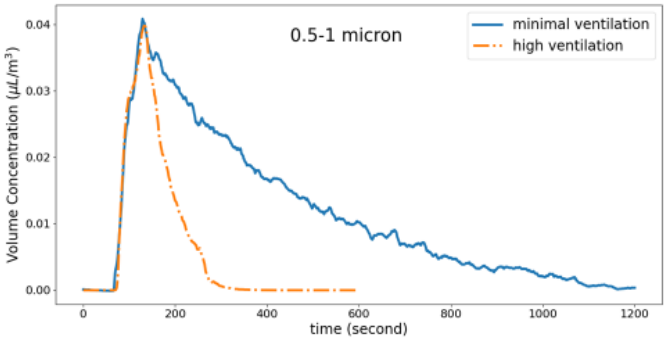

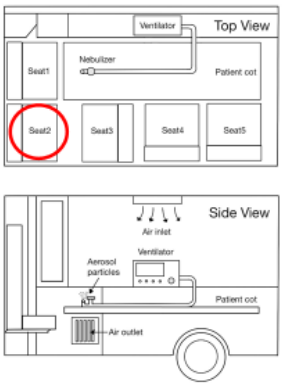

AEROSOL VOLUME CONCENTRATION OVER TIME AT EMS WORKERS' FACE

SEAT 3

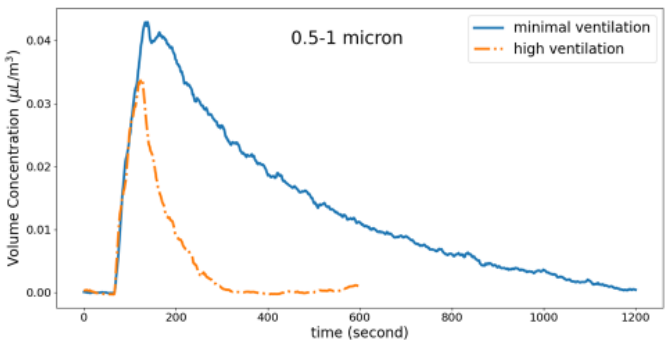

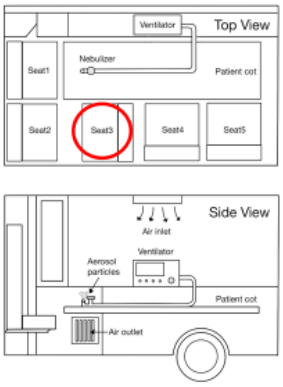

AEROSOL VOLUME CONCENTRATION OVER TIME AT EMS WORKERS' FACE

SEAT 4

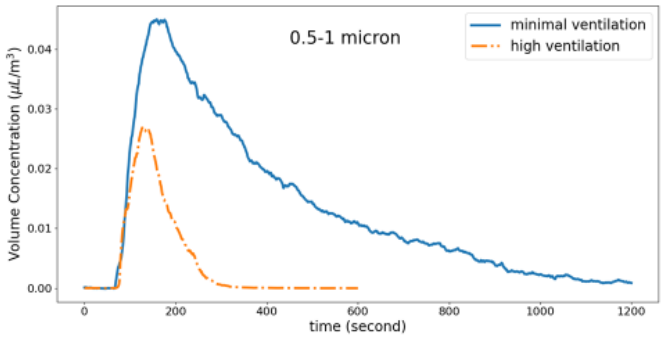

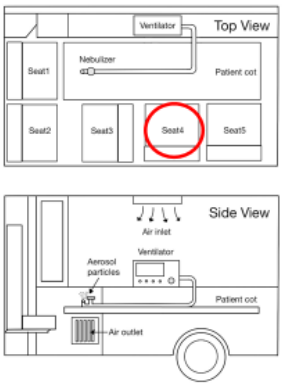

AEROSOL VOLUME CONCENTRATION OVER TIME AT EMS WORKERS' FACE

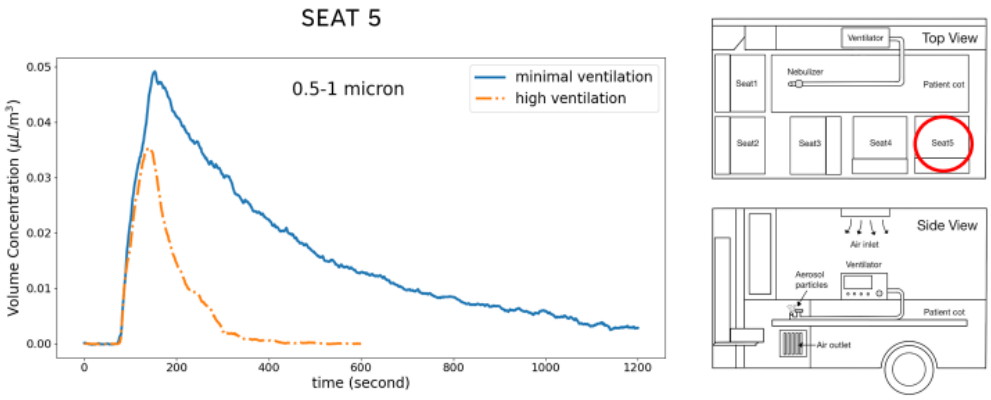

RETURN- TO-BACKGROUND TIME (SECOND)

(time is measured at the start of injection)

Seat 1		
Size Range (micron) \ Ventilation Rate	MV	HV
0.5-1	-	290
1-2.5	-	340
2.5-5	1040	260

Seat 2		
Size Range (micron) \ Ventilation Rate	MV	HV
0.5-1	1100	290
1-2.5	1140	350
2.5-5	960	420

Seat 3		
Size Range (micron) \ Ventilation Rate	MV	HV
0.5-1	-	280
1-2.5	1120	340
2.5-5	1120	290

Seat 4		
Size Range (micron) \ Ventilation Rate	MV	HV
0.5-1	-	290
1-2.5	1140	300
2.5-5	1120	290

Seat 5		
Size Range (micron) \ Ventilation Rate	MV	HV
0.5-1	-	350
1-2.5	-	340
2.5-5	1120	330

AEROSOL VOLUME CONCENTRATION OVER TIME AT EMS WORKERS' FACE

(summary)

- the decay is exponential
- the minimal ventilation case return to background time is approximately 17 minutes for all size ranges (after injection period is stopped)
- the high ventilation case return to background time is approximately 4 minutes for all size ranges (after injection period is stopped)

RESULTS

- THREE-DIMENSIONAL VISUALIZATION
- HORIZONTAL CONTOUR PLANE AT FACE LEVEL OF EMS WORKERS
- VERTICAL CONTOUR PLANE AT INJECTION POSITION ALONG PATIENT COT
- SPATIAL-AVERAGED AEROSOL VOLUME CONCENTRATION OVER TIME
- AEROSOL VOLUME CONCENTRATION OVER TIME AT EMS WORKERS' FACE
- MAXIMUM AEROSOL VOLUME CONCENTRATION AT EMS WORKERS' FACE
- TEMPORAL-AVERAGED AEROSOL VOLUME CONCENTRATION AT EMS WORKERS' FACE

MAXIMUM AEROSOL VOLUME CONCENTRATION

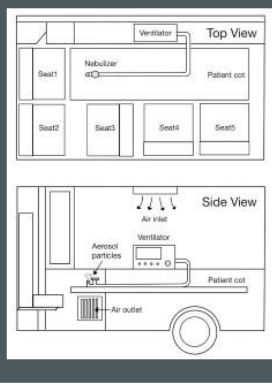

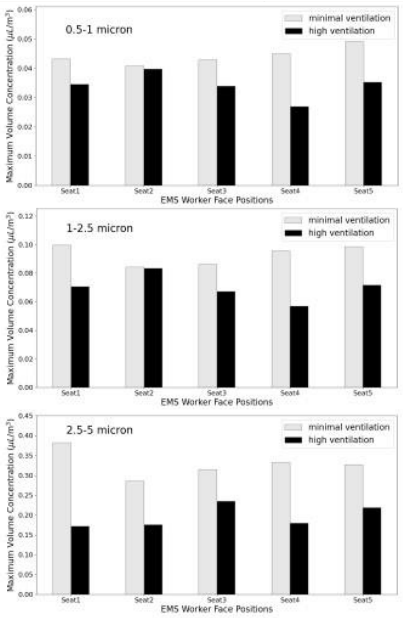

97

MAXIMUM AEROSOL VOLUME CONCENTRATION AT EMS WORKERS' FACE

(summary)

- **the air exhaust system can reduce maximum concentration by approximately 25%**
- **Minimal Ventilation:**
  - Seat 5 for 0.5-1 microns and seat 1 for others have the highest aerosol exposure
  - Seat 2 has the lowest aerosol exposure across all size ranges
- **High Ventilation:**
  - Seat 3 for 2.5-5 microns and seat 2 for others have the highest aerosol exposure
  - Seat 1 for 2.5-5 microns and seat 4 for others have the lowest aerosol exposure

RESULTS

- THREE-DIMENSIONAL VISUALIZATION
- HORIZONTAL CONTOUR PLANE AT FACE LEVEL OF EMS WORKERS
- VERTICAL CONTOUR PLANE AT INJECTION POSITION ALONG PATIENT COT
- SPATIAL-AVERAGED AEROSOL VOLUME CONCENTRATION OVER TIME
- AEROSOL VOLUME CONCENTRATION OVER TIME AT EMS WORKERS' FACE
- MAXIMUM AEROSOL VOLUME CONCENTRATION AT EMS WORKERS' FACE
- TEMPORAL-AVERAGED AEROSOL VOLUME CONCENTRATION AT EMS WORKERS' FACE

TEMPORAL-AVERAGED AEROSOL VOLUME CONCENTRATION

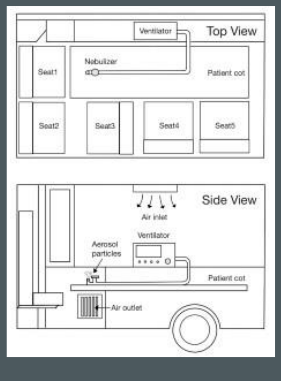

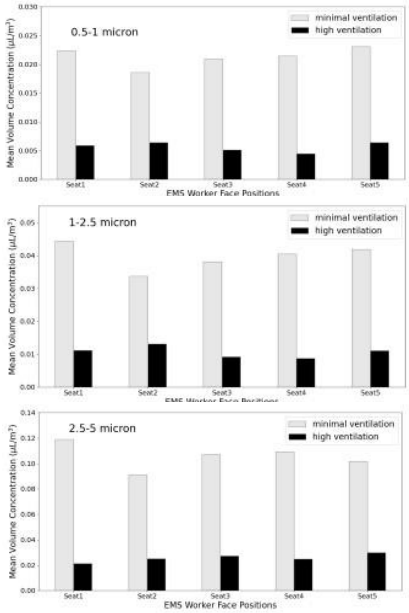

TEMPORAL-AVERAGED AEROSOL VOLUME CONCENTRATION AT EMS WORKERS' FACE

(summary)

- **the air exhaust system can reduce temporal-averaged concentration by 70%.**
- **Minimal Ventilation:**
  - Seat 5 for 0.5-1 microns and seat 1 for others have the highest aerosol exposure
  - Seat 2 has the lowest aerosol exposure across all size ranges.
- **High Ventilation:**
  - Seat 5 for 2.5-5 microns and seat 2 for others have the highest aerosol exposure
  - Seat 1 for 2.5-5 microns and seat 4 for others have the lowest aerosol exposure

CONCLUSION

Aerosol Distribution Characteris

Quantitativeness

CONCLUSION

Aerosol Distribution Characteristic

Start

- cloud of aerosols occurs at above patient face in patient compartment only a few seconds after the start of injection

During Injection Period

- minimal ventilation: concentration mainly distributes in the area above patient face and seat 1
- high ventilation: concentration mainly distributes in the area above patient face adjacent to the exhaust outlet
- smaller -size particles have a relatively wider distribution area than larger particles
- peak concentration throughout the experiment occurs immediately after the stop of injection

103

CONCLUSION

Aerosol Distribution Characteristic

Decreasing Period (almost uniform across control volume)

- minimal ventilation: at approximately 7-8 minutes after the injection is stopped
- high ventilation: approximately 1-2 minutes after the injection is stopped

Time to Return to (or Become Comparable with) Background after Injection Period is Stopped

- minimal ventilation: approximately 9 minutes for 2.5-5 microns, 12 minutes for 1-2.5 microns, and 16 minutes for 0.5-1 microns
- high ventilation: is approximately 3 minutes for 2.5-5 microns, 3 minutes for 1-2.5 microns, and 4 minutes for 0.5-1 microns

104

CONCLUSION

Quantitativeness

Minimal Ventilation (turn off air exhaust system):

- return to background time of spatial -averaged concentration is approximately 15 minutes for all size ranges (after injection period is stopped)
- return to background time of all seat positions combined is approximately 17 minutes for all size ranges (after injection period is stopped)
- highest exposure to aerosols among seating positions are at seat 5 for 0.5-1 microns and seat 1 for 1-5 microns
- lowest exposure to aerosols among seating positions is at seat 2 for all size ranges

105

CONCLUSION

Quantitativeness

High Ventilation (turn on air exhaust system):

- return to background time of spatial -averaged concentration is approximately 4 minutes for all size ranges (after injection period is stopped)
- return to background time of all seat positions combined is approximately 4 minutes for all size ranges (after injection period is stopped)
- highest maximum concentration among seating positions is at seat 3 for 2.5-5 microns
- highest temporal -averaged concentration among seating positions is at seat 5 for 2.5-5 microns
- highest exposure to aerosols among seating positions is at seat 2 for 0.5-2.5 microns
- lowest exposure to aerosols among seating positions are at seat 1 for 2.5-5 microns and seat 4 for 0.5-2.5 microns

106

OBJECTIVE

- To assess the effectiveness of an ambulance air exhaust system in reducing the volume density of airborne particles

THESIS CONTRIBUTION

- the air exhaust system can reduce 'return -to-background ' time by approximately 75%
- the air exhaust system can reduce peak spatial -averaged aerosol volume concentration about 2 times
- the air exhaust system can reduce maximum concentration (all seat positions and sizes combined) by approximately 25%
- the air exhaust system can reduce temporal -averaged (all seat positions and sizes combined) concentration by 70%.

107

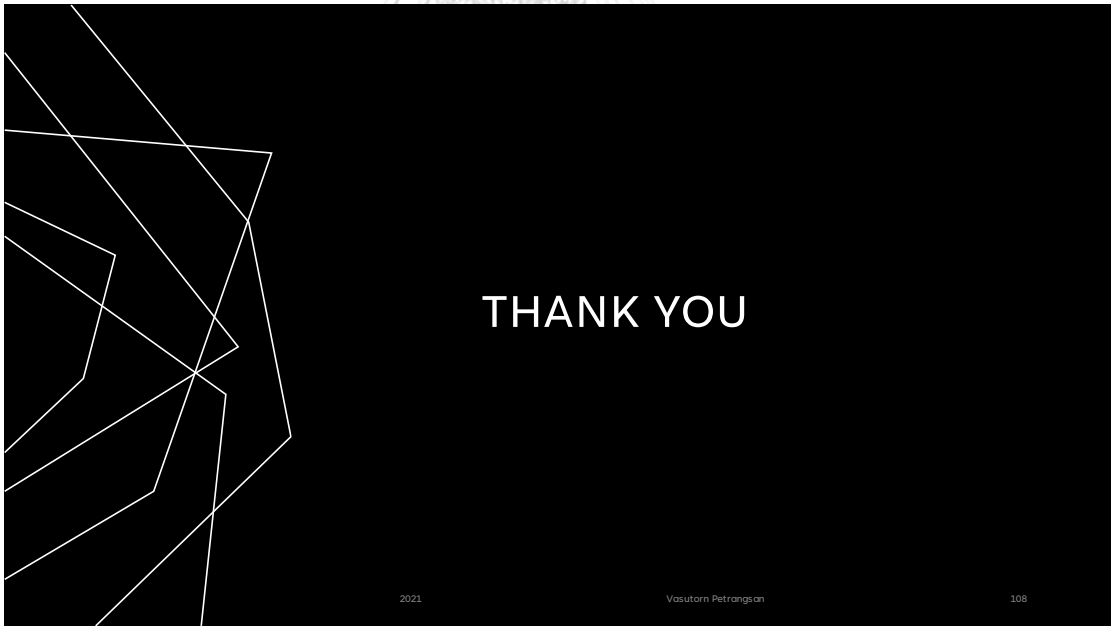

VITA

NAME	Vasutorn Petrangsan
DATE OF BIRTH	9 September 1995
PLACE OF BIRTH	Bangkok, Thailand
INSTITUTIONS ATTENDED	B.Eng. Mechanical Engineering, Chulalongkorn University
HOME ADDRESS	85 Ramkhamhaeng 9, Ramkhamhaeng Road, Plubpla, Wang Thonglang, Bangkok, 10310
PUBLICATION	Petrangsan, V., Rojanasarntikul, T., & Chongsiripinyo, K. (2021). Efficacy of the Ambulance Air Purifier System for Airborne Particle Reduction. The 35th Conference of the Mechanical Engineering Network of Thailand.
AWARD RECEIVED	Runners-up Best Paper in the 35th Conference of the Mechanical Engineering Network of Thailand (ME-NETT 2021) from the Paper "Efficacy of the Ambulance Air Purifier System for Airborne Particle Reduction" presented on July 22, 2021 via Zoom online meeting

จุฬาลงกรณ์มหาวิทยาลัย
Chulalongkorn University